

EXPERIMENTAL TESTING AND
ANALYSIS OF SURFACE WATER
HEAT EXCHANGERS

By

GARRETT MICHAEL HANSEN

Bachelor of Science in Mechanical Engineering

Oklahoma State University

Stillwater, Oklahoma

2011

Submitted to the Faculty of the
Graduate College of the
Oklahoma State University
in partial fulfillment of
the requirements for
the Degree of
MASTER OF SCIENCE
December, 2011

EXPERIMENTAL TESTING AND ANALYSIS OF
SURFACE WATER HEAT EXCHANGERS

Thesis Approved:

Dr. Jeffrey Spitler

Thesis Adviser

Dr. Lorenzo Cremaschi

Dr. Daniel Fisher

Dr. Sheryl A. Tucker

Dean of the Graduate College

ACKNOWLEDGMENTS

I would first like to start off by thanking those who are closest to me. Without my family and friends to keep my spirits high, making it through this long and exhausting process would have been nearly impossible. They continuously reminded me that my hard work and dedication would ultimately pay off, which it has. Thank you for your love and support!

Secondly I would like to bestow my deepest thanks to my advisor, Dr. Jeffrey Spitler. Throughout the duration of the project, Dr. Spitler provided guidance, knowledge, and encouragement. His reputation among the engineering field is highly regarded and I have learned this to be true first hand. Thank you for sharing your wisdom!

Third, I would like to extend my appreciation to my other two committee members whom doubled as my professors while attending Oklahoma State University. Dr. Lorenzo Cremaschi and Dr. Daniel Fisher provided additional advice and recommendations in further improve the material in this thesis. Thank you both for your knowledge & encouragement!

Fourth, I would like to recognize my colleagues in both the masters program and the undergraduate program. Having fellow workers to bounce ideas off of and helping hands when things required more than just me was invaluable. Thank you for your manpower and listening ears!

Finally I would like to thank the American Society of Heating, Refrigeration, and Air Conditioning Engineers (ASHRAE) for sponsoring this project. Without their funding, my going to graduate school and this work would not be possible. Thank you!

TABLE OF CONTENTS

Chapter	Page
I. INTRODUCTION	1
Overview	1
Background – Open-Loop Systems	8
Background – Closed-Loop Systems.....	10
Svenson (1985)	11
Kavanaugh & Co-Authors (1989-2006)	12
Chiasson et al. (2000)	16
Literature Review – Inside Pipe Forced Convection	16
Straight Pipe.....	17
Curved Pipe.....	18
Helical Pipe	19
Literature Review – Outside Natural/Free Convection	19
Straight Pipe.....	20
Helical Pipe.....	21
Objectives and Organization.....	24
II. EXPERIMENTAL APPARATUS	27
In-Situ Trailer (Austin 1998)	27
In-Situ Trailer Modifications	29
Heat Exchanger Construction	32
Frame Construction.....	34
Bundle Coil Construction	36
Spiral-Helical Coil Spacing Grid.....	38
Spiral-Helical Coil Construction.....	38
Flat-Spiral Coil Construction	44
Slinky Coil Construction.....	45
System Deployment	47
Temperature Sensor Attachment.....	47
Coil Deployment.....	52
System Purging and Data Acquisition Procedure	54
Coil Submersion and Rising	58

Chapter	Page
III. CALIBRATION OF MEASUREMENT DEVICES	60
Thermistors	60
Thermistor Calibration Procedure.....	60
Flow Meter.....	61
Watt Transducer.....	63
IV. ANALYSIS METHODOLOGY	64
Data Averaging	64
Outside Convection Coefficient – HDPE Tube-Based Heat Exchangers.....	64
Outside Convection Coefficient – Vertical Flat-Plate Heat Exchanger.....	68
Uncertainty Analysis Methodology	69
Uncertainty Analysis Results.....	74
Spiral-Helical Coil Uncertainty Results.....	74
Flat-Spiral Coil Uncertainty Results.....	76
Slinky Coil Uncertainty Results	77
Vertical Flat-Plate Heat Exchanger Coil Uncertainty Results.....	78
Bundle Coil Uncertainty Results	79
V. RESULTS AND DISCUSSION	81
HDPE SDR-11 Spiral-Helical SWHE Results	81
Outside Convection Coefficients	83
Spiral-Helical Correlation Development	88
Correlation to Experimental Comparisons.....	93
Correlation Refinement.....	95
Lake Bottom Proximity Testing Results.....	102
Bundled Coil Results	104
Flat-Spiral Coil Results.....	106
Vertical & Horizontal Slinky Coil Results	109
Vertical Flat-Plate Heat Exchanger Results.....	112
VI. APPLICATIONS	117
Approach Temperature Sizing Design Graphs	117
Kavanaugh & Rafferty Design Graphs	117
Lake Temperature & Heat Pump Load Dependence	118
Typical Condition Design Graph	123
Alternate SWHE Designs	127
HDPE Wall Thickness Influence	128
Thermally Enhanced SDR-11 HDPE Coils	131
Copper Tubing Coils.....	132
Comparison of Tubing Alternatives.....	134

Vertical Flat-Plate Heat Exchanger	135
Coil Selection Economics	136
Design Graphs or Software Design Tools	139
VII. SUMMARY, CONCLUSIONS, AND RECOMMENDATIONS	140
Summary of Experimental Testing, Apparatus, and Procedure.....	140
Conclusions: Convection Research.....	144
Conclusions: Applications Research.....	145
Recommendations: Convection Research.....	147
Recommendations: Applications Research.....	148
REFERENCES	149
APPENDICES	151
Spiral-Helical Experimental Data & Reference Calculations.....	151
Bundle Coil Experimental Data & Reference Calculations.....	161
Flat-Spiral Experimental Data & Reference Calculations	166
Vertical and Horizontal Slinky Experimental Data & Reference Calculations...	168
Vertical Flat-Plate Experimental Data & Reference Calculations.....	171

LIST OF TABLES

Table	Page
1-1 HDPE Thermal Conductivities According to Rauwendaal (1986)	5
1-2 Outside Convection Coefficient Scenario Results	7
1-3 Minimum Required Flow Rate (GPM) for Nonlaminar Flow (Modified from Kavanaugh and Rafferty 1997)	15
1-4 Prabhanjan et al. (2004) Nusselt-Rayleigh Number Correlations Results ($Nu_{o,L}=a(Ra_L)^b$)	22
2-1 Spiral-Helical Coil Configuration Numbering	33
2-2 Bundle Testing Coil Geometries	36
2-3 Set Point Nominal Power Input Values & Controller Positioning	57
2-4 Coil Buoyancy Analysis	58
2-5 Buoy Buoyancy Analysis	59
3-1 Flow Meter Calibration Results	62
4-1 Heat Transfer Uncertainty Example	70
4-2 Vertical Slinky Coil Uncertainty in Length Results	72
5-1 19 mm ($\frac{3}{4}$ ") Nominal SDR-11 HDPE Spiral-Helical SWHE Test Matrix	82
5-2 25 mm (1") Nominal SDR-11 HDPE Spiral-Helical SWHE Test Matrix	82
5-3 32 mm (1- $\frac{1}{4}$ ") Nominal SDR-11 HDPE Spiral-Helical SWHE Test Matrix	83
5-4 Thermal Resistance Breakdown SDR-11 HDPE by Tube Size	88
5-5 Statistics and Coefficients of the Two Parameter Nusselt-Rayleigh Correlation	90
5-6 Statistics and Coefficients of the Three Parameter Nusselt-Rayleigh Correlation	91
5-7 Statistics and Coefficients of the Four Parameter Nusselt-Rayleigh Correlation	92
5-8 Statistics and Coefficients of the Five Parameter Nusselt-Rayleigh Correlation	92
5-9 Correlation Equations for Refinement	96
5-10 Data Point Distribution for Uncertainty Filter Results	98
5-11 $\pm 70\%$ Uncertainty Filter Correlation Results	99
5-12 Vertical Flat-Plate Heat Exchanger Testing Conditions	113
5-13 Vertical Flat-Plate Heat Exchanger Thermal Resistance Distribution	113
6-1 Heat Pump Cooling Data	120
6-2 High Density Polyethylene Tubing Dimensions	128
6-3 Cost Analysis of HDPE and Copper Tubing	137

LIST OF FIGURES

Figure	Page
1-1 Small Closed-Loop SWHP System with SWHE in Spiral-Helical Configuration	2
1-2 Small Open-Loop SWHP System with Water Intake Screen	3
1-3 Open-Loop Direct Cooling System (Modified from Leraand and Van Ryzin 1995)	9
1-4 Open-loop Direct Cooling with Auxiliary Chiller (Modified from Leraand and Van Ryzin 1995)	9
1-5 Required Length for Spread/Slinky Coils in Cooling Mode (Modified from Kavanaugh and Rafferty 1997)	13
1-6 Required Length for Loose Bundle Coils in Cooling Mode (Modified from Kavanaugh and Rafferty 1997)	13
1-7 Required Length for Spread/Slinky Coils in Heating Mode (Modified from Kavanaugh and Rafferty 1997)	14
1-8 Required Length for Loose Bundle Coils in Heating Mode (Modified from Kavanaugh and Rafferty 1997)	14
1-9 Prabhanjan et al. (2004) Experimental Setup	21
2-1 In-Situ Trailer Setup	28
2-2 Outside of the In-Situ Trailer	29
2-3 In-Situ Trailer Pipe Insulated	30
2-4 Indoor SWHE Testing Pool	31
2-5 Flat-spiral Coil Prior to Submerging	33
2-6 Warped Spiral-Helical Coil in Pool without Metal Frame	34
2-7 Coil Base Frame with Supports	35
2-8 Flat-spiral Coil Adaptor	35
2-9 Loose Bundle Piping Circumference	36
2-10 Submerged Loose Bundled Coil	37
2-11 Loose-Spaced Bundled Coil	37
2-12 Single Spacer Frame	38
2-13 Assembled Spacing Grid	38
2-14 Finished Coil Platform-Hub Assembly	40
2-15 Spiral-Helical Coil Wrapping Number Diagram (1 = Start, 31 = End)	41
2-16 Step 1: Start of Spiral-Helical Coil Wrapping	42
2-17 Step 2: Spiral-Helical Coil Wrapping Continued	42
2-18 Step 3: Spiral-Helical Coil Wrapping Continued	43
2-19 Step 4: Spiral-Helical Coil Wrapping Continued	43
2-20 Step 5: Finished Spiral-Helical Coil Wrapping	44

Figure	Page
2-21 Flat-Spiral Coil	45
2-22 Slinky Coil Assembly Guide Rails	46
2-23 Constructed Slinky Coil	46
2-24 Slinky Coil Schematics & Dimensions	47
2-25 In-pipe Thermistor at the Coil Outlet	48
2-26 In-pipe Thermistor Probe (Part #: ON-410-PP)	49
2-27 Lake Temperature Thermistors at the Coil	50
2-28 Locations of Temperature Trees	51
2-29 Lake Temperature Tree Schematic	51
2-30 Sample Temperature Tree Data (6/2/2011-6/6/2011)	51
2-31 Braided Tube & HDPE Connection	52
2-32 Female Coupler Cam-Groove Connection	53
2-33 PVC Union Coil Connection	54
2-34 Purging 3-Way Valve Controls by Step (Modified from Austin (1998))	56
2-35 Coil & Frame Suspension Schematic	59
3-1 Lake Temperature Thermistor Calibration: $\ln(R)$ vs. $1/T_{\text{ref}}$	61
3-2 Flow Meter Calibration Curve	63
4-1 Vertical Slinky Spatial Uncertainty Diagram	72
4-2 Spiral-Helical SWHE Uncertainty on Heat Transfer Rate	75
4-3 Outside Convection Coefficient Uncertainty vs. Heat Transfer Rate (Spiral-Helical)	76
4-4 Outside Convection Coefficient Uncertainty vs. Heat Transfer Rate (Flat-Spiral)	77
4-5 Outside Convection Coefficient Uncertainty vs. Heat Transfer Rate (Slinky Coils)	78
4-6 Outside Convection Coefficient Uncertainty vs. Heat Transfer Rate (Vertical Flat-Plate)	79
4-7 Outside Convection Coefficient Uncertainty vs. Heat Transfer Rate (Bundle Coils)	80
5-1 Spiral-Helical $h_{o,exp}$ vs. ΔT (Individual Tests)	84
5-2 Spiral-Helical $h_{o,exp}$ vs. ΔT (Constant Heat Transfer Rates)	85
5-3 All 19 mm ($\frac{3}{4}$ in) Spiral-Helical SWHE Results ($h_{o,exp}$ vs. ΔT)	86
5-4 All 25 mm (1 in) Spiral-Helical SWHE Results ($h_{o,exp}$ vs. ΔT)	87
5-5 All 32 mm (1- $\frac{1}{4}$ in) Spiral-Helical SWHE Results ($h_{o,exp}$ vs. ΔT)	87
5-6 Spiral-Helical Results vs. Correlation ($h_{o,exp}$ vs. $h_{o,corr}$)	93
5-7 Spiral-Helical Results vs. Correlations ($Nu_{f,o,d}$ vs. $Ra_{f,o,d}^*$)	94
5-8 Spiral-Helical Results vs. Correlation ($Q_{c,exp}$ vs. $Q_{c,corr}$)	95
5-9 Correlation Refinement with RMSE % Results	97
5-10 Correlation Refinement with RMSE Results	98
5-11 Simulation Heat Transfer Rate Comparison (Filtered vs. Non-Filtered)	101
5-12 Spiral-Helical SWHE Lake Bottom Proximity Test Results	103
5-13 Bundled Coil Results in $Nu_{f,o,d}$ vs. $Ra_{f,o,d}^*$	104
5-14 Loose Bundle Heat Transfer Comparison with Simulation Model	106
5-15 Flat-Spiral SWHE Results ($h_{o,exp}$ vs. ΔT)	107

Figure	Page
5-16 Flat-Spiral SWHE Results ($Nu_{f,o,d}$ vs. $Ra_{f,o,d}^*$)	108
5-17 Vertical & Horizontal Slinky SWHE Results ($h_{o,exp}$ vs. ΔT)	109
5-18 Vertical & Horizontal Slinky SWHE Results ($Nu_{f,o,d}$ vs. $Ra_{f,o,d}^*$)	110
5-19 Flat-Spiral & Slinky SWHE Results with Equation 5-9 Correlation	111
5-20 Flat-Spiral & Slinky SWHE Results vs. Churchill & Chu (1975) Correlation	112
5-21 Vertical Flat-Plate Heat Exchanger Results ($h_{o,exp}$ vs. ΔT)	114
5-22 Vertical Flat-Plate Heat Exchanger Results ($Nu_{f,o,H}$ vs. $Ra_{f,o,H}^*$)	115
5-23 Vertical Flat-Plate Heat Exchanger Results vs. Churchill & Chu (1975) Correlation	116
6-1 Lake Temperature Effect on Small Spaced Configuration SWHE (19 mm, 3/4 in HDPE Tube)	119
6-2 Lake Temperature Effect on Large Spaced Configuration SWHE (32 mm, 1-1/4 in HDPE Tube)	119
6-3 Heat Pump Effects Design Graph (Medium Spaced Spiral-Helical SWHE 19 mm, 3/4 in SDR-11 HDPE)	122
6-4 Minnesota Scenario Sizing Design Graph for Medium Spaced SDR-11 HDPE SWHE	123
6-5 Tennessee Scenario Sizing Design Graph for Medium Spaced SDR-11 HDPE SWHE	124
6-6 Arizona Scenario Sizing Design Graph for Medium Spaced SDR-11 HDPE SWHE	125
6-7 Spiral-Helical SWHE Sizing Design Graph for SDR-11 HDPE (Combined Scenario Results)	126
6-8 Spiral-Helical SWHE Size-Range Design Graph for the Continental United States	127
6-9 Wall Thickness Influence on Medium Spaced SWHE (19 mm, 3/4 in)	129
6-10 Wall Thickness Influence on Medium Spaced SWHE (25 mm, 1 in)	130
6-11 Wall Thickness Influence on Medium Spaced SWHE (32 mm, 1-1/4 in)	130
6-12 Standard vs. Thermally Enhanced SDR-11 HDPE Design Graph (Medium Spaced Spiral-Helical SWHE)	131
6-13 Medium Spaced Copper Tube SWHE Sizing Design Graph (19 mm, 3/4 in)	133
6-14 Alternative SWHE Tubing Comparison Design graph	134
6-15 Vertical Flat-Plate SWHE Sizing Design graph	135
6-16 Spiral-Helical SWHE Material Pricing Design Graph	138

NOMENCLATURE

Variables

A	area (m^2)
C	coil minor circumference (m)
c_p	specific heat (J/kg-K)
d	tube diameter (m)
D	coil diameter (m)
De	Dean number
f	Darcy friction factor
g	gravitational acceleration (m/s^2)
h	convection coefficient ($\text{W/m}^2\text{-K}$)
H	coil height (m)
k	thermal conductivity (W/m-K)
L	tube length (m)
\dot{m}	mass flow rate (kg/s)
n	empirical constant
Nu	Nusselt number
NTU	number of transfer units
Pr	Prandtl number
q	heat flux (W/m^2)
Q	heat transfer rate (W)
r	radius (m)
R	electrical resistance (Ω)
R'	thermal resistance (K/W)
Ra	Rayleigh number
Ra^*	modified Rayleigh number
Re	Reynolds number
t	time (seconds)
T	temperature (K)
U	overall heat transfer coefficient ($\text{W/m}^2\text{-K}$)
\vec{v}	velocity (m/s)
ΔV	voltage (V)
V	volume (m^3)
\dot{V}	volumetric flow rate (m^3/s)

Subscripts

avg	average
b	bulk
c	coil
$corr$	correlation
cr	cross-section
d	tube diameter
exp	experimental
f	film
H	coil height
$HDPE$	high density polyethylene
i	inside
in	inlet
L	characteristic length
max	maximum
MFT	mean fluid temperature
o	outside
out	outlet
p	pond/lake
s	surface
t	tube
w	wall
Δx	horizontal tube spacing (m)
Δy	vertical tube spacing (m)

Greek Symbols

α	thermal diffusivity (m^2/s)
β	thermal expansion coefficient ($1/\text{K}$)
γ	dimensionless pitch coefficient
ε	thermal effectiveness
μ	dynamic viscosity (kg/m-s)
ν	kinematic viscosity (m^2/s)
ρ	density (kg/m^3)
π	mathematical constant

CHAPTER I

1) INTRODUCTION

1.1 Overview

Heat pumps are an efficient means of providing heating and cooling to buildings. Their efficiency depends partly on the heat sink or heat source being used. Different heat sinks and sources have been used, with air being the most common. In recent years, using the ground as a heat sink and source has become very popular. A less well known but also utilized heat sink/source is surface water; i.e. ponds, lakes, reservoirs, etc.

A surface water heat pump (SWHP) system utilizes a body of water to either reject or absorb heat depending on the building or process requirements. Small closed-loop SWHP systems typically have four main components as seen in Figure 1-1. The four components are the heat pump, the piping, circulating pump, and the surface water heat exchanger (SWHE) immersed in a body of water. The heat pump may be either an air-to-water or a water-to-water heat pump. Larger closed-loop systems will have multiple heat pumps and multiple SWHE.

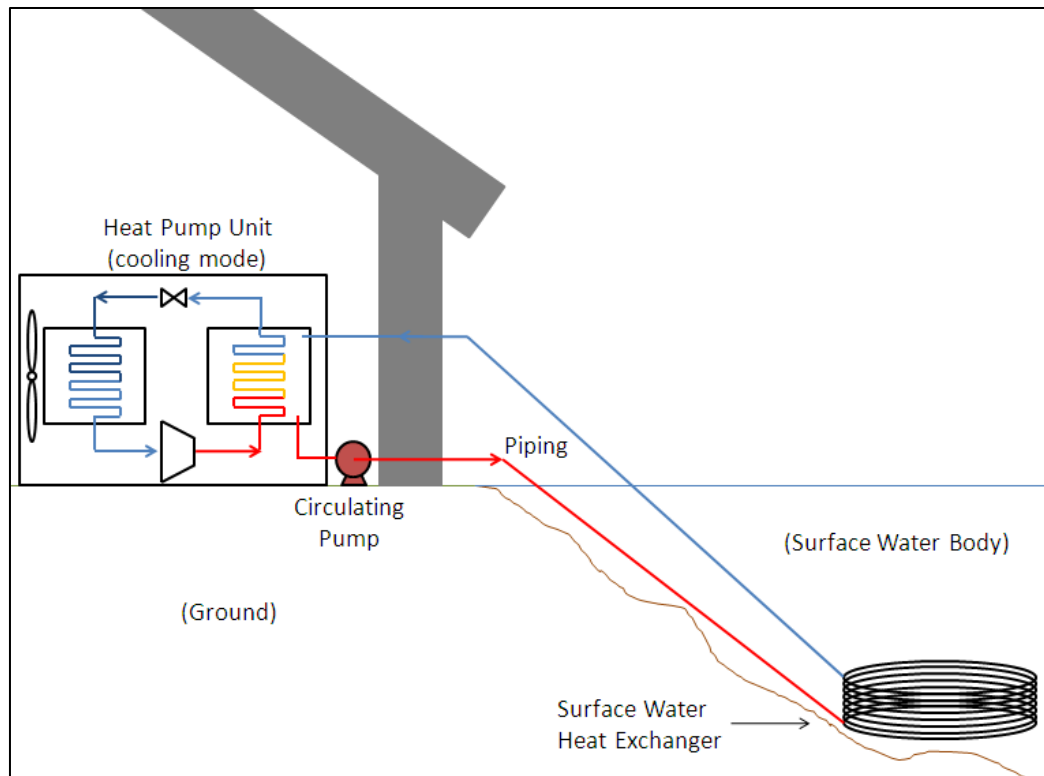


Figure 1-1. Small Closed-Loop SWHP System with SWHE in Spiral-Helical Configuration

There are also open-loop surface water heat pump systems. A small open-loop SWHP system is shown in Figure 1-2. The open-loop system is the same as the closed-loop system except the heat exchanger is replaced by a water intake structure that screens large objects and biological organisms. After the intake water is run through the heat pump it is discharged back into the surface water body at a temperature either warmer or colder than the intake depending on the mode (cooling or heating) of operation. The distance between the intake and the discharge should be fairly large to prevent short circuiting.

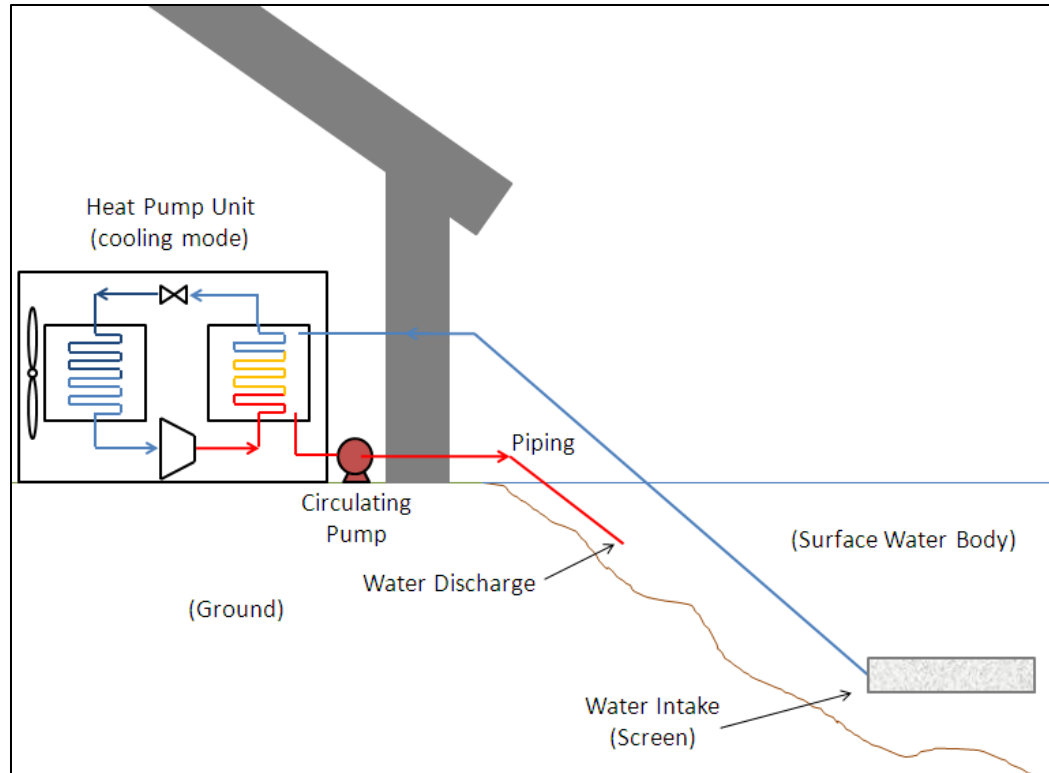


Figure 1-2. Small Open-Loop SWHP System with Water Intake Screen

There are many different types of surface water bodies in which SWHP systems can be used. Ponds, lakes, and reservoirs are all water bodies with relatively low inflows and outflows. Large lakes and reservoirs can remain stratified such that they have cool water year-round at significant depths. Water flow outside the SWHE is stagnant generally in these water bodies and thus natural convection is dominant for closed-loop systems. Streams and rivers fall in the category of flowing water bodies. This means that forced convection is present on the exterior of closed-loop heat exchangers in flowing water bodies and higher heat transfer is possible. However, due to water-borne debris such as fallen trees that can be destructive to SWHEs, many river and streams are unsuitable for closed-loop SWHP systems. Therefore this thesis is focused on SWHEs located in ponds, lakes and reservoirs. From here on, all three water bodies will be referred to as lakes unless otherwise specified since they exhibit similar characteristics.

The piping material of choice at present is high density polyethylene (HDPE). HDPE provides high durability with low cost. The connecting pipes are typically buried underground until they reach the surface water body. The header location in the trench or in the lake should be protected with either PVC or flexible drain pipe to prevent damage (Kavanaugh and Rafferty 1997).

The final main component of the SWHP system is the surface water heat exchanger that resides in the water. Many different types of SWHEs exist and are used in SWHP systems. Some of the different types include straight HDPE piping, slinky coils, spiral-helical coils, vertical-flat metal plates (Slim Jim®), and flat-spiral heat exchangers. The different SHWEs provide different benefits and drawbacks.

In many closed-loop SWHP systems, the SWHE is formed from HDPE pipe by wrapping it around a spindle device into a spiral-helical coil. Such a device is described more in Section 2.3.4. The disadvantage of using HDPE is that its thermal conductivity is relatively low. According to Rauwendaal (1986), the thermal conductivity of polyethylene is a function of both density and temperature as shown in Equation 1-1.

$$k_t = 0.17 + 5(\rho_{HDPE} - 0.90) - 0.001T_{HDPE} \quad (1-1)$$

Where: k_t is the thermal conductivity of the HDPE tube in W/m-K

ρ_{HDPE} is the density of the HDPE in g/cm³

T_{HDPE} is the temperature of the HDPE less than 135°C

HDPE has densities ranging from 0.941-0.971 g/cc (58.7-60.6 lb/ft³) (Müller 2007).

Thermal conductivities for the range of densities and the range of temperatures typically encountered in our experiments are shown in Table 1-1. Helical coils made of copper tubing have also been used because the thermal conductivity is almost 900 times higher than that of HDPE, or around 400 W/m-K (231 Btu/hr-ft-°F).

Table 1-1. HDPE Thermal Conductivities According to Rauwendaal (1986)

Density	Temperature				
g/cm³	0°C	10°C	20°C	30°C	40°C
0.941	0.38	0.37	0.36	0.35	0.34
0.956	0.45	0.44	0.43	0.42	0.41
0.971	0.53	0.52	0.51	0.50	0.49

In addition to the spiral-helical and single helix coils, other configurations made of HDPE such as loose bundle, slinky, flat-spiral, and straight piping coils do exist. On the HDPE coils, heat transfer between the lake water and the heat exchanger is highly dependent on the geometry. When a SWHE has pipes that run near to one another, tube-to-tube interference may occur and diminish the heat transfer. In general, the more spaced out the configuration, the larger the heat transfer capacity is per unit length of piping.

Metal plate heat exchangers (e.g. Slim Jim®) provide compactness and high heat transfer rates but in some environments may degrade significantly over time and need replacing more frequently than HDPE coils. The metal of choice for plate SWHEs is stainless-steel when in freshwater environments but when dealing with saltwater bodies such as oceans or gulfs, titanium is the better material due to fouling reasons (Keens 1977). Titanium provides higher corrosion resistance but at a much higher cost. Pugh et al. (2005) provides additional guidelines on the fouling of heat exchangers in different environments.

This thesis is focused on closed-loop SWHP systems and in particular, the SWHE. The least understood aspect of the design when constructing a SWHE is the outside convection coefficient. Little or no data is available for the prediction of exterior convection coefficients that vary with geometry, orientation, loop temperatures, and lake temperatures.

When performing a surface water heat exchanger analysis, a design engineer needs to know the inside convective resistance, the conductive resistance through the material, and the

outside convective resistance to accurately predict the amount of heat transfer that will occur.

Equation 1-2 shows how the overall heat transfer coefficient (UA) is calculated.

$$\frac{1}{UA} = \frac{1}{h_i A_i} + \frac{\ln(d_o/d_i)}{2\pi k_t L_t} + \frac{1}{h_o A_o} \quad (1-2)$$

The number of transfer units ($NTUs$) is then obtained using Equation 1-3.

$$NTU = \frac{UA}{\dot{m} c_{p,MFT,i}} \quad (1-3)$$

An important assumption made is that the thermal mass of the lake is so large that the lake temperature is not changed by the heat transfer to/from the SWHE on a noticeable level. The lake (from a heat exchanger perspective) acts like a flow with infinite capacitance. The infinite capacitance heat exchanger relationship can be derived from the ε -NTU correlation for either a parallel flow or counter flow heat exchanger with a capacitance ratio of zero. The infinite capacitance ε -NTU relationship is then used in order to determine the heat exchanger effectiveness (ε_c) as shown in Equation 1-4.

$$\varepsilon_c = 1 - e^{-NTU} \quad (1-4)$$

The heat exchanger effectiveness and the maximum thermodynamically possible heat transfer rate between the fluid and the lake water is then used in Equation 1-5 to determine the actual heat transfer rate (Q_c).

$$Q_c = \varepsilon_c \left(\dot{m} c_{p,MFT,i} (T_{c,in} - T_p) \right) \quad (1-5)$$

This value can be compared to the load size and then the length of tube (L_t) can be adjusted iteratively or Equation 1-6 can be used explicitly to solve for the required length of tubing for a given load through the SWHE.

$$L_t = \frac{1}{h_i \pi d_i} + \frac{\ln(d_o/d_i)}{2\pi k_t} + \frac{1}{h_o \pi d_o} \left/ \frac{1}{\dot{m} c_{p,MFT,i} \ln \left(1 - \frac{Q_c}{\dot{m} c_{p,MFT,i} (T_{c,in} - T_p)} \right)} \right. \quad (1-6)$$

The importance of knowing the outside convection coefficient is evident if we look at the tube lengths required for a range of outside convection coefficients. On the low end of the spectrum a design engineer may use a value for h_o around 75 W/m²-K (426 Btu/hr-ft²-°F) while the top end of the spectrum may be a value of 500 W/m²-K (2,839 Btu/hr-ft²-°F), a rough value for a single straight tube with natural convection in water. We may then make a comparison for a case where the actual outside convection coefficient is in the middle, around 300 W/m²-K (1,703 Btu/hr-ft²-°F). Table 1-2 shows the required tube lengths necessary to reject a load of 3 tons (36,000 Btu/hr or 10.55 kW) at the SWHE through ¾ in SDR-11 HDPE when the coil inlet water temperature is 35°C (95°F), the coil outlet water temperature is 30°C (86°F), the lake water temperature is 20°C (68°F) and the volumetric flow rate is 0.315 L/s (5.0 GPM).

In this case, using the low value would double the cost of the lake heat exchanger, possibly making the project appear infeasible and uneconomical. If the high value is assumed, heat pump entering fluid temperature may exceed projected, damaging the company's reputation. It is quite evident to see from the example why obtaining the correct value of the outside convection coefficient is highly important from a design engineer's point of view.

Table 1-2. Outside Convection Coefficient Scenario Results

Value Compared to Actual	Outside Convection Coefficient		Required Tube Length		Length Increase Compared to Actual
	W/m ² -K	Btu/hr-ft ² -°F	m	ft	%
Low	75	426	511	1680	100% (oversized)
Actual	300	1703	256	840	-
High	500	2839	223	730	-13% (undersized)

This thesis is focused on the experimental testing of spiral-helical, flat-spiral, and slinky type heat exchanger configurations within an actual lake to obtain values of the outside convection coefficients. From the collected data, new correlations are developed in order to predict the exterior convection heat transfer so that a design engineer could use the correlation to more accurately size the SWHE.

1.2 Background – Open Loop Systems

Open-loop systems utilize water pumped from the lakes. It may be possible under some water conditions to directly use the water as shown in Figure 1-2. In applications where the water conditions are not ideal, an isolation heat exchanger is often used to prevent excessive fouling throughout the system. For cases with larger water-to-refrigerant heat exchangers it may be possible to clean the isolation heat exchanger in an inexpensive manner (Kavanaugh and Pezent 1990). Additionally, preventative measures such as flow direction reversal and water screening to remove fine particulates is recommended to reduce the fouling of open-loop systems (Kavanaugh and Rafferty 1997). The other disadvantage of an open-loop system is the increase in pumping power required since the elevation head is also present. Also mentioned by Kavanaugh and Rafferty is the benefit of being able to use the water temperature from the lake instead of the circulated water temperature which tends to be between 2.2°C-6.7°C (4°F-12°F) different.

Before discussing the open-loop SWHP system, there is also a direct cooling system that utilizes an open-loop configuration. In this system, the water is typically pumped through a large plate frame heat exchanger. After the water is pumped through the heat exchanger it is dumped back into the surface water body at a shallower depth. A simplified diagram is shown in Figure 1-3.

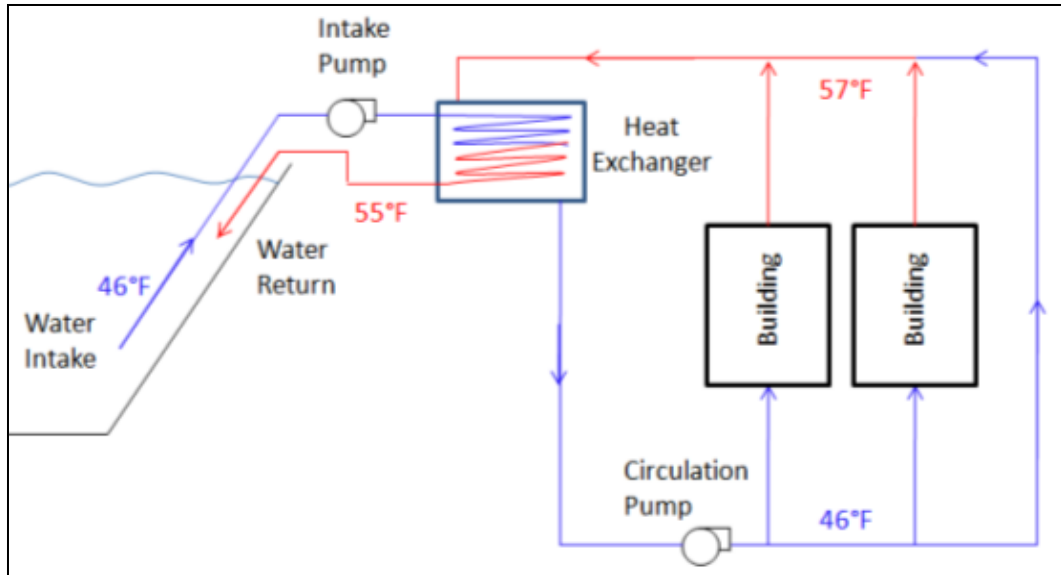


Figure 1-3. Open-loop Direct Cooling System (Modified from Leraand and Van Ryzin 1995)

Another method utilized by open-loop systems is the auxiliary chiller method. This uses the intake water and runs it first through the direct cooling heat exchanger and then additionally through the condenser side of a chiller (Leraand and Van Ryzin 1995). The direct cooling portion of the indirect method is optional; therefore the intake water can run directly into the condenser. This augmentation to the open-loop system can be found in Figure 1-4.

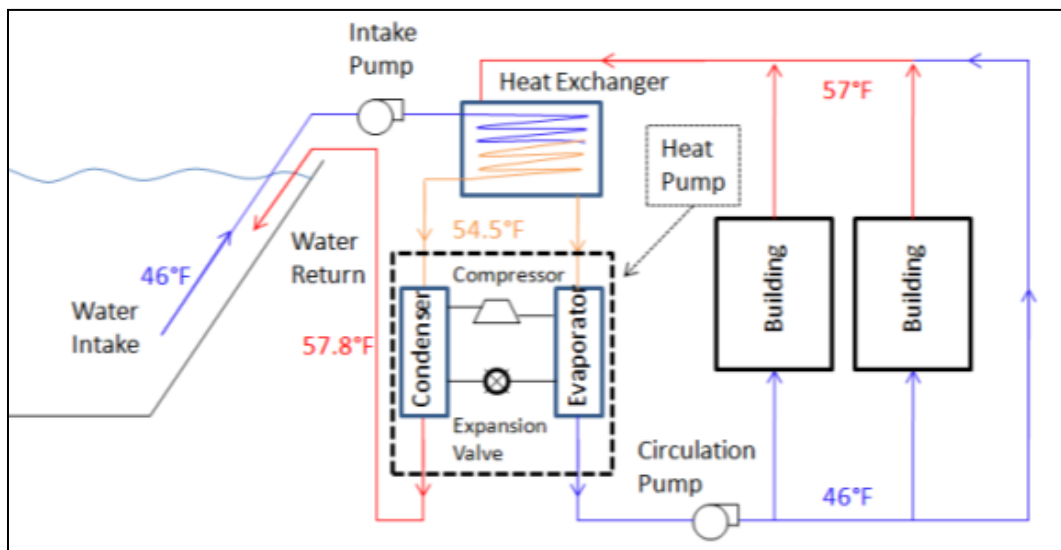


Figure 1-4. Open-loop Direct Cooling with Auxiliary Chiller (Modified from Leraand and Van Ryzin 1995)

Examples of direct open-loop systems can be found in Leraand and Van Ryzin (1995), Viquerat (2007), and Newman and Herbert (2009) while open-loop systems with chillers can be found in Chen et al. (2006), Looney and Olney (2007), and Zogg et al. (2008). The aforementioned systems are similar in type but do vary dramatically in size. The smallest system (Diego Garcia, India) is around 5.45 MW (1550 tons) of cooling while the largest system (Stockholm, Sweden) is around 180 MW (51182 tons).

1.3 Background – Closed Loop Systems

The second configuration, closed-loop systems, moves the heat exchanger (Kavanaugh and Pezent 1990) into the heat source/sink and connects it back to the heat pump with piping. Kavanaugh and Pezent summarize the benefits and disadvantages:

1. Fouling to the system is reduced dramatically because the circulating water is clean instead of dirty lake water.
2. A reduction in pumping power is experienced since the elevation head is no longer present.

Closed-loop systems do have their disadvantages as well:

- 1) The circulation fluid temperatures degrade 2°C to 7°C (4°F-12°F) compared to using the lake water in open-loop systems.
- 2) Damage is also a possibility to the SWHE located in the lake.
- 3) Fouling on the outside of the SWHE.

An example of a large closed-loop system (Kremposky 2007) that is currently in place is the Whitmore Lake High School in Whitmore Lake, MI. The 13,935 m² (150,000 ft²) high school opened in 2007 and was the first high school in Michigan to achieve LEED® Silver certification. The system has 72 heat pump units, four energy heat recovery units, and a capacity of 1.51 MW

(430 tons) which is dissipated through its 75.64 km (47 miles) of tubing. One third of the tubing is located beneath the surface of a 20,234 m² (5 acres or 217,800 ft²) lake. For this system the maximum amount of heat rejected per unit length of tubing is around 37 W/m (419 Btu/hr-ft) assuming a heat pump COP of 4 and equal loads in the ground-loop and lake-loop.

Another example of a large closed-loop surface water heat pump system (Hampton 2008) that is in place and working is located in Elgin, IL at the Sherman Health Facility. The 60,387 m² (650,000 ft²) hospital was completed in 2011 and has an extensive 750 water-to-air heat pump system that is connected to 171 underwater heat exchangers. This comes out to be nearly 26 km (16.2 miles or 85,500 ft) of ¾ in HDPE in just heat exchangers. In total there is approximately 241.4 km (150 miles or 792,000 ft) of HDPE piping when adding the headers and leads. Inside the tubing is an 80/20 mixture of water and methyl alcohol. The tubing loops are stretched out through a 60,703 m² (15 acres or 653,400 ft²) lake that is located next to the hospital. The lake is man-made and has a depth of 5.5 m (18 ft). The total cooling capacity of the closed-loop heat pump system is 8.62 MW (2,450 tons). This equates to a max heat rejection of 45 W/m (500 Btu/hr-ft) under the assumption that the heat pump COP is equal to 4 and the maximum load is dissipated through all of the HDPE piping and not just the heat exchanger piping.

1.3.1 Svensson (1985)

An early example of a closed-loop system is described by Svensson (1985). The system was connected to heat exchangers made from low density polyethylene pipe. The heat exchangers were spread out along the bottom of Lake Ö. Grevie at depths ranging from 2-3 meters (6.6-9.8 feet). Because freezing could be present at the coils, and thus cause floating, the tubes with brine solution in them were anchored roughly 10 cm (4 in) into the sediments by metal rods that were driven into the lake bottom. Since this system was designed for heating, the burying of the tubes in the sediments allowed for additional heat energy to be absorbed as it moved from the earth and into the lake. Additional studies done on the system show a majority of the heat energy comes

from the ground and not the water in the lake. Over the three years of testing conducted on the system, December 1981 through May 1984, it was shown to provide on average between 13.9-15.8 W/m (156-177 Btu/hr-ft) of heat extraction over the heating seasons.

1.3.2 Kavanaugh & Co-Authors (1989-2006)

Professor Stephen Kavanaugh at the University of Alabama in Tuscaloosa has carried out research on SWHP systems reported in a series of papers, much of which is summarized in Kavanaugh and Rafferty (1997). Their work covers such topics as temperature profiles in southern water bodies, lake water design temperatures for engineers to use throughout the United States (Hattemer and Kavanaugh 2005), existing water-to-air heat pump system performance (Kavanaugh and Pezent 1989) (Kavanaugh and Pezent 1990), environmental impacts of SWHP systems (McCrary et al. 2006), and a one-dimensional heat transfer simulation model for lakes (Pezent and Kavanaugh 1990).

Of particular relevance to this thesis, Kavanaugh and Rafferty (1997) also introduce the concept of an approach temperature and defined it as the temperature difference between the coil exit temperature and the lake temperature. They present a series of graphs to help with sizing two types of coils; spread/slinky coils and loose bundle coils. Spread/slinky coils are also utilized for ground heat exchangers and are constructed with a specific loop diameter and pitch, neither of which are defined in Kavanaugh and Rafferty (1997). The loose bundle coils have a few retaining bands to hold the tubes in its torus shape and in one general area. The circumference of the retaining band was not specified by Kavanaugh and Rafferty. Another crucial detail omitted by them was the basis of the design graphs. If based on experimental data, the heat transfer and the outside convection coefficient would have heavily depended on the geometry and lake conditions.

Never the less, the graphs were constructed for both heating and cooling scenarios. In all cases the flow rate per unit of heat absorbed/rejected was a constant 0.054 L/s-kW (3 GPM/ton). The design graphs from Kavanaugh and Rafferty (1997) can be seen in Figures 1-5 through 1-8.

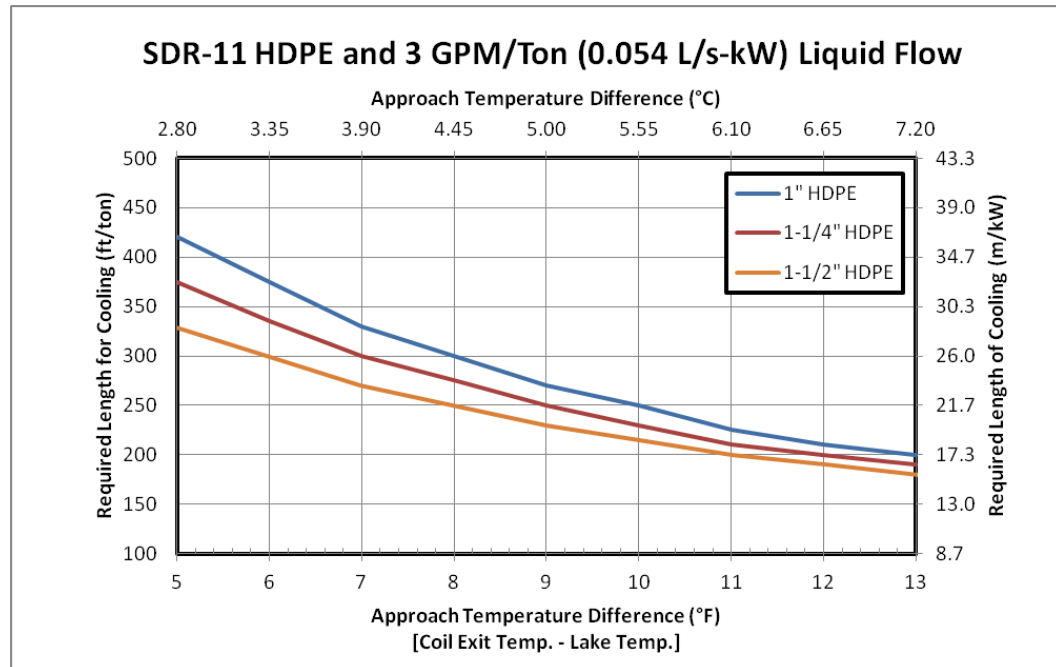


Figure 1-5. Required Length for Spread/Slinky Coils in Cooling Mode (Modified from Kavanaugh and Rafferty 1997)

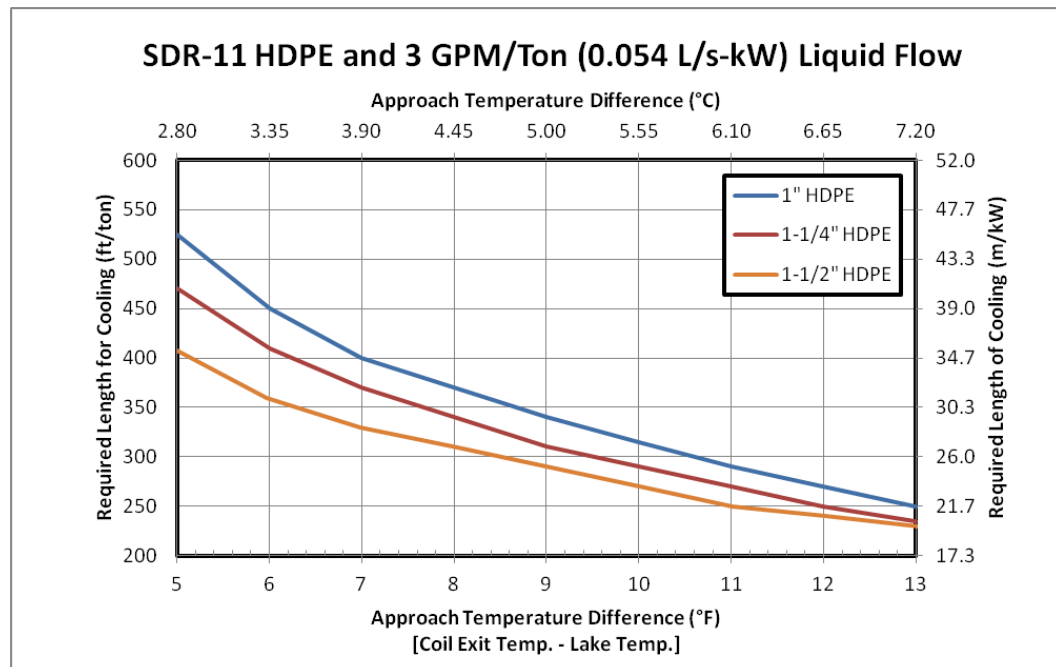


Figure 1-6. Required Length for Loose Bundle Coils in Cooling Mode (Modified from Kavanaugh and Rafferty 1997)

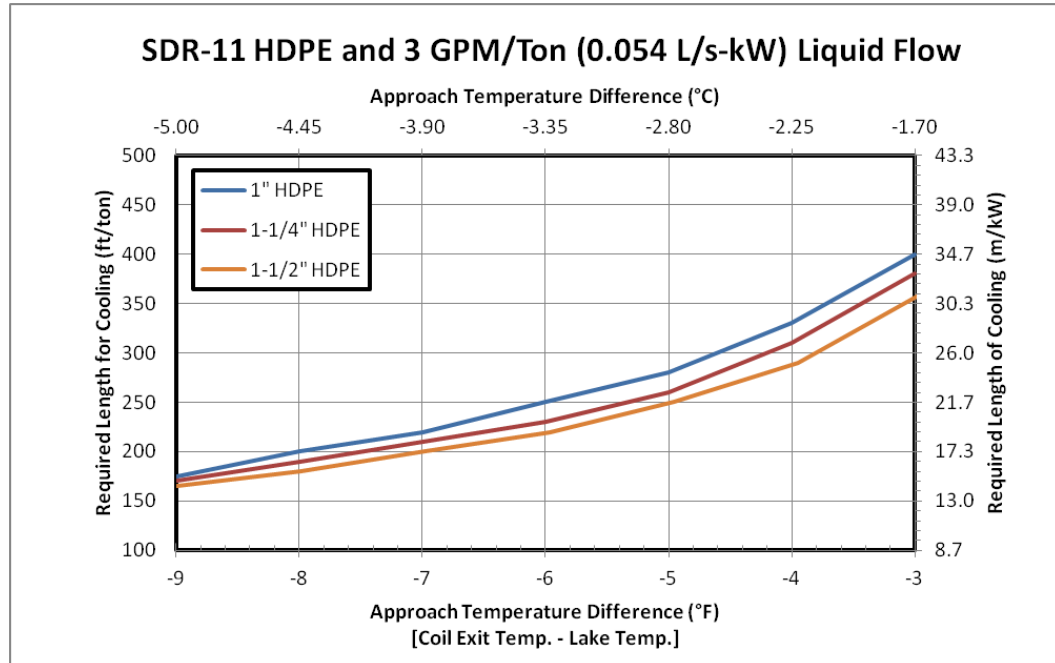


Figure 1-7. Required Length for Spread/Slinky Coils in Heating Mode (Modified from Kavanaugh and Rafferty 1997)

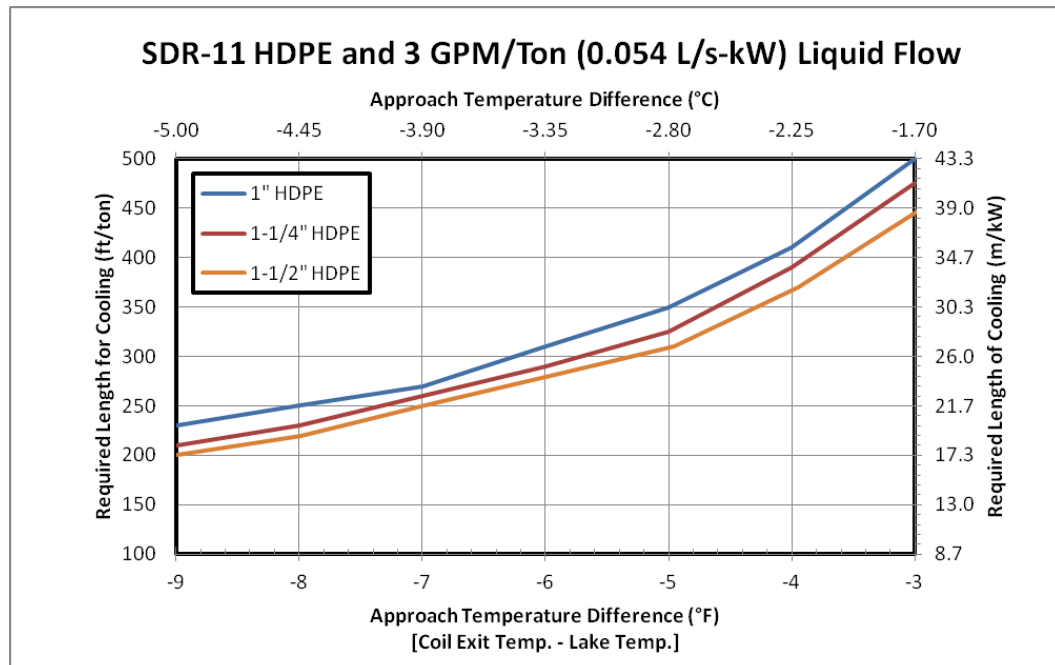


Figure 1-8. Required Length for Loose Bundle Coils in Heating Mode (Modified from Kavanaugh and Rafferty 1997)

In order to use the sizing graphs that Kavanaugh and Rafferty developed, a designer would need to ensure that the minimum flow rate remains turbulent within the tubing. With many systems having the potential to reach temperatures where freezing may occur, Kavanaugh also provides a table for five different water-antifreeze solutions that gives the minimum flow rate in

order to reach a Reynolds number of greater than 3000. This table has been recreated and is shown in Table 1-3 below.

Table 1-3. Minimum Required Flow Rate (GPM) for Nonlaminar Flow (Modified from Kavanaugh and Rafferty 1997)

Fluid (% by weight)	T = 30°F				T = 50°F			
	Nominal Diameter SDR-11 Pipe				Nominal Diameter SDR-11 Pipe			
	3/4 in.	1 in.	1 1/4 in.	1 1/2 in.	3/4 in.	1 in.	1 1/4 in.	1 1/2 in.
20% Ethanol	3.8	4.8	6.0	6.9	2.6	3.2	4.0	4.6
20% Ethylene Glycol	2.5	3.1	3.9	4.5	1.8	2.2	2.8	3.1
20% Methanol	2.9	3.6	4.5	5.2	2.0	2.5	3.1	3.5
20% Propylene Glycol	3.4	4.2	5.4	6.1	2.3	2.8	3.6	4.1
Water	-	-	-	-	1.1	1.4	1.7	2.0

After describing the design procedure, Kavanaugh and Rafferty give some sample calculations for heat transfer through the headers that are buried in the ground followed by installation guidelines. They give a five step process for installing a closed-loop surface water coil and header assembly.

For determining the minimum reservoir size, Kavanaugh and Rafferty recommend that the design engineer perform a detailed energy balance on the body of water using the peak loads as well as the seasonal energy. Included in this energy balance should be all, but not limited to, the terms located in Equation 1-7.

$$\rho c_p V (\Delta T / \Delta t) = Q_{solar} + Q_{evap} + Q_{conv} + Q_{grnd,cond} + Q_{ice,cond} + Q_{inflow} + Q_{outflow} + Q_{leak} + Q_{coil} \quad (1-7)$$

Where: Q_{solar} is the solar radiation incident on the lake (W)

Q_{evap} is the evaporation heat transfer from the lake (W)

Q_{conv} is the convection heat transfer from the surface of the lake (W)

$Q_{grnd,cond}$ is the ground conduction heat transfer to the lake (W)

$Q_{ice,cond}$ is the conduction heat transfer through ice that covers the lake (W)

Q_{inflow} is the heat transfer from infiltrating water to the lake (W)

$Q_{outflow}$ is the heat transfer from exfiltration water leaving the lake (W)

Q_{leak} is the heat transfer from system leakage (W)

Q_{coil} is the heat transfer from the surface water heat exchanger (W)

This analysis recommended by Kavanaugh and Rafferty is however strictly for shallow, unstratified lakes and thus not applicable to the majority of reservoirs where SWHP systems would be implemented. To accurately predict the impact of SWHP systems on a reservoir, additional research is needed and a highly complex computer simulation that performs an energy balance on the entire lake would be required. The program should incorporate weather data, geological formations, the different heat transfer components, and many other transient variables.

1.3.3 Chiasson et al. (2000)

Additional work was done on shallow pond heat exchangers by Chiasson et al. (2000). ³/₄ in HDPE slinky coil heat exchangers were submerged in a 12.2m by 0.9m by 0.6m (40 ft x 3 ft x 2 ft) and 12.2m by 0.9m by 1.1m (40 ft x 3 ft x 3.5 ft) rectangular shallow ponds filled with water in order to reject heat from a circulating fluid. The coils were oriented both vertically and horizontally in the shallow ponds. The cumulative heat rejection over a 25 day period was calculated and compared to a simulation model developed for the project. The simulation model used a heat balance on the shallow pond to predict the water temperature while a heat exchanger model was used to determine the fluid temperature for the slinky coil. Inside convection was assumed to follow the Dittus-Boelter equation which is discussed in further details later. The outside convection was assumed to be natural convection from a straight pipe according to Churchill and Chu (1975). Difference between the measured and simulated heat rejection differed by a maximum of 5.20%.

1.4 Literature Review – Inside Pipe Forced Convection

With each of the different SWHE designs come different geometries and thus different thermal and fluid calculations must be made for each specific coil. This thesis is focused on

exterior convection heat transfer. In order to measure the exterior convective heat transfer it is necessary to use a heat exchanger analysis which includes an overall thermal resistance of the SWHE, the inside convective resistance, the material conductive resistance, and the outside convection resistance. Methods for determining the conductive resistance are through a hollow cylinder are well known and thus do not require a literature review. The areas of high importance are the inside and outside convection and thus more thorough investigations were conducted on them.

Forced convection on the inside of a pipe is not an unknown phenomenon. Numerous studies have been conducted on different piping shapes, sizes, orientations, and flow rates. Depending on the velocity of the fluid and the pipe size, three different flow regimes can occur; namely laminar, transitional, and turbulent. Laminar flow occurs when the Reynolds number is below the critical value of 2300. Transitional flow occurs between the Reynolds numbers of 2300-4000. Turbulent flow takes place at Reynolds numbers above 4000. The heat transfer from the fluid is maximized under turbulent flow conditions. All experiments conducted were under turbulent flow and thus use turbulent flow correlations.

1.4.1 Straight Pipe

The simplest geometry for inside pipe convection is that of a straight pipe. Numerous studies were conducted on liquids through straight pipes and correlations were developed by Dittus-Boelter (Sleicher and Rouse 1975), Sieder-Tate (Sieder and Tate 1936), and Petukhov (Petukhov 1970). The three correlation equations are given below in respective order.

$$Nu_{b,d_i} = 0.023 * Re_{b,d_i}^{0.8} * Pr_b^n \quad \text{(Dittus-Boelter)} \quad (1-8)$$

Where $Re_{b,d_i} = \frac{\rho_b \bar{v} d_i}{\mu_b}$

$$Pr_b = \frac{c_{p_b} \mu_b}{k_b}$$

$$n = 0.3 \text{ for fluid cooling, } 0.4 \text{ for fluid heating}$$

$$Nu_{b,d_i} = 0.023 * Re_{b,d_i}^{0.8} * Pr_b^n (\mu_b / \mu_w)^{0.14} \quad (\text{Sieder-Tate}) \quad (1-9)$$

Where $n = 0.3$ for fluid cooling, 0.4 for fluid heating

$$Nu_{b,d_i} = \left(\frac{Re_{b,d_i} Pr_b (f/8)}{1.07 + 12.7 (Pr_b^{2/3} - 1) \sqrt{f/8}} \right) (\mu_b / \mu_w)^n \quad (\text{Petukhov}) \quad (1-10)$$

Where $f = (1.82 \log Re_{b,d_i} - 1.64)^{-2}$

$n = 0.11$ for fluid heating, 0.25 for fluid cooling

For $0.5 < Pr_b < 2000$ and $1 \times 10^4 < Re_{b,d_i} < 5 \times 10^6$

1.4.2 Curved Pipe

This simple geometry of a straight pipe is not a good fit however for the inside convection correlation because it does not include the increased heat transfer due to centrifugal forces on fluid flowing through curved pipes. Seban & McLaughlin (1963), Rogers & Mayhew (1964), and many others noticed the secondary flow that was introduced when the pipe went from being straight to curved and thus increased the inside convection heat transfer. To account for this augmentation the ratio of tube diameter (d_i) to coil diameter (D_c) was included in the correlations of both Seban & McLaughlin (1963) and Rogers & Mayhew (1964). Rogers & Mayhew (1964) is commonly used and was selected for use here because of its convenient forms. Equation 1-11 shows the Rogers & Mayhew correlation when using properties calculated at the inside film temperature while Equation 1-12 when using the properties calculated at the bulk fluid temperature.

$$Nu_{b,d_i} = 0.021 (Re_{b,d_i})^{0.85} (Pr_b)^{0.4} \left(\frac{d_i}{D_c} \right)^{0.1} \quad (1-11)$$

$$Nu_{f,i,d_i} = 0.023 (Re_{f,i,d_i})^{0.85} (Pr_{f,i})^{0.4} \left(\frac{d_i}{D_c} \right)^{0.1} \quad (1-12)$$

1.4.3 Helical Pipe

The final improvement to the inside convection comes on the experimental correlation obtained using single-helix coils by Salimpour (2009). Salimpour's correlation (Equation 1-13) includes the effects of fluid flow, fluid type, pipe curvature, as well as the pitch change through the coil.

$$Nu_{f,i,d_i} = 0.152 De_{f,i,d_i}^{0.431} Pr_{f,i}^{1.06} \gamma^{-0.277} \quad (1-13)$$

Where De_{f,i,d_i} = Dean number $\left(De_{f,i,d_i} = Re_{f,i,d_i} \sqrt{\frac{d_i}{D_c}} \right)$

γ = dimensionless pitch ratio $\left(\gamma = \frac{\Delta y}{\pi D_c} \right)$

1.5 Literature Review – Outside Natural/Free Convection

The other convection term that needs to be taken into consideration is the outside convection which will be natural convection rather than forced convection. Water has a unique property, a maximum density point at 4°C (39.2°F) just above the freezing point. Because of that, when water above 4°C (39.2°F) is heated, its density decreases and thus has the tendency to rise. The rising, warmer fluid is replaced by incoming cooling fluid, which in turn is heated and a convection flow is generated. When water below 4°C (39.2°F) is cooled, it also becomes more buoyant. Natural convection is often correlated to Rayleigh number (Equation 1-14).

$$Ra_L = \frac{g \beta_{f,o} (T_{s,o} - T_{\infty}) L^3}{\nu_{f,o} \alpha_{f,o}} \quad (1-14)$$

Where: g is the acceleration constant due to gravity (m/s^2)

$\beta_{f,o}$ is the thermal expansion coefficient calculated at the outside film temperature (1/K)

$T_{s,o}$ is the outside surface temperature (°C)

T_{∞} is the reference temperature (°C)

L is the characteristic length (m)

$\nu_{f,o}$ is the kinematic viscosity calculated at the outside film temperature (m²/s)

$\alpha_{f,o}$ is the thermal diffusivity calculated at the outside film temperature (m²/s)

1.5.1 Straight Pipe

Churchill & Chu (1975) and Morgan (1975) both developed separate natural convection correlations for horizontal cylinders with different forms at roughly the same time. The Churchill & Chu correlation, shown in Equation 1-15, includes both the Prandtl number as well as the Rayleigh number.

$$Nu_{f,o,d_o} = \left[0.6 + \left(\frac{0.387 Ra_{d_o}^{1/6}}{\left[1 + \left(\frac{0.559}{Pr_{f,o}} \right)^{9/16} \right]^{8/27}} \right) \right]^2 \quad (1-15)$$

Also stated in the Churchill & Chu work is the use of a modified Rayleigh number (Ra_L^*) when correlating natural convective heat transfer. Under uniform heating conditions the modified Rayleigh number is selected to prevent the use of the outside surface temperature. Churchill & Chu do caution the use of the modified Rayleigh number though because it masks the fact that the Nusselt-Rayleigh dependence is the same for uniform heating and uniform wall temperature. Equation 1-16 is how the modified Rayleigh number is calculated using the coil heat flux instead of a temperature difference.

$$Ra_L^* = \frac{g \beta_{f,o} q_c L^4 Pr_{f,o}}{k_{f,o} \nu_{f,o}^2} \quad (1-16)$$

The Morgan correlation, shown in Equation 1-17, has a simple form only involving the Rayleigh number.

$$Nu_{f,o,d_o} = 0.48 Ra_{d_o}^{1/4} \quad (1-17)$$

These two correlations are useful for comparison purposes; however, use for helical-spiral coils is not recommended because these correlations do not account for tube-to-tube heat transfer interferences. Note that all properties are calculated at the outside film temperature.

1.5.2 Helical Pipe

Natural convection for helical coils was investigated by Prabhanjan et al. (2004) when they experimentally tested four helical coils in a constant temperature bath of water. Their experimental setup can be viewed in Figure 1-9.

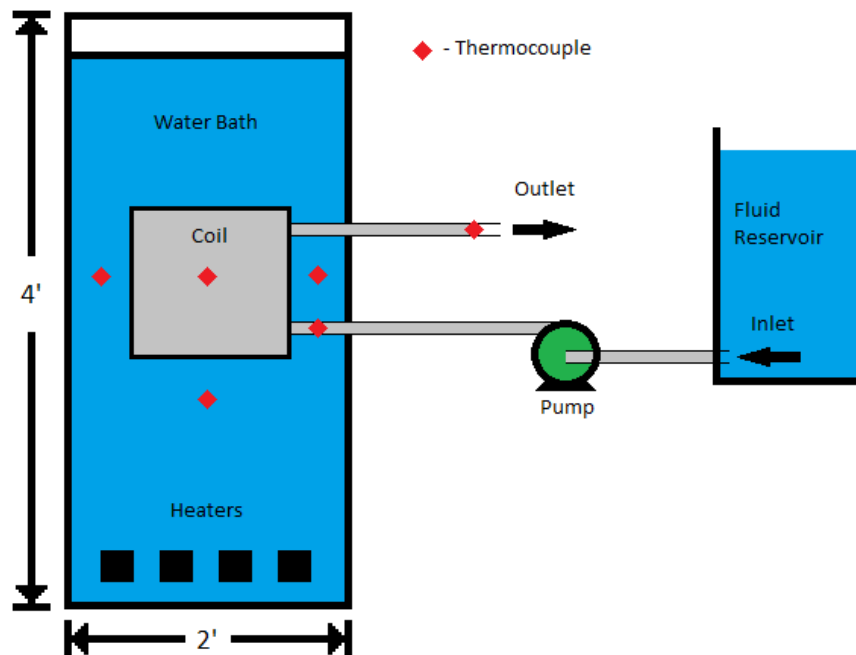


Figure 1-9. Prabhanjan et al. (2004) Experimental Setup

There are a few differences between this experimental setup and a typical lake heat exchanger. To start, Prabhanjan et al. used coils made of copper in a single helix configuration and not SDR-11 HDPE arranged in a spiral-helical design. Additional differences in the geometries are also present. The tube diameters and coil diameters are both quite smaller than typical HDPE lake heat exchangers. The two pipe diameters used were 12.7 mm (0.5 in) and 15.9 mm (0.625 in) and the two coil diameters were 30.5 cm (12 in) and 20.3 cm (8 in). Between the four different coils they ran, the pitch was varied from 12.7 mm (0.5 in) to 47.5 mm (1.87 in).

ASTM standards have HDPE piping with outside pipe diameters of 26.7 mm (1.050 in), 33.4 mm (1.315 in), and 42.2 mm (1.660 in). Common coil diameter and pitch dimensions for SWHE range are around 1 m (3 ft) to 3 m (9 ft) and 38.1 mm (1.5 in) and up respectively. Their correlation also differed from customary natural convection correlations in that they used the coil height as the characteristic length instead of the outside pipe diameter

From the data Prabhanjan et al. collected in their 24 tests (4 coils, 3 flow rates, and 2 water bath temperatures) they formulated Nusselt-Rayleigh correlations for three different characteristic lengths as shown in Table 1-4. The improvement that their correlations make on single tube natural convection correlations is that now the vertical tube-to-tube heat transfer interference is included and since the experimental testing was done on a single-helix helical coil, pipe curvature was indirectly taken into account in the coefficients. Once again this correlation is an improvement but the horizontal tube-to-tube interference that may be present in spiral-helical coils is not included. Also there is the issue that the coil and pipe diameters have been excluded from the correlation.

Table 1-4. Prabhanjan et al. (2004) Nusselt - Rayleigh Number Correlations Results ($Nu_{f,o,L}=a(Ra_L)^b$)

Characteristic Length	a	b	Rayleigh Range	Correlations Coefficient
Tube Length	0.00976	0.397	$5 \times 10^{14} - 3 \times 10^{15}$	0.8684
Coil Height	0.0749	0.342	$9 \times 10^9 - 4 \times 10^{11}$	0.9306
Normalized Length	2.0487	0.177	$2 \times 10^6 - 3 \times 10^9$	0.9341

Ali (2006) also conducted experiments on 15 vertical helical coils, using both water and heat transfer oil. He varied the configurations by different coil diameter-to-tube diameter ratios and number of turns. The helix coil diameter-to-tube diameter ratios were 30, 20.83, 17.5, 13.33, and 10 while each of the ratios were tested for a number of turns at 2, 5, and 10. Ali concluded that for the coils with the number of turns equal to 2 or 10 that the exterior flow was laminar because the average heat transfer coefficient decreased as the diameter ratio increased. Also included with the previous conclusion was that the average heat transfer coefficient for the coils

with two turns were higher than the coils with 10 turns. For the coils that contained five turns, Ali decided to classify the mode of exterior heat transfer as a transition regime because the average heat transfer was highly unstable as the diameter ratio increased. His final conclusion was that the average heat transfer coefficient decreased as the number of coil turns increased for a constant coil diameter-to-tube diameter ratio.

In Ali's analysis of the data he used the heat exchanger method in order to find the four thermal resistances of the system; inside convective resistance, outside convective resistance, material conductive resistance, and the total thermal resistance. To find the overall thermal resistance (R'_c) he used the log mean temperature difference ($LMTD$) and divided it by the heat transfer rate (Q_c) as shown by Equation 1-18.

$$R'_c = \frac{LMTD}{Q_c} = \frac{\left(\frac{T_{in} - T_{out}}{\ln \left(\frac{T_{in} - T_{\infty}}{T_{out} - T_{\infty}} \right)} \right)}{Q_c} \quad (1-18)$$

The correlation by Rogers and Mayhew (1964) was used to find the inside Nusselt number (Equation 1-19).

$$Nu_{f,i,d_i} = 0.023 Re_{f,i,d_i}^{0.85} Pr_{f,i}^{0.4} \left(\frac{d_i}{D_c} \right)^{0.1} \quad (1-19)$$

The inside convection coefficient was determined using the definition of the Nusselt number that is shown in Equation 1-20.

$$h_i = \frac{Nu_{f,i,d_i} k_f}{d_i} \quad (1-20)$$

From there the outside convection coefficient was backed out from Equation 1-21.

$$h_o = A_o \left[R'_c - \left(\frac{1}{h_i A_i} + \frac{\ln \left(\frac{d_o}{d_i} \right)}{2\pi k_c L_c} \right) \right] \quad (1-21)$$

Ali formulated three equations from his experimental data for outside convection coefficients. The first one (Equation 1-22) was for strictly oil with $250 \leq Pr \leq 400$, $4.37 \times 10^{10} \leq Ra_L \leq 5.5 \times 10^{14}$, and $10 \leq D_e/d_o \leq 30$.

$$Nu_L = 0.619 Ra_L^{0.3} \quad (1-22)$$

The second (Equation 1-23) was for the differentiation between natural heat transfer in oil and water. The limitations on the equation are $1 \times 10^8 \leq Gr_L \leq 5 \times 10^{14}$ and $4.4 \leq Pr \leq 345$.

$$Nu_L = 0.555 Gr_L^{0.301} Pr^{0.314} \quad (1-23)$$

The third correlation that Ali provided combined the oil and water data into a single equation (Equation 1-24) where $4.35 \times 10^{10} \leq Ra_L \leq 8 \times 10^{14}$.

$$Nu_L = 0.714 Ra_L^{0.294} \quad (1-24)$$

For all of the correlations obtained by Ali, L is not the generic variable for characteristic length but instead it is the length of the coil.

1.6 Objectives and Organization

From the onset of this research project there were several tasks that were to be investigated in detail. Within this thesis, four main points of emphasis or objectives are discussed in detail. They are listed as follows:

- 1) Provide experimentally-validated guidance for designers of SWHPs
- 2) Develop correlations for exterior convective heat transfer that can be used in design and simulation.
- 3) Develop an experimental facility, instrumentation, and an analysis procedure to support the first two objectives.

- 4) Since the physical scaling of the natural convection heat transfer for these complex geometries is not well understood it is desirable to perform the experiments in full-scale with typical heat transfer rates.

In order to complete the objectives, a significant amount of testing was conducted on a self-fabricated apparatus. To better explain how everything was constructed, recorded, and analyzed, the remainder of this thesis is organized as follows:

- 2) Experimental Apparatus

A detailed explanation of the equipment used in testing the different surface water heat exchangers is given. The various SWHE construction procedures are provided with all of the pertinent dimensions specified. Temperature sensor types and locations are also provided. Data acquisition, system purging, and coil deployment procedures are discussed as well.

- 3) Calibration of Measurement Devices

All of the measurement devices are described in regards to their accuracy from the manufacturer. The procedure to calibrate all of the thermistors and the flow meter are discussed in detail. The calibration curve for the flow meter is also presented.

- 4) Analysis Methodology

The process of which the collected data is analyzed is presented based on the literature review performed. The heat exchanger method is described in full detail and the exterior convection coefficient is obtained. The uncertainty analysis method according to Holman and Gajda (1984) was implemented on the heat exchanger method to show how accurate the measurements are. Included in the uncertainty analysis are both the sensor and special uncertainties. Finally, the overall uncertainty procedure for the heat transfer rate, exterior convection coefficient, and Nusselt numbers are obtained.

- 5) Results and Discussion

Experimental results for the 19 mm ($\frac{3}{4}$ in) spiral-helical, 25 mm (1 in) spiral-helical, and 32 mm (1- $\frac{1}{4}$ in) spiral-helical, flat-spiral, slinky, and vertical flat-plate SWHEs are presented. Numerous correlation forms are presented and compared with the experimental exterior convection coefficients for the spiral-helical coils. The optimal correlation is then selected and applied to a heat exchanger model where experimental values of heat transfer are compared with predicted values for a SWHE simulation model.

6) Applications

Design tools similar to the design graphs presented in Kavanaugh and Rafferty (1997) are discussed in more detail with respect to the influence of lake temperatures and heat pump efficiencies. Updated SWHE sizing design graphs are presented and discussed. Design improvements such as thinner walled tubing and metal tubing are discussed and represented in sizing design graphs. Finally a simple first cost analysis of the different types of SWHEs is presented.

7) Conclusions and Recommendations

Final thoughts, equations, and findings are reiterated for the different types of SWHEs. Recommendations for further testing and analysis are also provided.

CHAPTER II

2. EXPERIMENTAL APPARATUS

2.1 In-Situ Trailer (Austin 1998)

In a previous research project at OSU, *Development of an In-Situ System for Measurement for Ground Thermal Properties*, Austin (1998) designed and constructed a trailer for the mobile measurement of ground thermal properties for ground source heat pump (GSHP) systems. All of the components were located inside of a 3 m (10 ft) long by 1.8 m (6 ft) wide by 1.7 m (5.5 ft) tall enclosed trailer. Since the testing locations had neither electricity nor water hookups, the In-Situ trailer was originally designed to be independent of utilities and thus housed its own water storage tank and came with generators to supply power for the electrical equipment.

The trailer was modified by Austin to allow for the installation of fiberglass insulation behind an interior plywood wall. Both 120V and 240V electrical supply wires were run through conduit behind the plywood for the equipment that was to be mounted on the walls. Two Grundfos UP26-99F circulating pumps, one Omega flow meter, three threaded ports with screw in electric water heaters (heat input), a watt transducer, purging water tank and pumps, piping, filter, and valves were then installed inside of the trailer.

Also located inside of the trailer was the data acquisition system. For this project, two Fluke Hydra data loggers were used to record all of the temperatures, flow rate, and watt transducer readings. All of the mechanical components, except the water storage tank, can be seen in Figure 2-1.

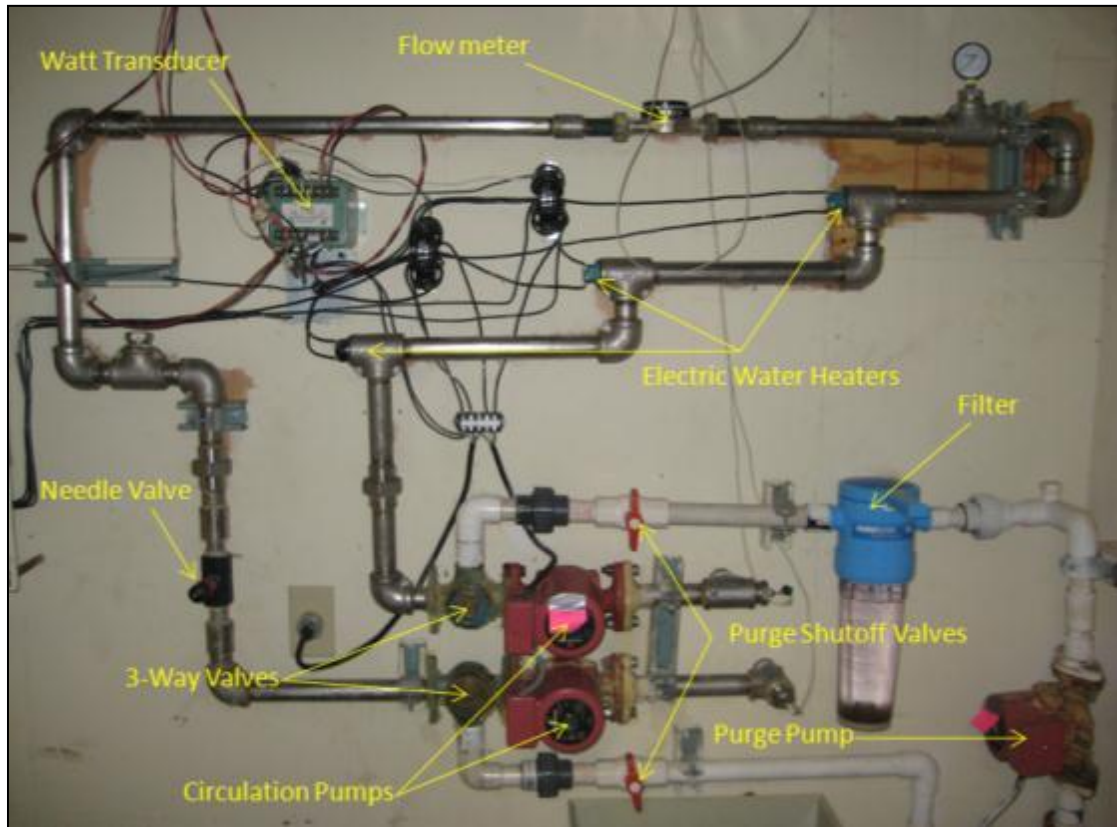


Figure 2-1. In-Situ Trailer Setup

On the exterior of the trailer there are two access doors; one small door on the side and one large swinging door in the rear. On the exterior of the same wall as the mechanical equipment, two ports where HDPE leads can be connected to the trailer piping system are located. This allows for quick and easy coil changing from test to test. In the front of the trailer are two 240V-30A female electrical outlets. The two female outlets were not connected to the generators as in Austin's work but instead they were connected to outlets in a nearby building via two long extension cords. On the top of the trailer is the air conditioning unit allowing for the climate control inside of the trailer during hot summer months. However, all the power available

was dedicated to the water heating, so the AC was not available. Figure 2-2 shows the exterior of the In-Situ trailer.



Figure 2-2. Outside of the In-Situ Trailer

2.2 In-Situ Trailer Modifications

The In-Situ trailer was the perfect type of system for use on this project because of the mobility and availability. Only some slight modifications had to be made to the trailer in order to bring it back up to running condition. Cleaning out the inside of the trailer and plumbing was a must due to its lack of use over the previous years. Required mechanical changes were:

- One circulation pump replaced
- Needle valve removed to increase flow rate
- Larger water heater elements installed
- Insulation of the piping inside the trailer, as seen in Figure 2-3
- In-pipe thermistors added at the coil inlet and coil outlet

- Lake temperature measurement trees with seven thermistors installed in the lake



Figure 2-3. In-Situ Trailer Pipe Insulated

With the mechanical system in place, initial shakedown testing was performed. To test the apparatus, an above ground swimming pool was set up inside of the Electronics Research Laboratory on the northwest side of the OSU campus. This pool was used as a mock “lake”. The pool is 4.6 m (15 ft) in diameter and roughly 1.2 m (4 ft) in depth. The volume of the pool is about 20 m³ (707 ft³). Figure 2-4 shows the pool inside of the laboratory filled up with water ready for testing.



Figure 2-4. Indoor SWHE Testing Pool

Inside the laboratory space, the In-Situ trailer was parked next to the pool so that the leads connecting the trailer to the testing coil needed to only be around 3 m (10 ft) – 4.6 m (15 ft) long. Located inside of the pool was a PVC temperature tree that had three thermocouples taped to the vertical shaft at three different heights. The three heights were the top, middle, and bottom of the coil when it was submerged in the pool. The coil itself was placed on 102 mm (4 in) thick rigid foam insulating blocks to keep it off of the floor and then weighed down with a heavy metal bar to prevent it from floating.

The method for changing out coils was a highly time consuming process. In order to get the coil out of the pool, the pool itself had to be completely drained and the metal bar removed. This would take anywhere from two to three hours depending on if the pool was allowed to drain via gravity and the drain plug or if an auxiliary pump was used to empty it. Submerging the coil took even longer as the only means of filling the pool was a water tap and a garden hose. Later on, methods for deploying coils in a more efficient manner were implemented.

2.3 Heat Exchanger Construction

One of the driving factors for the different outside convection coefficients between heat exchangers is the geometry. Studies done on tube banks and other heat exchangers show that increasing the density of tubes packed into a confined area reduces the total amount of heat transfer capacity. In order to compare results between heat exchangers, maintaining the coil geometry and spacing dimensions is important. To achieve this, different devices such as a metal suspension frame, coil winding apparatus, slinky assembly guide rails, and different spacers were designed, fabricated, and utilized.

The different types of coils that are constructed include the bundled, spiral-helical, flat-spiral, and slinky heat exchangers. There are three different types of bundled coils. The first one that would be tested would be the factory banded coil that came directly from the manufacturer. The second coil would be the factory banded coil except the bands would be cut and the coil would be allowed to freely expand out to a set minor circumference (+50% from factory banded). The third bundled coil would be the same as the second except the minor circumference allowance would be increased to +75% from the factory banded value.

There were nine test configurations of the spiral-helical type coils arranged in a “testing matrix”. The testing matrix is shown in Table 2-1. The asterisk next to the first column and row dimension is due to the fact that the 32 mm (1- ¼ in) tube could only be reduced down to a dimension of 48.5 mm (1.91 in). Test configurations 1, 5, and 9 from here on will be referred to as the “small”, “medium”, and “large” spaced configurations. Likewise, these numbering assignments apply to the different tube sizes. To control the spacing for the spiral-helical coils, PVC spacers were constructed and attached to the metal frame.

Table 2-1. Spiral-Helical Coil Configuration Numbering

SDR-11 HDPE Spiral-Helical Pond HX				
		Horizontal Spacing		
		38.1 mm (1.5 in)*	66.7 mm (2.625 in)	104.8 mm (4.125 in)
Vertical Spacing	38.1 mm (1.5 in)*	1	2	3
	66.7 mm (2.625 in)	4	5	6
	104.8 mm (4.125 in)	7	8	9

The flat-spiral coil was constructed directly on the metal frame with the vertical support rails removed. Spoke extensions were added to accommodate for the approximately 3.7 m (12 ft) wide outside diameter. The inside diameter was set at 0.9 m (3 ft) and the distance between each loop was set to a value of roughly twice the pipe diameter, 51 mm (2 in). In total, there were 18 concentric loops in the flat-spiral coil. Figure 2-5 shows the flat-spiral coil waiting to be submerged in the test lake.



Figure 2-5. Flat-spiral Coil Prior to Submerging

2.3.1 Frame Construction

The steel suspension frame serves as a means to hold the coil in the upright and stable position when the coil is submerged in the water. From testing in the pool it was obvious that we needed something to hold the spacers in place otherwise they would warp and the spacing would shift to an unknown quantity (see Figure 2-6).



Figure 2-6. Warped Spiral-Helical Coil in Pool without Metal Frame

To prevent the warping from happening, a steel frame was fabricated from 25 mm by 25 mm by 2 mm (1 in x 1 in x 14 gauge) square tubing. The shape of the frame was that of a hexagon and the long diagonals were 2.4 m (8 ft) long. Attached on the six spokes were 12 upright supports (2 on each spoke) which were to prevent the coil from warping shape. All together the metal frame weighed about 31 kg (68 lbs). This additional weight was to the coil was sufficient enough to force the coil to sink to the bottom when it was filled with water as later described in the coil buoyancy analysis. The frame also served as a connection point for the buoys in order to suspend the coil off of the lake bottom. Figure 2-7 shows the frame with supports attached to the spokes.



Figure 2-7. Coil Base Frame with Supports

There were also adaptor pieces that were fabricated for the coil base frame which were for the flat-spiral coil. These adaptors were 0.6 m (2 ft) extensions because the outside diameter of the flat-spiral coil was approximately 3.7 m (12 ft). A schematic of the adaptors can be seen in Figure 2-8. They are held in place via U-bolts that clamp the adaptors to the spokes of the base frame.

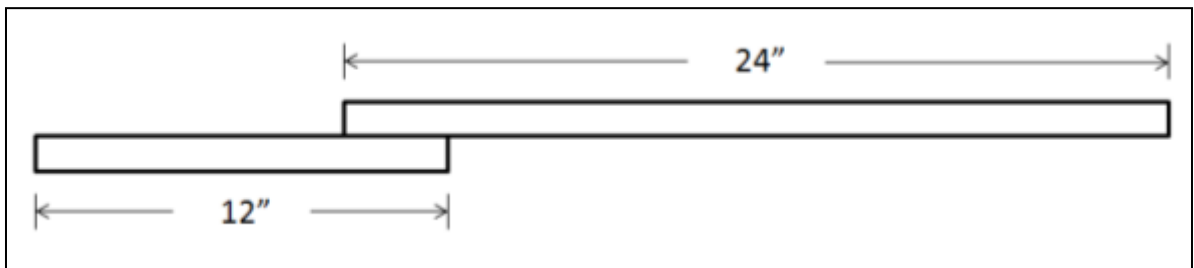


Figure 2-8. Flat-spiral Coil Adaptor

2.3.2 Bundle Coil Construction

As stated earlier, the bundle tests consisted of the three variations from the factory bundle. The way these were constructed were to simply test the factory bundle as it came and then to space out the factory bundle to the desired minor circumference. For the +50% spaced bundle, large industrial zip ties were placed around the minor circumference at the increased value. After this was completed, the factory bands were cut and sections of PVC or HDPE piping were wedged between the tubes in a semi-random manner until the zip ties were fairly tight. For the +75% spaced bundle the zip ties were adjusted to the larger value and more PVC or HDPE piping sections were added until the zip ties were taut. A summary of the geometries for all of the bundle coils can be found in Table 2-2. The minor circumference is the distance around the cross sectional area of the coil pipes as shown in Figure 2-9.

Table 2-2. Bundle Testing Coil Geometries

Test Date	Description	Test Location	Vertical Spacing		Horizontal Spacing		Tube ID		Tube OD		Coil Height		Minor Circumference		Coil ID		Coil OD		Tube Length	
			mm	in	mm	in	mm	in	mm	in	cm	in	cm	in	m	ft	m	ft	m	ft
1/15/2010	Loose Bundle Pool Test (3/4")	Pool	55.9	2.2	30.5	1.2	21.8	0.86	26.7	1.05	25	10	79	31	1.4	4.5	1.9	6.3	152.4	500
1/19/2010	Loose Spaced Bundle Pool Test (3/4")	Pool	86.4	3.4	30.5	1.2	21.8	0.86	26.7	1.05	38	15	118	47	1.4	4.5	1.9	6.3	152.4	500
4/28/2011	Factory Banded Spiral-Helical Coil (3/4")	Pond	27.9	1.1	27.9	1.1	21.8	0.86	26.7	1.05	28	11	86	34	0.6	1.9	1.1	3.5	152.4	500
5/20/2011	+50% Loose Spiral-Helical Coil (3/4")	Pond	30.5	1.2	30.5	1.2	21.8	0.86	26.7	1.05	41	16	130	51	0.6	1.9	1.1	3.5	152.4	500
5/27/2011	+75% Loose Spiral-Helical Coil (3/4")	Pond	38.1	1.5	33.0	1.3	21.8	0.86	26.7	1.05	51	20	151	60	0.6	1.9	1.1	3.5	152.4	500
5/3/2011	Factory Banded Spiral-Helical Coil (1")	Pond	33.4	1.3	33.4	1.3	27.3	1.08	33.4	1.32	23	9	91	36	0.8	2.6	1.2	4.1	152.4	500
5/31/2011	50% Loose Spiral-Helical Coil (1")	Pond	44.3	1.7	33.4	1.3	27.3	1.08	33.4	1.32	43	17	132	52	0.8	2.6	1.2	4.1	152.4	500
6/3/2011	75% Loose Spiral-Helical Coil (1")	Pond	55.1	2.2	33.4	1.3	27.3	1.08	33.4	1.32	58	23	152	60	0.8	2.6	1.2	4.1	152.4	500
5/10/2011	Factory Banded Spiral-Helical Coil (1.25")	Pond	42.2	1.7	42.2	1.7	34.5	1.36	42.2	1.66	20	8	97	38	1.2	4.0	1.8	6.0	152.4	500
6/7/2011	50% Loose Spiral-Helical Coil (1.25")	Pond	72.0	2.8	62.7	2.5	34.5	1.36	42.2	1.66	33	13	140	55	1.2	4.0	1.8	6.0	152.4	500
6/9/2011	75% Loose Spiral-Helical Coil (1.25")	Pond	70.2	2.8	47.4	1.9	34.5	1.36	42.2	1.66	53	21	163	64	1.2	4.0	1.8	6.0	152.4	500

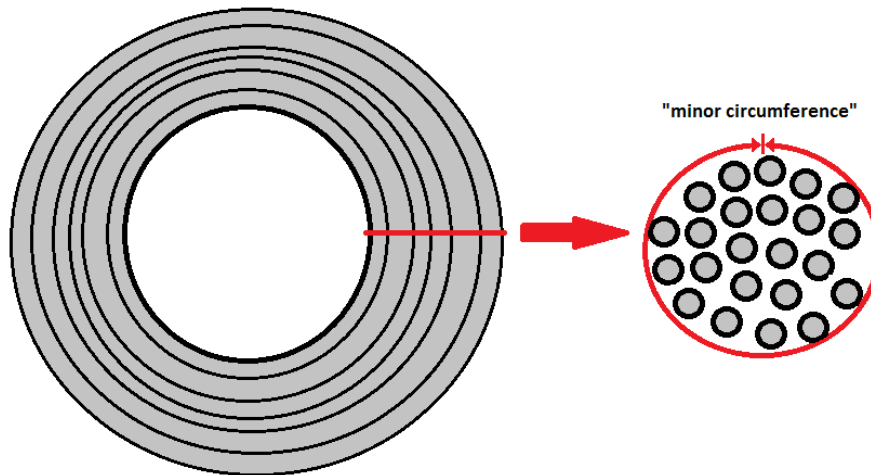


Figure 2-9. Loose Bundle Piping Circumference

Testing in the pool required the placement of a large cast iron pipe to prevent the coil from floating to the surface. Figure 2-10 shows the submerged loosely bundled coil at the bottom of the pool ready for testing. Figure 2-11 shows the loose spaced coil prior to submersion with the HDPE spacers inserted in it. Testing in the lake did not have the metal bar but instead had the metal frame to weigh it down as told previously in the frame construction section.

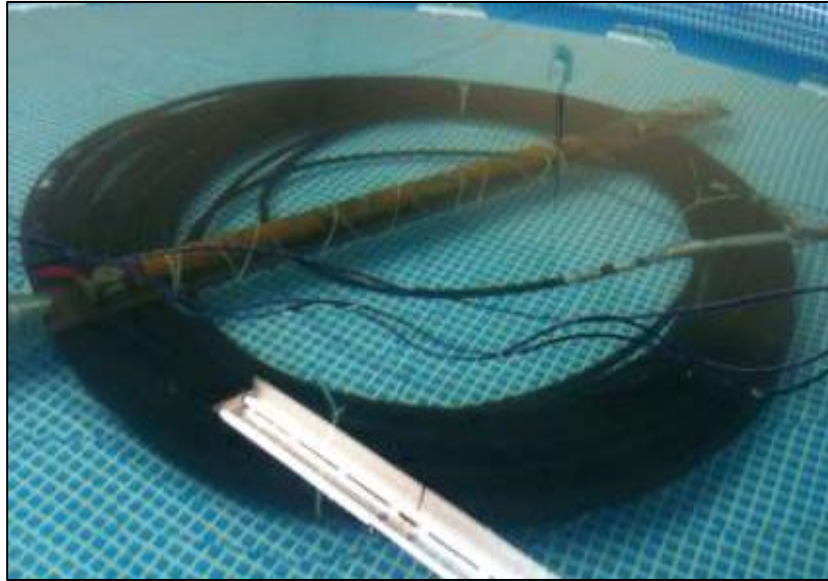


Figure 2-10. Submerged Loose Bundled Coil



Figure 2-11. Loose-Spaced Bundled Coil

2.3.3 Spiral-Helical Coil Spacing Grid

The next step for testing coils was to develop a method for spacing out the coils in a uniform manner. To do this, PVC fitting spacers were determined to be the easiest to implement while also allowing for flexibility. The components on each spacer manifold included 19 mm ($\frac{3}{4}$ in) PVC pipe, five tees, and two elbows. These were arranged such that the end of one tee or elbow would butt-up flush with the next tee or elbow. This gives a center to center (CC) spacing distance of 66.7 mm (2.625 in). Figure 2-12 is a picture of two manifolds joined together by 19 mm ($\frac{3}{4}$ in) PVC pipe to form one spacer frame. By combining two spacer frames (one horizontally and one vertically), a grid pattern is formed, as shown in Figure 2-13.



Figure 2-12. Single Spacer Frame



Figure 2-13. Assembled Spacing Grid

2.3.4 Spiral-Helical Coil Construction

When a HDPE coil comes from the factory it comes tightly bound with bands. The moment when the bands are cut and the coil is allowed to expand out on its own, problems occur. To prevent kinks and tube tangles from occurring, a method of unwinding and rewinding the coil into the uniform spacing grid was a must. The system that was decided upon was to wrap the coil tubing around a central hub and guide it into the vertical slots of the PVC spacers.

A platform made of wood was designed to allow for easy coil removal upon winding completion as well as flexibility with minimal cost. The base of the platform is 2.4 m by 2.4 m (8 ft x 8 ft). 51 mm by 102 mm (2 in x 4 in) studs line the outer edge of the platform while additional 51 mm by 102 mm (2 in x 4 in) studs are spaced on 41 cm (16 in) centers through the middle. Four sheets of plywood with dimensions of 1.2 m by 2.4 m by 4.8 mm (4 ft x 8 ft x 3/16 in) were then screwed and glued together on the top of the 51 mm by 102 mm (2 in x 4 in) framing to create a flat surface.

Next a six spoke central hub was constructed with 51 mm by 102 mm (2 in x 4 in) and 51 mm by 51 mm (2 in x 2 in) studs. The horizontal boards were all cut to 1.2 m (4 ft) lengths so that the inside diameter of the spiral-helical coils would be 1.2 m (4 ft). 51 mm by 51 mm (2 in x 2 in) studs were then screwed to a vertical 51 mm by 102 mm (2 in x 4 in) stud on each of the six spokes to create channels that the PVC spacers would be able to slide in and out of freely. Radially along the platform surface from each spoke, 51 mm by 51 mm (2 in x 2 in) studs were screwed to the platform to make a channel as well. After the channels were created along the platform surface, an outside retainer was constructed at the edge of the central hub spokes. The retainer could be widened or removed all together for larger width coils. This allowed for the outside major diameter to range from as little as 1.6 m (5.25 ft) for the horizontal spacing of 38.1 mm (1.5 in) center-to-center all the way up to around 2.6 m (8.5 ft) when the horizontal spacing was 105 mm (4.125 in) center-to-center. The completed coil platform-hub assembly can be seen in Figure 2-14.



Figure 2-14. Finished Coil Platform-Hub Assembly

To start the winding process of a spiral-helical coil, a PVC manifold was placed in each channel that runs along the platform surface. Second, seven pieces of PVC pipe were placed into the manifold. Third, the bound up coil from the factory was placed on top of the central hub and the first metal band was cut off. Fourth, the start of the HDPE pipe was secured to the platform to prevent it from unraveling. Fifth, the winding process starts at the inside spacer slot and progresses outward until all six spacer slots are filled. Once all slots are filled, horizontal PVC pipes were placed on top of the HDPE pipe at every spoke. The next wrap around the hub would go through the outside slot again and then any subsequent wraps would proceed inward toward the hub. The numbering diagram for the coil wrapping can be seen in Figure 2-15 starting at 1 and ending at 31.

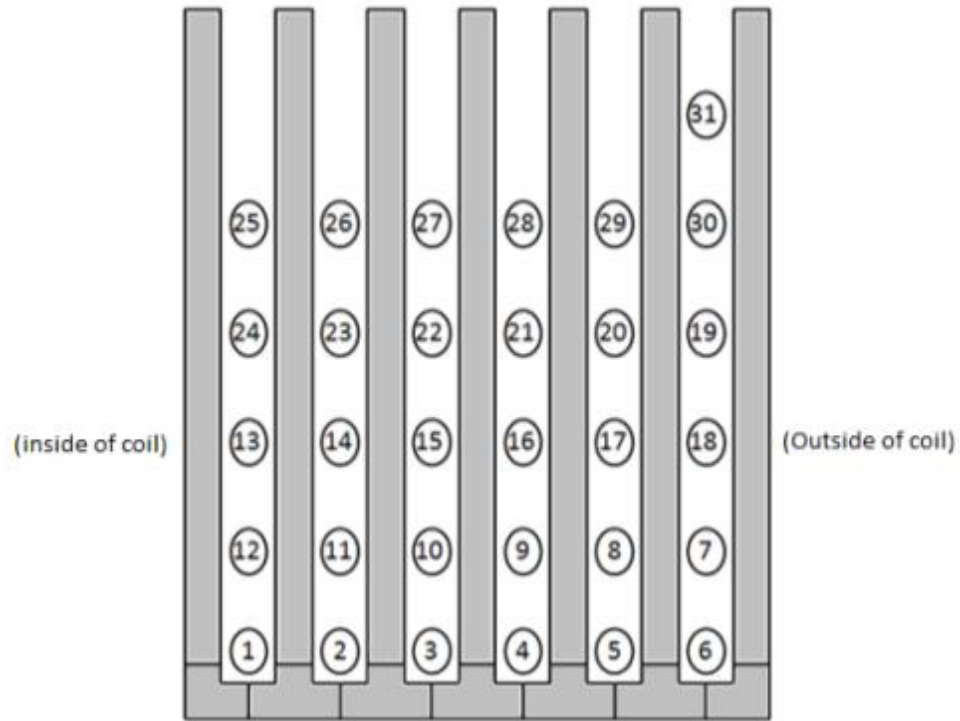


Figure 2-15. Spiral-Helical Coil Wrapping Number Diagram (1 = Start, 31 = End)

Figure 2-16 through Figure 2-20 show the step by step process of wrapping a 105 mm (4.125 in) vertical by 67 mm (2.625 in) horizontal spaced coil from a bound factory product into a uniformly spaced coil. Upon completion of the uniformly spaced coil it would be securely fastened to the metal frame support rails either by zip ties or rope to prevent warping as described earlier.



Figure 2-16. Step 1: Start of Spiral-Helical Coil Wrapping



Figure 2-17. Step 2: Spiral-Helical Coil Wrapping Continued (1)



Figure 2-18. Step 3: Spiral-Helical Coil Wrapping Continued (2)



Figure 2-19. Step 4: Spiral-Helical Coil Wrapping Continued (3)



Figure 2-20. Step 5: Finished Spiral-Helical Coil Wrapping

2.3.5 Flat-Spiral Coil Construction

As mentioned previously, the outside diameter of the flat-spiral coil exceeded that of the 2.4 m (8 ft) base frame so the adaptors had to be attached to extend the frame to 3.7 m (12 ft). With the frame set up for the coil, the inside diameter of the flat-spiral coil was to be 0.9 m (3 ft) in diameter because any smaller would require too much bending of the semi-rigid HDPE and potentially cause permanent deformation in the tube. The next dimension that needed to be set was the spacing between the tubes. This dimension was set at roughly twice the diameter of the HDPE pipe which was 51 mm (2 in). With the dimensions set, the only remaining step was to wrap the coil on to the frame and secure it down. This was done with 51 mm (2 in) PVC spacers, hundreds of 28 cm (11 in) long zip ties, and a lot of patience. The final outside spiral diameter ended up being approximately 3.5 m (11.5 ft). The resulting flat-spiral coil is shown in Figure 2-21. The waviness in the flat-spiral coil is due to shape retention of the coil from the factory and does not deviate above or below the frame by more than 51 mm (2 in).



Figure 2-21. Flat-Spiral Coil

2.3.6 Slinky Coil Construction

In order to construct a slinky coil from the 152.4 m (500 ft) HDPE pipe, a guide rail system and spacers were designed. These were constructed from 51 mm by 102 mm (2 in by 4 in) boards that ran parallel to each other. The guide rail system was built such that the center to center loop diameter was 0.9 m (3 ft) while the guide length was 3 m (10 ft). Figure 2-22 shows the slinky assembly guide rails during a coil construction. The spacer lengths used for setting up the coil were equal to the coil pitch. These were chosen to be 12.7 cm (5 in), 25.4 cm (10 in), and 38.1 cm (15 in). As the coils were being wrapped up, zip ties were used in numerous locations to prevent the coil from unraveling. Figure 2-23 shows a constructed slinky coil using the guide rails and spacers while Figure 2-24 provides the dimensions for all three slinky coil types.



Figure 2-22. Slinky Coil Assembly Guide Rails



Figure 2-23. Constructed Slinky Coil

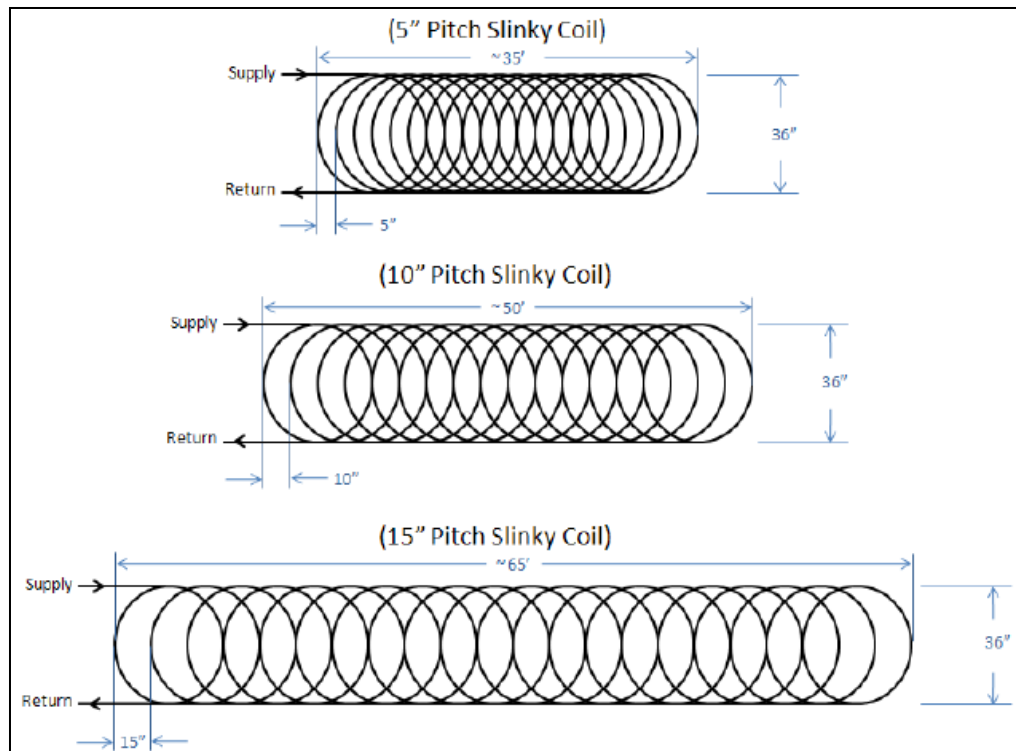


Figure 2-24. Slinky Coil Schematics & Dimensions

2.4 System Deployment

With the mechanical system set up in the trailer and the coils constructed, the next thing to do is to assemble everything together, get the equipment in place, and start the testing process. To do this a few different components needed to be either added to the system or simply connected together. Thermistors were added for temperature measuring for both inside the piping system and the lake temperatures. Instrumentation and calibration will be discussed in chapter 3. Here, we will discuss sensor placement. SDR-11 HDPE connecting lines were run from the trailer to the coil where they were fastened and sealed thoroughly. After an onshore leak check the coil would be loaded up onto the boat and deployed for testing.

2.4.1 Temperature Sensor Attachment

Before temperature data acquisition could begin, the temperature sensors themselves need to be attached in and around the coil to be tested as well as inside the trailer. There are two

different thermistor types used for measuring temperatures. One is a sheathed in-pipe thermistor that screws into a threaded tee pipe fitting. This thermistor was purchased from Omega Engineering Inc. (Part #: ON-410-PP) which was used for the measurement of the fluid temperature inside of the piping system. The second type of thermistor is a small bead thermistor, or lake temperature thermistor, for measuring temperatures outside of the piping system.

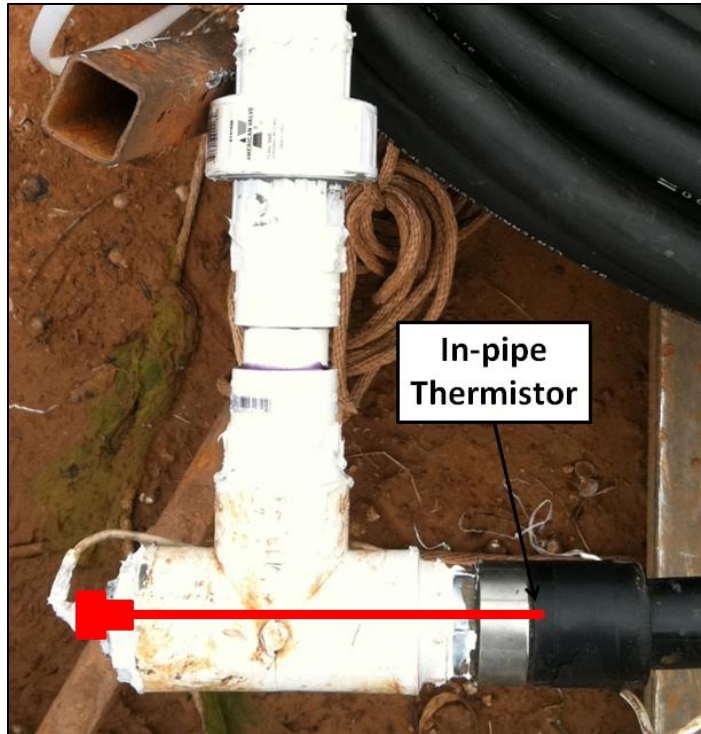


Figure 2-25. In-pipe Thermistor at the Coil Outlet

The in-pipe thermistor probes (Figure 2-26) were used to measure four specific temperatures. The first location was immediately after the three heater elements and second pump for measuring the trailer supply temperature. The second thermistor probe was positioned directly at the start of the test coil to measure the coil inlet temperature. The third one is located at the outlet of the test coil while the fourth temperature probe is located just after the piping enters the trailer again to measure the trailer return temperature. These four temperature probes allow for the determination of heat transfer to and from the coil, through the coil, and also inside of the trailer.

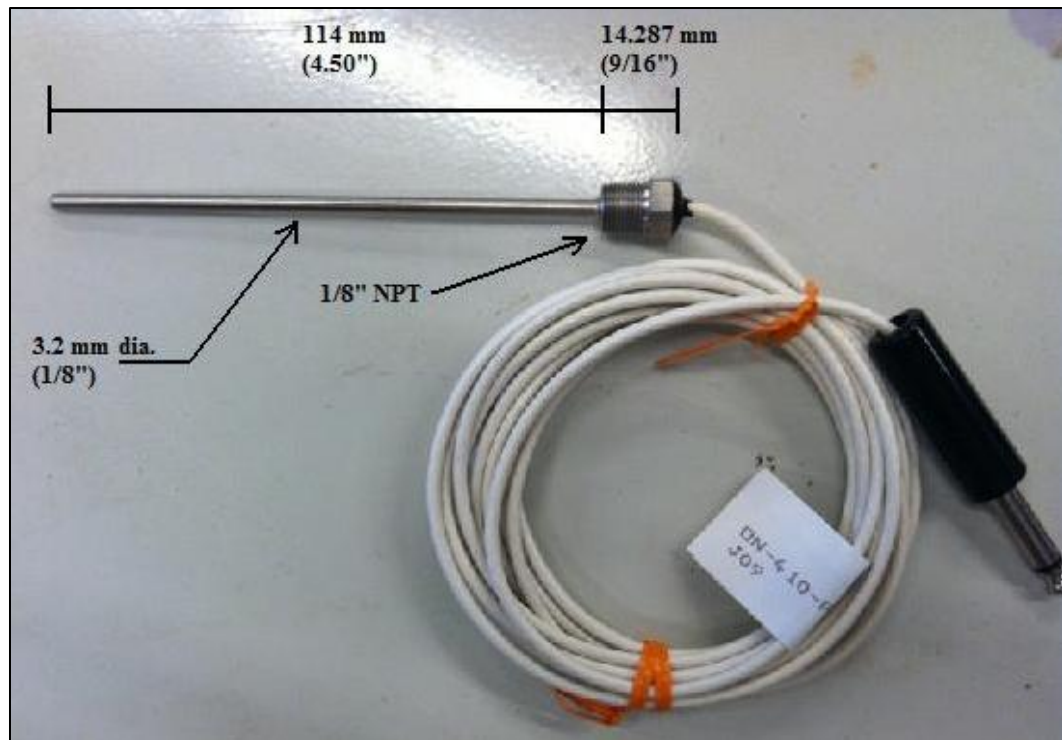


Figure 2-26. In-pipe Thermistor Probe (Part #: ON-410-PP)

The lake temperature thermistors were either a 1000 or 5000 ohm negative temperature coefficient (NTC) thermistors. An NTC thermistor means that as the temperature goes up, the resistance decreases. The process for assembling the lake temperature thermistors is described below:

1. Solder the thermistor to the plain copper leads.
2. Cover the exposed thermistor leads in epoxy so as to prevent a short in the electrical signal from occurring.
3. Allow the epoxy to dry for at least six hours.
4. Calibration (see the Calibration of Measurement Devices section for more details as to the procedure)
5. Locate the lake temperature thermistors where the temperature reading was desired.

A picture of the local lake temperature thermistors on the coil temperature tree can be seen in Figure 2-27.



Figure 2-27. Lake Temperature Thermistors at the Coil

The main function of the lake temperature thermistors were for measuring the local and undisturbed lake temperatures. On each coil tested there were three to five thermistors for measuring the local lake temperature located on an arm 1.2 m (4 ft) from the edge of the coil. They were height oriented to the top, middle, and bottom of the coil and spaced approximately 0.15 m to 0.46 m (0.5-1.5 ft) from the outer edge of the spiral-helical coils (The flat-spiral coil thermistors were all at the same height and were about 0.3 m (1 ft) beyond the outside loop. The slinky coils had the three thermistors about 0.15 m (0.5 ft) away from the HDPE piping).

To measure the local and the undisturbed lake temperature (or serve as a check to the local thermistors), two temperature sensing trees were constructed and located at distances of around 3 m (10 ft) and 30.5 m (100 ft) from the test coil (Figure 2-28). Each temperature tree has seven small bead thermistors spaced 0.46 m (1.5 ft) apart each. Located at the bottom of the PVC pipe are three 6.8 kg (15 lbs) concrete weights to hold the whole assembly to the bottom of the lake. At the top of each temperature there are three buoys securely fastened to the 7.6 cm (3 in)

nominal PVC pipe to hold the assembly upright as long as the water level of the lake does not drop below them. Figure 2-29 shows the general schematic of the temperature tree. Figure 2-30 shows a sample of the temperatures that the two trees record over a period of 4 days at the beginning of June.

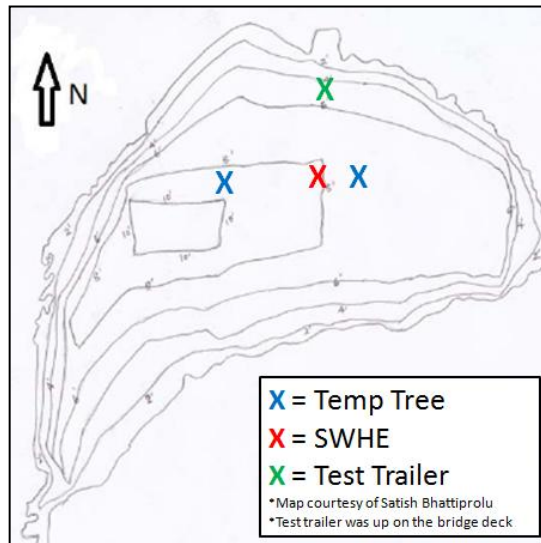


Figure 2-28. Locations of Temperature Trees

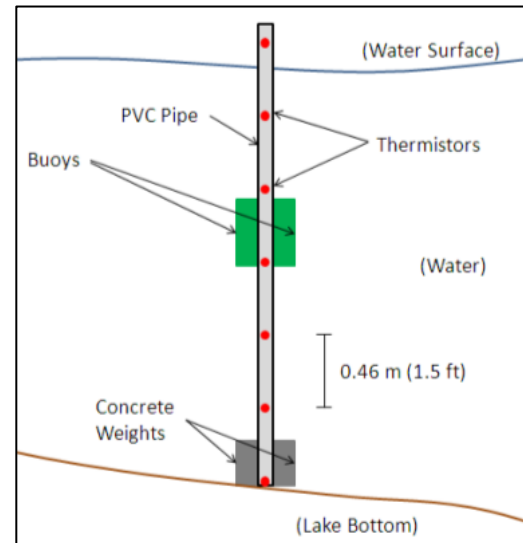


Figure 2-29. Lake Temperature Tree Schematic

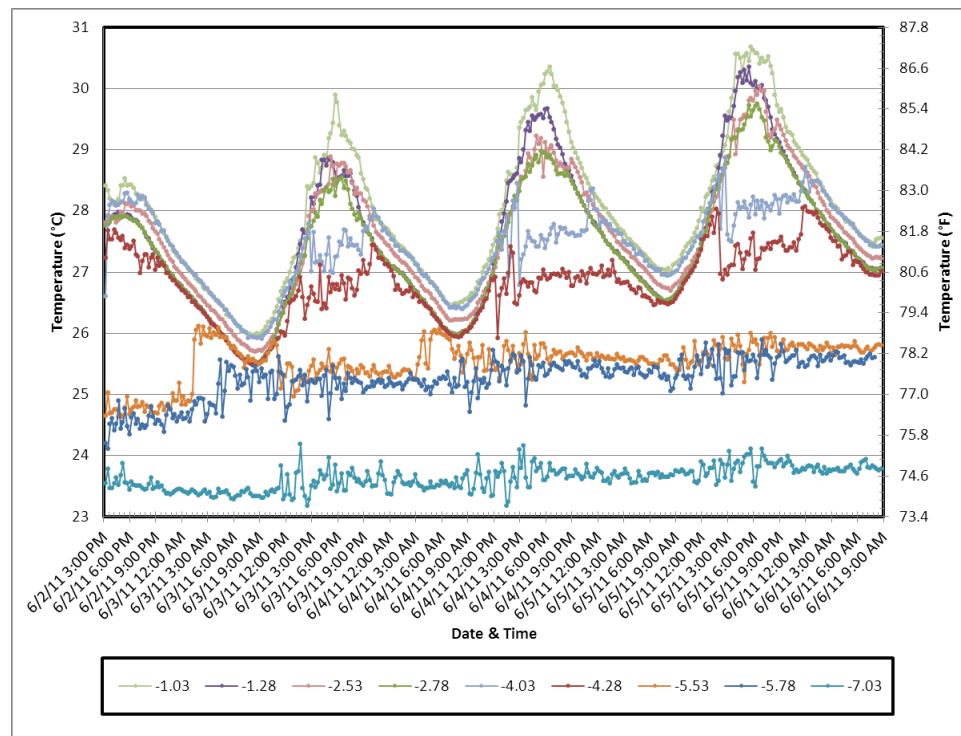


Figure 2-30. Sample Temperature Tree Data (6/2/2011-6/6/2011)

2.4.2 Coil Deployment

Upon completion of setting up the coil with the spacers and moving it from the laboratory to the lake, the coil would be loaded onto the back of the boat (if it was on the frame). Flat-spiral and slinky coils it were simply floated out into the water and tethered to the boat with rope. Before being brought out onto the testing pond, the lead pipes that run from the trailer to the coil were attached and sealed to and prevent leaking.

Three different connection types were used throughout the duration of all the testing. The first was braided tubing with pipe clamps shown in Figure 2-31. This was the worst of three and simply relied on friction to prevent leaking. The main problem with this connection was the connection coming apart when the water was removed from the coil via compressed air. Also, leakage would occur if the tubing was bent slightly or if the clamp was not constantly checked for tightness.



Figure 2-31. Braided Tube & HDPE Connection

The second connection type used was the cam-groove locking mechanism shown in Figure 2-32. This type worked well for when the connection was visible and no torque was put on the connection. When torque was applied to the cam-groove connection, small leaking would occur because the seal ring would separate from the male side of the coupling. This change was however good enough for the above water trailer connection because it made connecting and disconnecting really fast and leaking could be seen and prevented. Below water however was not a good choice because we couldn't always tell if there was torque on the connection and so the third modification was made.



Figure 2-32. Female Coupler Cam-Groove Connection

The final device that was decided upon for the connection to the coil was the PVC union coupling shown in Figure 2-33. With ample Teflon tape, Teflon paste, and tight assembly the union was resistant to leaking regardless of the forces applied to it. For extra protection against leaking though, silicone caulk was also applied to every joint in a generous manner.



Figure 2-33. PVC Union Coil Connection

Once the silicone on the leads dried, the coil could then be brought out to the testing location and dumped into the water. Another key step in coil deployment is attaching the tether line from the coil frame to the anchor buoy line. This prevents the coil from being able to move around the lake whether by winds on the surface of the lake or under-surface currents. With the coil in the water and the tether line attached, the purging process can begin to allow the coil to sink to its final testing location.

A secondary check may need to be done once the coil has sunk down to the bottom of the buoy lines. If the buoy lines are not under tension then it generally means the frame is on the bottom and some adjustments need to be made. Either the coil can be pulled out manually to a deeper location or the whole coil-frame assembly needs to be floated back up to the surface and the buoy line lengths need to be shortened.

2.4.3 System Purging and Data Acquisition Procedure

The procedure for performing the experiment has many different steps to it. These different steps include purging the system of air, adjusting the heat input setting, transition time period delay, and data recording. In closed-loop hydronic systems, air inside of the piping can

cause the circulation pumps to surge (flow rate goes up and down rapidly) or even air lock (flow stops all together). To remove the air from the piping and other components, a purging loop was built into the system by Austin (1998). The proper sequence for purging the system is listed below.

- 1) Arrange the three-way valves so that the flow from the water storage tank goes only through the coil and then back to the storage tank (valve position 1 in Figure 2-34).
- 2) Allow the purge pumps to run for approximately 10-15 minutes to remove the air from within the heat exchanger
- 3) Shut off the purge pumps before switching valve position to prevent damaging of the pumps.
- 4) Turn the three-way valves so the flow is directed through the trailer piping only and then back to the storage tank (valve position 2 in Figure 2-34).
- 5) Allow the purge pumps to run another 10-15 minutes to remove the air from inside the trailer piping.
- 6) Shut off purge pumps.
- 7) Turn the three-way valves so that the flow can go both directions, either through the coil and back to the storage tank or through the trailer piping and back to the storage tank (valve position 3 in Figure 2-34).
- 8) Allow the purge pumps to run roughly 10 minutes.
- 9) Shut off purge pumps.
- 10) Rotate the valves to the position that isolates the coil and trailer piping from the storage tank (valve position 4 in Figure 2-34). This creates a closed-loop between the two and now the circulation pumps must be used to flow water through the pipes.
- 11) Start the test using the circulation pumps and commence data acquisition

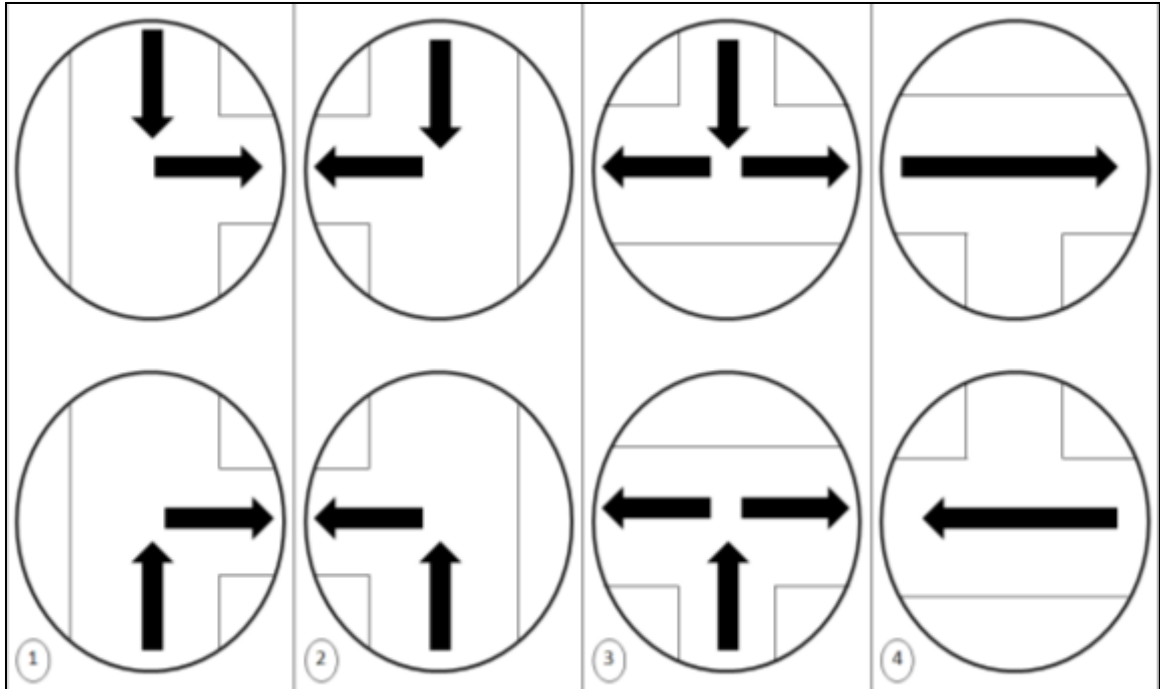


Figure 2-34. Purging 3-Way Valve Controls by Step (Modified from Austin (1998))

For this project, a time interval of 10 seconds was used between scans. The total time length that data was collected during each set point was usually around 30 minutes but it depended on how long it would take for the coil inlet and outlet to reach a steady-state (little to no changes). From all of the data points recorded, the final five minutes of data was averaged and thus reduced down to a single data point. In all, there are typically eight different set points yielding eight data points for each test. These were predetermined points based on the size of the electric water heaters used inside the trailer. When Austin (1998) constructed the trailer, he used two 1.5kW (5,118 Btu/hr) nominal heaters and one 2.0kW (6,824 Btu/hr) nominal heater. These have since been replaced twice now. The first time was to replace the 1.5kW (5,118 Btu/hr) nominal heaters for 3.5kW (11,943 Btu/hr) nominal heaters. The second time was to even further increase the heat input in hopes of reducing uncertainty due to small temperature differences. Two new 4.5kW (15,355 Btu/hr) nominal heaters and one 3.5kW (11,943 Btu/hr) nominal heater were implemented into the three heater locations. The 3.5kW (11,943 Btu/hr) heater and one of the 4.5kW (15,355 Btu/hr) heaters are set up on two separate ON/OFF breakers. The other 4.5kW

(15,355 Btu/hr) heater was wired up on a third breaker which was then connected to a proportional controller so that different heat inputs can be obtained between the range of 8.0kW (27,297 Btu/hr) nominal and 12.5kW (42,652 Btu/hr) nominal. Table 2-3 shows the different configuration controls and set points used during each coil test.

Table 2-3. Set Point Nominal Power Input Values & Controller Positioning

Set Point	Nominal Power Input		Breaker 1	Breaker 2	Breaker 3	Proportional Controller
#	kW	Btu/hr	ON/OFF	ON/OFF	ON/OFF	%
1	4.5	15,355	ON	OFF	OFF	0%
2	8.0	27,297	ON	ON	OFF	0%
3	10.0	34,121	ON	ON	ON	44%
4	10.5	35,827	ON	ON	ON	56%
5	11.0	37,534	ON	ON	ON	67%
6	11.5	39,240	ON	ON	ON	78%
7	12.0	40,946	ON	ON	ON	89%
8	12.5	42,652	ON	ON	ON	100%

One event that is nice to be able to observe is the transitioning between each set point. This helps confirm when steady-state has been reached. The steps to recording data for each set point are described below:

1. To record the transition period, the data logger is started prior to turning on the first heater. Allow the data acquisition equipment to log several points.
2. Flip on the first breaker (#1) to engage the first resistance water heater.
3. Continue to log data while observing the transition period.
4. When steady-state conditions are met, usually takes around 20-25 minutes, then the experimental data recording period begins. This is recorded for a minimum of five minutes and usually up to ten minutes.
5. Steps 2-4 are repeated according to Table 2-3 until all set points have been recorded.

2.4.4 Coil Submersion and Rising

The easiest and most efficient method for sinking and floating coils was the buoyancy approach. By balancing out the buoyancy forces correctly, it could be set up so that a coil full of water would sink while a coil full of air would float. Another problem that could be taken care of with this design is keeping the coil off of the lake bottom and also keeping the coil level.

The buoyancy calculation on the coil and frame is summarized in Table 2-4 when the coil is filled with air. Included in the table are the three different nominal tube sizes, displacement volume, frame and coil buoyancy forces, and finally a net buoyancy force. Note that a positive value for buoyancy force means the force is directed upward (floats)

Table 2-4. Coil Buoyancy Analysis

	Nominal SDR-11 Tube Size											
	3/4"				1"				1-1/4"			
V_{air}	0.057	m ³	2.0	ft ³	0.089	m ³	3.2	ft ³	0.142	m ³	5.0	ft ³
V_{HDPE}	0.028	m ³	0.99	ft ³	0.044	m ³	1.56	ft ³	0.070	m ³	2.49	ft ³
V_{steel}	0.0039	m ³	0.14	ft ³	0.0039	m ³	0.14	ft ³	0.0039	m ³	0.14	ft ³
F_{air}	560	N	126	lbs _f	874	N	197	lbs _f	1395	N	314	lbs _f
F_{HDPE}	12	N	3	lbs _f	20	N	4	lbs _f	31	N	7	lbs _f
F_{steel}	-263	N	-59	lbs _f	-263	N	-59	lbs _f	-263	N	-59	lbs _f
$F_{\text{net,air}}$	309	N	69	lbs _f	631	N	142	lbs _f	1163	N	262	lbs _f
$F_{\text{net,water}}$	-251	N	-56	lbs _f	-243	N	-55	lbs _f	-232	N	-52	lbs _f

The other force balance that is needed is for when the coil is filled with water. Through further analysis the net downward force with the coil and the frame filled with water was calculated. To counteract the downward force, buoys are attached via 1.5 m (5 ft) ropes. The dimensions of the cylindrical buoys that were used throughout the testing were 10 cm (4 in) diameter by 36 cm (14 in) length. A summary of the buoyancy analysis for the buoys on the frame is shown in Table 2-5. For any of the three tube diameters, the most buoys that we would be needed to hold the coil up off the bottom was eight total.

Table 2-5. Buoy Buoyancy Analysis

	Nominal SDR-11 Tube Size											
	3/4"				1"				1-1/4"			
F_{net,water}	-251	N	-56	lbs _f	-243	N	-55	lbs _f	-232	N	-52	lbs _f
V_{buoy}	33	cm ³	0.12	ft ³	33	cm ³	0.12	ft ³	33	cm ³	0.12	ft ³
F_{buoy}	32	N	7	lbs _f	32	N	7	lbs _f	32	N	7	lbs _f
buoys	8	#	8	#	8	#	8	#	8	#	8	#
F_{total}	7.6	N	1.7	lbs _f	14.8	N	3.3	lbs _f	26.3	N	5.9	lbs _f

The length of the buoy lines can be adjusted for the lake bottom contour. Careful attention needed to be made toward the lake level and buoy lines to prevent the coil and frame from being on/near the bottom and thus the possibility of interference from the bottom. Figure 2-35 shows a schematic of how the coil is suspended in the lake.

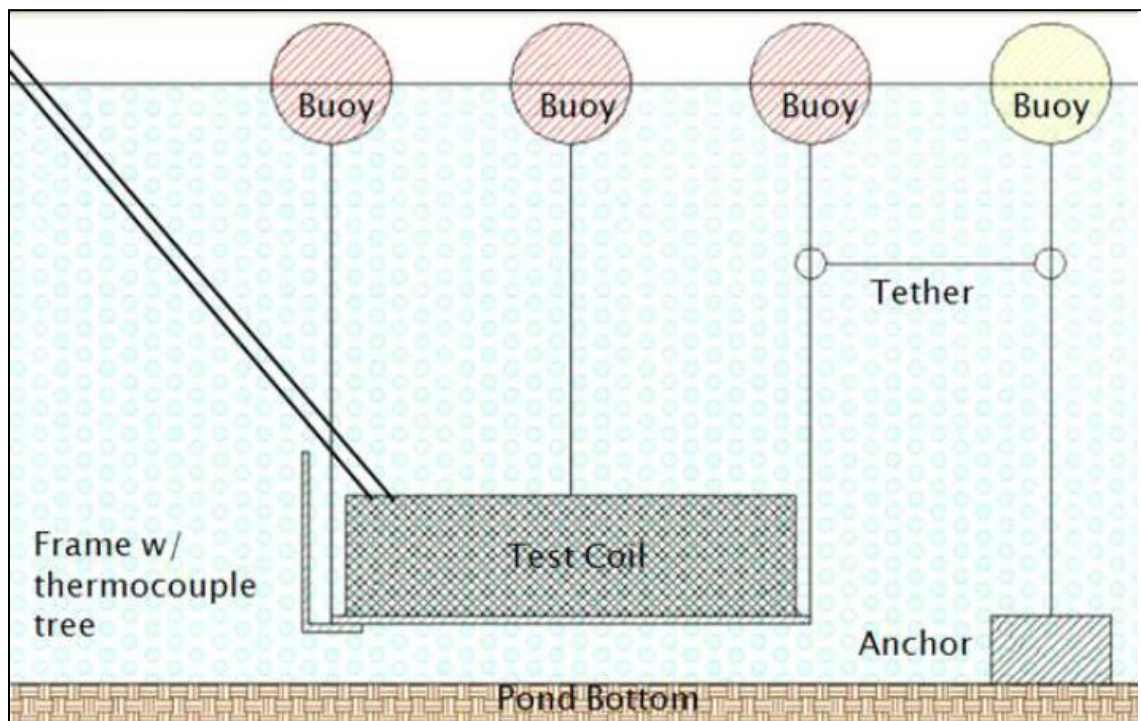


Figure 2-35. Coil & Frame Suspension Schematic

CHAPTER III

3. CALIBRATION OF MEASUREMENT DEVICES

3.1 Thermistors

Originally for this experiment thermocouples were used to measure temperatures. At this time the Fluke data logger was placed in a floating waterproof case. However, water penetration into the case led to aberrant temperature readings. Thermistors are relatively cheap and the wire needed to transport the signal back to the trailer and into the data logger is far less expensive than thermocouple wire. It was the low cost that ultimately allowed us to relocate the data logger into the trailer.

3.2 Thermistor Calibration Procedure

The calibration of the constructed thermistors and the thermistor probes was done using a temperature bath, high precision thermometer, data logger, and the thermistors themselves. Set points from 5°C (41°F) to 50°C (122°F), in increments of 5°C (8.1°F), were recorded over 10 minute intervals. Each data set was then averaged to a single mean resistance and used in the Steinhart-Hart equation (Equation 3-1).

$$\frac{1}{T} = A + B \ln(R) + C \ln(R)^2 + D \ln(R)^3 \quad (3-1)$$

Where: T = measured temperature (K)
 R = electrical resistance (Ω)

To generate the coefficients A , B , C , and D , the natural log of the resistance is graphed against the inverse temperature and a best curve fit for a third order polynomial is used (Figure 3-1).

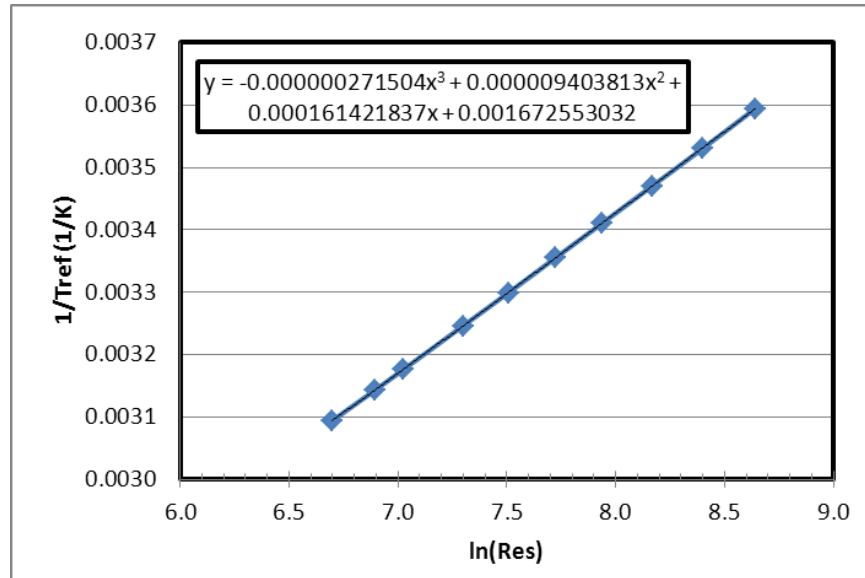


Figure 3-1. Lake Temperature Thermistor Calibration: $\ln(R)$ vs. $1/T_{ref}$

Once the coefficients were found (to assure accuracy they needed to be carried out to high decimal precision), the equation based predictions were then compared to the high precision thermometer values in order to generate the uncertainty values for each thermistor (always $< \pm 0.1^{\circ}\text{C}$ (0.18°F) and usually around the $\pm 0.06^{\circ}\text{C}$ (0.11°F)). These uncertainty values will be used in the uncertainty analysis.

3.3 Flow Meter

The flow meter that is used inside the testing trailer is a FTB-4607H from Omega Engineering Inc. This flow meter has a maximum volumetric flow measurement of 1.262 L/s (20 GPM) and a minimum volumetric flow measurement of 0.014 L/s (0.22 GPM). The uncertainty rating for the flow meter is given as $\pm 1\%$ of the full scale measurement by the manufacturer. Calculated, this is ± 0.0125 L/s (0.198 GPM).

To check the calibration on the flow meter a 0.114 m³ (30 gallon) container, a scale, and a stop watch was used. The water collected during a period of time recorded was weighed on the scale. Equation 3-2 was used to determine the flow rate from the amount of water and the time of collection. The recorded voltages from the data logger were next graphed against the flow rate. The different flow rate results are shown in Table 3-1.

$$\dot{V} = \frac{m/\rho}{t} \quad (3-2)$$

Where: \dot{V} = volumetric flow rate (m³/s, gal/min)
 m = mass of the collected water (kg, lb_f)
 ρ = density of the water collected (kg/m³, lb_f/gal)
 t = time measured by the stopwatch (s, min)

Table 3-1. Flow Meter Calibration Results

	Mass	Density	Volume	Time	ΔV	Flow Rate	Flow Rate
Setting	kg	kg/m ³	m ³	s	volts	m ³ /s	gal/min
1	17.45	998.5	0.0175	26.2	4.88	0.000667	10.57
2	17.45	998.5	0.0175	29.0	4.40	0.000603	9.55
3	16.75	998.5	0.0168	39.4	3.13	0.000426	6.75
4	17.20	998.5	0.0172	64.7	1.94	0.000266	4.22
5	16.10	998.5	0.0161	130.1	0.90	0.000124	1.96
6	7.90	998.5	0.0079	125.7	0.43	0.000063	1.00

By using the linear regression feature within Excel®, the calibration curve was determined and is shown graphically in Figure 3-2 and numerically in Equation 3-3 where \dot{V} is the flow rate in gallons per minute (GPM) and ΔV is the measured voltage from the flow meter. The SI version of the flow rate equation in m³/s is provided in Equation 3-4.

$$\dot{V}_{c,i} = 2.156357(\Delta V) + 0.036831 \quad (\text{GPM}) \quad (3-3)$$

$$\dot{V}_{c,i} = 1.36 \times 10^{-4}(\Delta V) - 2.32 \times 10^{-6} \quad (\text{m}^3/\text{s}) \quad (3-4)$$

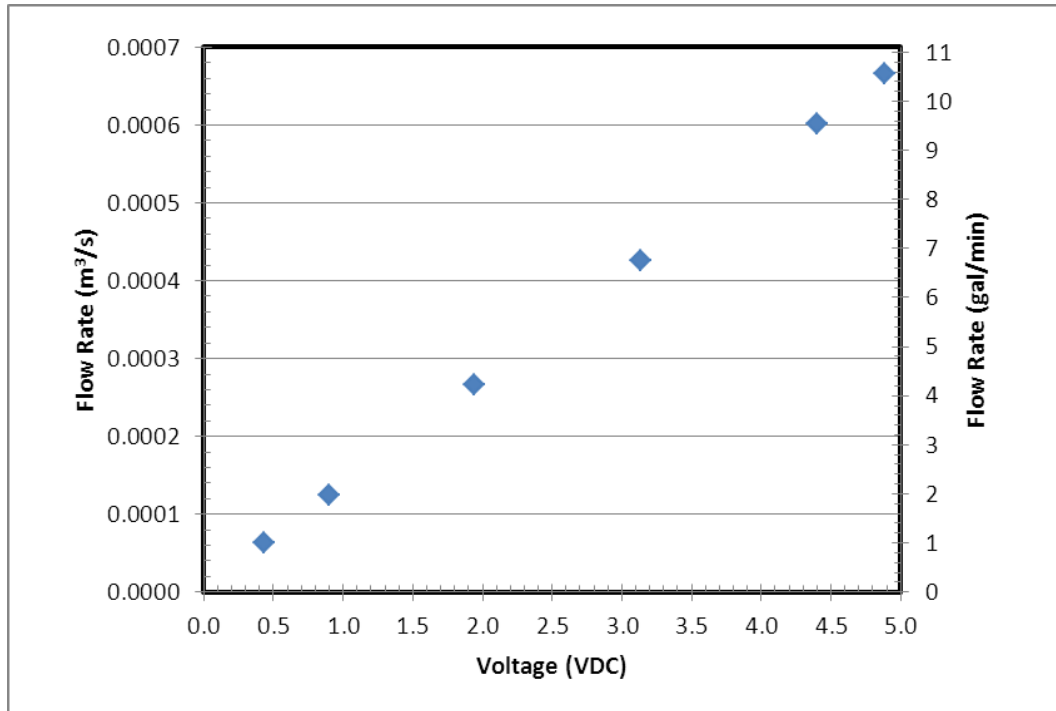


Figure 3-2. Flow Meter Calibration Curve

The uncertainty in the flow meter readings were calculated using a 95% confidence interval. This uncertainty was found to be approximately 0.0023 L/s (0.036 GPM) which is well within the uncertainty specified by the manufacturer.

3.4 Watt Transducer

The watt transducer that was used inside the testing trailer is a PC5-0610Y24 from Ohio Semitronics Inc. This watt transducer has a minimum to maximum power reading of 0-20 kW. The uncertainty on the readings is said to be $\pm 0.5\%$ of the full scale measurement. This results in an uncertainty of ± 100 watts. The main reason for using the measured power input was for data organization. By looking at the power input it could be determined which set point was running at that time. Also it was very easy to spot when the set point was switched from one to the next. Aside from these two reasons, the measured power input by the watt transducer was not used in the analysis at all since high losses were obtained from the leads running from the trailer to the test coils.

CHAPTER IV

4. ANALYSIS METHODOLOGY

4.1 Data Averaging

As stated in the System Purging and Data Acquisition section of this thesis, readings are taken every 10 seconds from the start of the test till approximately 10 minutes after the system reaches a semi-steady state. The last 5 minutes of data for each set point are taken for the analysis. To smooth out the data, averages for the 30 set point readings are taken. This means that only 8 points are run through the analysis procedure, one for every set point. With the averages for each reading calculated, they can be converted from their raw data form to their actual form (i.e. thermistor resistance measurements are converted to temperatures, flow rates are converted to correct units, etc.).

4.2 Outside Convection Coefficient – HDPE Tube-Based Heat Exchangers

The heat exchanger analysis first determines the overall thermal resistance, and from this, the outside convection coefficient is determined. The first major step is to find the total thermal resistance of the heat exchanger. The start of this process is to calculate the heat transfer rate (Q_c) through the coil (Equation 4-1) using the volumetric flow rate ($\dot{V}_{c,i}$), coil inlet temperature ($T_{c,in}$), coil outlet temperature ($T_{c,out}$), fluid density ($\rho_{MFT,i}$), and fluid specific heat ($c_{p,MFT,i}$) calculated at the mean fluid temperature (MFT) which is the average between the inlet and outlet temperatures. In our case the circulating fluid is water but this may be a water-antifreeze solution if the design calls for near freezing temperatures in the system.

$$Q_c = \dot{V}_{c,i} * \rho_{MFT,i} * c_{p,MFT,i} * (T_{c,in} - T_{c,out}) \quad (4-1)$$

The next step is to calculate the theoretical maximum heat transfer rate ($Q_{c,max}$) that could take place for the warm entering fluid temperature and lake temperature. This is found by the following equation.

$$Q_{c,max} = \dot{V}_{c,i} * \rho_{MFT,i} * c_{p,MFT,i} * (T_{c,in} - T_p) \quad (4-2)$$

With the actual heat transfer rate and theoretical maximum heat transfer rate known, a thermal effectiveness (ε_c) of the coil can be calculated.

$$\varepsilon_c = \frac{Q_c}{Q_{c,max}} \quad (4-3)$$

Next, the number of transfer units (NTU) for an infinite capacity heat exchanger can be calculated with Equation 4-4.

$$NTU = -\ln(1 - \varepsilon_c) \quad (4-4)$$

From knowing the number of transfer units, the UA can be found as shown in Equation 4-5.

$$UA = NTU * \dot{V}_{c,i} * \rho_{MFT,i} * c_{p,MFT,i} \quad (4-5)$$

The inverse of UA is the total thermal resistance of the coil (R'_c).

$$R'_c = \frac{1}{UA} \quad (4-6)$$

The second major step is to calculate the inside thermal resistance which is due to convection under turbulent conditions. To start this next process, the kinematic viscosity ($\nu_{MFT,i}$), thermal conductivity ($k_{MFT,i}$), and thermal diffusivity ($\alpha_{MFT,i}$) need to be calculated as a function of the mean fluid temperature. The velocity of the fluid ($\vec{v}_{c,i}$) is first calculated as follows.

$$\bar{v}_{c,i} = \frac{\dot{V}_{c,i}}{A_{cr,i}} \quad (4-7)$$

Next the Reynolds number ($Re_{d,i}$) is calculated by multiplying the fluid velocity by the inside pipe diameter (d_i) and then dividing it by the kinematic viscosity of the fluid.

$$Re_{MFT,d_i} = \frac{\bar{v}_{c,i} * d_i}{\nu_{MFT,i}} \quad (4-8)$$

The bulk fluid Prandtl number (Pr_i) calculation is next. It is calculated by taking the kinematic viscosity and dividing it by the thermal diffusivity. Both properties are evaluated at the mean fluid temperature of the coil.

$$Pr_{MFT} = \frac{\nu_{MFT,i}}{\alpha_{MFT,i}} \quad (4-9)$$

The inside Nusselt number ($Nu_{d,i}$) can now be calculated using the Rogers & Mayhew (1964) or the Salimpour (2009) correlation. For convenient use in simulation coding, the Rogers and Mayhew correlation was selected which uses bulk fluid temperature properties instead of film temperature properties. The coil diameter is also taken at an average value ($D_{c,avg}$).

$$Nu_{MFT,d_i} = 0.021 Re_{MFT,d_i}^{0.85} Pr_{MFT}^{0.4} \left(\frac{d_i}{D_{c,avg}} \right)^{0.1} \quad (4-10)$$

With the Nusselt number on the inside of the pipe known, the inside convection coefficient (h_i) can be determined by multiplying the inside Nusselt number by the thermal conductivity of the inside fluid then dividing it by the inside pipe diameter.

$$h_i = \frac{k_{MFT} * Nu_{MFT,d_i}}{d_i} \quad (4-11)$$

The inside convection resistance (R'_i) is then calculated by taking the inverse of the inside convection coefficient multiplied by the inside pipe surface area ($A_{s,i}$).

$$R'_i = \frac{1}{h_i * A_{s,i}} \quad (4-12)$$

The third resistance needed for the heat exchanger model is the conductive thermal resistance from the HDPE tube material (R'_t). The equation for the tube thermal resistance is as follows.

$$R'_t = \frac{\ln\left(\frac{d_o}{d_i}\right)}{2\pi * k_t * L_t} \quad (4-13)$$

Where: d_o is the outside tube diameter (m)

d_i is the inside tube diameter (m)

$k_t = 0.17 + 5(\rho_{HDPE} - 0.9) - 0.001T_{HDPE}$ (W/m-K) (Rauwendaal 1986)

L_t is the length of the HDPE tubing (m)

The next to last step of the heat exchanger model is to calculate the outside thermal resistance (R'_o). This is done by subtracting the inside convective resistance and pipe conductive resistance from the total thermal resistance of the coil.

$$R'_o = R'_c - R'_i - R'_t \quad (4-14)$$

The final step is the calculation of the outside convection coefficient (h_o). To do this, the outside thermal resistance is multiplied by the outside pipe surface area and then it is inverted as shown.

$$h_o = \frac{1}{R'_o * A_{s,o}} \quad (4-15)$$

From here different Nusselt numbers can be calculated by using the definition of Nusselt number with the desired characteristic length. The fluid conductivity used in the Nusselt number is calculated at the outside film temperature. Likewise, the Rayleigh number and modified Rayleigh number can be calculated for different characteristic lengths and properties at the outside film temperature according to Equation 1-14 and Equation 1-16 respectively.

4.3 Outside Convection Coefficient – Vertical Flat-Plate Heat Exchanger

Because of highly complex geometry involved in the Slim Jim® vertical flat-plate, many unknowns were present and approximations had to be made. The channel dimensions of height (y) and width (x) (28cm, 11 in and 6.4 mm, 0.25 in respectively) were approximated assuming a flow cross section of a rectangle. The length of the flow path (L) was estimated as the average length (6.9 m, 22.6 ft) traveled down the center of the channel of a four-pass plate. The thickness of the stainless steel (Δx) was estimated at 1.6 mm (0.0625 in). Dimensional uncertainties for the vertical flat-plate were all obtained through engineering judgments. To increase the accuracy of this method, exact values for the inside and outside surface areas should be obtained as well as the channel dimensions and plate material properties.

The heat exchanger analysis on the vertical flat-plate first starts by calculating the hydraulic diameter (D_h) using equation 4-16.

$$D_h = \frac{4(xy)}{(2x+2y)} \quad (4-16)$$

The inside and outside rectangular surface areas ($A_{s,i}$, $A_{s,o}$) were assumed to be equal since wall thickness was small. The inside cross-sectional area ($A_{cr,i}$) was also calculated and used with the volumetric flow rate (\dot{V}) measured to find the velocity of the fluid (\vec{v}) flowing through the channel via Equation 4-17.

$$\vec{v} = \frac{\dot{V}}{A_{cr,i}} \quad (4-17)$$

Using the hydraulic diameter as the characteristic length and the velocity of the fluid inside the channel, the inside Reynolds number ($Re_{MFT,i}$) was calculated using Equation 4-18.

$$Re_{MFT,i} = \frac{\vec{v}D_h}{\nu_{MFT,i}} \quad (4-18)$$

The inside Nusselt number ($Nu_{MFT,i,Dh}$) was then obtained using the Dittus-Boelter equation (Equation 1-8). Through the definition of the Nusselt number, the inside convection coefficient (h_i) was calculated using Equation 4-19 and the inside convective resistance (R'_i) can be found using Equation 4-12.

$$h_i = \frac{Nu_{MFT,i,Dh} k_{MFT,i}}{D_h} \quad (4-19)$$

The conductive thermal resistance (R'_w) was calculated by assuming the thermal conductivity of stainless steel (k_w) as 16 W/m-K (9.2 Btu/hr-ft-°F) and using Equation 4-20 where Δx is the thickness of the stainless steel wall.

$$R'_w = \frac{\Delta x}{k_w A_i} \quad (4-20)$$

The total thermal resistance of the heat exchanger (R'_c) can be calculated in the same manner as described at the start of Section 4.2 up through Equation 4-6. From there the outside convective resistance (R'_o) can be found using Equation 4-14 and the outside convection coefficient (h_o) using Equation 4-15.

4.4 Uncertainty Analysis Methodology

When making measurements of any type, there is some form of error that is associated with it. A temperature measurement is a good example of this. When a temperature bath is actually at 20.0°C (68°F), a thermometer may read a value in the range of 19.1-20.1°C (67.8-68.2°F). In this instance, the accuracy of the thermometer is said to be $\pm 0.1^\circ\text{C}$ (0.2°F). It is this slight error in numerous measurements that causes the necessity for an uncertainty analysis on research projects. When an uncertainty analysis of a project is completed, the range of possible outcomes is presented in error bars of the calculated values. For the case of a convection coefficient experiment, the final results may be a value of $200 \pm 40 \text{ W/m}^2\text{-K}$ ($35 \pm 7 \text{ Btu/hr-ft}^2\text{-}^\circ\text{F}$) which means that the reading has a possible error of 20%.

To calculate the uncertainty on the measurements, Chapter 3 from Holman and Gajda (1984) provides a general approach. The method involves using the individual uncertainties from all of the measurements and combining them into a single uncertainty on a final parameter. In our case, the final parameter is either the outside Nusselt number or the outside convection coefficient.

The generic formula for calculating the uncertainty in a given parameter (w_R) as given in Holman and Gajda is found in Equation 4-21. The assumption of this equation is that each of the individual variables are independent of each other. Each of the measured variables involved in the calculation have their individual uncertainties ($w_1, w_2, w_3... w_n$) included in the equation as well as the partial derivative contributions of each variable ($\partial R/\partial x_1, \partial R/\partial x_2, \partial R/\partial x_3... \partial R/\partial x_n$)

$$w_R = \sqrt{\left(\frac{\partial R}{\partial x_1} w_1\right)^2 + \left(\frac{\partial R}{\partial x_2} w_2\right)^2 + \left(\frac{\partial R}{\partial x_3} w_3\right)^2 + \dots \left(\frac{\partial R}{\partial x_n} w_n\right)^2} \quad (4-21)$$

Applying this uncertainty methodology to the equation for calculating the heat transfer of the fluid inside the coil yields the following partial derivatives and the uncertainty that is associated to each variable (Table 4-1). The property calculation functions are assumed to accurate and thus have negligible uncertainty.

Table 4-1. Heat Transfer Uncertainty Example

Given Conditions	$\partial R/\partial x_1, \partial R/\partial x_2, \partial R/\partial x_3, \dots, \partial R/\partial x_n$	$w_1, w_2, w_3, \dots, w_n$
$\dot{V}_{c,i} = 0.000279 \text{ m}^3/\text{s}$	$\partial \dot{q}_c / \partial \dot{V}_{c,i} = \rho_{MFT} c_{p,MFT} (T_{c,in} - T_{c,out})$ $\partial \dot{q}_c / \partial \dot{V}_{c,i} = 13811715$	$w_{\dot{V}_{c,i}} = 0.00000292 \text{ m}^3/\text{s}$
$\rho_{MFT} = 999.3 \text{ kg}/\text{m}^3$	$\partial \dot{q}_c / \partial \rho_{MFT} = \dot{V}_{c,i} c_{p,MFT} (T_{c,in} - T_{c,out})$ $\partial \dot{q}_c / \partial \rho_{MFT} = 3.86$	$w_{\rho_{MFT}} = 0 \text{ kg}/\text{m}^3$
$c_{p,MFT} = 4188.3 \text{ J}/\text{kg} \cdot ^\circ\text{C}$	$\partial \dot{q}_c / \partial c_{p,MFT} = \dot{V}_{c,i} \rho_{MFT} (T_{c,in} - T_{c,out})$ $\partial \dot{q}_c / \partial c_{p,MFT} = 0.92$	$w_{c_{p,MFT}} = 0 \text{ J}/\text{kg} \cdot ^\circ\text{C}$
$T_{c,in} = 15.2 ^\circ\text{C}$	$\partial \dot{q}_c / \partial T_{c,in} = \dot{V}_{c,i} \rho_{MFT} c_{p,MFT}$ $\partial \dot{q}_c / \partial T_{c,in} = 1168$	$w_{T_{c,in}} = 0.1 ^\circ\text{C}$
$T_{c,out} = 11.9 ^\circ\text{C}$	$\partial \dot{q}_c / \partial T_{c,out} = -\dot{V}_{c,i} \rho_{MFT} c_{p,MFT}$ $\partial \dot{q}_c / \partial T_{c,out} = -1168$	$w_{T_{c,out}} = 0.1 ^\circ\text{C}$

Finally, the uncertainty on just the heat transfer for the given conditions is found to be ± 165 Watts (563 Btu/hr) out of the calculated heat transfer rate of 3,885 Watts (13,256 Btu/hr). This means that there is a 4.2% uncertainty in just the heat transfer rate alone for this set point of the experiment. Note that this sample calculation does not include spatial uncertainty.

When talking about the uncertainty analysis for the testing apparatus, there is more than just the uncertainty due to the sensors. There is also spatial uncertainty that is present. This is the uncertainty due to the coil not being at the same depth as the lake temperature sensors everywhere. If the lake temperature sensors are measuring at the top, middle and bottom of the coil and the coil is tilted at all, then parts of the coil that are not exactly where the temperature sensors are will be at a different depth and thus a different temperature than we are calculating for.

The amount of spatial uncertainty that is involved with each different test has two components, a vertical and horizontal temperature uncertainty. For the vertical spatial uncertainty of the spiral-helical coil setup, it can be estimated from the buoy length because the entire coil resides inside the frame perimeter. The uncertainty of the buoy lengths is estimated at ± 25 mm (1 in). Using the estimation for the vertical spatial uncertainty length, the lake temperatures are checked using the range of possible depths that the coil could be located in. The maximum difference in lake temperature compared to the original location is taken for each test as the vertical spatial uncertainty in temperature.

To calculate the spatial quantity for the vertical oriented slinky coil, the procedure is a slightly different. The thermistors are located at the first buoy along the coil. The spatial uncertainty to the far end of the coil is a function of the rope length uncertainty. If the rope lengths are estimated to be ± 25.4 mm (1 in), the spatial depth difference from the first buoy to the last buoy can be calculated (see Figure 4-1 and Table 4-2 for more details).

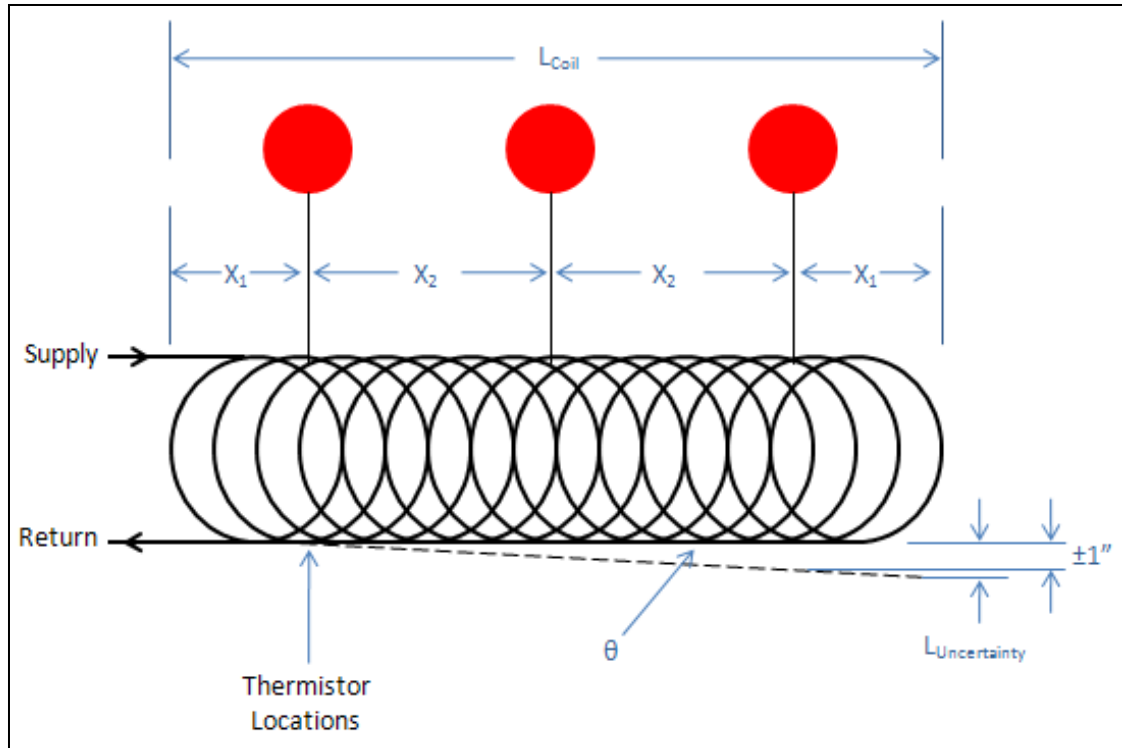


Figure 4-1. Vertical Slinky SWHE Spatial Uncertainty Diagram

Table 4-2. Vertical Slinky Coil Uncertainty in Length Results

Pitch (Inches)	L_{Coil} (feet)	X_1 (feet)	X_2 (feet)	θ (degrees)	$L_{Uncertainty}$ (Inches)
5	35	5	12.5	0.1910	1.200
10	50	5	20	0.1194	1.125
15	65	10	22.5	0.1061	1.222

To calculate how the temperature is influence by the spatial uncertainty, the gradients between the top and middle thermistors as well as the middle and bottom thermistors is calculated. The temperature difference is the obtained by projecting the two gradients in their respective direction to the uncertainty length. The largest temperature change between the original position and the projected position is taken as the vertical spatial uncertainty in temperature.

The horizontal slinky and the flat-spiral coils are also different from all of the previous coils. The method for calculating the uncertainty in the lake temperature could not be done like the vertical or horizontal slinky coils because all of the thermistors were located at the same depth

and thus a small change in temperature would result in a large gradient. If the gradient was used to project the temperature, the uncertainty would be outrageous. The method that was decided upon instead was to take the average of the three thermistors and compare them to the individual readings. The largest deviation from the average was used as the vertical spatial uncertainty in temperature.

The determination of the horizontal spatial uncertainty in temperature for a lake is a highly complex three dimensional problem. To best approximate such a complex task the horizontal spatial uncertainty in temperature was determined by using the two lake temperature sensor trees. Because they were located in different regions of the lake, the temperatures were compared at similar depths and over several averaged periods of time. With the coil being located between the two, The average of the maximum temperature difference between the two trees was decided as the best estimate for the spatial uncertainty in lake temperature.

Finally there is calculating the combined uncertainty value for the lake temperatures. To do this, the uncertainty values due to spatial effects are added with the uncertainty of the sensor itself by using Equation 4-22.

$$U_{total} = \sqrt{(U_{sensor})^2 + (U_{spatial,vertical})^2 + (U_{spatial,horizontal})^2} \quad (4-22)$$

Where: U_{total} is the total uncertainty of the measurement (°C)

U_{sensor} is the uncertainty of the sensor measurement (°C)

$U_{spatial,vertical}$ is the vertical spatial uncertainty in lake temperature (°C)

$U_{spatial,horizontal}$ is the horizontal spatial uncertainty in lake temperature (°C)

The highest estimated value for the total uncertainty on the pond temperature occurred when the sensor uncertainty was 0.1°C (0.18°F), the vertical spatial uncertainty was 0.17°C

(0.31°F), and the horizontal uncertainty was 0.15°C (0.27°F). This resulted in a maximum total uncertainty of 0.25°C (0.45°F) for the pond temperature.

4.5 Uncertainty Analysis Results

Using the uncertainty methods previously discussed the uncertainty for the different coils tested were calculated. The results from this analysis are too lengthy to list in a table so they have been displayed in graphical form. The main areas of interest are the uncertainties of the heat transfer rate and the outside convection coefficients.

4.5.1 Spiral-Helical Coil Uncertainty Results

When calculating the heat transfer rate inside the coils, the main influence on the uncertainty comes from the in-pipe thermistors. The difference between the inlet and outlet temperatures is directly related to the heat transfer rates measured for the coils. It is because of this relationship that we see the downward decreasing trend that is shown in Figure 4-2. As the heat transfer rate increases from the coil, the temperature difference between the coil inlet and outlet also increases. The larger that the difference becomes, the more the effects of the thermistor uncertainty are diminished.

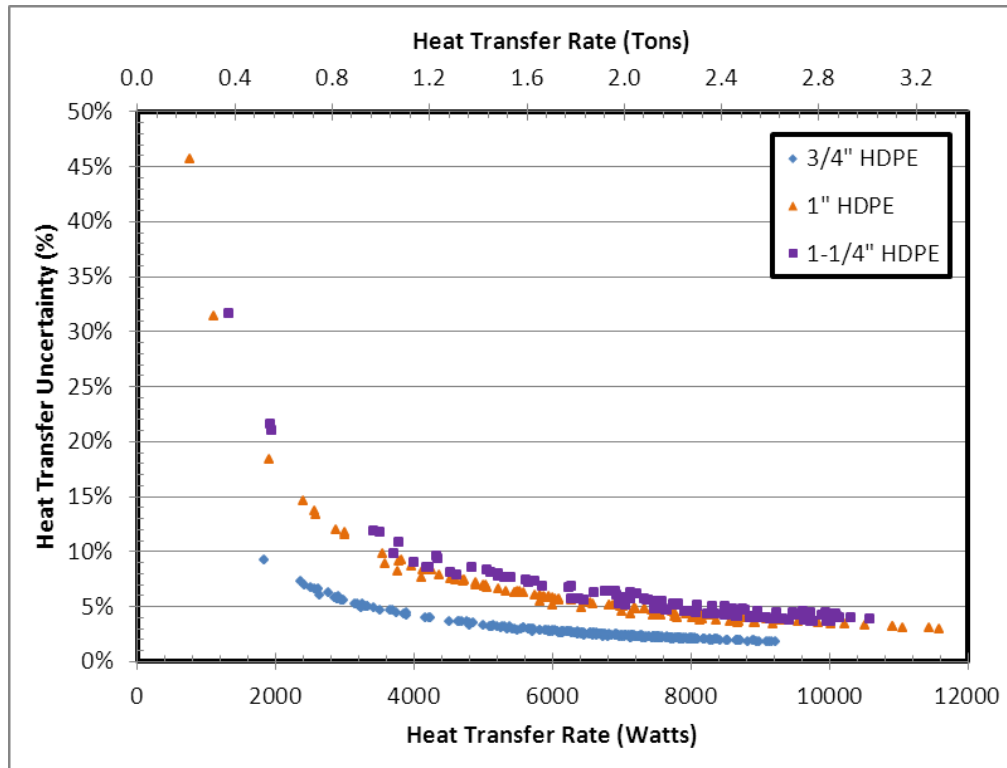


Figure 4-2. Spiral-Helical SWHE Uncertainty on Heat Transfer Rate

Another interesting recognition that can be made from the spiral-helical uncertainty percentage in heat transfer is that there is a definite separation between the three tube sizes. The highest uncertainty in heat transfer rate was for the largest, thickest walled HDPE piping. This is then followed by the middle and smallest tubes sizes that were tested. This is a direct result from the increase in flow rate due to the larger cross-sectional areas of the different tube sizes. Larger flow rate results in a lower temperature difference between the inlet and outlet and thus causes higher uncertainty for same heat transfer rates. For the spiral-helical testing though, less than 3% of the total points (15/528) were above the 10% uncertainty. Of those 15 points, all of them were below a heat transfer rate of 4 kW (13,649 Btu/hr).

To get a better understanding on the outside convection coefficient uncertainty, it was graphed against the heat transfer rate as shown in Figure 4-3. From this graph it is obvious to see that the large uncertainty points are associated with the low values of heat transfer rates.

Additionally these points mainly comprised of the larger tubes but there are a few small tube points that approach the 100% uncertainty mark. These high error values will be investigated later as to their contribution to the development of a spiral-helical coil outside convection coefficient correlation.

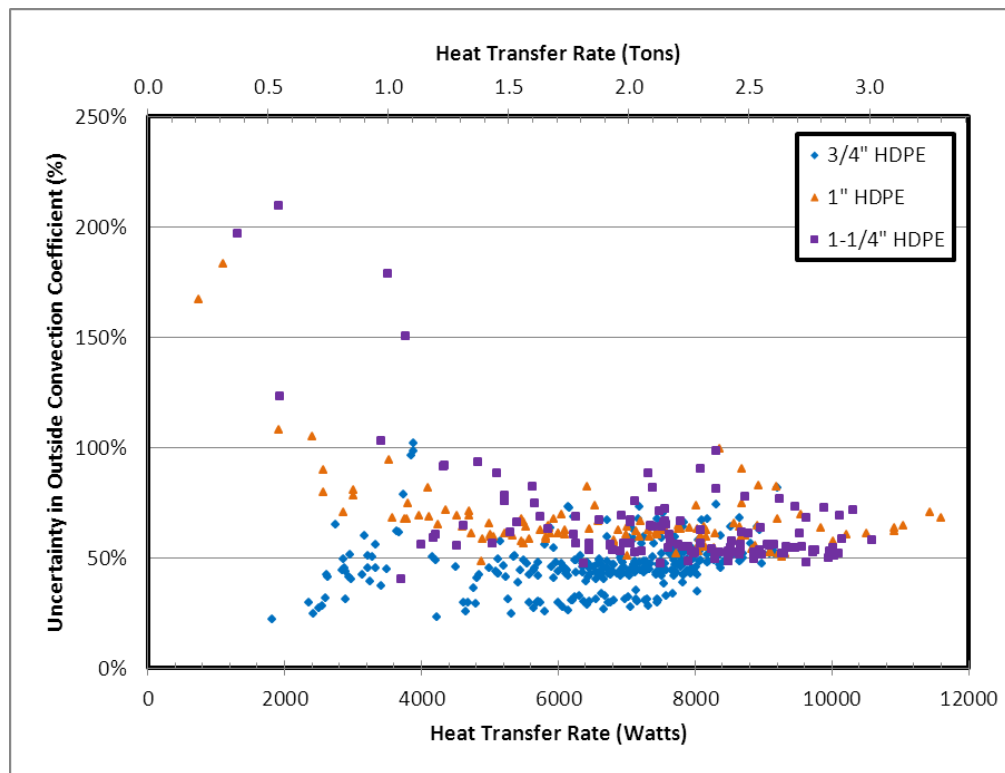


Figure 4-3. Outside Convection Coefficient Uncertainty vs. Heat Transfer Rate (Spiral-Helical)

4.5.2 Flat-Spiral Coil Uncertainty Results

The same uncertainty analysis as the spiral-helical was conducted for the flat-spiral coil testing. Similar results of uncertainty to heat transfer rate were found. As the heat transfer rate of the flat-spiral coil increased from 1.2 kW (4,095 Btu/hr) to 4.8 kW (16,378 Btu/hr), the uncertainty percentage decreased from slightly under 11% (1.2 kW, 4095 Btu/hr) to just below 3%.

As for the uncertainty of the outside convection coefficient, Figure 4-4 shows the uncertainty percentage with respect to the heat transfer rate. Unlike the spiral-helical coil

uncertainty, the flat-spiral coil uncertainty did not show that low values of heat transfer rate were associated with high uncertainty rates. This is presumably due to the much smaller range of conditions that were tested in.

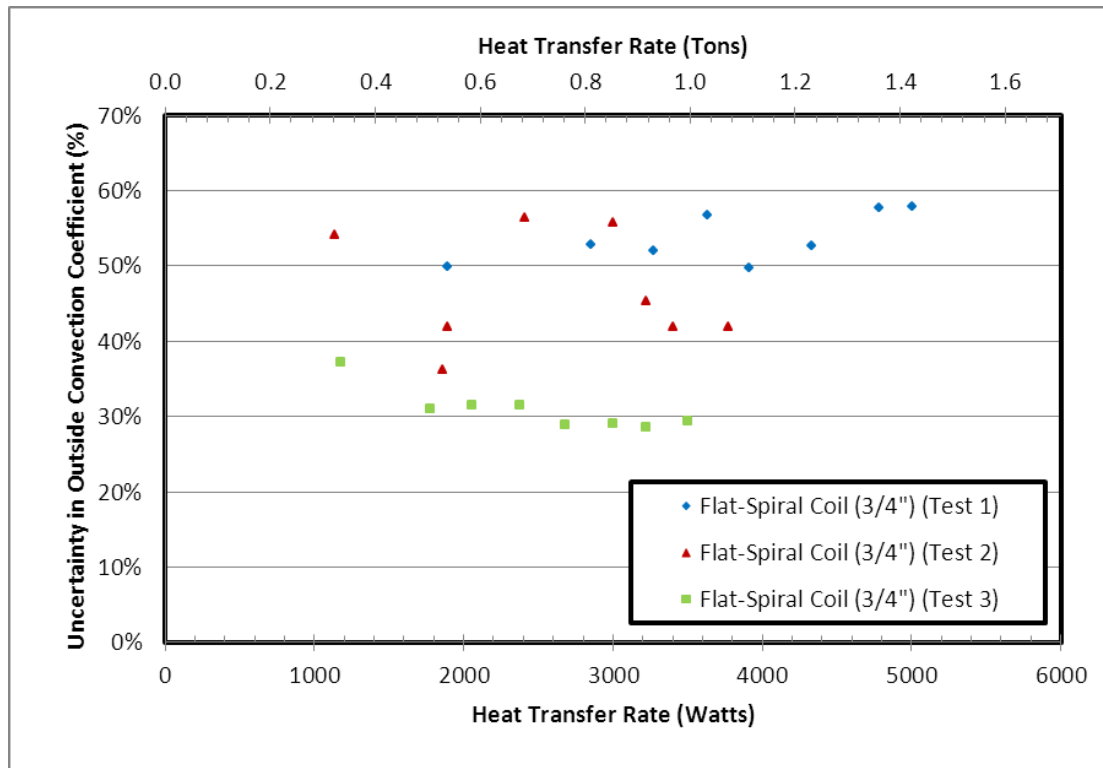


Figure 4-4. Outside Convection Coefficient Uncertainty vs. Heat Transfer Rate (Flat-Spiral)

4.5.3 Slinky Coil Uncertainty Results

Again, the uncertainty results for the slinky coil were similar to those of the spiral-helical and flat-spiral coils. The uncertainty percentage in heat transfer rate decreased from 21% down to 3% as the heat transfer rate increased from 1 kW (3,412 Btu/hr) to 7.6 kW (25,932 Btu/hr). The percent uncertainty of the outside convection coefficient is provided in Figure 4-5. For the most part the graph shows the uncertainty staying relatively constant with the exception of a few points below 2 kW (6,824 Btu/hr) where the uncertainty percentage increased. It may be of interest to eliminate these high uncertainty points from a correlation development.

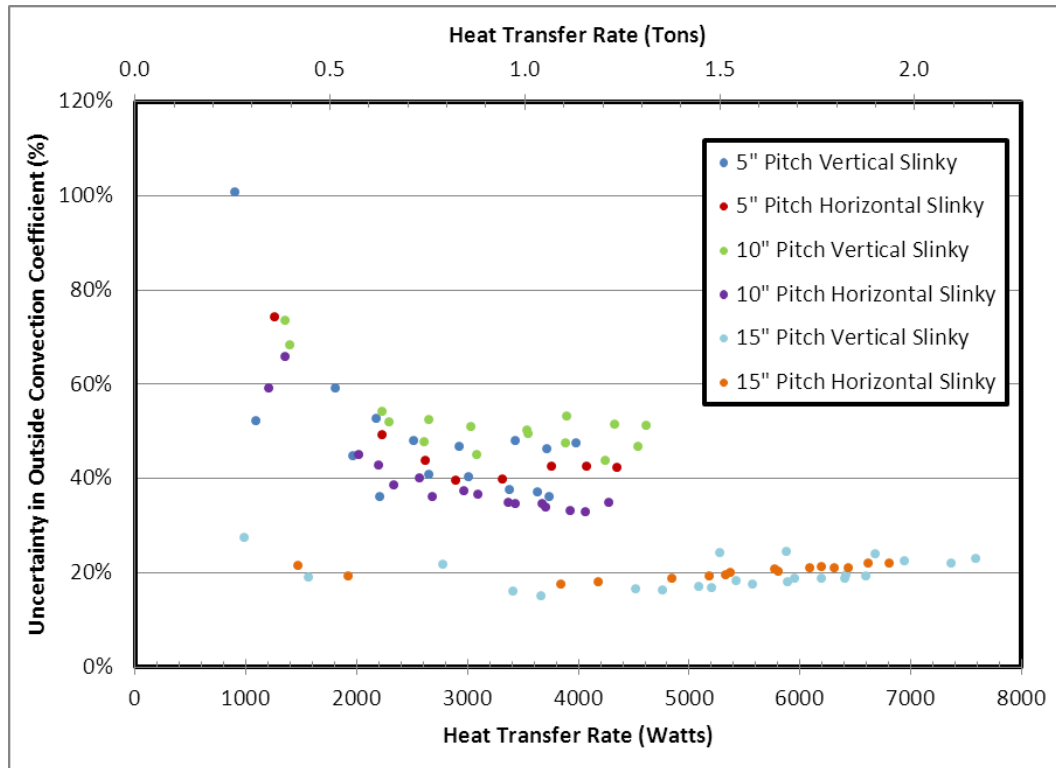


Figure 4-5. Outside Convection Coefficient Uncertainty vs. Heat Transfer Rate (Slinky Coils)

4.5.4 Vertical Flat-Plate Heat Exchanger Uncertainty Results

Even with all of the assumptions that were taken into account in the analysis methodology of the vertical flat-plate heat exchanger, the uncertainty results were similar to those of the spiral-helical, flat-spiral, and slinky coils on a heat transfer level. The uncertainty percentage in heat transfer rate decreased from 35% down to 3% as the heat transfer rate increased from 600 W (2,047 Btu/hr) to 6.1 kW (20,814 Btu/hr). The percent uncertainty of the outside convection coefficient is provided in Figure 4-6. The most obvious feature of the graph is that after 2 kW (6,824 Btu/hr), the uncertainty levels off at a value around 30%. This was investigated and found out to be strictly the dimensional uncertainties that were estimated. Improvement to the dimensional uncertainties would most likely provide higher accuracy in the uncertainty analysis. With all things considered, the uncertainty below 2 kW (6,824 Btu/hr) does increase as the heat transfer rate decreases. Again it may be of interest to eliminate these higher uncertainty points from a correlation development.

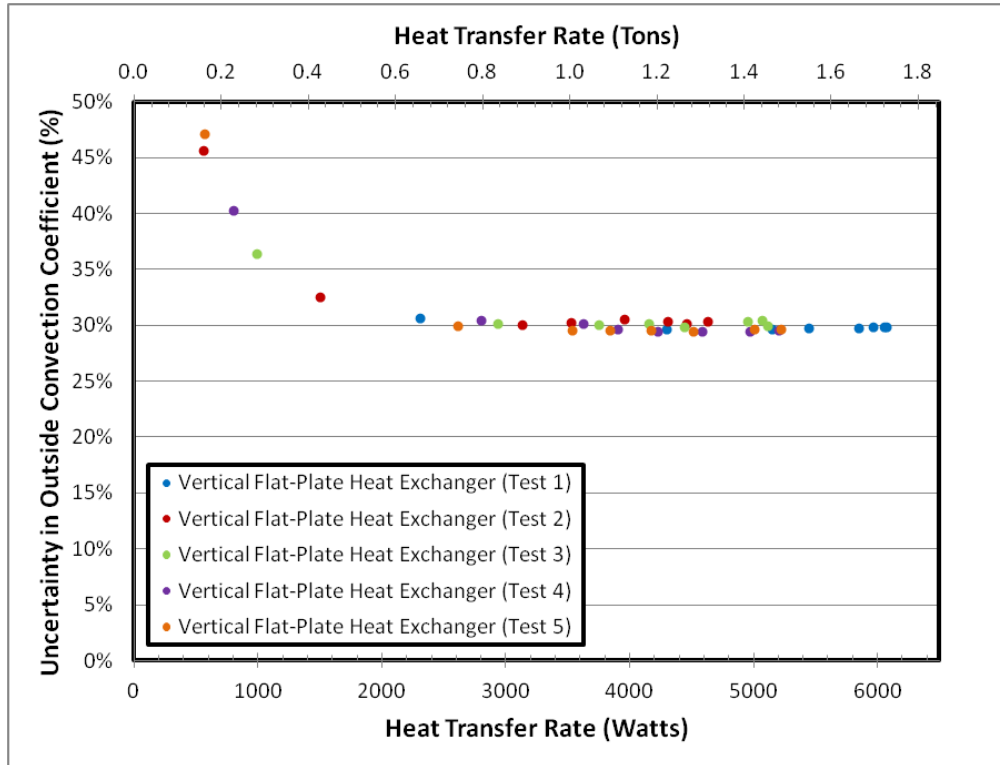


Figure 4-6. Outside Convection Coefficient Uncertainty vs. Heat Transfer Rate (Vertical Flat-Plate)

4.5.5 Bundle Coil Uncertainty Results

The percent uncertainty of the outside convection coefficient is provided in Figure 4-7. With respect to the heat transfer rate, the uncertainty percentage in outside convection coefficient for the bundled coils ranged from 8% to just below 50% (with two outliers) as the heat transfer rate ranged from 0.9 kW (3,071 Btu/hr) to 11 kW (37,534 Btu/hr). For the most part the graph shows the uncertainty staying relatively constant with the exception of a first few points of each coil being slightly higher. Like the spiral-helical coils, there is again the separation between the different tube diameters. Again this is because of the dimensional uncertainties and the flow rate differential causing lower temperature differences in the larger tubing.

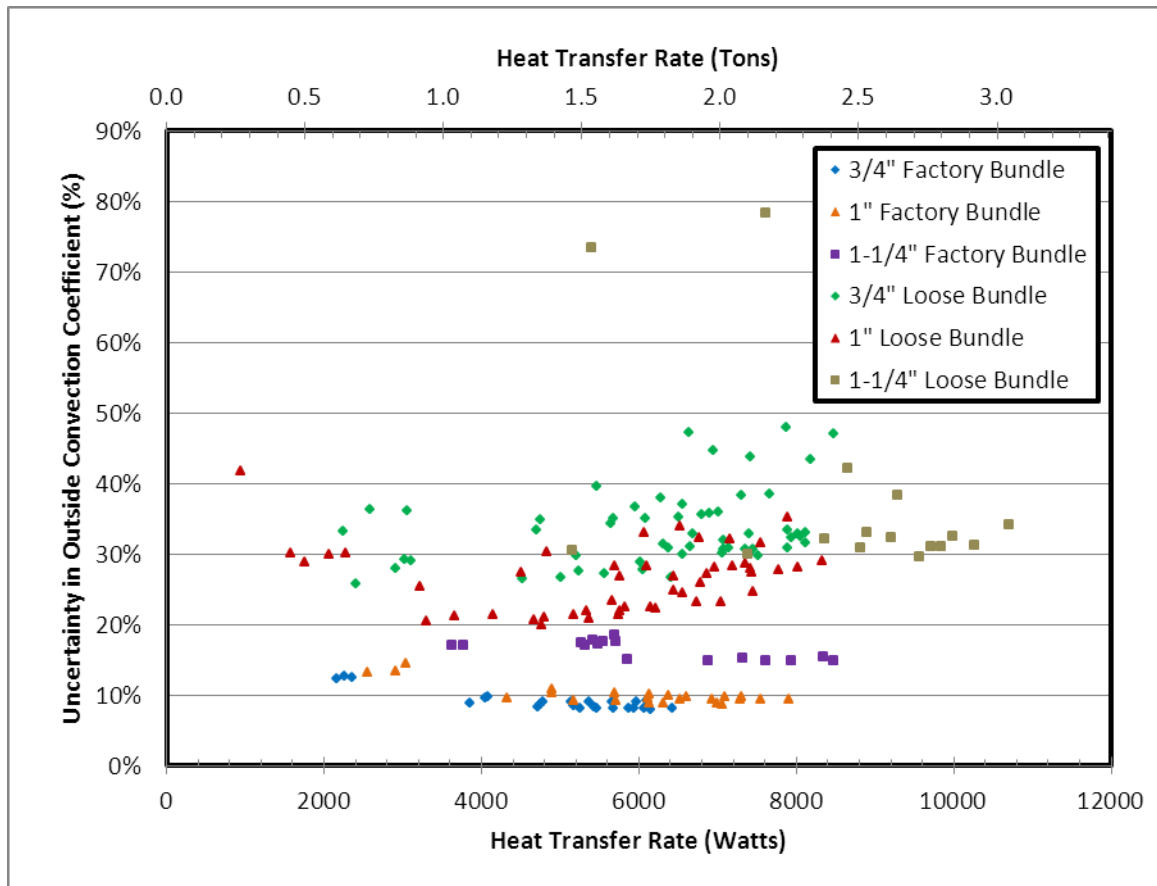


Figure 4-7. Outside Convection Coefficient Uncertainty vs. Heat Transfer Rate (Bundled Coils)

CHAPTER V

5. RESULTS AND DISCUSSION

5.1 HDPE SDR-11 Spiral-Helical SWHE Results

Over the course of 18 months, 66 tests were completed on the three different diameter tube coils. Each “test” contains eight heat transfer rates thus resulting in 528 data points. Although 66 tests over 18 months may seem like a low rate of productivity, there were delays caused by adverse weather conditions (e.g. the pond was frozen over for about a month) and the general adverse environment found when trying to make measurements on a submerged coil. Additional tests were performed, but failures in the piping (e.g. some of the joints leaked and/or separated), instrumentation (e.g. some of the thermistor leads were damaged, but as we were recording resistances, this was not always obvious until the resistances were converted back into temperature), or data acquisition (the computer got rained on when a sudden thunderstorm occurred) precluded their use in the correlations.

The successfully completed tests are described in more detail in Tables 5-1 through 5-3. Included in the testing matrix tables are the vertical and horizontal spacing of the configurations, the number of tests performed on each configuration, the number of set points for each test, and other pertinent geometrical dimensions.

Table 5-1. 19 mm ($\frac{3}{4}$ ") Nominal SDR-11 HDPE Spiral-Helical SWHE Test Matrix

3/4" Nominal SDR-11 HDPE Spiral-Helical Pond HX							
		Horizontal Spacing					
		38.1 mm (1.5 in)		66.7 mm (2.625 in)		104.8 mm (4.125 in)	
		Test Description	Coil Height	Test Description	Coil Height	Test Description	Coil Height
Vertical Spacing	38.1 mm (1.5 in)	3 Tests; 8 H.T. Rates (4/19/2011-4/20/2011)	21.6 cm (8.5 in)	3 Tests; 8 H.T. Rates (3/28/2011-3/29/2011) 3 Tests; 8 H.T. Rates (4/8/2011-4/11/2011)	17.8 cm (7 in)	1 Test; 8 H.T. Rates (3/8/2011)	17.8 cm (7 in)
	66.7 mm (2.625 in)	3 Tests; 8 H.T. Rates (4/21/2011)	36 cm (14.2 in)	3 Tests; 8 H.T. Rates (3/26/2011-3/27/2011) 3 Tests; 8 H.T. Rates (4/13/2011-4/14/2011)	36 cm (14.2 in)	6 Tests; 8 H.T. Rates (3/2/2011-3/5/2011)	29.5 cm (11.6 in)
	104.8 mm (4.125 in)	3 Tests; 8 H.T. Rates (4/22/2011-4/25/2011)	55.1 cm (21.7 in)	3 Tests; 8 H.T. Rates (3/30/2011-4/1/2011)	55.1 cm (21.7 in)	5 Tests; 8 H.T. Rates (3/17/2011-3/18/2011)	44.5 cm (17.5 in)
	Coil Inside Diameter	1.22 m (4 ft)		1.22 m (4 ft)		1.22 m (4 ft)	
	Coil Outside Diameter	1.67 m (5.5 ft)		1.98 m (6.5 ft)		2.44 m (8 ft)	

There are three independent geometric parameters for these tests: pipe diameter, vertical spacing, and horizontal spacing. Since all spiral-helical tests used 152.4 m (500 ft) coils, two other parameters, height and outside coil diameter, are dependent on these three parameters. For each of the independent parameters, three levels were utilized during the testing – three diameters, three horizontal spacings, and three vertical spacings. This represents 27 possible geometric configurations. Time has only allowed tests on 17 of the 27 configurations, though all parameters have been varied.

Although it would have been preferable to complete all 27 configurations, and for that matter to have additional levels of parameters, the 17 different configurations will all three parameters varied should be sufficient for correlation development. These correlations will be necessarily limited in their range of application.

Table 5-2. 1" Nominal SDR-11 HDPE Spiral-Helical Coil Test Matrix

1" Nominal SDR-11 HDPE Spiral-Helical Pond HX							
		Horizontal Spacing					
		38.1 mm (1.5 in)		66.7 mm (2.625 in)		104.8 mm (4.125 in)	
		Test Description	Coil Height	Test Description	Coil Height	Test Description	Coil Height
Vertical Spacing	38.1 mm (1.5 in)	3 Tests; 8 H.T. Rates; (10/04/2011-10/05/2011)	25.4 cm (10 in)	3 Tests; 8 H.T. Rates; (9/15/2011)	20.3 cm (8 in)	-	-
	66.7 mm (2.625 in)	-	-	3 Tests; 8 H.T. Rates; (9/7/2011-9/8/2011)	30.5 cm (12 in)	-	-
	104.8 mm (4.125 in)	-	-	3 Tests; 8 H.T. Rates; (9/13/2011)	43.2 cm (17 in)	3 Tests; 8 H.T. Rates; (6/17/2011-6/20/2011)	43.2 cm (17 in)
	Coil Inside Diameter	1.22 m (4 ft)		1.22 m (4 ft)		1.22 m (4 ft)	
	Coil Outside Diameter	1.7 m (5.6 ft)		1.98 m (6.5 ft)		2.16 m (7.8 ft)	

Table 5-3. 1-1/4" SDR-11 HDPE Spiral-Helical Coil Test Matrix

1-1/4" Nominal SDR-11 HDPE Spiral-Helical Pond HX							
		Horizontal Spacing					
		48.3 mm (1.9 in)		66.7 mm (2.625 in)		104.8 mm (4.125 in)	
		Test Description	Coil Height	Test Description	Coil Height	Test Description	Coil Height
Vertical Spacing	48.3 mm (1.9 in)	-	-	3 Tests; 8 H.T. Rates; (6/20/2011-6/22/2011)	25.4 cm (10 in)	3 Tests; 8 H.T. Rates (9/20/2011-9/21/2011)	25.4 cm (10 in)
	66.7 mm (2.625 in)	-	-	3 Tests; 8 H.T. Rates; (6/15/2011-6/16/2011)	35.6 cm (14 in)	3 Tests; 8 H.T. Rates (9/22/2011)	35.6 cm (14 in)
	104.8 mm (4.125 in)	-	-	-	-	3 Tests; 8 H.T. Rates (9/26/2011)	45.7 cm (18 in)
	Coil Inside Diameter	-		1.22 m (4 ft)		1.22 m (4 ft)	
	Coil Outside Diameter	-		1.98 m (6.5 ft)		2.44 m (8 ft)	

5.1.1 Outside Convection Coefficients

Using the methodology described in the previous section, the raw data was analyzed for all 66 tests. The variable of particular interest is the outside convection coefficient. Convective heat transfer generally has the form shown in Equation 5-1.

$$\dot{q}_{convection} = hA(T_s - T_{\infty}) \quad (5-1)$$

Where: $\dot{q}_{convection}$ is the convective heat transfer rate from a surface (W, Btu/hr)

h is the convection coefficient for the surface (W/m²-K, Btu/hr-ft²-°F)

A is the surface area (m², ft²)

T_s is the temperature of the surface (K or °F)

T_{∞} is the temperature of the surrounding ambient fluid (K or °F)

For buoyancy-driven convection heat transfer, it is expected that as the temperature difference between the surface and the fluid medium increases that the outside convection coefficient will also increase. Figure 5-1 shows several single tests for different configurations. As can be seen, the outside convection coefficient does in fact increase as the temperature difference increases.

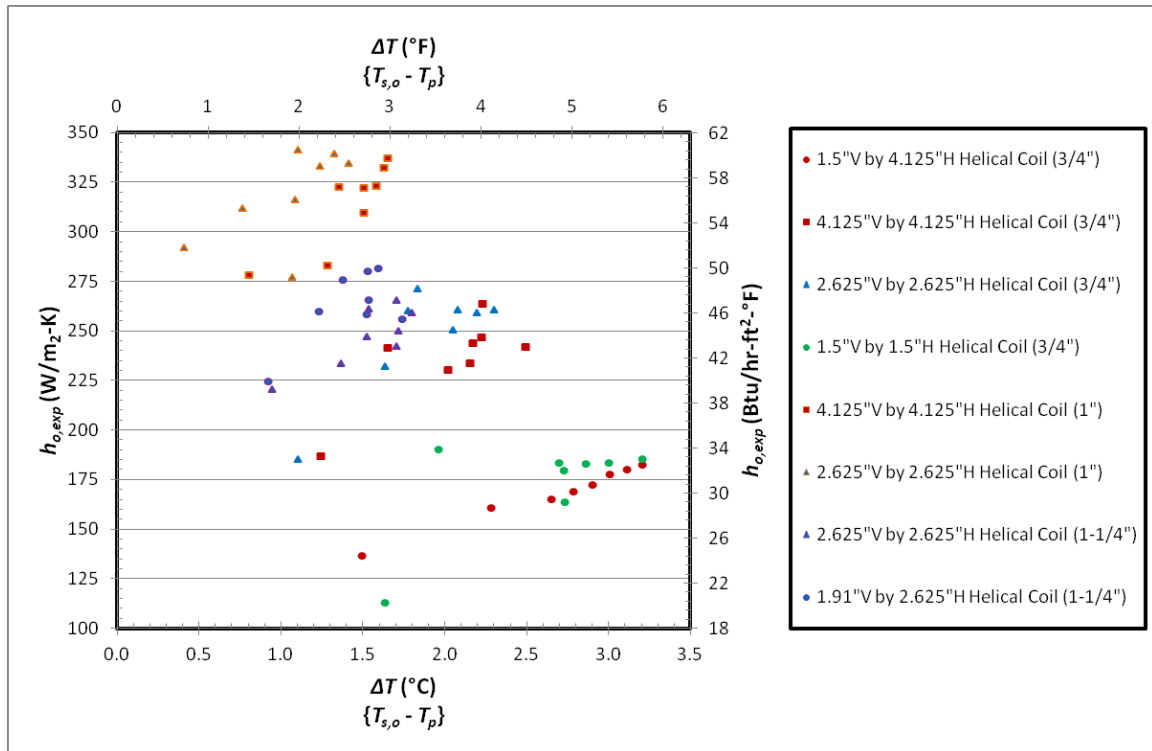


Figure 5-1.Spiral-Helical $h_{o,exp}$ vs. ΔT (Individual Tests)

Interestingly though, if data points from a narrow band of heat transfer rates are examined, it can be observed that the outside convection coefficient actually decreases as the temperature difference increases. To illustrate this, Figure 5-2 was created using heat transfer rates of $4,000 \pm 300$ W ($13,649 \pm 1,024$ Btu/hr), $7,000 \pm 300$ W ($23,885 \pm 1,024$ Btu/hr), and $10,000 \pm 300$ W ($34,121 \pm 1,024$ Btu/hr). This is a direct result of Equation 5-1. If the convection heat transfer is fixed and the geometry is changed while area is held constant, h and ΔT will be inversely related.

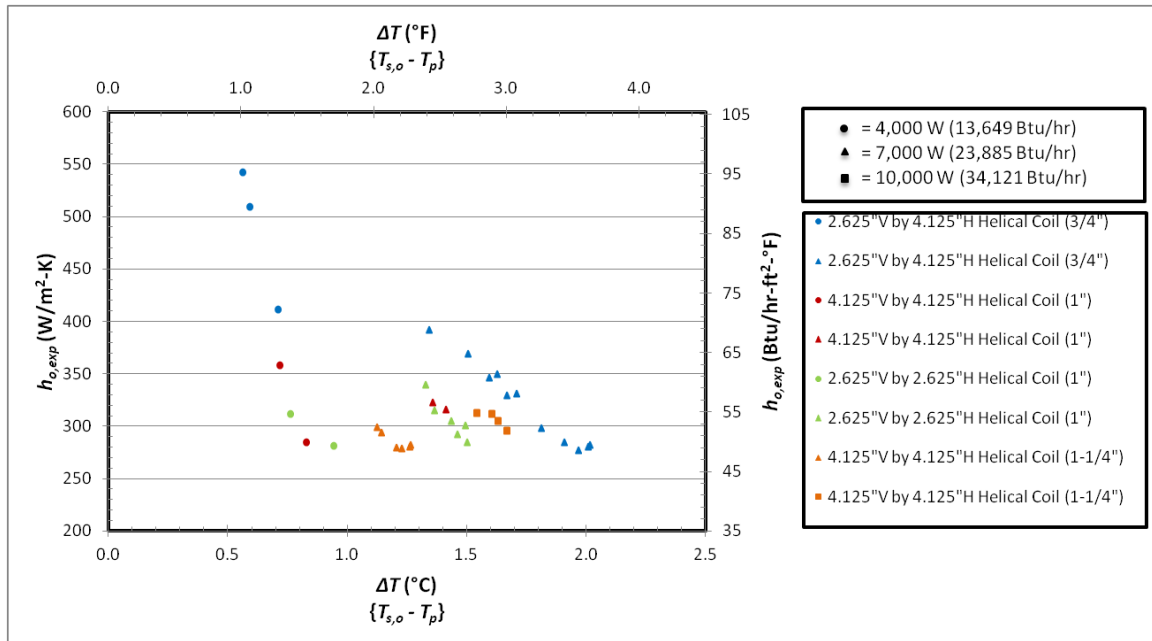


Figure 5-2. Spiral-Helical $h_{o,exp}$ vs. ΔT (Constant Heat Transfer Rates)

When all data points for a single coil diameter (with a fixed area) are plotted for experiments that used fixed heat input rates, this inverse relationship can be seen as shown in Figure 5-3. Figure 5-3 is all of the data points for the 19 mm ($\frac{3}{4}$ in) spiral-helical coils. Subtly hidden in the graph is that positive relationship between the heat transfer rate and the temperature difference. The heat transfer rate dependence is discussed in more detail later on about how it will be taken into account in the correlation development.

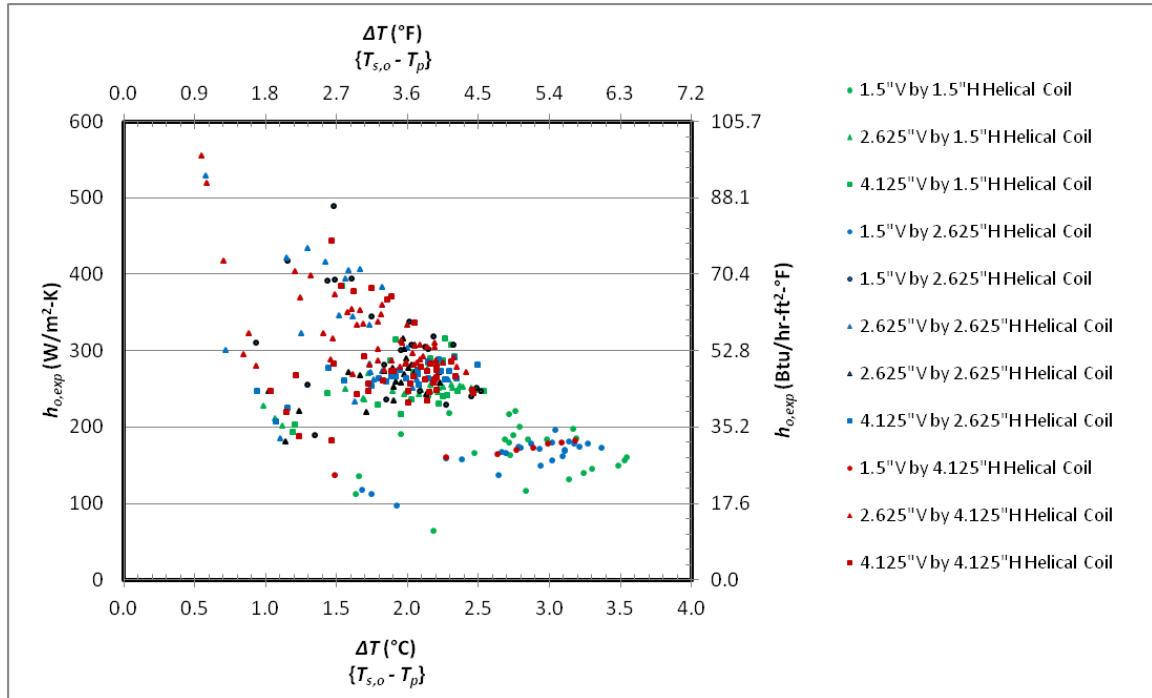


Figure 5-3. All 19 mm (3/4 in) Spiral-Helical SWHE Results ($h_{o,exp}$ vs. ΔT)

Figures 5-4 and 5-5 show the outside convection coefficient plotted against the outside pipe temperature difference for the 25 mm (1 in) and 32 mm (1-1/4 in) coils. In these two graphs the inverse relationship between the convection coefficient and the outside pipe temperature difference is diminished. As the power input is increased and the temperature difference increased the outside convection coefficient stays fairly constant for both tube diameters.

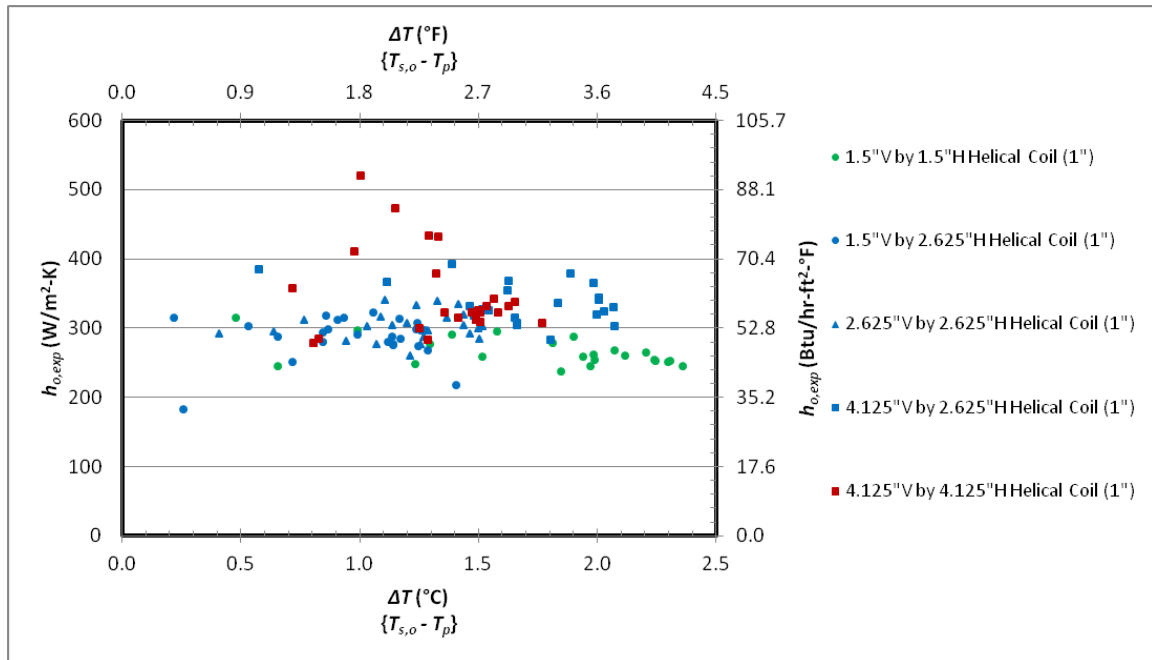


Figure 5-4. All 25 mm (1 in) Spiral-Helical SWHE Results ($h_{o,exp}$ vs. ΔT)

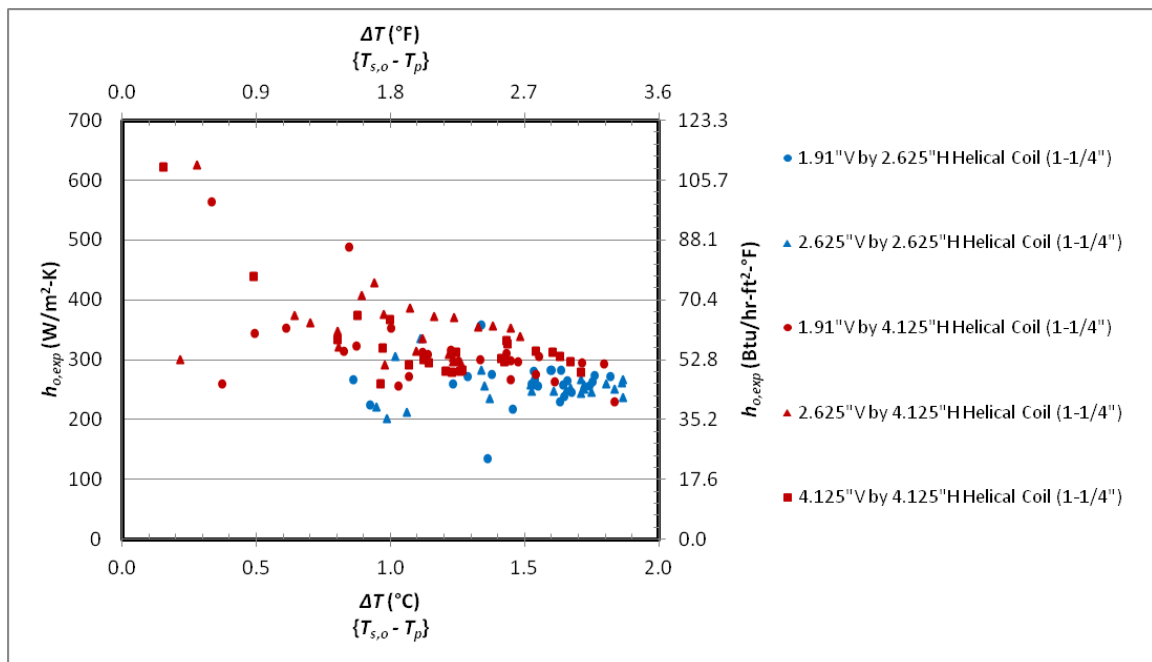


Figure 5-5. All 32 mm (1-1/4 in) Spiral-Helical SWHE Results ($h_{o,exp}$ vs. ΔT)

Further investigation into general performance trends for the 25.4 mm (1 in) and 32 mm (1-1/4 in) diameter coils led to a discovery involving the thermal resistances. Table 5-4 shows the

average percentage of the three thermal resistance quantities with respect to the total thermal resistance.

Table 5-4. Thermal Resistance Breakdown SDR-11 HDPE by Tube Size

Nominal Tube Size		Inside Convective Resistance	Tube Conductive Resistance	Outside Convective Resistance
19 mm	(3/4")	4%	59%	38%
25 mm	(1")	3%	69%	29%
32 mm	(1-1/4")	3%	73%	25%

Table 5-4 shows that as the HDPE tube increases in diameter, the effect of the outside convection is reduced. The dominant heat transfer resistance in SWHE using HDPE is the conductive resistance of the HDPE tube, at least at SDR-11 tube wall thicknesses.

The fact that the tube has such a high resistance and that the conductivity of the tube is not known as accurately as desired leads to high uncertainties in the value of $h_{o,exp}$. This may partly explain Figures 5-2 and 5-3. Other factors include the limited number of tests done for these tube diameters and the fact that buoyancy effects with water depend somewhat on how close the lake temperature near the coil is to the maximum density.

This leads to several recommendations for future research: additional tests of the 19 mm (1 in) and 32 mm (1-1/4 in) coils; a separate measurement of the conductive resistance could be used to reduce uncertainty; and, especially for application purposes, use of thinner-walled tube and/or tube with higher thermal conductivity should be investigated.

5.1.2 Spiral-Helical Correlation Development

As shown previously in the literature review, Nusselt-Rayleigh correlations are the dominant method for explaining natural/free convective heat transfer. Many different characteristic lengths have been used for correlations including outside tube diameter (Churchill and Chu 1975), tube length (Ali 2006), and coil height (Prabhanjan et al. 2004). For this

particular study, the correlations were tested with the different characteristic lengths of outside tube diameter (d_o), vertical spacing length (Δy), horizontal spacing length (Δx), and coil height (H). To account for the positive relationship between the power input and the outside convection coefficient, the modified Rayleigh number (Ra_L^*) suggested by Churchill and Chu (1975) was also tested in the different correlations.

For each of the forms, four different analysis parameters were calculated. The first was the mean bias error (MBE). This quantity is calculated using Equation 5-2 and shows on average how the correlation is predicting the outside convection coefficient. A positive value shows that the correlation is in general over predicting while a negative value means under prediction.

$$MBE = \frac{1}{n} \sum_{i=1}^n (h_{o,corr} - h_{o,exp}) \quad (5-2)$$

The second statistical measurement calculated between the correlation and the experimental data is the mean bias error percent (MBE %). This is calculated using Equation 5-3. This measurement will be different than the MBE divided by the average heat transfer coefficient, as errors for experimental points with small absolute values get equal weighting.

$$MBE \% = \frac{1}{n} \sum_{i=1}^n \left(\frac{h_{o,corr} - h_{o,exp}}{h_{o,exp}} \right) \quad (5-3)$$

The third correlation comparison that was calculated was the root mean square error (RMSE). Equation 5-4 shows how the RMSE was calculated. This measurement is often used as a goodness-of-fit measure.

$$RMSE = \sqrt{\frac{1}{n} \sum_{i=1}^n (h_{o,corr} - h_{o,exp})^2} \quad (5-4)$$

The fourth and final parameter used for comparing the between the correlations was the root mean square error percent (RMSE %). Again errors for measurements with small absolute values

get equal weighting. This means that a few data points with small heat transfer rates and high uncertainty can make the RMSE % quite high.

$$RMSE \% = \sqrt{\frac{1}{n} * \sum_{i=1}^n \left(\frac{h_{o,corr} - h_{o,exp}}{h_{o,exp}} \right)^2} \quad (5-5)$$

The simplest form of the correlations tested was similar to that of Prabhanjan et al. (2004). Nusselt number is correlated using two empirical parameters (a,b) and a Rayleigh number (either the standard form of Rayleigh or the modified form) as shown in Equation 5-6.

$$Nu_L = a(Ra_L)^b \text{ OR } Nu_L = a(Ra_L^*)^b \quad (5-6)$$

The two-parameter correlations are shown in Table 5-5. The highlighted last column is the only correlation that yielded an RMSE % of less than 25%. This correlation form will be refined later using only measurements with uncertainties less than $\pm 70\%$, as described in Section 5.1.4.

Table 5-5. Statistics and Coefficients of the Two-Parameter Nusselt-Rayleigh Correlation

	$Nu_L = a(Ra_L)^b \text{ or } Nu_L = a(Ra_L^*)^b$							
Parameter	$T_{ref} = T_{pond,tree,avg}$							
	$L = D$		$L = H$		$L = \Delta y$		$L = \Delta x$	
	Ra_D	Ra_D^*	Ra_H	Ra_H^*	$Ra_{\Delta y}$	$Ra_{\Delta y}^*$	$Ra_{\Delta x}$	$Ra_{\Delta x}^*$
MBE	-6.38	-2.15	-9.59	-2.88	-10.25	-3.16	-10.30	-3.2
MBE,%	5.8%	5.1%	4.4%	4.4%	3.7%	4.0%	3.2%	3.3%
RMSE	86.4	70.8	91.5	70.9	91.7	70.2	90.2	66.9
RMSE,%	39.2%	28.8%	39.5%	27.5%	37.9%	26.2%	36.0%	24.0%
a	1.31	0.37	0.27	0.21	0.14	0.17	0.063	0.083
b	0.179	0.230	0.309	0.260	0.345	0.273	0.394	0.310

To increase the accuracy of the correlation, a correction factor was added onto the first correlation form to account for either the influence of the vertical spacing or the horizontal spacing. To make the correction factor dimensionless, the spacing term was divided by the

outside tube diameter. The results of the correlations with a single correction factor are shown in Table 5-6. The increase in accuracy from the two-parameter correlation to the three-parameter correlation for the regular Rayleigh form is between 1.6% and 4.4% in the RMSE %. For the modified Rayleigh form, the increase was between almost 0% and 4.1% Again, the highlighted correlation columns have an RMSE % of less than 25% and will be further refined in Section 5.1.4.

Table 5-6. Statistics and Coefficients of the Three-Parameter Nusselt-Rayleigh Correlation

	$Nu_L = a(Ra_L)^b (CF)^c$ or $Nu_L = a(Ra_L^*)^b (CF)^c$											
Parameter	$T_{ref} = T_{pond, tree, avg}$											
	$L_{char} = D$				$L_{char} = H$				$L_{char} = \Delta y$		$L_{char} = \Delta x$	
	Ra_D		Ra_D^*		Ra_H		Ra_H^*		$Ra_{\Delta y}$	$Ra_{\Delta y}^*$	$Ra_{\Delta x}$	$Ra_{\Delta x}^*$
	$CF = \Delta y/D$	$CF = \Delta x/D$	$CF = \Delta y/D$	$CF = \Delta x/D$	$CF = \Delta y/D$	$CF = \Delta x/D$	$CF = \Delta y/D$	$CF = \Delta x/D$	$CF = \Delta x/D$	$CF = \Delta x/D$	$CF = \Delta y/D$	$CF = \Delta y/D$
MBE	-6.61	-5.88	-2.49	-1.95	-6.07	-7.12	-1.86	-1.78	-7.18	-1.79	-9.76	-3.14
MBE, %	5.3%	5.1%	4.5%	4.1%	5.4%	4.3%	5.0%	4.2%	4.3%	4.2%	3.0%	3.2%
RMSE	85.9	82.5	69.7	65.1	83.9	83.9	69.2	65.2	84.0	65.2	88.3	66.3
RMSE, %	37.7%	35.7%	26.7%	24.6%	37.4%	35.1%	27.6%	24.7%	34.9%	24.7%	34.0%	23.4%
a	0.95	0.44	0.27	0.16	2.25	0.18	0.50	0.18	0.15	0.19	0.070	0.088
b	0.199	0.244	0.245	0.266	0.190	0.315	0.220	0.257	0.319	0.257	0.381	0.304
c	0.083	0.277	0.107	0.293	0.443	0.362	0.188	0.276	0.374	0.269	0.155	0.070

In the third correlation form (four-parameter) there are two correction factors for the vertical spacing and the horizontal spacing. In this correlation form, the characteristic length was limited to either the outside tube diameter or the coil height to prevent duplicate representation of a single variable in the correlation. The four-parameter correlations are found in Table 5-7. Improvements to the accuracy for the four-parameter correlation from the three-parameter correlation are smaller than those found going from two parameters to three parameters. This shows that the addition of more terms is not necessarily beneficial in proportion to the increased complexity of the correlation.

Table 5-7. Statistics and Coefficients of the Four-Parameter Nusselt-Rayleigh Correlation

	$Nu_L = a(Ra_L)^b (\Delta y/D)^c (\Delta x/D)^d$ or $Nu_L = a(Ra_L^*)^b (\Delta y/D)^c (\Delta x/D)^d$			
Parameter	$T_{ref} = T_{pond,tree,avg}$			
	$L_{char} = D$		$L_{char} = H$	
	Ra_D	Ra_D^*	Ra_H	Ra_H^*
MBE	-5.92	-1.99	-6.04	-1.93
MBE,%	5.0%	4.0%	4.9%	4.1%
RMSE	82.5	65.1	82.4	65.1
RMSE,%	35.5%	24.5%	35.6%	24.5%
a	0.43	0.16	0.73	0.14
b	0.245	0.267	0.243	0.266
c	0.012	0.014	0.262	-0.042
d	0.272	0.286	0.208	0.299

A final form of the correlation (five-parameter) that was examined used the outside tube diameter as the characteristic length, a vertical spacing correction factor, a horizontal spacing correction factor, and a coil height correction factor. However, since all coils have the same length, the vertical spacing correction and the height of the coil are not independent of each other and in fact; no improvement in RMSE is gained over the four-parameter correlation. The results of the five-parameter correlations are shown in Table 5-8.

Table 5-8. Statistics and Coefficients of the Five-Parameter Nusselt-Rayleigh Correlation

	$Nu_D = a(Ra_D)^b (\Delta y/D)^c (\Delta x/D)^d (H/D)^e$	
	$Nu_D = a(Ra_D^*)^b (\Delta y/D)^c (\Delta x/D)^d (H/D)^e$	
Parameter	$T_{ref} = T_{pond,tree,avg}$	
	Ra_D	Ra_D^*
MBE	-6.0	-2.0
MBE,%	5.0%	4.0%
RMSE	82.4	65.1
RMSE,%	35.6%	24.5%
a	0.66	0.16
b	0.241	0.267
c	0.193	0.015
d	0.223	0.286
e	-0.197	-0.001

5.1.3 Correlation to Experimental Comparisons

A simple way to compare how well a correlation predicts the actual values is to graph them against each other. If the data points lie on the positive diagonal (solid purple line) then the correlation predicts the experimental value exactly. If the data point lies above the diagonal then the correlation is over-predicting. Alternatively, if the data point lies below the diagonal then the correlation is under-predicting. Figure 5-6 is an example of one such plot using the four-parameter correlation given in the 2nd column of Table 5-7. Reference lines of $\pm 25\%$ and $\pm 50\%$ have been added to the graph.

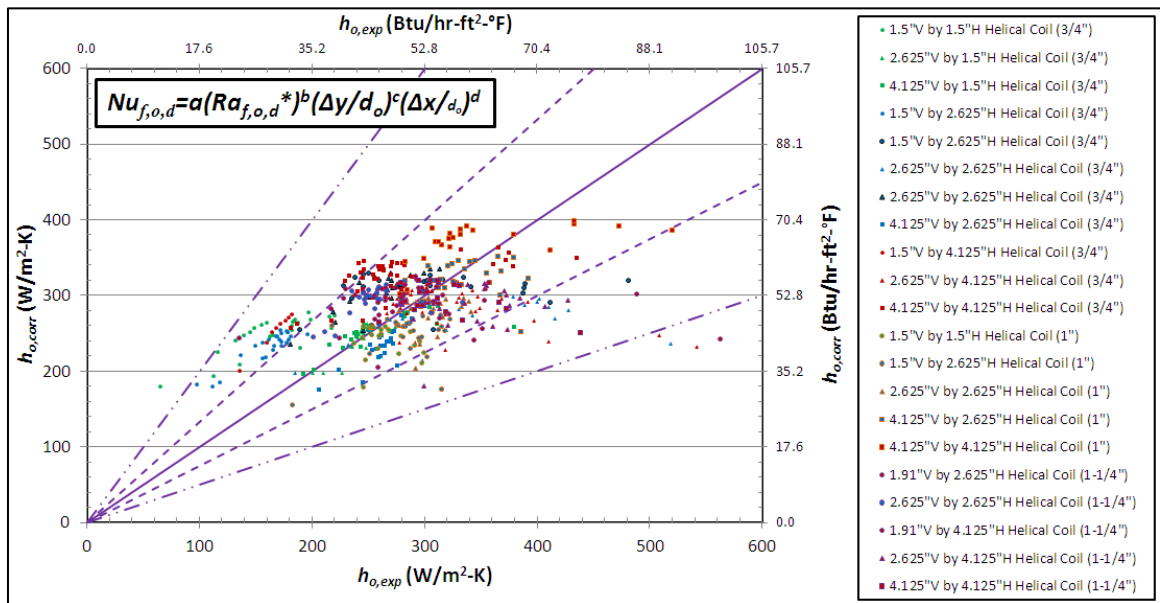


Figure 5-6. Spiral-Helical Results vs. Correlation ($h_{o,exp}$ vs. $h_{o,corr}$)

Figure 5-6 shows that this particular correlation fits the experimental data well because a majority of the data points lie inside the error lines of $\pm 25\%$. There are a fair number of points that lie outside the $\pm 25\%$ error lines as well as five points that fall outside of the $\pm 50\%$. Also, The slope of the data points for similar configurations is important to the correlation form. If the points are scattered horizontally then the form of the correlation does not account for all pertinent factors. If the data points have a 1-to-1 slope (equality line slope) then the form of the correlation is correct or near correct.

Another way the correlation was checked to see how well it matched the experimental data was in a Nusselt-Rayleigh plot. Figure 5-7 shows all of the spiral-helical data points graphed in terms of Nusselt number and the modified Rayleigh number which uses the outside tube diameter as the characteristic length. Also graphed on the plot are correlations (using 2nd column of Table 5-7) for the smallest configuration of the 19 mm (¾ in) diameter tube and largest configuration for the 32 mm (1-¼ in) diameter tube. Again it can be seen that a majority of the data points fall in near the correlation curves, with some notable outliers.

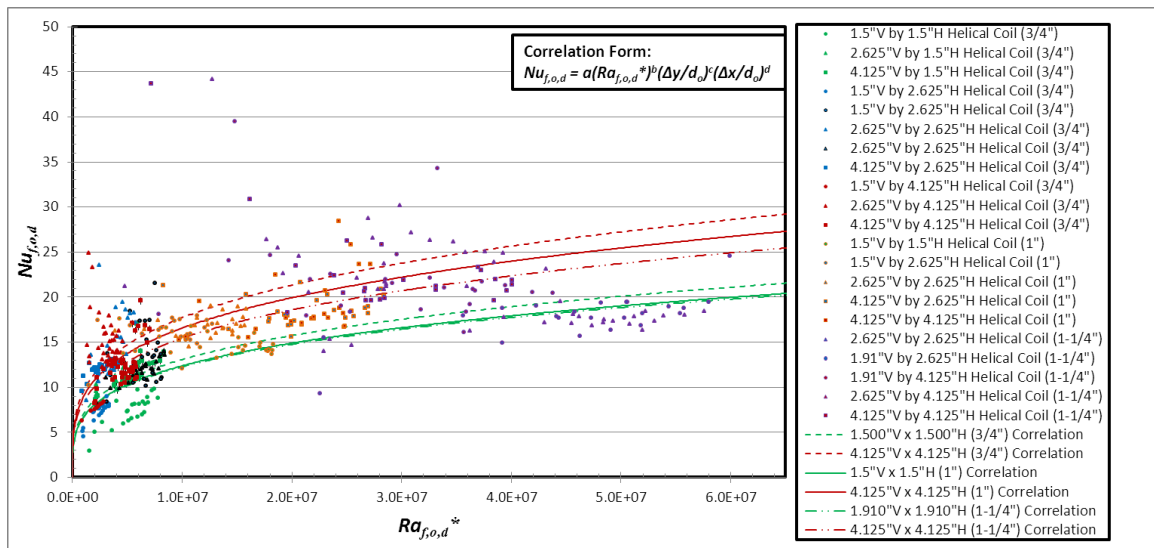


Figure 5-7. Spiral-Helical Results vs. Correlation ($Nu_{f,o,d}$ vs. $Ra_{f,o,d}^*$)

The final check to see how well the correlations were working came in the form of a comparison between the experimental and correlation heat transfer rates. Like the outside convection coefficient plot, when the data points lie on the equality line (solid purple) than the correlation is predicting the heat transfer rate perfectly. Included in Figure 5-8 are reference error lines of $\pm 10\%$, $\pm 20\%$, and $\pm 30\%$.

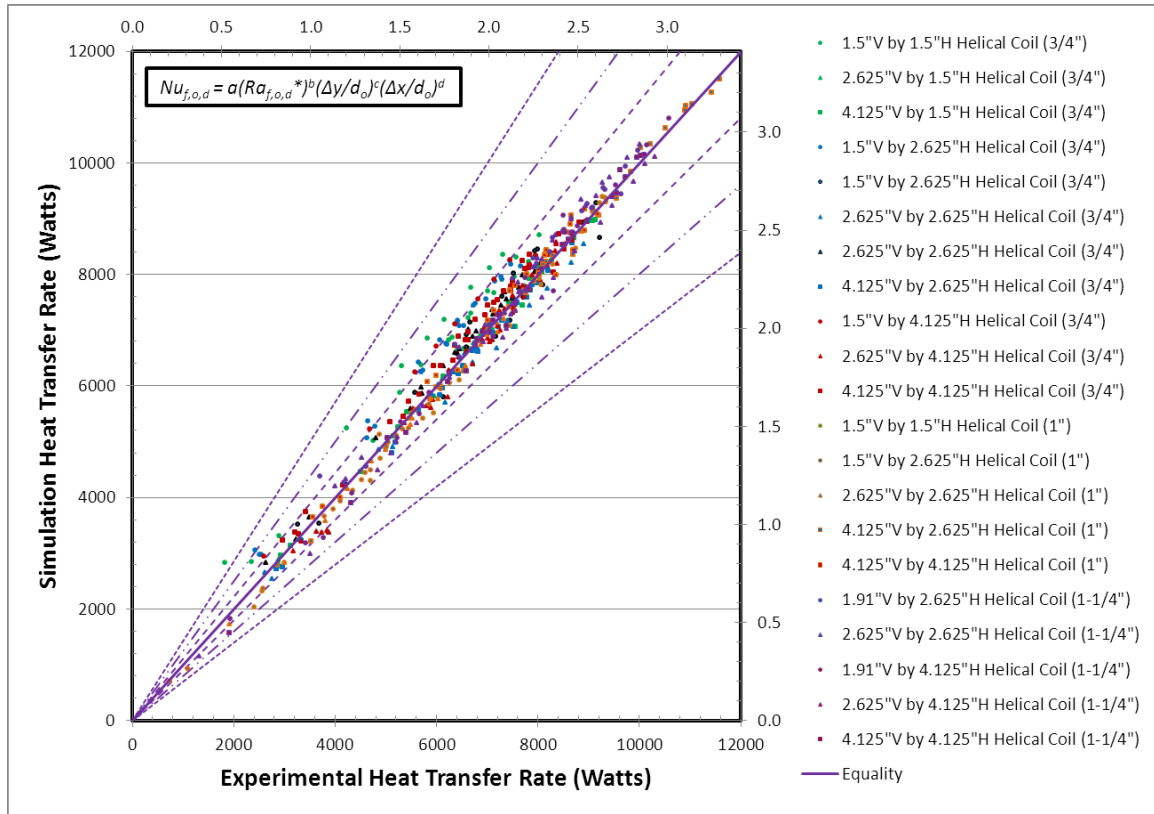


Figure 5-8. Spiral-Helical Results vs. Correlation ($Q_{c,exp}$ vs. $Q_{c,corr}$)

Figure 5-8 shows that even though there are a number of data points that show relatively high values of error in the outside convection coefficient, the heat transfer rate is still predicted accurately. Of the 528 data points, only 38 of them (~8%) are outside of the $\pm 10\%$ error lines. This is because of the dominant effect of the tube conductive resistance on the heat transfer. E.g. for a typical 32 mm (1-1/4 in) coil, a 25% error in the exterior convection coefficient would only represent a 5.4% error in the total thermal resistance, a 5.7% error in the UA, and a 4.4% error in the heat transfer rate.

5.1.4 Correlation Refinement

Despite the fact that the exterior convection correlation gives very good predictions of the total heat transfer rate, the RMSE % errors reported for the convection coefficients are fairly high – close to 25%. As these values tend to be dominated by a small number of experimental measurements at the lower heat transfer rates with higher uncertainties, some concern arose as to

whether the correlations might be unduly influenced by a few high-uncertainty measurements. Furthermore, these high-uncertainty measurements correspond to the lowest heat transfer rates, well away from design conditions, where the correlations are most important. This was shown in Figure 4-4. Therefore, the effect of removing some experimental measurements from the data set used for the correlations was investigated. This took the form of a “data filter” where measurements that had percentage uncertainties above a certain value were removed from the data set.

Instead of testing all of the correlation forms, the ones with an RMSE % less than 25% were chosen to be refined. Table 5-9 is a list of the correlations that were used with a data filter. A number was assigned to each correlation to make identification easier.

Table 5-9. Correlation Equations for Refinement

Correlation #	Correlation
1	$Nu_{\Delta x} = a(Ra_{\Delta x}^*)^b$
2	$Nu_D = a(Ra_D^*)^b (\Delta x/D)^c$
3	$Nu_H = a(Ra_H^*)^b (\Delta x/D)^c$
4	$Nu_{\Delta y} = a(Ra_{\Delta y}^*)^b (\Delta x/D)^c$
5	$Nu_{\Delta x} = a(Ra_{\Delta x}^*)^b (\Delta y/D)^c$
6	$Nu_D = a(Ra_D^*)^b (\Delta y/D)^c (\Delta x/D)^d$
7	$Nu_H = a(Ra_H^*)^b (\Delta y/D)^c (\Delta x/D)^d$
8	$Nu_D = a(Ra_D^*)^b (\Delta y/D)^c (\Delta x/D)^d (H/D)^e$

The data filter values that were selected for comparison were $\pm 100\%$, $\pm 80\%$, $\pm 70\%$, $\pm 60\%$ and $\pm 50\%$. Any data point that contained an uncertainty value of greater than the data filter value was removed from the data set used for the correlation. A comparison graph of the different filter values is provided in Figure 5-9. Each correlation is graphed with the RMSE % vs. the filter value. Also incorporated in the graph is the number of data points at each filter value. As the filter value was decreased, the number of data points was also decreased. A lower boundary value was

determined based on the results and the number of data points included in the correlation. Too small of data set could result in an erroneous correlation.

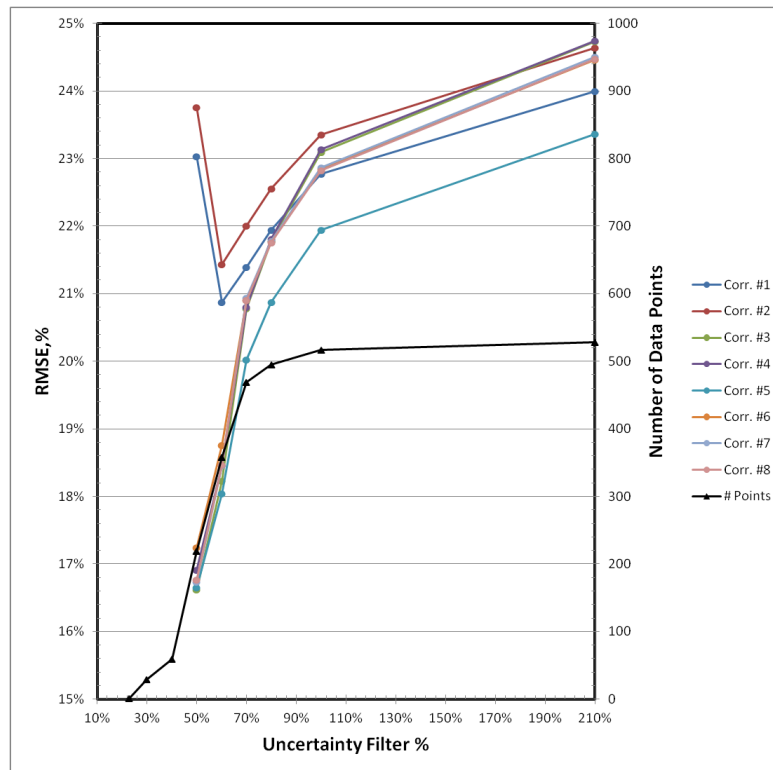


Figure 5-9. Correlation Refinement with RMSE % Results

When the data filter is reduced to 100% uncertainty, the RMSE % of all of the equations drops by roughly 1% while filtering out 11 data points. As the filter is continually reduced to 70% uncertainty, the RMSE % continues to drop for all correlations. At this uncertainty, the data pool has been reduced by 59 data points or roughly 11%. Of the eight correlations, the RMSE % on six of them was reduced below 21% with the smallest one being 20%.

The additional two filters of $\pm 60\%$ and $\pm 50\%$ uncertainty were applied to the correlations but adverse effects started to appear due to the shrinking data pool size. When the data filter was set to $\pm 60\%$, the number of data points was reduced from 528 down to 370 meaning that the data pool was reduced by nearly one-third. Although the RMSE % was again reduced by another 1% in most cases, an investigation revealed that much of the 25 mm (1 in)

and 32 mm (1-¼ in) tube data had been removed. The breakdown of the points for each tube size with respect to the filter level is given in Table 5-10.

Table 5-10. Data Point Distribution for Uncertainty Filter Results

Nominal Tube Size		Uncertainty Data Filter					
		All	100%	80%	70%	60%	50%
19 mm	0.75 in	288	287	284	279	258	209
25 mm	1 in	120	116	107	97	34	1
32 mm	1.25 in	120	114	104	93	66	9

Looking at the $\pm 50\%$ data filter results in Figure 5-9 shows another interesting consequence that comes from reducing the filter too much. For correlations #1 and #2 the RMSE % actually goes up from filter levels $\pm 60\%$ to $\pm 50\%$. This is not an error in the graph but instead a result of how the optimization routine works as well as too many data points being removed from the data pool, mostly from the two larger tube sizes. The Nelder-Mead simplex optimizes on RMSE, not RMSE %. Figure 5-10 shows how the RMSE varies with the different filter levels. Note that for each filter, the RMSE does in fact decrease.

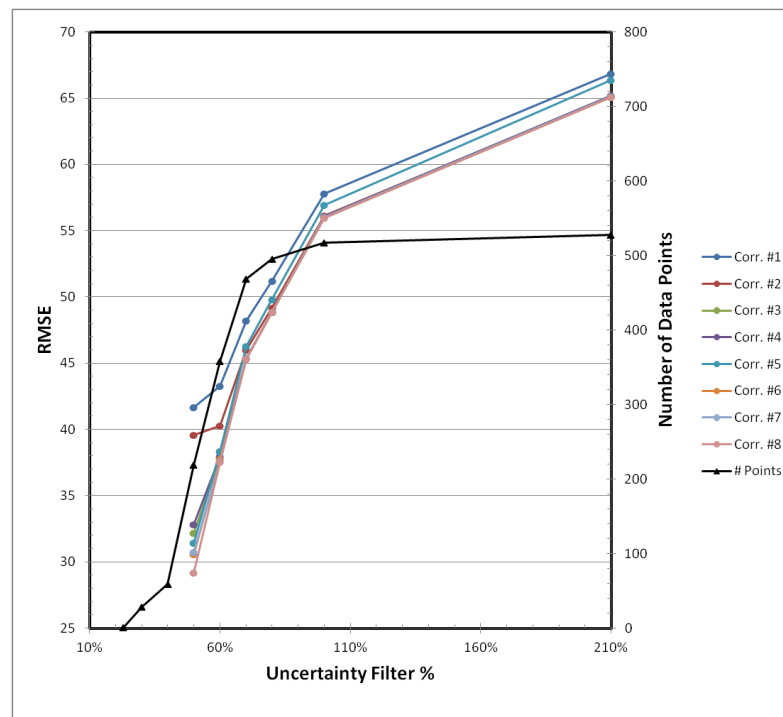


Figure 5-10. Correlation Refinement with RMSE Results

After taking into account all of the evidence previously presented, it was decided that an uncertainty filter level of $\pm 60\%$ was too high in order to maintain sufficient quantities of 25 mm (1 in) and 32 mm (1-¼ in) data points. The filter level of $\pm 70\%$ provides ample data points for all tube sizes as well as a decent reduction in RMSE and RMSE% and thus was chosen as the best filter level. Table 5-11 gives the statistical values as well as the coefficients for each of the eight correlations at the $\pm 70\%$ filter level.

Table 5-11. $\pm 70\%$ Uncertainty Filter Correlation Results

Correlation Form:	$Nu_L = a(Ra_L^*)^b (\Delta y/d_o)^c (\Delta x/d_o)^d (H/d_o)^e$							
Correlation #:	1	2	3	4	5	6	7	8
MBE	-1.8	-0.5	-0.7	-0.8	-1.5	-0.7	-0.6	-0.7
MBE, %	2.6%	3.4%	3.1%	3.0%	2.5%	3.1%	3.2%	3.1%
RMSE	48.2	46.0	45.4	45.3	46.3	45.3	45.4	45.3
RMSE, %	21.4%	22.0%	20.8%	20.8%	20.0%	20.9%	20.9%	20.9%
L	Δx	d_o	H	Δy	Δx	d_o	H	d_o
a	0.091	0.18	0.127	0.15	0.099	0.16	0.15	0.16
b	0.303	0.258	0.269	0.268	0.294	0.264	0.263	0.264
c	0	0	0	0	0.120	0.078	0.029	0.082
d	0	0.260	0.250	0.229	0	0.223	0.234	0.222
e	0	0	0	0	0	0	0	-0.005

From Table 5-11 it is obvious to see that correlations #3 through #8 provide the best RMSE and RMSE %. Correlations #3, #4, and #5 are essentially the same for the reason that the tube length was a constant 152.4 m (500 ft) and thus the coil height and vertical spacing are not independent of each other. They do however provide a RMSE % of about 21% and for all practical purposes work for calculations.

From a buoyancy-driven flow perspective, the vertical spacing or height should have some influence on the outside convection coefficient. Yet correlation #5 performs slightly better than the other correlations from the perspective of RMSE %, though it has the highest RMSE of 45.3.

Correlations #6 and #8 are the same with the five-parameter form having an additional term for the height. From a theoretical, buoyancy-driven heat transfer stand point, these two correlations make the most sense because the tube diameter effects, vertical spacing effects, and the horizontal spacing effects all have their own parameter that can adjust for different configurations. Looking at the coefficients provides evidence that there is negligible influence from the coil height beyond that which is already included in the vertical spacing parameter. The statistical values for the two correlations are identical but the complexity of adding a fifth parameter for almost no improvement makes correlation #8 less desirable. For the above mentioned reasons, correlation #6 shown as Equation 5-7 below is recommended for use. All further analysis on spiral-helical coils and applications of spiral-helical coils.

$$Nu_{f,o,d_o} = 0.16(Ra_{f,o,d_o}^*)^{0.264} \left(\frac{\Delta y}{d_o}\right)^{0.078} \left(\frac{\Delta x}{d_o}\right)^{0.223} \quad (5-7)$$

Where: Nu_{f,o,d_o} is the outside Nusselt number calculated at the outside film temperature using the outside tube diameter as the characteristic length

Ra_{f,o,d_o}^* is the outside modified Rayleigh number calculated at the outside film temperature using the outside tube diameter as the characteristic length

Δy is the vertical center-to-center distance between tubes (mm, in)

Δx is the horizontal center-to-center distance between tubes (mm, in)

d_o is the outside tube diameter (mm, in)

Range of applicability: $3.3 \times 10^5 < Ra_{f,o,d_o}^* < 6.0 \times 10^7$

$38.1 \text{ mm (1.5 in)} < \Delta y < 104.8 \text{ mm (4.125 in)}$

$38.1 \text{ mm (1.5 in)} < \Delta x < 104.8 \text{ mm (4.125 in)}$

$21.8 \text{ mm (0.86 in)} < d_i < 34.5 \text{ mm (1.358 in)}$

$26.7 \text{ mm (1.050 in)} < d_o < 42.2 \text{ mm (1.660 in)}$

$1.2 \text{ m (4 ft)} < D_c < 2.4 \text{ m (8 ft)}$

$L_c = 152.4 \text{ m (500 ft)}$

To compare the improvement between the non-filtered and filtered correlations two tests were conducted. The first was to see how much the RMSE % decreased on the heat transfer rate from one to the other. The non-filtered correlation yielded an RMSE % of 6.0% while the filtered correlation was only 5.8%. The second comparison was to graph the values of heat transfer rates against each other, similar to how the experimental heat transfer rates were graphed against the simulation results. Again, if the data points lie on a straight line with a slope of one, the two values are identical. Figure 5-11 shows the non-filtered heat transfer rates plotted against the filtered heat transfer rates.

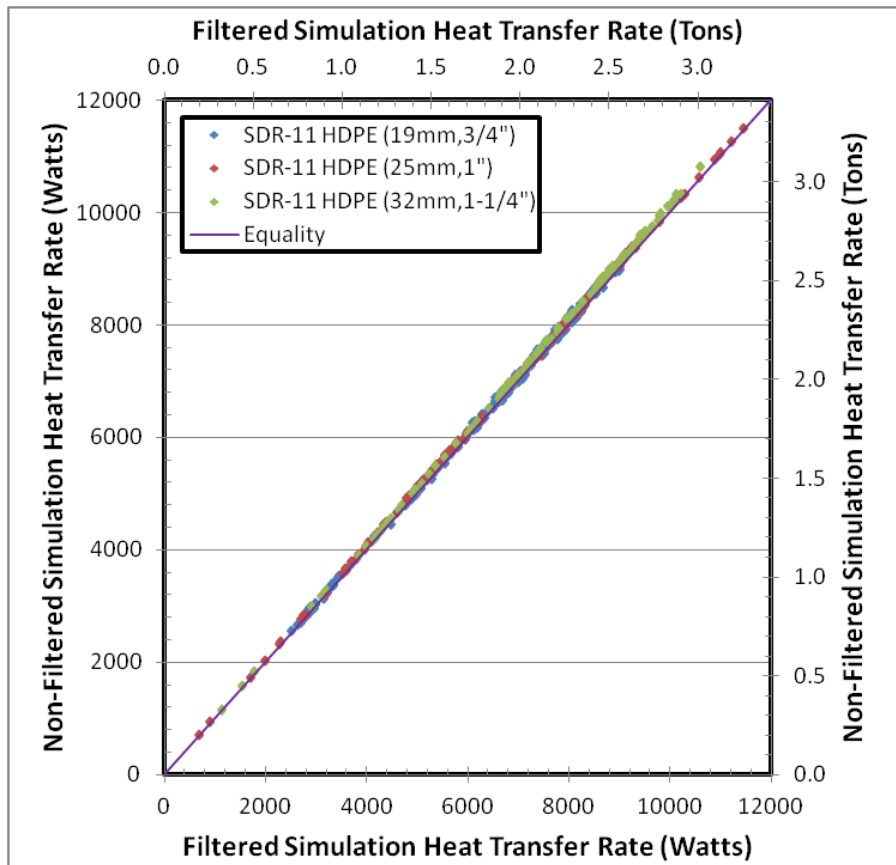


Figure 5-11. Simulation Heat Transfer Rate Comparison (Filtered vs. Non-Filtered)

Looking at the two tests used to compare the filtered and non-filtered correlations only leaves one conclusion to be made: very minimal improvement is gained in filtering the data. Even though this is true, Equation 5-7 will still be used throughout the remainder of this thesis.

5.2 Lake Bottom Proximity Testing Results

An aspect of testing that was looked into when testing the spiral-helical coil configurations was whether or not the suspension of the coil above the lake bottom really caused a significant increase in outside convection. To test this hypothesis, a 1" SDR-11 HDPE coil with 6.7 cm (2.625") vertical spacing and with 6.7 cm (2.625") horizontal spacing was tested suspended 0.7 m (2.2 ft) above the pond bottom, then lowered to the pond bottom and retested.

The coil was suspended in the water with the bottom of the coil at a depth of 1.5 m (5 ft) and the test was started. Data was recorded every ten seconds for a period of approximately four hours, of which two hours was needed to achieve a steady-state condition. At 12:32 PM on 9/6/2011 the coil was lowered to the bottom of the testing pond which was measured to be 2.2 m (7.2 ft) in depth from the surface of the pond. A transition period of ten minutes followed where the conditions were changing until a new steady state was reached. The temperatures of the testing pond at the top, middle, and bottom of the coil (squares with line) as well as the outside convection coefficient (circles) for the coil are graphed together in Figure 5-12.

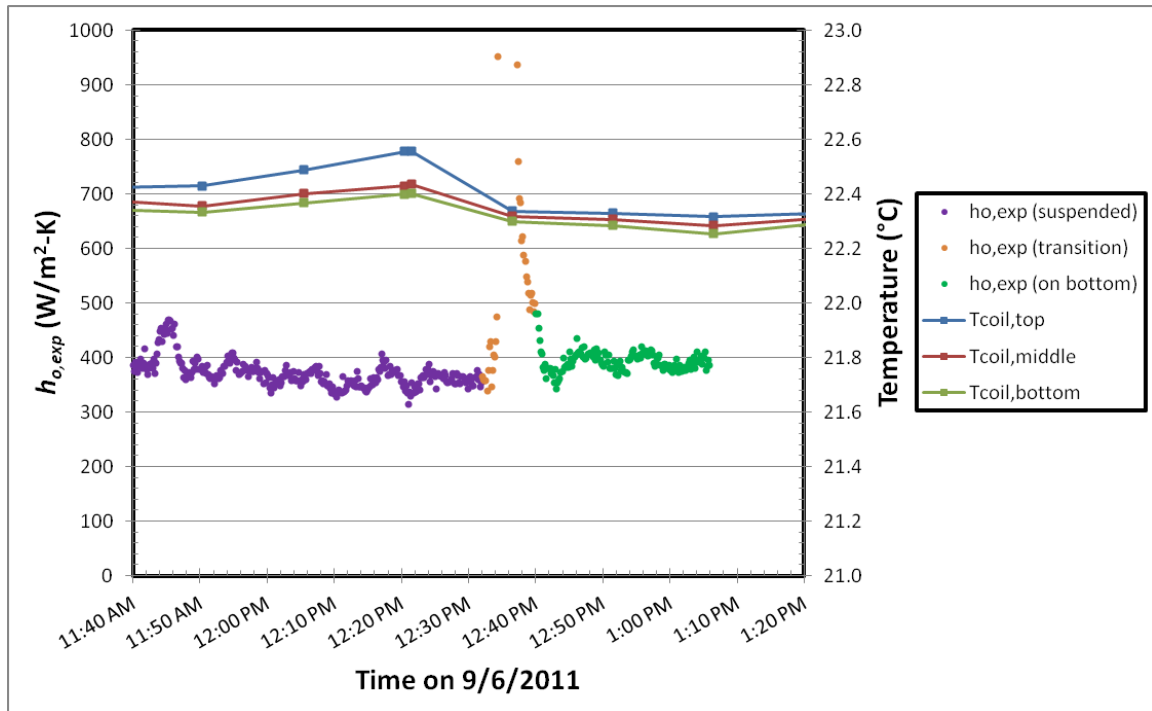


Figure 5-12. Spiral-Helical SWHE Lake Bottom Proximity Tests Results

By looking at the graph it can be seen that the temperature of the testing pond around the coil became cooler once the coil was lowered to the bottom of the testing pond. This is because of the slight stratification in the pond. Also noticeable is a sharp rise in the convection coefficient. This increase may be due to several effects: disturbances in the boundary layer, the extra motion created when lowering the heat exchanger, and the dynamics of changing the exterior pond temperature while the interior fluid temperatures were still in equilibrium with the previous exterior pond temperatures. However, this was not investigated further because of the limited practical application. The change in the outside convection coefficient from an average value of $360 \text{ W/m}^2\text{-K}$ ($63 \text{ Btu/hr-ft}^2\text{-}^\circ\text{F}$) before lowering the coil to $390 \text{ W/m}^2\text{-K}$ ($69 \text{ Btu/hr-ft}^2\text{-}^\circ\text{F}$) afterward is an increase of about 8%. This is within the uncertainty of our calculated outside convection coefficient and therefore no definitive conclusion can be drawn from the test.

It seems likely that a coil on the bottom of the lake might have a lower outside convection than one that is raised up off the bottom, because the natural convection flow might be

impeded if the coil sinks into the lake bottom. In this case, the steel frame plus the spacer frame will support the coil so that the bottom of the coil is approximately 51 mm (2 in) above the bottom of the steel frame. The steel frame that the coil sits on likely only sank in a negligible amount and thus the buoyancy-driven flow was not impeded.

5.3 Bundled Coil Results

The purpose for testing the bundled coils was to gain a better understanding of how much the heat transfer is reduced by leaving the coils banded up (factory-banded coils) or by simply rebanding them, cutting the factory bands and inserting some spacers into fill out the new bands instead of uniformly spacing them out. To achieve this, 11 bundled configurations (Table 2-2) equaling 30 tests were conducted. Figure 5-13 shows how the outside film Nusselt numbers compare to that of the small and large spaced spiral-helical SWHE correlations for the different bundled experiments conducted.

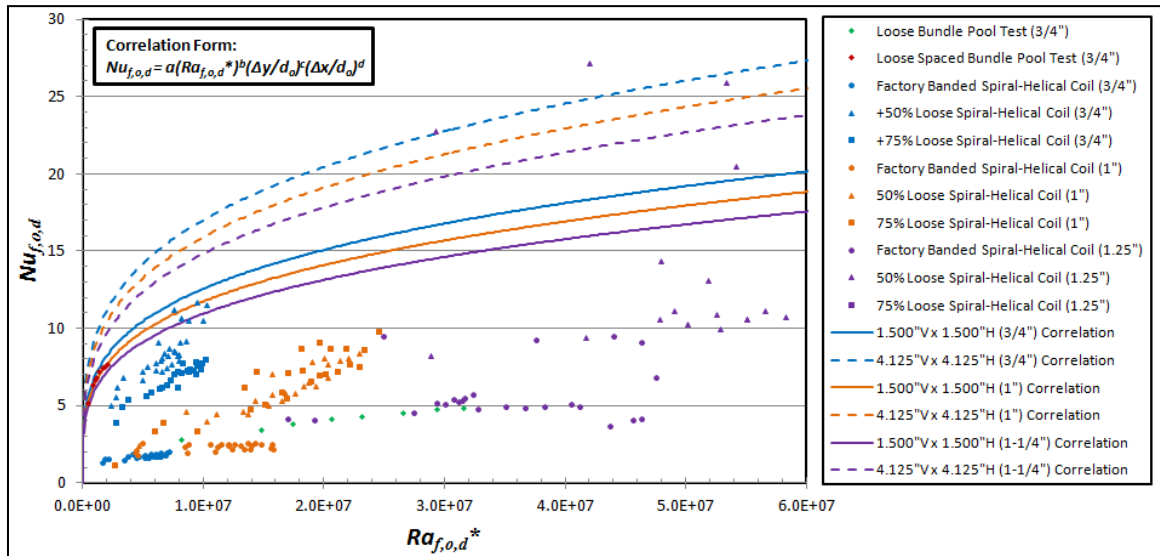


Figure 5-13. Bundled Coil Results in $Nu_{f,o,d}$ vs. $Ra_{f,o,d}^*$

The factory bundle coils (circles) are not recommended for installation but these tests do provide a lower boundary on the heat transfer capacity of the coils. The spaced out bundles (triangles and squares) show insight into the performance that can occur with the commonly used

configuration in the SWHE installation field. Since the spacing of the coil was done in a haphazard manner, the outside convection coefficients have high variation. This variation in outside convection leads to lower heat transfer rates in most cases.

It seems like it should be possible to apply the correlation developed for controlled-spacing spiral-helical coils to these loose bundles if approximate horizontal and vertical spacings can be determined. These were estimated from the vertical and horizontal dimensions of the loose bundles and are given in Table 2-2. Figure 5-14 compares the actual experimental heat transfer rates to those that would be obtained with a simulation applying the correlation (Equation 5-7) with the spacings given in Table 2-2. These are approximately equivalent to the reductions in heat transfer that come from the random spacing and tube-to-tube interference found in the loose bundles compared to the controlled-spacing coils. In turn, these percentages also represent the penalty in required size. So, they might be considered as degradation factors that could be applied to any sizes determined with a simulation or design graph based on Equation 5-7.

For each tube size, the decrease in heat transfer ranges as follows:

- 3/4": 0%-30% for loose bundles; 50%-60% for factory bundles
- 1": 10%-30% for loose bundles; 45%-55% for factory bundles
- 1 1/4": 5%-15% for loose bundles; 30%-40% for factory bundles

This suggests that a degradation factor be applied for loose-bundled coils for each tube diameter as follows:

$$Q_c = F_{deg}(Q_{c,corr}) \quad (5-8)$$

Where: $Q_{c,exp}$ is the heat transfer rate for the factory and loose bundle coils (Watts)

$Q_{c,corr}$ is the predicted heat transfer rate using Equation 5-7 (Watts)

F_{deg} is the degradation factor associated with the factory and loose bundle configuration coils. They are assigned as follows:

- 3/4": 0.7 for loose bundles; 0.4 for factory bundles

- 1": 0.7 for loose bundles; 0.45 for factory bundles
- 1 1/4": 0.85 for loose bundles; 0.6 for factory bundles

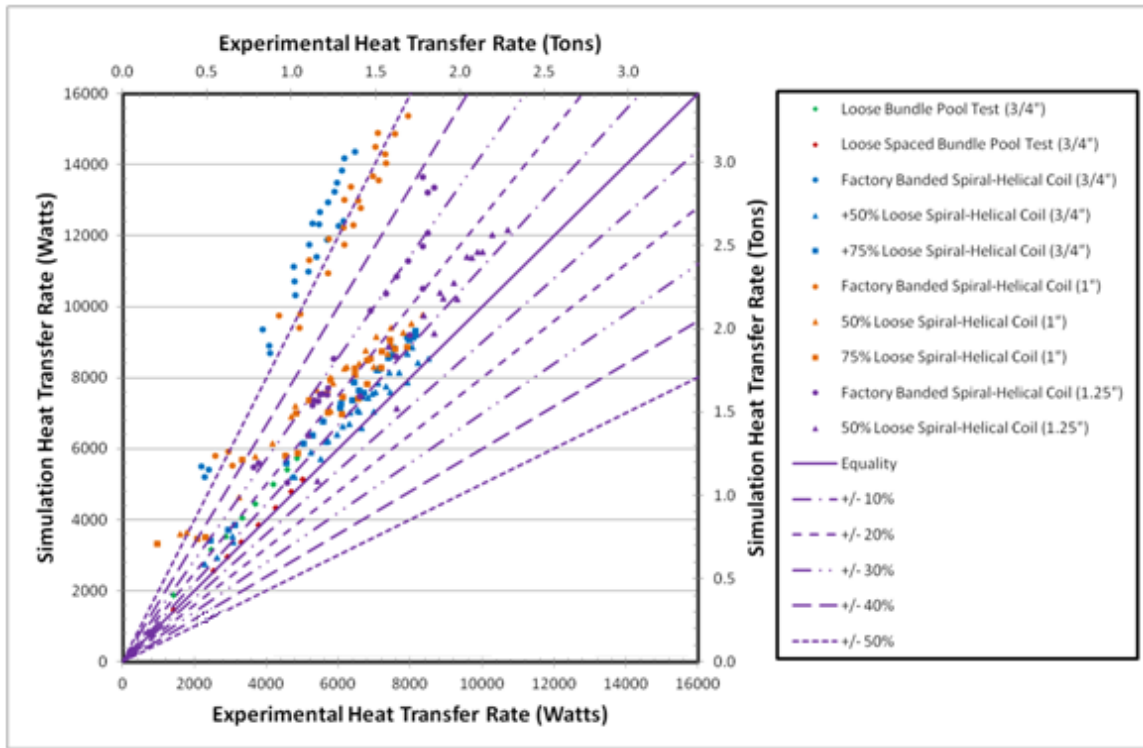


Figure 5-14. Loose Bundle Heat Transfer Comparison to Simulation Model

From Figure 5-14 it can be seen that the experimental heat transfer rates of the loose bundle coils are between 10%-30% lower than that of the simulation model using Equation 5-7 with the exception of a few points. This would mean that if a system were to use a simulation with the developed correlation on loose bundle coils, they would be undersized. The lower heat transfer performance also leads to the recommendation that a uniform spacing throughout the entire coil be used.

5.4 Flat-Spiral Coil Results

Three separate tests were conducted on the flat-spiral yielding 24 data points. The tests were conducted over a time span of 13 days with the first one on 9/3/2010 and the final two on the 9/14/2010 and 9/16/2010 respectively. Like the spiral-helical coils, the outside convection

coefficients have been graphed against the temperature difference between the outside surface of the tube and the lake temperature in Figure 5-15.

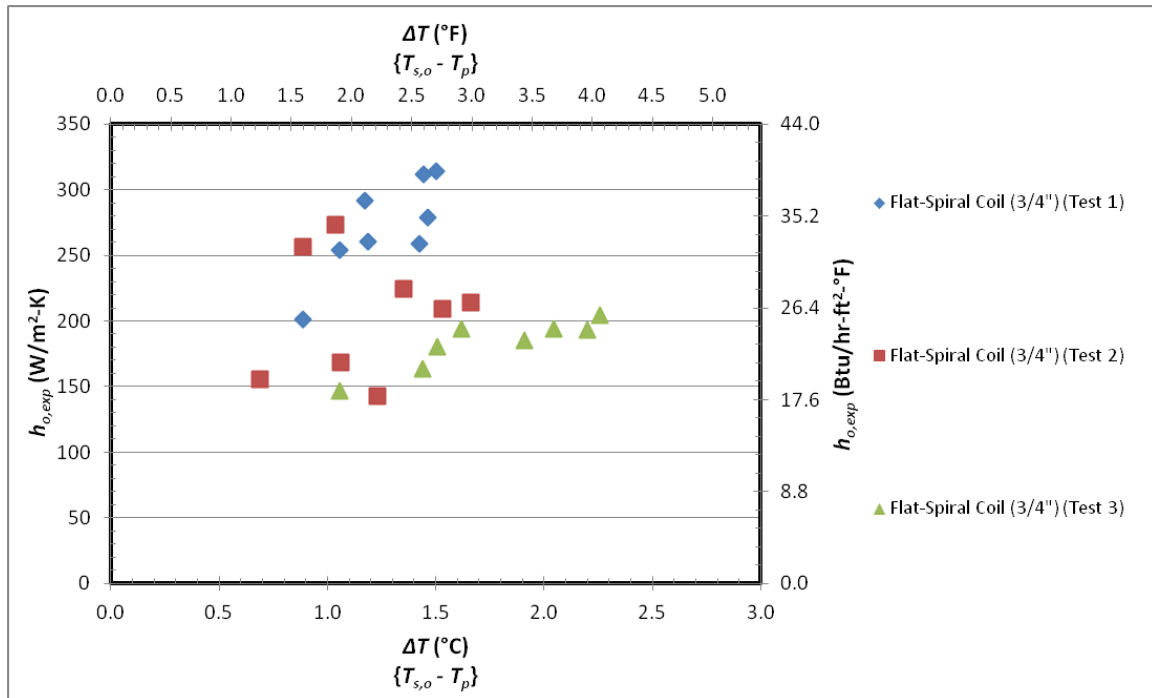


Figure 5-15. Flat-Spiral SWHE Results ($h_{o,exp}$ vs. ΔT)

Similar to the spiral-helical coils tested, the individual tests have a positive trend with the exception of 2nd test which appears to have some erratic points. To check if the testing conditions may have had an influence, the data is graphed using their respective Nusselt and modified Rayleigh numbers using the outside tube diameter as the characteristic length in Figure 5-16. The error bars for the data points have been added to the graph as well to show the level of uncertainty in the measurements.

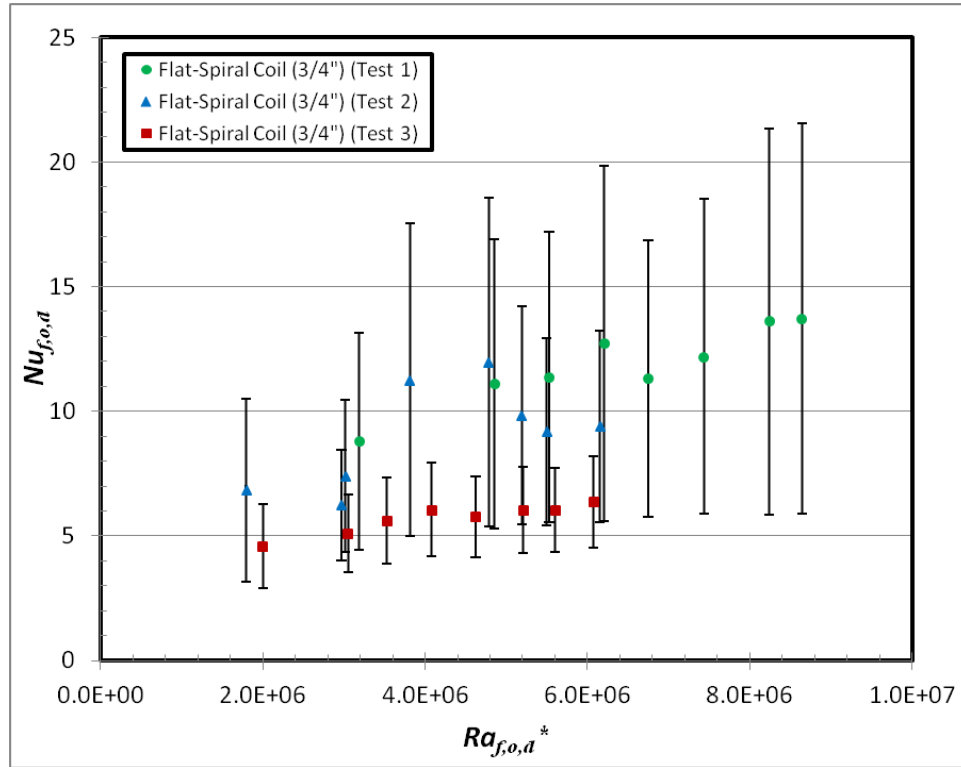


Figure 5-16. Flat-Spiral SWHE Results ($Nu_{f,o,d}$ vs $Ra_{f,o,d}^*$)

From Figure 5-16 it can be seen that the data points have been consolidated down to the point where the error bars for all data points overlap. There is still however significant separation between the two tests which arises the recommendation that additional tests be conducted in order to more accurately gain a better understanding of the flat-spiral coils performance.

From the limited data that was obtained, a comparison to the values for the spiral-helical coils can be made. A typical “small” 19 mm (¾ in) spiral-helical coil would have a Nusselt number ranging from 8 to 12 for the same range of modified Rayleigh number as the flat-spiral coil. This means that the spiral-helical correlation matches the flat-spiral coil data fairly well. A correlation development for the flat-spiral coil will be discussed in conjunction with that of the vertical and horizontal slinky coil results in the next subsection since they are more closely related by only having a few interfering tubes instead of a whole bundle of them.

5.5 Vertical & Horizontal Slinky Coil Results

For the slinky coil testing there were two orientations and three pitches. In total there were 12 tests or 95 data points (one test only had seven set points instead of eight). The testing for the slinky coils took place between 9/30/2010 and 1/7/2011 which resulted in large changes in testing conditions as the seasons changed from summer to winter. Figure 5-17 shows the results of the slinky coil testing in terms of the outside convection coefficients and the outside surface temperature difference.

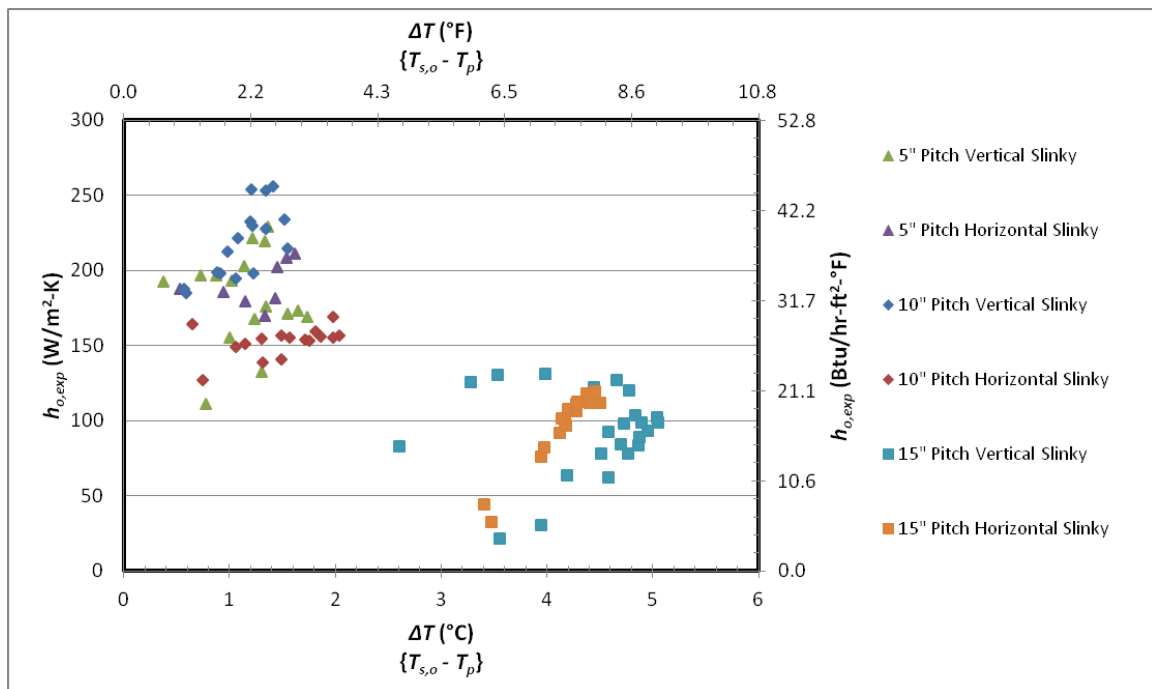


Figure 5-17. Vertical & Horizontal Slinky SWHE Results ($h_{o,exp}$ vs. ΔT)

Just like the spiral-helical coil results the outside convection coefficient increases with temperature difference for an individual test. Also, the decrease in outside convection coefficient as the temperature difference increases is present. This is extremely noticeable when looking at the 38 cm (15 in) pitch slinky coils compared to the other tests.

The first four slinky configurations were tested before winter set in and thus they are clustered together on the upper left hand-side of Figure 5-17. The final two configurations were

tested after the Christmas and New Year holiday period where the temperatures of the pond were much lower than the first four configurations. To be more specific, the average testing pond temperature for the first cluster of tests was 18.5 °C (65.3°F) while the second cluster is only at 5.0°C (41.0°F). In order to form a better method of predicting the outside convection while also taking into account the influence of the testing conditions, the Nusselt number is graphed with the modified Rayleigh number in Figure 5-18.

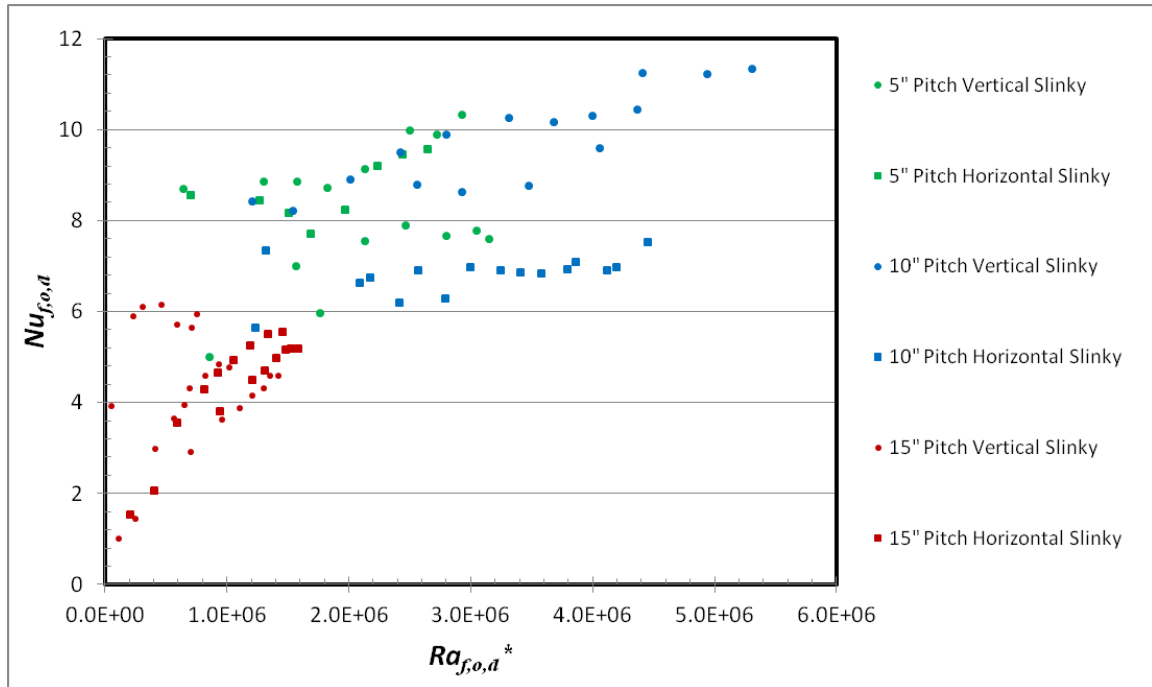


Figure 5-18. Vertical & Horizontal Slinky SWHE Results ($Nu_{f,o,d}$ vs. $Ra_{f,o,d}^*$)

An extreme improvement in overall correlation of the points is obtained using the $Nu_{f,o,d}$ vs. $Ra_{f,o,d}^*$ graph compared to the $h_{o,exp}$ vs. ΔT . With this improvement it may be possible to obtain an equation to predict the outside Nusselt number for the flat-spiral coils, vertical slinky coils, and the horizontal slinky coils. Using the Nelder-Mead simplex as described earlier, Equation 5-9 is a very simple correlation that can predict the outside convection coefficient with an MBE, MBE %, RMSE, and RMSE % of -2.8, 6.9%, 39.3, and 34.3% respectively. A graphical

representation of how the experimental data compares with the simple correlation is shown in Figure 5-19.

$$Nu_{f,o,d_o} = 0.047(Ra_{f,o,d_o}^*)^{0.34} \quad (5-9)$$

Range of applicability: $5.2 \times 10^4 < Ra_{f,o,d_o}^* < 8.6 \times 10^6$

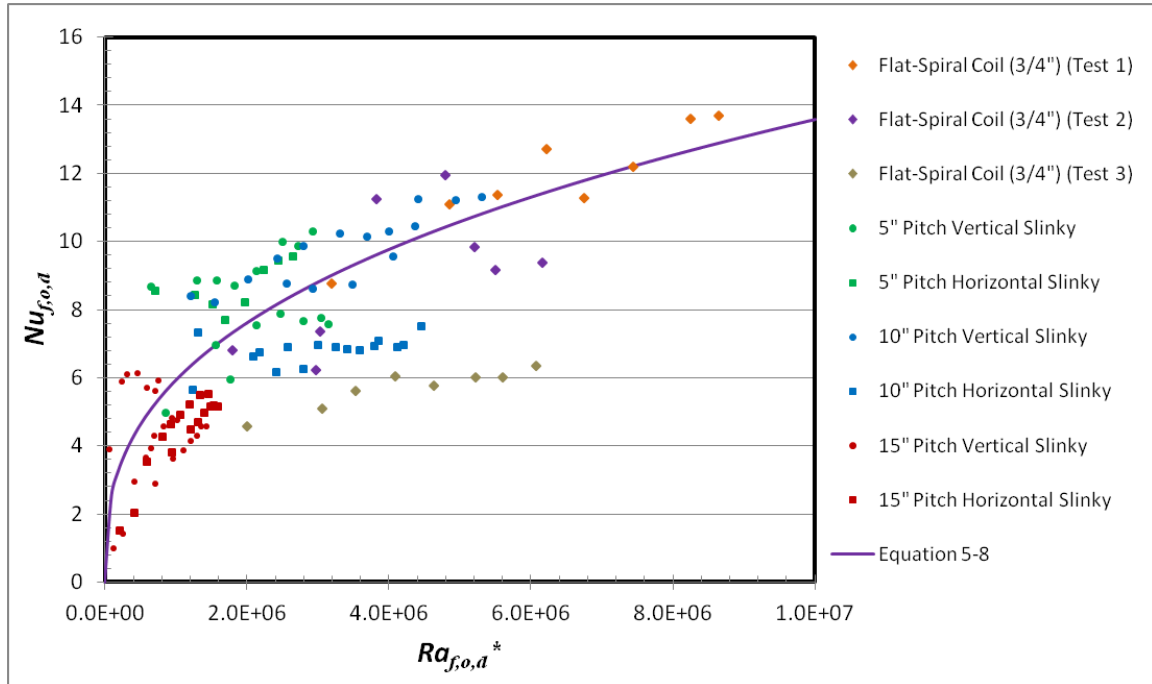


Figure 5-19. Flat-Spiral & Slinky SWHE Results With Equation 5-9 Correlation ($Nu_{f,o,d}$ vs. $Ra_{f,o,d}^*$)

Because the coil configurations of the flat-spiral and slinky coils tend to have primarily a single tube that might only interact with only a few tubes, a comparison with the Churchill & Chu (1975) correlation for a single horizontal cylinder was made. Figure 5-20 shows how the experimental values for the outside convection coefficient (horizontal axis) compares with the values obtained using the Churchill & Chu correlation (vertical axis). Reference lines of $\pm 25\%$, $\pm 50\%$, and $\pm 75\%$ have been added to the graph.

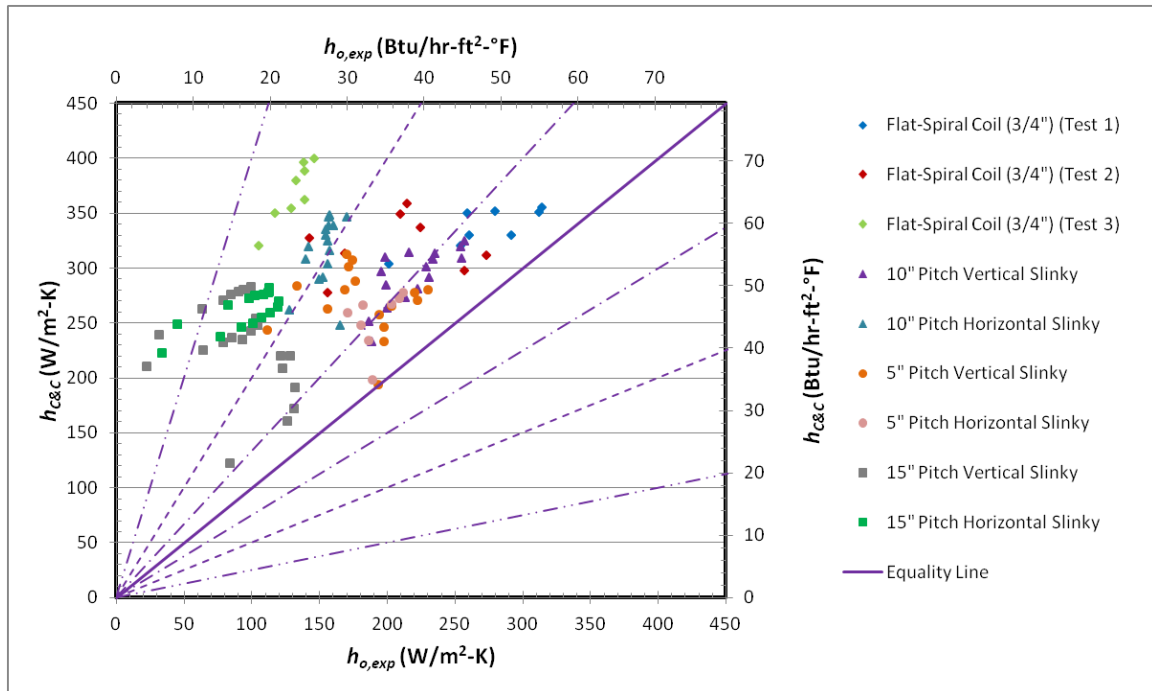


Figure 5-20. Flat-Spiral & Slinky SWHE Results vs. Churchill & Chu (1975) Correlation

It is quickly evident when looking at Figure 5-20 that using the Churchill & Chu correlation will result in the outside convection coefficient being over predicted. The reasons for this cannot be completely determined but possible explanations include the fact that the Churchill and Chu correlation for horizontal cylinders does not take into account the tube-to-tube interference and thus will over predict the outside convection coefficient. Furthermore, the effect of the curvature on exterior convection is really unknown.

5.6 Vertical Flat-Plate Heat Exchanger Results

The testing on the vertical flat-plate heat exchanger (Slim Jim®) was administered in the spring of 2011. A total of 5 tests were completed yielding 40 data points. A major point of interest with testing the vertical flat-plate is to see how much the outside convection coefficient influences the heat transfer through this type of SWHE because the heat exchanger material is no longer an insulator but is now stainless steel. Table 5-12 shows some the different conditions that the vertical flat-plate heat exchanger was under for each of the tests.

Table 5-12. Vertical Flat-Plate Heat Exchanger Testing Conditions

Test Description	Date	Average Pond Temp		Average Flow Rate		Plate Bottom Depth	
		°C	°F	L/s	GPM	m	ft
Flat-Vertical Plate Test 1	4/1/2011	11.8	53.3	0.37	5.9	1.5	5
Flat-Vertical Plate Test 2	4/4/2011	16.0	60.8	0.34	5.4	1.5	5
Flat-Vertical Plate Test 3	4/4/2011	16.5	61.7	0.36	5.7	1.5	5
Flat-Vertical Plate Test 4	4/4/2011	15.9	60.7	0.37	5.9	1.5	5
Flat-Vertical Plate Test 5	4/5/2011	14.6	58.3	0.37	5.8	1.5	5

Upon completion of the testing, an analysis was conducted (Section 4.4.4) on the experimental data. A review of the thermal resistances revealed that the balance of thermal resistance was no longer centered over the heat exchanger material. To recall, the conductive thermal resistance of SDR-11 HDPE was found to be around 60% in the 19 mm (¾ in) spiral-helical coils. The analysis of the vertical flat-plate heat exchanger shows that the majority of the thermal resistance now resides in the outside convection term of the heat exchanger analysis. This makes sizing the outside convection coefficient that much more critical than in the spiral-helical SWHEs made from HDPE. The breakdown of the thermal resistances for each of the vertical flat-plate tests is given in Table 5-13.

Table 5-13. Vertical Flat-Plate Heat Exchanger Thermal Resistance Distribution

Test Description	Inside Convective Resistance	Wall Conductive Resistance	Outside Convective Resistance
	% of total	% of total	% of total
Flat-Vertical Plate Test 1	12%	2%	86%
Flat-Vertical Plate Test 2	10%	1%	89%
Flat-Vertical Plate Test 3	11%	1%	87%
Flat-Vertical Plate Test 4	10%	1%	89%
Flat-Vertical Plate Test 5	8%	1%	91%

The results from the testing on the vertical flat-plate heat exchanger are displayed in Figure 5-21 in terms of outside convection coefficient and the outside temperature difference.

From the graph it is evident that the outside convection coefficient increases with an increase in the outside temperature difference.

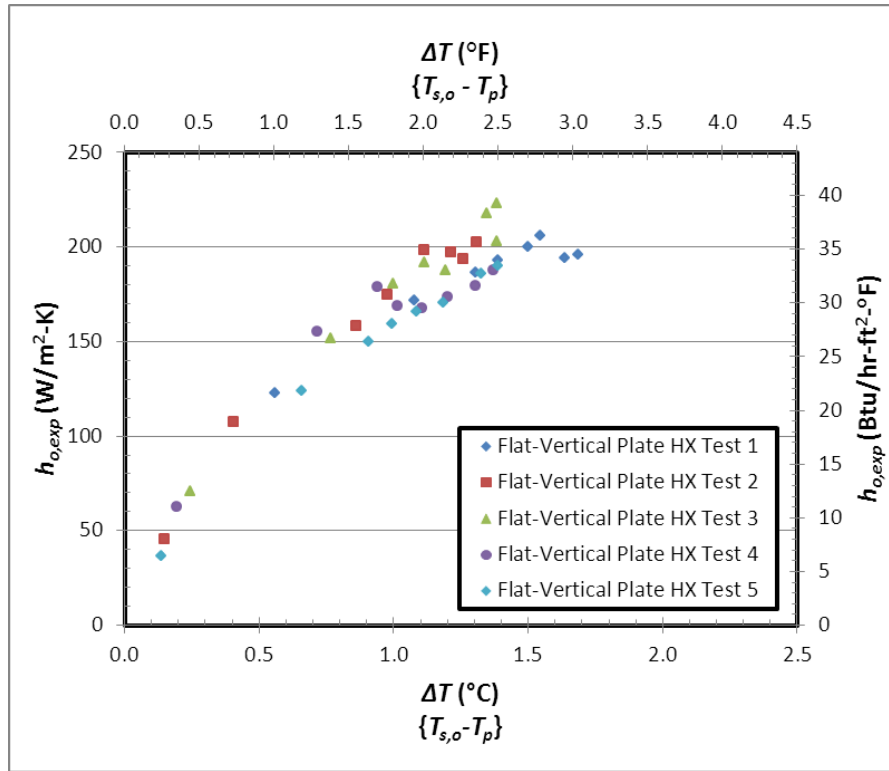


Figure 5-21. Vertical Flat-Plate Heat Exchanger Results ($h_{o,exp}$ vs. ΔT)

In order to check the influence from the testing pond conditions, the results are presented in the same Nusselt-Rayleigh method as the previous HDPE coils. Instead of using the inside tube diameter, because the vertical flat-plate does not have any tubes, the plate height was used in conjunction with how testing was done on vertical plates by Churchill and Chu (1975). The modified Rayleigh number described by Churchill and Chu is also utilized in Figure 5-22.

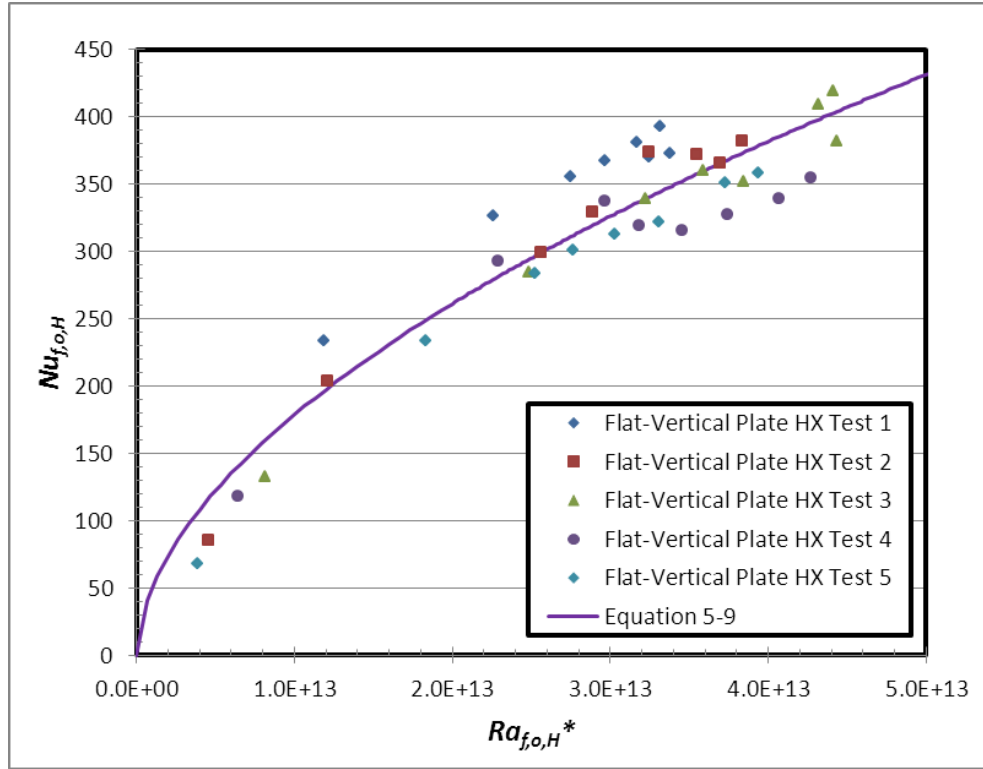


Figure 5-22. Vertical Flat-Plate Heat Exchanger Results with Equation 5-10 ($Nu_{f,o,H}$ vs. $Ra_{f,o,H}^*$)

The Nusselt number is well-correlated to the modified Rayleigh number. Again, using the Nelder-Mead Simplex optimization, a simple correlation curve was developed and is shown in Equation 5-10. The statistical parameters for the correlation are 0.32, 2.7%, 14.3, and 13.7% for the mean bias error, MBE %, RMSE, and RMSE % respectively.

$$Nu_{f,o,H} = 1.35 \times 10^{-5} (Ra_{f,o,H}^*)^{0.55} \quad (5-10)$$

$$\text{Range of applicability: } 1.7 \times 10^9 < Ra_{f,o,H}^* < 2.2 \times 10^{10}$$

A comparison with the correlation for vertical flat-plates by Churchill and Chu (1975) was also conducted. Figure 5-23 shows that the data matches the correlation very well with the exception that the Churchill and Chu correlation slightly over predicts the outside convection coefficients at the low coefficient values. This may be due to the uncertainties at the low heat

transfer rates. This may also be due to the method used for estimating inside convection, which may introduce a systematic error. Additional testing is recommended.

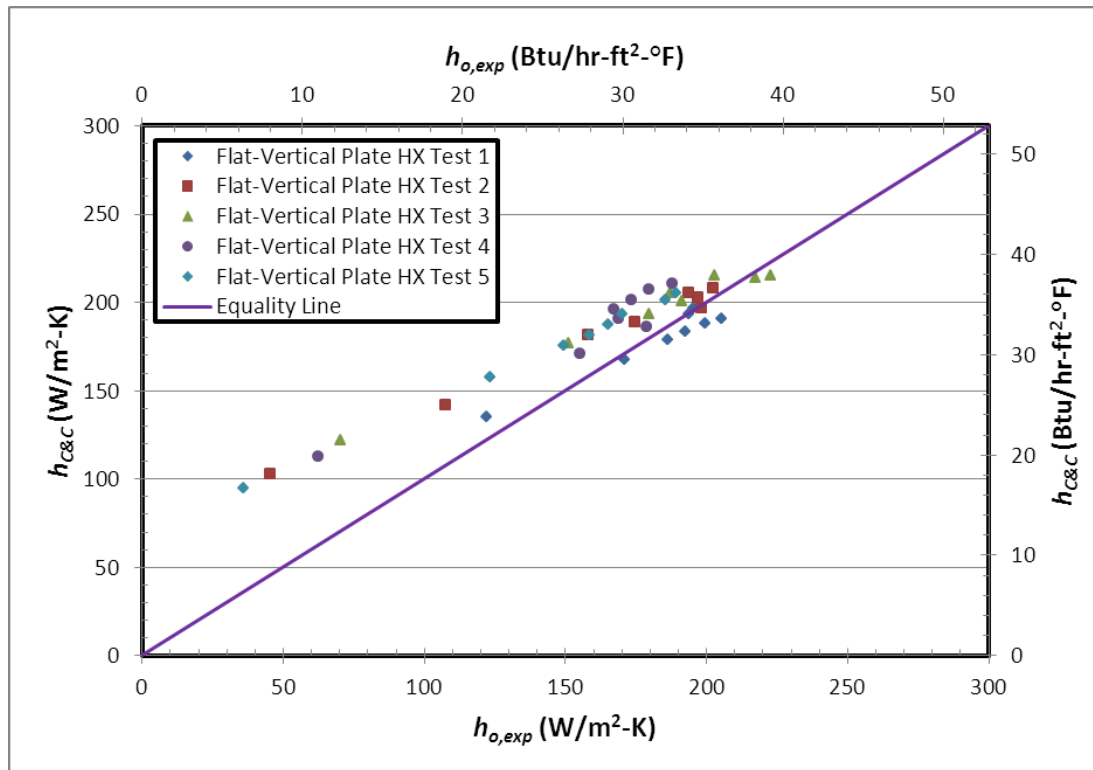


Figure 5-23. Vertical Flat-Plate Heat Exchanger Results vs. Churchill & Chu (1975) Correlation

CHAPTER VI

6. APPLICATIONS

6.1 Approach Temperature Sizing Design Graphs

Designing a SWHP system can be a lengthy process for engineers. A method of sizing the SWHE off of a chart would save significant time if the charts were accurately developed. As mentioned in Chapter 1, Kavanaugh and Rafferty (1997) provide a series of approach temperature sizing design graphs to aid in the design of SWHEs that utilize HDPE tubing. Specifically, two charts were provided for sizing loose and spaced bundle coils in both cooling and heating modes. Similar design graphs were developed using the results preserved in Chapter 5. Included in the updated design graphs will be lake temperature effects and heat pump efficiency for many of the SWHEs mentioned previously.

6.1.1 Kavanaugh & Rafferty Design Graphs

Although the Kavanaugh and Rafferty design graphs are convenient, there are several significant questions about them. Lake temperature plays a vital role in the buoyancy forces present on the outside of the coil particularly near the maximum density point, where the derivative of density with respect to temperature changes rapidly. Kavanaugh and Rafferty do not mention for what lake temperatures their graphs are valid. They do not indicate whether the ft/ton are based on tons of installed capacity, tons of cooling load, or tons of heat rejection.

If it was per ton of installed capacity or ton of cooling load, the assumed energy efficiency ratio (EER) or coefficient of performance (COP) is not stated. Either the EER or the COP should be provided so that the amount of heat rejected at the coil can be backed out in a calculation if needed. Heat pump COPs are variable from model to model and have improved over the years so clarification on this is needed. Finally, the coils are described by Kavanaugh and Rafferty as “loose” or “spaced” but the actual spacing, shown to be important in Chapter 5, is not described.

6.1.2 Lake Temperature & Heat Pump Load Dependence

The first area of concern that requires attention from the Kavanaugh and Rafferty work is the influence of the lake temperature on the required length of coil for a specific heat rejection. To show how the different lake temperatures affect the coil length, Equation 5-7 was used in a series of heat exchanger simulations to determine the outside convection coefficient. The inside convection was determined using the Rogers and Mayhew (1964) correlation (Equation 4-10) while the conductive resistance was calculated using Equation 4-13. The flow rate was set at 0.19 L/s (3 GPM) and the coil length was initially set at 152.4 m (500 ft). A series of simulations with different inlet temperatures were run and the length per heat rejection at the coil was calculated for each inlet temperature. This length per heat rejection was then used to calculate the new length of coil and the simulation was run again. Numerous iterations were conducted until the flow rate per unit of heat rejection was stable at 0.054 L/s-kW (3 GPM/ton of heat rejection). For each inlet temperature, the end result is a converged configuration with 3.52 kW (1 ton or 12,000 Btu/hr) of heat rejection, flow rate of 0.054 L/s-kW (3 GPM/ton), entering and exiting fluid temperatures, and an approach temperature difference. From the approach temperature differences and the corresponding lengths per unit of heat rejection, design graphs were created for a range of lake temperatures from 5°C (41°F) to 35°C (95°F). Two coil configuration design graphs are provided in Figures 6-1 and 6-2.

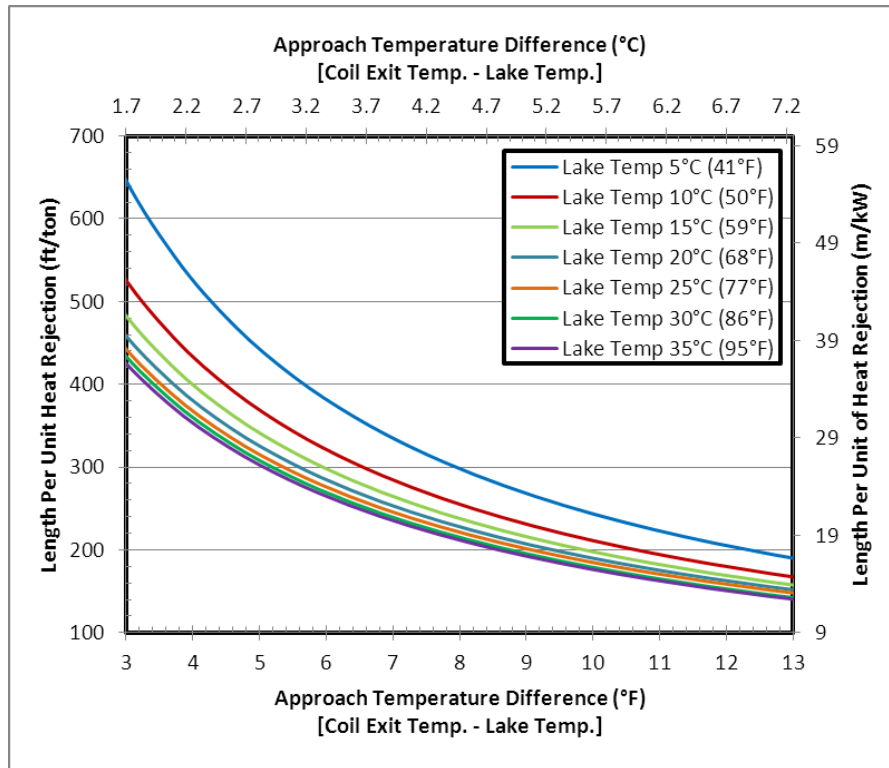


Figure 6-1. Lake Temperature Effect on Small Spacing Configuration SWHE (19 mm, 3/4" HDPE Tube)

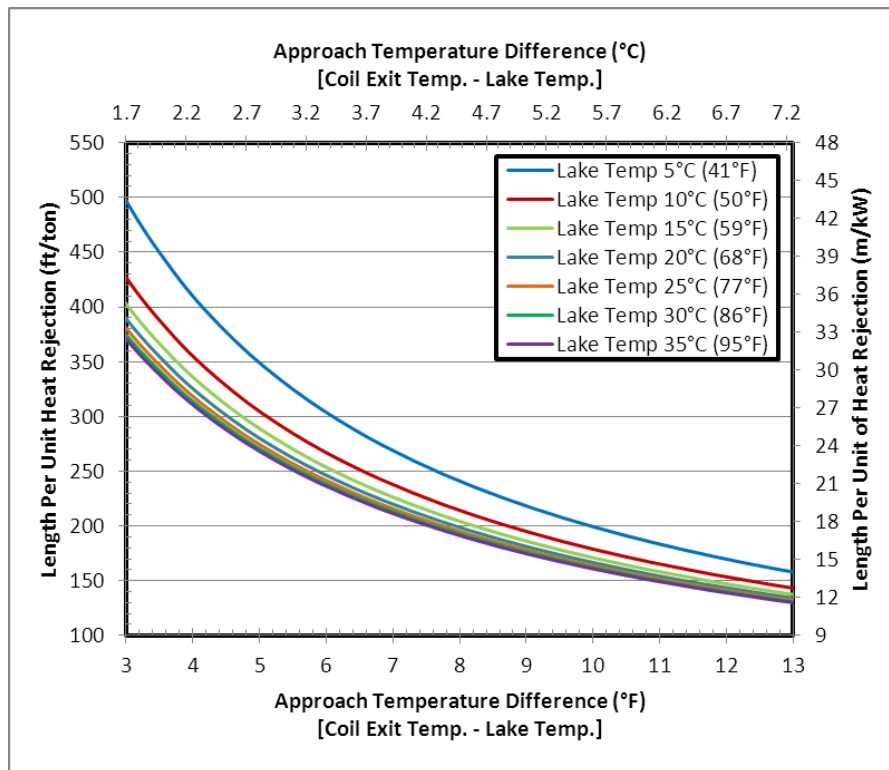


Figure 6-2. Lake Temperature Effect on Large Spacing Configuration SWHE (32 mm, 1-1/4" HDPE Tube)

From the two design graphs it is clear that the lake temperature plays a large role in the sizing of a SWHE. The difference between the 5°C (41°F) and the 35°C (95°F) lake temperatures is about 11 m/kW (180 ft/ton) and 2.5 m/kW (30 ft/ton) for respective approach temperature differences of 1.7°C (3°F) and 7.2°C (13°F). For the operating ranges that might be typical in much of the continental United States where the approach temperature difference is greater than 2.8°C (5°F) and the lake temperature is greater than 20°C (68°F), the percent error in the length per unit of heat rejection compared to the 20°C (68°F) lake condition is no larger than 7.2% for all configurations. However, there are situations where cooling may be required and where lake temperatures are considerably lower than 20°C (68°F).

The second issue to address is the influence of the heat pump efficiency on the HDPE coil sizing design graph. To study the influence of the heat pump on the design graph, three different heat pumps are looked at with respect to the medium configuration, 19mm (¾ in) tube size coil. The three different heat pumps that are looked at are listed in Table 6-1 with their respective performance data. The 1997 data were obtained from an old Florida Heat Pump (FHP) data sheet used in a class example (Spitler 2011) created in 1997. The heat pump may have been manufactured prior to 1997.

Table 6-1. Heat Pump Cooling Data

FHP Model (Year)	Flow Rate		EWT		EAT _{wb}		Heat Rejection		EER	COP _c
	L/s	GPM	°C	°F	°C	°F	MW	MBtuH	Btu/hr-W	-
SX030 (~1997)	0.44	7.0	7.2	45	19.4	67	13.0	44.3	29.9	8.8
	0.44	7.0	10.0	50	19.4	67	12.8	43.8	27.8	8.1
	0.44	7.0	15.6	60	19.4	67	12.4	42.4	24.1	7.1
	0.44	7.0	21.1	70	19.4	67	12.0	40.9	21.0	6.2
	0.44	7.0	29.4	85	19.4	67	10.6	36.0	15.0	4.4
	0.44	7.0	37.8	100	19.4	67	9.7	33.2	12.5	3.7
EC030 (2011)	0.44	7.0	10.0	50	19.4	67	11.8	40.2	19.4	5.7
	0.44	7.0	15.6	60	19.4	67	11.5	39.4	16.9	5.0
	0.44	7.0	21.1	70	19.4	67	11.3	38.6	14.9	4.4
	0.44	7.0	29.4	85	19.4	67	11.0	37.4	12.3	3.6
	0.44	7.0	37.8	100	19.4	67	10.6	36.2	10.3	3.0
ES030 (2011)	0.47	7.5	10.0	50	19.4	67	11.8	40.2	30.3	8.9
	0.47	7.5	15.6	60	19.4	67	11.5	39.1	25.6	7.5
	0.47	7.5	21.1	70	19.4	67	11.1	37.9	21.9	6.4
	0.47	7.5	29.4	85	19.4	67	10.6	36.2	17.5	5.1
	0.47	7.5	37.8	100	19.4	67	10.1	34.5	14.2	4.2

From the data in Table 6-1, 3rd order polynomial fit lines were made for the three heat pumps in order to predict the heat pump cooling COP_c ($COP_c = \frac{EER}{3.412}$) based on the temperature of the water entering the heat pump. Equations 6-1 through 6-3 are the equations for the SX030, EC030, and the ES030 respectively.

$$COP_{c,SX030} = 1.36 \times 10^{-4}(T_{EWT})^3 - 0.0072(T_{EWT})^2 - 0.078(T_{EWT}) + 9.6 \quad (6-1)$$

$$COP_{c,EC030} = -1.65 \times 10^{-5}(T_{EWT})^3 - 0.0026(T_{EWT})^2 - 0.19(T_{EWT}) + 7.3 \quad (6-2)$$

$$COP_{c,ES030} = -4.98 \times 10^{-5}(T_{EWT})^3 - 0.0066(T_{EWT})^2 - 0.39(T_{EWT}) + 12.2 \quad (6-3)$$

Where: COP_c is the coefficient of performance in cooling mode for the given heat pump

T_{EWT} is the entering water temperature to the heat pump (°C)

Using the COP_c of the heat pump, the actual amount of heat rejection at the coil is obtained using Equation 6-4.

$$Q_c = Q_{load} \times \left(1 + \frac{1}{COP_c}\right) \quad (6-4)$$

Where: Q_c is the required total amount of heat rejected through the coil (kW, tons)

Q_{load} is the cooling load of the space (kW, tons)

With the nominal load calculated, the parameters for the design graph can be obtained. Figure 6-3 shows a coil sizing design graph for the three heat pumps, a theoretical heat pump with a constant COP_c of four, and the sizing if it was simply the heat rejection rate at the coil used. Hidden in the graph is an underlying constant flow rate per unit heat pump cooling load of 0.054 L/s-kW (3 GPM/ton). This will hold true for all design graphs in the remainder of this thesis.

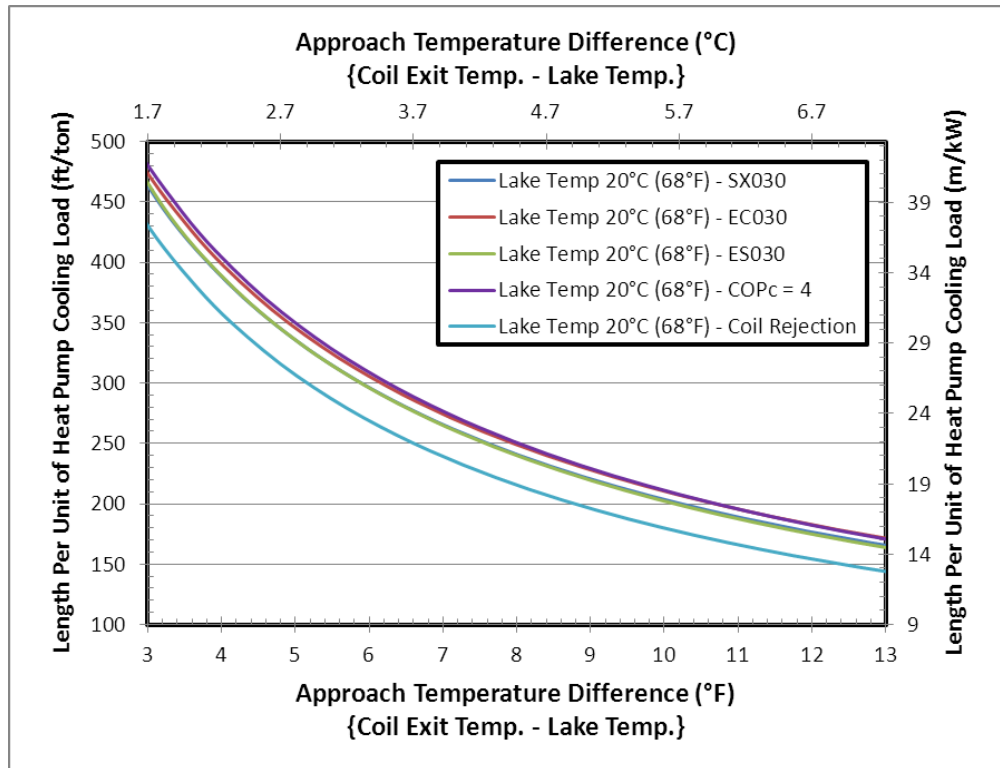


Figure 6-3. Heat Pump Effects Design Graph (Medium Spaced Spiral-Helical SWHE 19 mm, 3/4 in SDR-11 HDPE)

Visible in the figure is the separation between the curves for design loads and heat rejection at the coil. Also noticeable is the separation between the different heat pump efficiencies. For the coil inlet temperature range of about 21°C (70°F) to 28°C (82°F), the EC030 Florida Heat Pump requires an additional 2.7 m/kW (31 ft/ton) when compared to the ES030 Florida Heat Pump. These effects could further be magnified if the COPs between the different heat pumps had a larger difference and also at the different lake temperatures. In a more general comparison between the different heat pumps and the heat pump with a constant COP_c of four shows that the largest average percent error was only 4.7% for approach temperature differences greater than 5°C (2.8°F). For the constant COP_c and the coil rejection line the average percent error was 16.5% when the approach temperature difference was above 5°C (2.8°F).

6.1.3 Typical Condition Design Graph

The Kavanaugh and Rafferty sizing design graphs may need updating to include the lake temperature effects as well as the heat pump efficiency influence to more accurately size the HDPE coils to be used in a SWHP system. For the updating of the sizing design graphs, three scenarios will be considered. The sizing design graphs for the scenarios are provided after the description. Each scenario has a medium configuration for the 19mm (¾ in) and the 32 mm (1-¼ in) tube sizes.

1. A heat pump system that is rejecting heat to a lake in central Minnesota at a depth of 9 m (30 ft) in September. The average temperature of Grindstone Lake at the given depth is roughly 14°C (57°F) (Hattemer and Kavanaugh 2005). A heat pump with a constant COP_c of four and the medium spaced spiral-helical SDR-11 HDPE coil configuration was selected for this system.

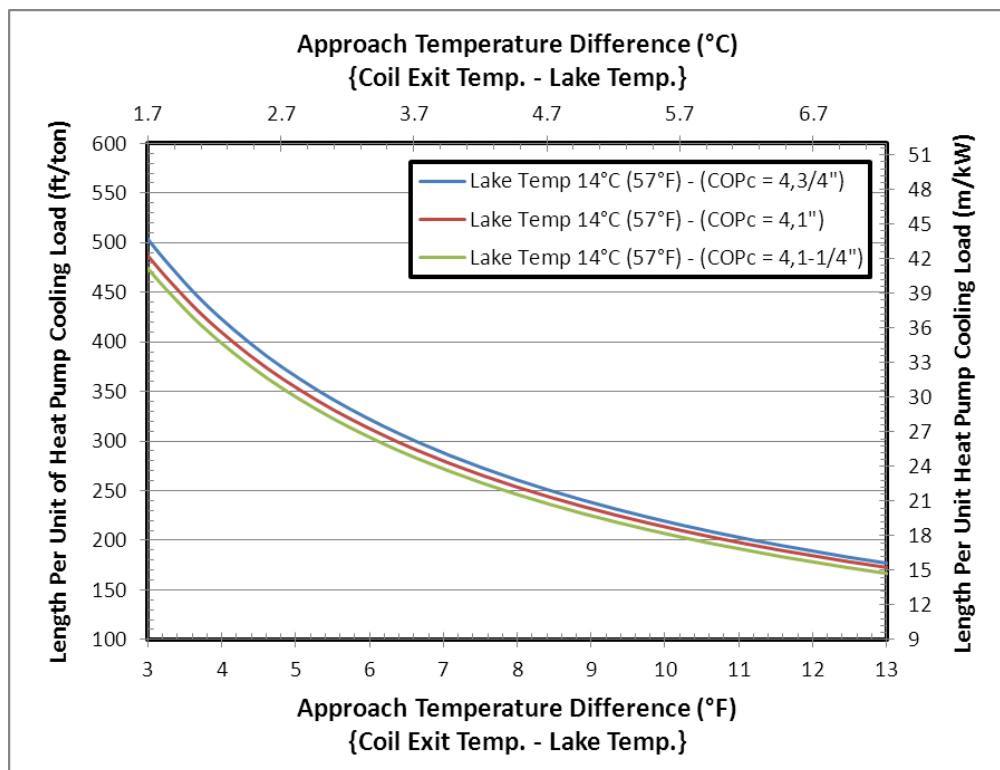


Figure 6-4. Minnesota Scenario Sizing Design Graph for Medium Spaced SDR-11 HDPE SWHE

2. A heat pump system that is rejecting heat to a lake in Tennessee at a depth of 9 m (30 ft) in September. The average temperature of Norris Reservoir at the given depth is roughly 24°C (75°F) (Hattemer and Kavanaugh 2005). A heat pump with a constant COP_c of four and the medium spaced spiral-helical SDR-11 HDPE coil configuration was selected for this system.

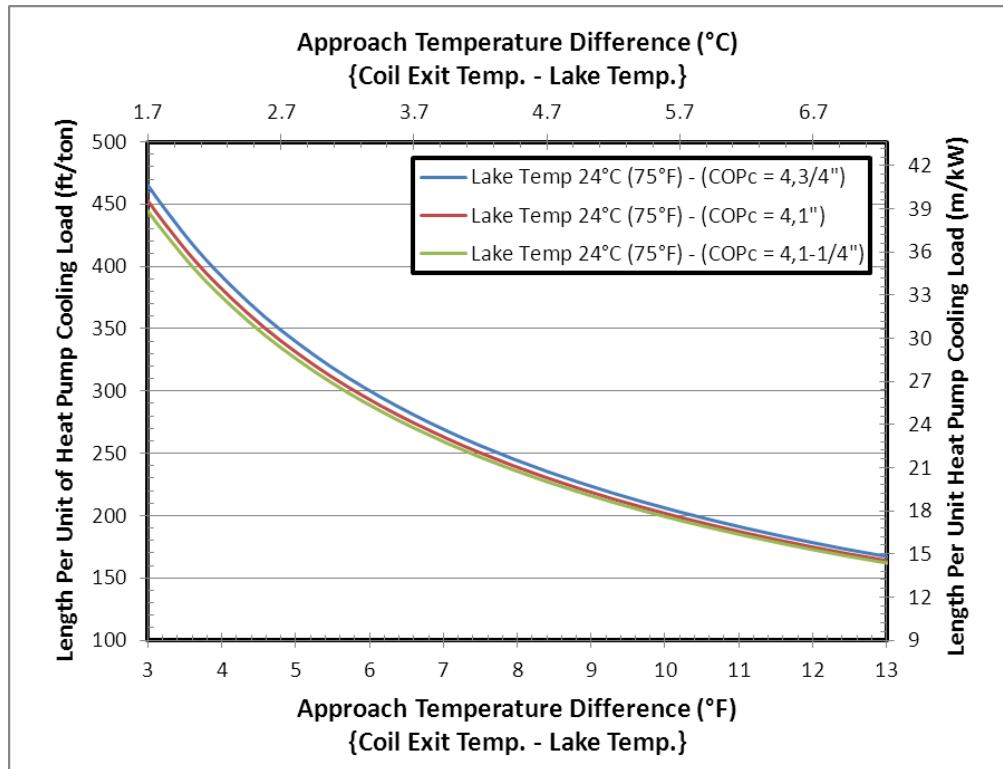


Figure 6-5. Tennessee Scenario Sizing Design Graph for Medium Spaced SDR-11 HDPE SWHE

3. A heat pump system that is rejecting heat to a lake in Arizona at a depth of 2 m (5 ft) in July. The average temperature of Ouachita Lake at the given depth is roughly 32°C (90°F) (Hattemer and Kavanaugh 2005). A heat pump with a constant COP_c of four and the medium spaced spiral-helical SDR-11 HDPE coil configuration was selected for this system.

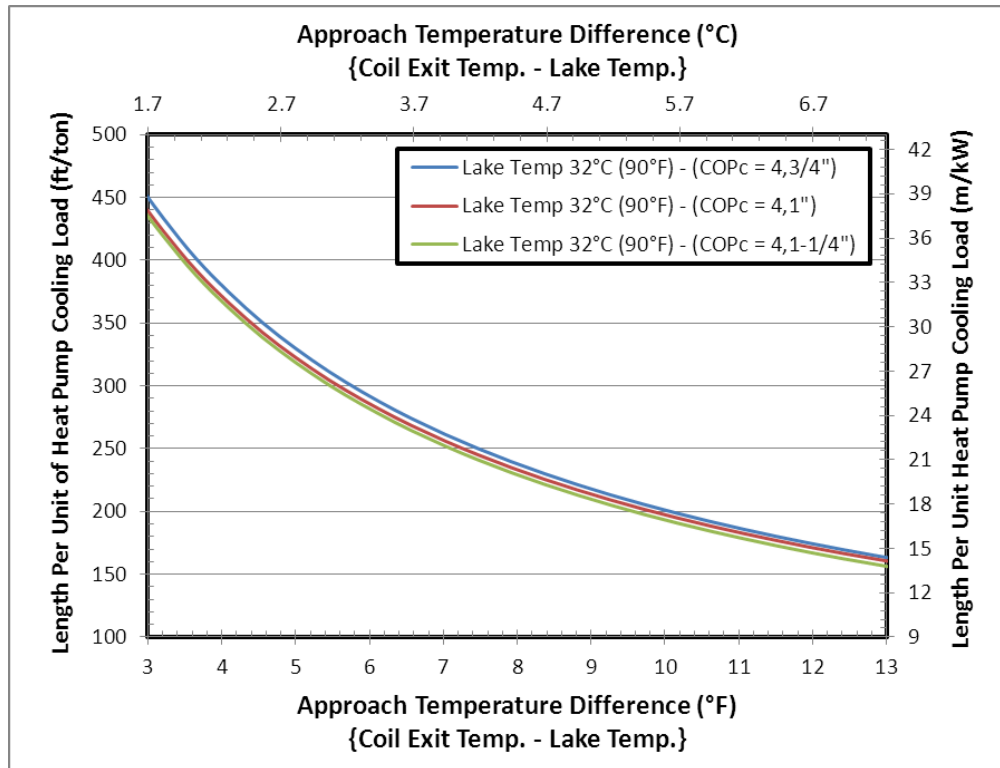


Figure 6-6. Arizona Scenario Sizing Design Graph for Medium Spaced SDR-11 HDPE SWHE

One thing to note about the updated design graphs is that they do look similar but there are subtle differences between each of them. When comparing them to the design graphs given by Kavanaugh and Rafferty (1997), also found in Section 1.3.2, there are a few differences. The one that sticks out the most is the separation between the different tube sizes. Kavanaugh and Rafferty show that there is significant separation between their three tube sizes while the updated design graphs shown little variation. This leads to the conclusion that the smaller tubing may be more cost effective than the larger tubing. More discussion on this can be found in Section 6.2.4. With this tentative hypothesis about the tube size it is worth noting that Kavanaugh and Rafferty do not include 19 mm ($\frac{3}{4}$ in) tube in their design graphs but instead have a 38 mm ($1\frac{1}{2}$ in) curve. Another difference has to do with the asymptotic decay of the curves. Kavanaugh and Rafferty have their curves leveling off at a length per unit heat pump cooling load (if that is what they were using) of 17.3 m/kW (200 ft/ton) while all three scenarios go no higher than 16 m/kW (175 ft/ton) at approach temperature differences of 7.2°C (13°F).

In order to further demonstrate the variations between the scenarios, Figure 6-7 was created. Shown in the figure is how each of the scenarios (blue = Minnesota, red = Tennessee, green = Arizona) influenced the design graph for the three tube sizes. The 19 mm ($\frac{3}{4}$ in) tube, solid lines, require the highest length while the 32 mm ($1\frac{1}{4}$ in) tube, dash dot dot lines, require the least amount of length per unit of heat pump cooling load.

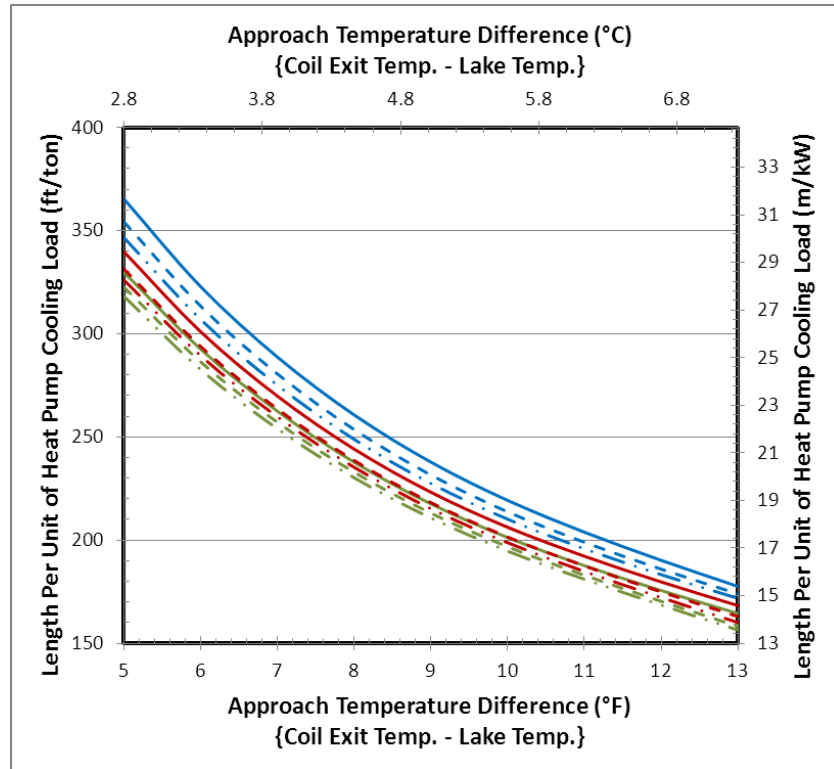


Figure 6-7. Spiral-Helical SWHE Sizing Design Graph for SDR-11 HDPE (Combined Scenario Results)

At the two extremes of the scenarios there are the 19 mm ($\frac{3}{4}$ in) tube with a small spacing configuration in Minnesota and the 32 mm ($1\frac{1}{4}$ in) tube with a large spacing configuration in Arizona. This may seem counter intuitive that Minnesota requires more length per unit of heat pump cooling load than Arizona at a given approach temperature difference. If, for example, a maximum heat pump entering fluid temperature of 35°C (95°F) were desired a 21°C (37.8°F) approach temperature difference can be used in Minnesota, leading to a 7.6 m/kW (88 ft/ton). For the same case, Arizona would require a 3°C (5.4°F) approach temperature difference leading to a

38.7 m/kW (446 ft/ton) size. Again, this difference in m/kW (ft/ton) at the two locations is caused by the different derivatives of density with respect to water temperature.

Most of the spiral-helical SWHEs that get designed in the United States for cooling should fall within the blue area of Figure 6-8 below regardless of their location, spacing configuration, and tube size. This figure can serve as a valuable check to make sure the SWHE is designed correctly. The other service that this could provide is for the conservative engineer. If he wanted to make sure his system was sized large enough he or she could simply use the upper boundary as their sizing criterion.

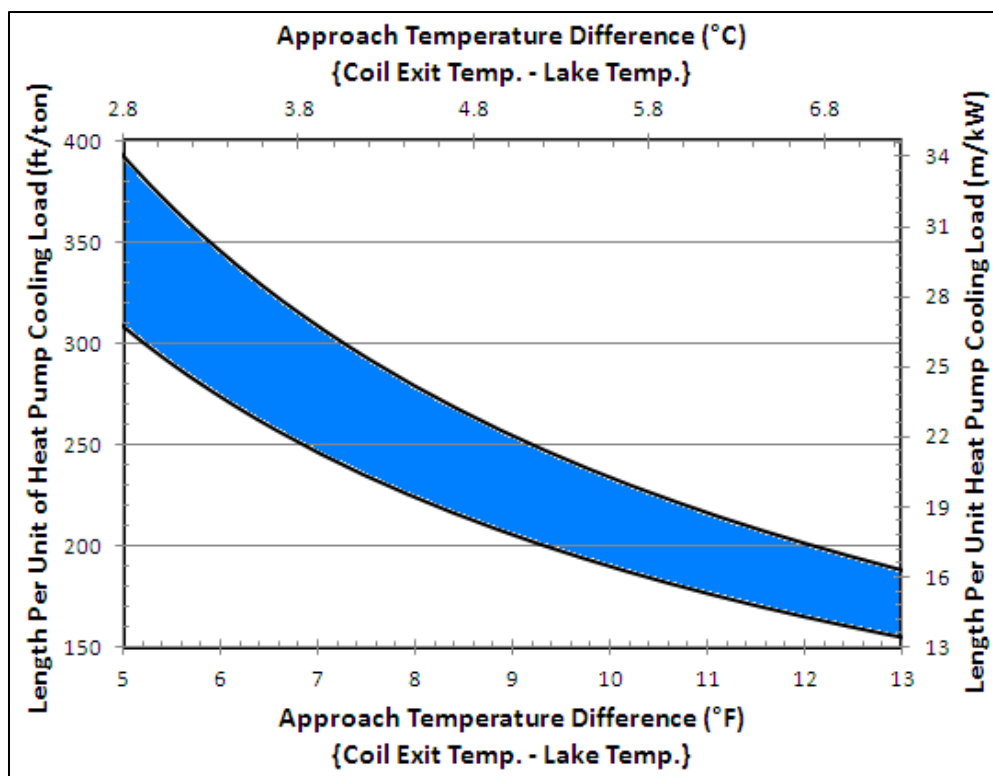


Figure 6-8. Spiral-Helical SWHE Size-Range Design Graph for the Continental United States

6.2 Alternate SWHE Designs

There are other SWHE designs that are either out in the market or could readily be utilized. These include spiral-helical coils that use different HDPE tube thicknesses, thermally

enhanced HDPE tubing, or copper tubing. Vertical flat-plate heat exchangers are also sold by at least two different manufacturers. Equation 5-7 will be used to create sizing design graphs for the different SWHE designs that contain tubing while Equation 5-10 will be used for the vertical flat-plate SWHE.

6.2.1 HDPE Wall Thickness Influence

After the discovery of the high influence of the tube conductive resistance in the HDPE coils, as discussed in Section 5.1.1, an improvement to the design became obvious – reduction of the tube wall thickness. This is possible for the SWHE portion of the system because high pressures are not present and therefore the tubing does not require high strength. If placed in public access waters, there is a possibility of tubing getting punctured by fishing lures, boat propellers, and boat anchors. Reducing the tube wall thickness is potentially risky and doing so should be done with extreme caution.

HDPE manufacturers do make different tube thicknesses other than SDR-11. The term SDR-11 comes from the diameter ratio obtained by dividing the outside tube diameter by the wall thickness. Two tubes with smaller wall thicknesses examined here are SDR-13.5 and SDR-15.5. The dimensions for the three tubes used in this comparison are shown in Table 6-2.

Table 6-2. High Density Polyethylene Tubing Dimensions

Nominal Tube Size		Tube Schedule	Tube OD				Wall Thickness				Nominal ID	
mm	in	SDR-XX	mm	± mm	in	± in	mm	± mm	in	± in	mm	in
19	0.75	11	26.7	0.10	1.050	0.004	2.4	0.51	0.095	0.02	21.8	0.860
		13.5	26.7	0.10	1.050	0.004	2.0	0.51	0.078	0.02	22.7	0.894
		15.5	26.7	0.10	1.050	0.004	1.7	0.51	0.068	0.02	23.2	0.915
25	1	11	33.4	0.13	1.315	0.005	3.0	0.51	0.120	0.02	27.4	1.077
		13.5	33.4	0.13	1.315	0.005	2.5	0.51	0.097	0.02	28.5	1.121
		15.5	33.4	0.13	1.315	0.005	2.1	0.51	0.084	0.02	29.1	1.145
32	1.25	11	42.2	0.13	1.660	0.005	3.8	0.51	0.151	0.02	34.5	1.358
		13.5	42.2	0.13	1.660	0.005	3.1	0.51	0.123	0.02	35.9	1.414
		15.5	42.2	0.13	1.660	0.005	2.7	0.51	0.107	0.02	36.7	1.446

Using the same simulation that was developed for obtaining the sizing design graphs for the SDR-11, SDR-13.5 and SDR-15.5 were added in to shown their impact on the sizing. Figures 6-9 through 6-11 show the variation in the coil sizing for the three tubes on the medium spaced configuration, at a constant lake temperature of 20°C (68°F), with the ES030 Florida Heat Pump, on the 19 mm (¾ in), 25 mm (1 in), and 32 mm (1-¼ in) tube sizes respectively.

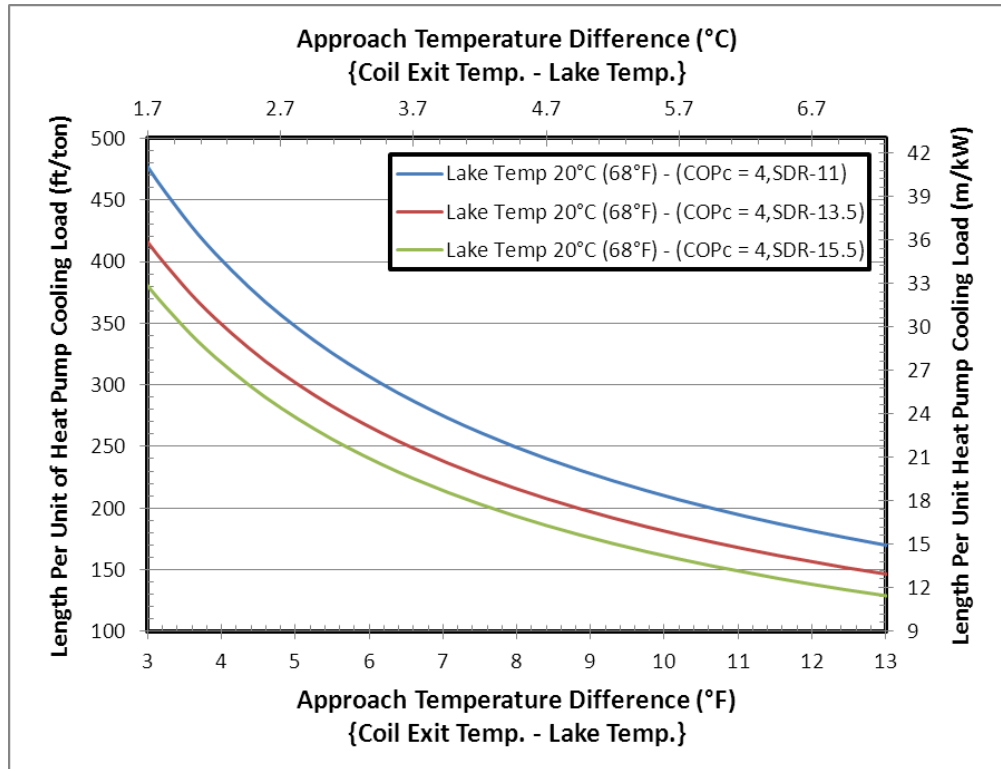


Figure 6-9. Wall Thickness Influence Design Graph (19 mm, ¾ in HDPE Medium Spaced SWHE)

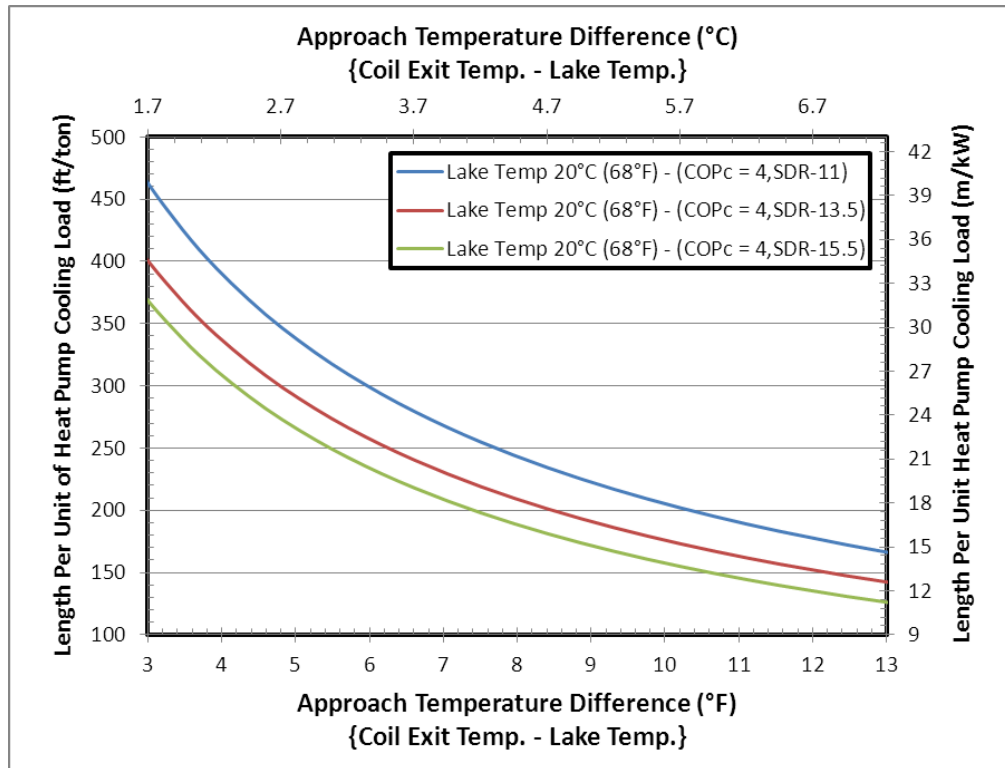


Figure 6-10. Wall Thickness Design Graph (25 mm, 1 in HDPE Medium Spaced SWHE)

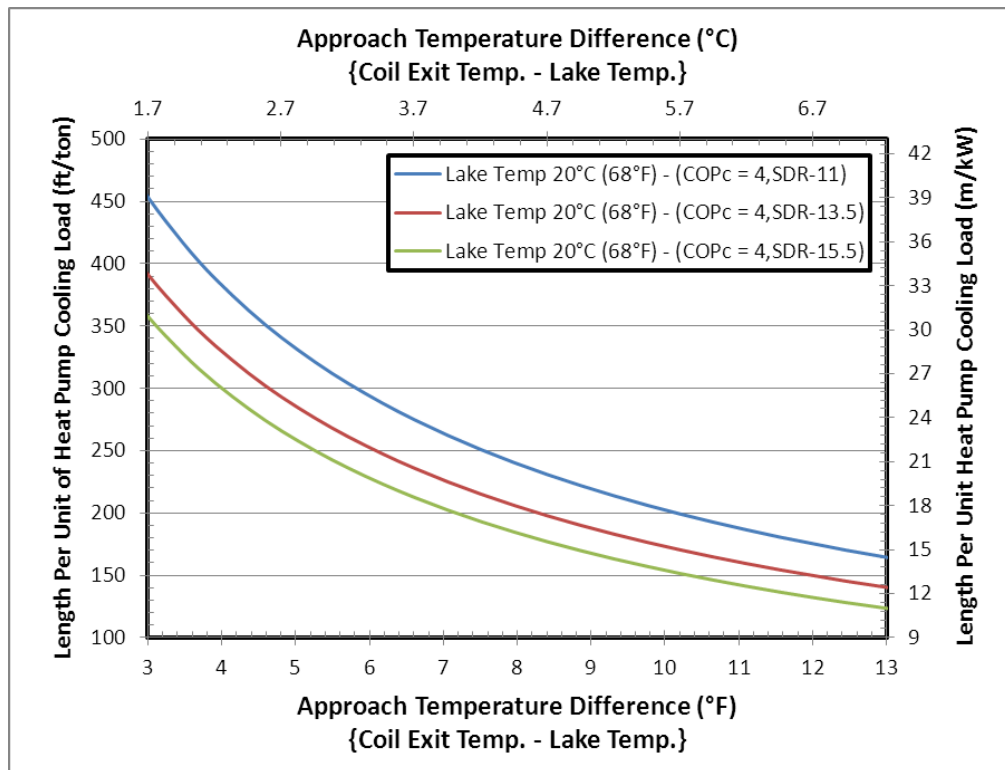


Figure 6-11. Wall Thickness Design Graph SWHE (32 mm, 1-1/4 in HDPE Medium Spaced SWHE)

As can be seen, the sizing of the coils is significantly reduced as the wall thickness is brought down from SDR-11 to SDR-15.5. On average, the reduction in sizing from SDR-11 to SDR-13.5 is 14% while it's 21% for SDR-11 to SDR-15.5 for cases where the approach temperature difference is between 1.7°C (3°F) and 7.2°C (13°F).

6.2.2 Thermally Enhanced SDR-11 HDPE Coils

Recently a Canadian manufacturer, IPL Plastics (Spitler 2011), has introduced thermally enhanced HDPE tubing with conductivity 75% higher than that of standard HDPE (~0.7 W/m-K instead of 0.4 W/m-K; 0.4 Btu/hr-ft-°F instead of 0.23 Btu/hr-ft-°F). This increase in thermal conductivity was investigated to determine the extent of the sizing decrease for three sizes of SDR-11 HDPE tubing. A comparison between the thermally enhanced HDPE and the standard HDPE tubing is shown in Figure 6-12.

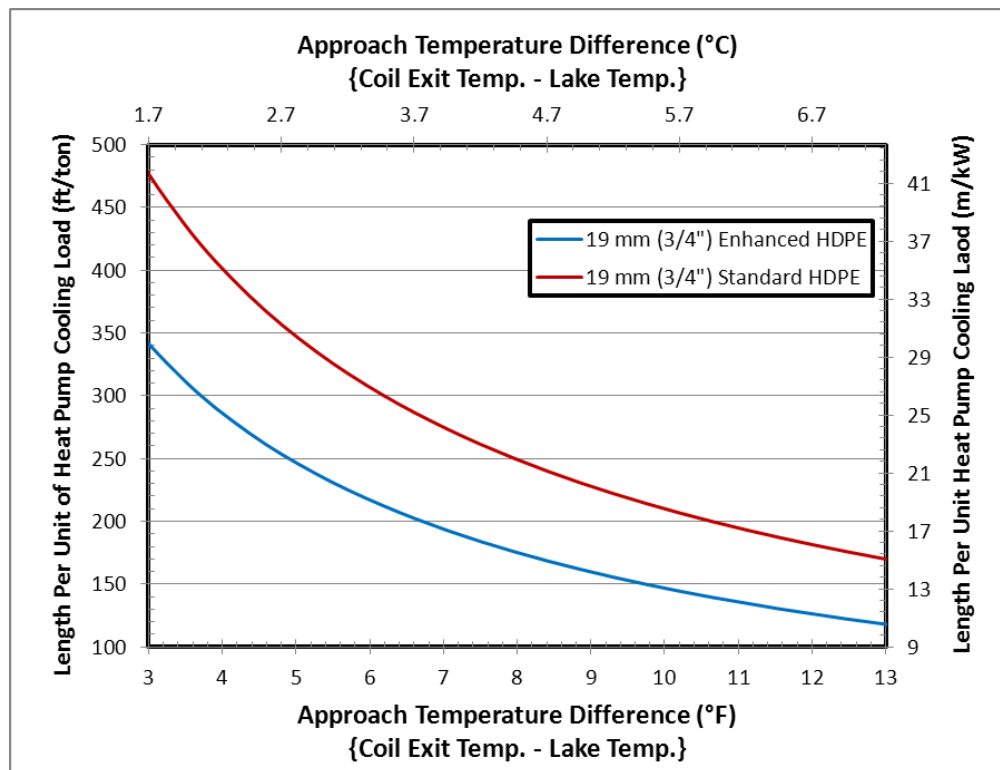


Figure 6-12. Standard vs. Thermally Enhanced SDR-11 HDPE Design Graph (Medium Spaced Spiral-Helical SWHE)

The sizing design graph shows precisely what was expected. The increase in thermal conductivity caused a reduction in the required size of the spiral-helical SWHE. A comparison between the original HDPE and the thermally enhanced HDPE shows that the reduction in size from standard HDPE is approximately 28-32% for approach temperature differences between 3-13°C (1.7-7.2°F).

6.2.3 Copper Tubing Coils

In order to create a coil sizing design graph for a copper tubing coil a few parameters need to be modified from the HDPE spiral-helical coil simulation. The main alteration is the thermal conductivity of the tube material. Instead of using the equation by Rauwendaal (1986) for HDPE, a value of 400 W/m-K (231 Btu/hr-ft-°F) was used. The tubing dimensions that were used for simulation were for 19 mm (¾ in) copper tube. This meant that the actual inside and outside diameters were 21 mm (0.81 in) and 22 mm (0.875 in) respectively. Again, Equation 5-7 was used to obtain the outside convection coefficient, the lake temperature was varied from 5°C (41°F) to 35°C (95°F), the heat pump COP_c was held constant at four, and the coil configuration was selected to be medium spaced. Figure 6-13 is the copper coil sizing design graph.

It should be noted that the use of Equation 5-7 for the copper coil did exceed the range of applicability at the upper end of the modified Rayleigh number. Further investigation showed that the places where the modified Rayleigh number exceeded the range was only in conditions where the lake temperature exceeded 25°C (77°F). The highest amount that the modified Rayleigh number exceeded the recommended range was a value of 1.1×10^8 . The use of extrapolation for the copper coil may introduce some minor additional error and thus further investigation should be conducted.

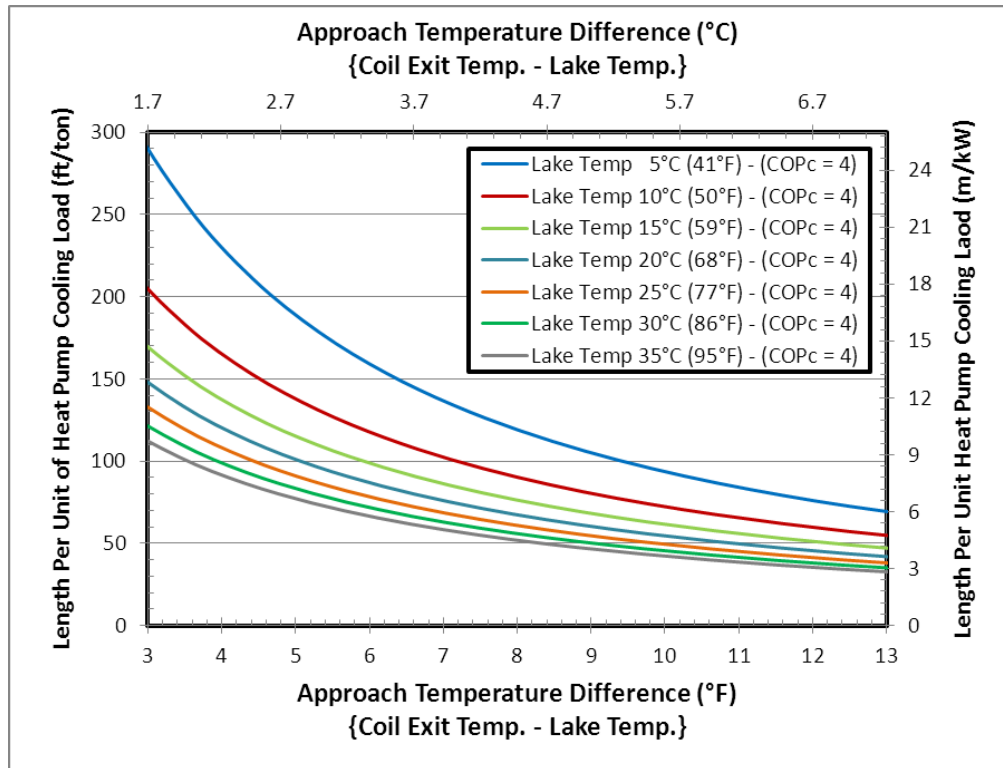


Figure 6-13. Medium Spaced Copper Tube SWHE Sizing Design Graph (19 mm, 3/4 in)

The use of copper tubing dramatically reduces the size of the heat exchanger required for the same amount of heat pump cooling load as seen by comparing the 20°C (68°F) lines of Figures 6-13 to 6-9. The reduction in size is on average from the SDR-11 HDPE at 20°C (68°F) is around 69% for low approach temperature differences and about 77% for high approach temperature differences. The lake temperature has a greater effect on the sizing of the copper coils compared to HDPE.

The problem with using copper as the SWHE material comes in the corrosion and the cost. Copper may corrode in lakes and rivers and the heat transfer capacity may as a result go down. Further research on the corrosion of metal heat exchangers is another area of importance for this field. The cost of 19 mm (3/4 in) copper tubing at present time is roughly \$9.45/m (\$2.88/ft) from a commercial chain store which is 10.6 times greater than the \$0.89/m (\$0.27/ft) for 19 mm (3/4 in) HDPE tubing. Further economic analysis is provided in Section 6.2.5.

6.2.4 Comparison of Tubing Alternatives

To better understand the how each of the alternative tubing options affect the sizing of the surface water heat exchanger, it is beneficial to plot all of the results on a single design graph.

To do this, several parameters had to be fixed. They include the following:

- The lake temperature was selected to be 20°C (68°F)
- The heat pump efficiency was a constant value of four ($COP_c = 4$)
- The nominal tube outside diameter was 19 mm (¾ inch)
- The coils were arranged in the medium spacing configuration

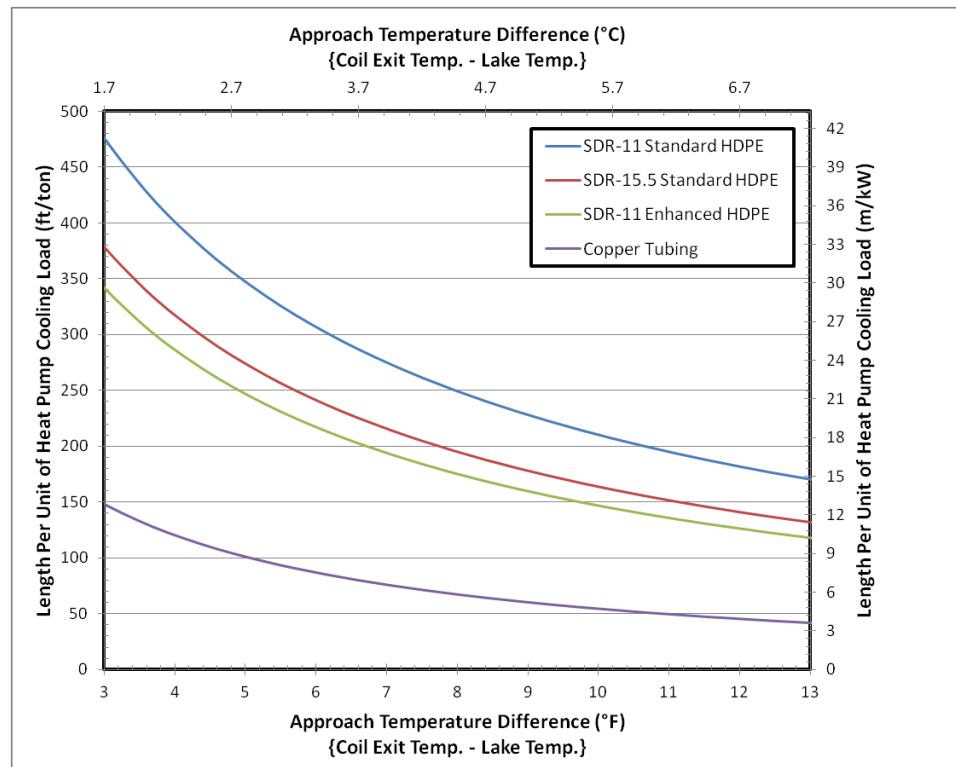


Figure 6-14. Alternative SWHE Tubing Comparison Design Graph

Figure 6-14 shows that each of the alternatives to the standard SDR-11 HDPE tubing does reduce the required size of the heat exchanger to reject the same amount of heat for a given approach temperature difference. As stated previously, the copper provides the greatest reduction in size followed by the thermally enhanced HDPE and SDR-15.5 HDPE respectively.

6.2.5 Vertical Flat-Plate Heat Exchanger

Using Equation 5-10 for vertical flat-plate heat exchangers, sizing design graphs were created to aid design engineers if this type of SWHE was selected for a SWHP system. A difference in these design graphs are that instead of on a per meter (ft) scale, they will be conducted on a per square meter (ft^2) basis. Figure 6-15 shows the vertical flat-plate heat exchanger design graph for different lake temperatures.

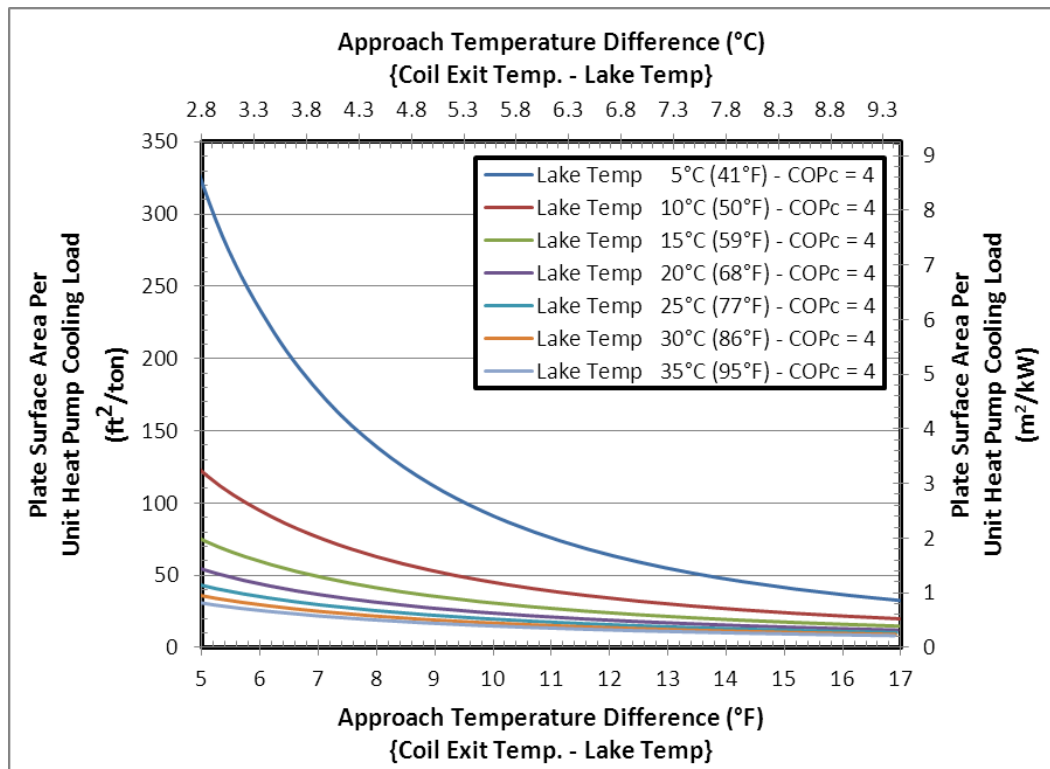


Figure 6-15. Vertical flat-plate SWHE Sizing Design Graph

The sizing design graph for a vertical flat-plate heat exchanger shows that the lake temperature causes more influence than for the HDPE spiral-helical coils at lower lake temperatures. It also shows that once the lake temperature goes above 20°C (68°F), the sizing only differs by 0.5 m^2/kW (20 ft^2/ton).

Similar to the copper spiral-helical SWHE, the vertical flat-plate heat exchanger will tend to provide better heat transfer because it is made from metal instead of HDPE. Also like the copper coil, both fouling and cost are large issues when using this type of a SWHE.

6.2.6 Coil Selection Economics

As with many topics in engineering, it all comes down to economics. If a SWHE can be designed with high heat transfer capacity, small size, no fouling, and minimal pressure drop but it has a price tag that is too high, the design will simply not be used. Several of the previously mentioned SWHEs have been further examined to determine their cost per unit of heat pump cooling load.

Current prices were obtained from local distributors for both HDPE and copper tubing. Copper tubing is sold in spools at a unit cost of about \$8.20/m (\$2.50/ft). The SDR-11 HDPE coils came in 152.4 m (500 ft) lengths and cost \$135, \$200, and \$310 for the 19 mm ($\frac{3}{4}$ in), 25 mm (1 in), and 1- $\frac{1}{4}$ in) tube sizes respectively. These prices were first broken down into a cost per length and then further broken down into a cost per volume of HDPE tubing. This was to price out the smaller wall thickness tubes. It may be worth noting that the estimation for the price of the smaller wall thickness tube is most likely on the low side because of fixed manufacturing costs. Never the less, the cost per volume was calculated and then used to calculate the cost per unit length. Table 6-3 shows the costs broken down for the different tubing.

Table 6-3. Cost Analysis of HDPE and Copper Tubing

HDPE	Nominal Tube Size		Weight/length		Price by Weight		Price by Length	
	mm	in	kg/m	lb/ft	\$/kg	\$/lb	\$/m	\$/ft
SDR-11	19	0.75	0.182	0.122	\$ 1.00	\$ 2.21	\$ 0.89	\$ 0.27
	25	1	0.284	0.191	\$ 0.95	\$ 2.09	\$ 1.31	\$ 0.40
	32	1.25	0.455	0.306	\$ 0.92	\$ 2.03	\$ 2.03	\$ 0.62
SDR-13.5	19	0.75	0.152	0.102	\$ 1.00	\$ 2.21	\$ 0.74	\$ 0.23
	25	1	0.237	0.159	\$ 0.95	\$ 2.09	\$ 1.09	\$ 0.33
	32	1.25	0.378	0.254	\$ 0.92	\$ 2.03	\$ 1.69	\$ 0.51
SDR-15.5	19	0.75	0.132	0.089	\$ 1.00	\$ 2.21	\$ 0.65	\$ 0.20
	25	1	0.210	0.141	\$ 0.95	\$ 2.09	\$ 0.97	\$ 0.30
	32	1.25	0.332	0.223	\$ 0.92	\$ 2.03	\$ 1.48	\$ 0.45
Copper	19	0.75	0.497	0.334	\$16.50	\$7.49	\$ 8.20	\$2.50

The prices per unit length were then applied to the design graphs previously created for spiral-helical SWHEs to obtain a cost per unit of heat pump cooling load in \$/kW (\$/ton). Figure 6-16 shows a design graph similar to the SWHE sizing design graphs except it is in terms of price for each type of SWHE. It is important to know that this is strictly a first cost view of the heat exchanger material. Some additional costs beyond the material that will be present are the pumping costs, heat pump operating costs, and fabrication/installation costs.

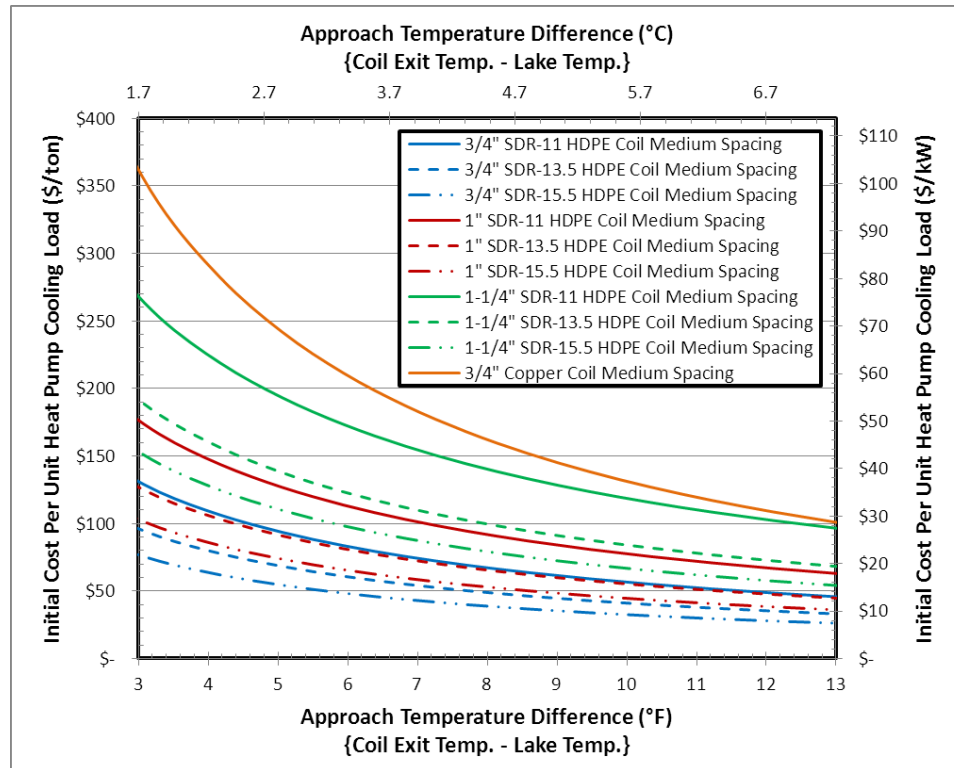


Figure 6-16. Spiral-Helical SWHE Tubing Material Pricing Design Graph

Even though Figure 6-16 is time dependent, the current findings that can be drawn from it are interesting. The copper tubing that was originally looked at as a significant reduction in sizing is actually the most expensive on a cost per length basis. This doesn't necessary rule out using copper tubing. In situations where large volumes of SWHEs may cause problems, compact copper coils may be the best design still especially when the approach temperature difference becomes quite large.

Similar to the copper tubing, the large HDPE tube size (32 mm, 1-1/4 in) was lowest on the sizing design graph but is some of the highest in terms of cost per unit of heat pump cooling load. As stated earlier though, this is strictly a material cost and the larger diameter tube may reduce the cost of pumping enough to make it a feasible design.

The main thing to grasp from the figure is that the smaller the tube and wall thickness, the cheaper the SWHE can be made. This could mean that it may be of interest to design a SWHE

that has extremely small-thin tubes so that the cost is reduced significantly. The caution with such a design has to do with the pressure loss through the smaller tube. Using too small of tubing could cause pump requirements to exceed the benefits of the gained by using the smaller tube. In order to protect a small-thin tube, an enclosure may be of interest so that damage to the tubing is avoided.

6.3 Design Graphs or Software Design Tool

In this chapter, numerous design graphs have been presented showing different design lengths per unit heat pump capacity or unit heat rejection. As shown in Figure 6-8, there can be a significant variation in required design lengths depending for spiral helical coils, even if they all utilize SDR-11 HDPE piping. Accordingly, a software design tool that can account for the effects of different:

- lake temperatures,
- pipe diameters,
- pipe spacing,
- pipe materials,
- antifreeze concentrations,
- heat pump performance,

and other factors may be preferable to design graphs. The design graphs shown here were all created with a simple spreadsheet/VBA based tool.

CHAPTER VII

7. SUMMARY, CONCLUSIONS, AND RECOMMENDATIONS

As discussed in Section 1.6 (Objectives and Organization), this thesis focuses on three main areas: The experimental apparatus and testing of closed-loop SWHEs, the analysis of the experimental data into correlations, and the development of application tools for SWHEs using the obtained correlations for the experimental analysis.

7.1 Summary of Experimental Testing, Apparatus, and Procedures

Over the course of one and a half years, 119 tests were conducted in the approximately 12,141 m² (3 acre or 130,680 ft²) testing pond. The breakdown of the testing is as follows:

- 66 spiral-helical tests
- 30 factory/loose bundle tests
- 3 flat-spiral tests
- 15 vertical and horizontal slinky tests
- 5 vertical flat-plate heat exchanger tests

The testing equipment, data acquisition, and experimental procedures were developed over a series of tests that preceded the 97 tests reported here. In the earlier tests, there were a number of lessons learned along the way through failure and these are reflected in the summary below.

A summary of the equipment and data acquisition devices that were used during the experimental testing is as follows:

Equipment

- 1) Air Compressor. A three gallon air compressor was used to remove water from the test coils allowing them to rise back to the surface. The size of the motor was 0.75 kW (1 hp) and it provided 1.75 L/s @ 276 kPa (3.7 SCFM @ 40 psi).
- 2) Boat. A simple 3 m (10 ft) flat-bottom boat was used for deploying the SWHEs in the test pond. Calm weather during deployment made the processes fast and simple since paddles were the primary source of propulsion. A motor would most likely have made deployment faster.
- 3) Coil Connections. Unions were found to be the best connection given the testing conditions and moments place on the connection joint. Although it was not the most time efficient it provided the best seal.
- 4) Coil Spacers. PVC and rod spacers were used to create a well-controlled spacing pattern between the spiral-helical coils. Space increments of 38.1 mm (1.5 in), 66.7 mm (2.625 in), and 104.8 mm (4.125 in) were varied in both the horizontal and vertical directions in order to form a 3 x 3 testing matrix.
- 5) Coil Suspension Frame. A fabricated steel frame with support uprights was used to suspend the test coil in a rigid manner (no deformation) at a predetermined depth via buoys and ropes. An anchor near the testing site is recommended with a tether line to the frame to prevent the test coil from drifting around the lake.
- 6) Heater Elements. Three electric water heater elements of at least 3.5 kW (11,942 Btu/hr) each were used to create a highly controllable load on the system. The heater elements were threaded directly into the piping system via a threaded tee connection. One of the three heaters was connected to a proportional controller to allow multiple set points to be obtained. Higher heat input minimizes heat transfer uncertainty because higher temperature differences between the inlet and outlet of the SWHE occur. This becomes difficult in winter months due to high heat losses through the connecting pipe from the trailer to the test coil.
- 7) Power Supply. Two large extension cords were connected to a local building with 240V/30A electricity. Power generators could be used if highly remote testing was required.
- 8) Pumps. Two circulating pumps and two purging pumps were used for the pumping of the water through the system. The circulating pumps were sized to flow between 0.25 L/s – 0.79 L/s (4 GPM – 12.5 GPM) at

approximately 7.3-9.1 m (24-30 ft) of head loss depending on if 19 mm ($\frac{3}{4}$ in) tube or 32 mm (1- $\frac{1}{4}$ in) tube was used for the connecting pipe to the SWHEs and the SWHEs themselves.

- 9) SWHEs. Five different SWHEs were tested in numerous configurations. The different SWHEs were the spiral-helical, flat-spiral, slinky, bundle, and vertical flat-plate.
- 10) Valves and Controls. Although a needle valve allows for precise control of the flow rates, a simple ball valve was used to control the flow rate since it was not of particular interest in this study and higher flow rates were desired. Three-way valves were also used to determine which piping circuit was being used: circulating or purging.
- 11) Water Source. City potable water was used from a garden hose to fill up the purging water tank. The water tank could be valuable for remote testing locations.

Data Acquisition Devices

- 1) Data Logger. A Fluke Hydra II data logger was used for recording the data in an organized manner. Other data loggers may be used depending on availability.
- 2) In-pipe Temperature Measurement. Sheathed thermistor probes were threaded directly into the flow of the circulating fluid via threaded tee connections at four locations: trailer supply, coil inlet, coil outlet, and trailer return. Calibration conducted on the thermistor probes were always below $\pm 0.1^{\circ}\text{C}$ (0.2°F).
- 3) Lake Temperature Measurement. Two temperature trees were utilized to measure the lake temperatures at seven different depths at two separate locations (total of 14 depths). The small-bead thermistors were calibrated to within $\pm 0.1^{\circ}\text{C}$ (0.2°F). But special effects add additional uncertainty, which was estimated to make the total uncertainty 0.25°C (0.45°F).
- 4) Flow Rate Measurement. The flow rate was measured with a flow meter that was calibrated to within ± 0.0023 L/s (0.036 GPM). The flow rate was used directly in the calculation of the inside convective resistance as well as the heat transfer rate from the SWHE.
- 5) Power Input. A watt transducer was used to measure the power input to the system. It was not required however because of the losses from the trailer to the test coil were significant since the connecting pipe could not be insulated as it was going into the water. It did allow for easy determination of set point changes though.

The following is the testing procedure used:

1. Prepare the SWHE for testing per spacing specifications on coil winding apparatus. Transport the SWHE to the testing pond. This includes placement of the SWHE on the steel frame if required. Securely fasten the SWHE to the frame.
2. Connect trailer to experimental apparatus. Seal the connection joints thoroughly using plumbing tape, paste, and silicone. This includes the installed in-pipe thermistor probes at the four specified locations.
3. Conduct an on-shore leak test prior to deploying the SWHE into the testing pond. If leaks are detected, remove the water from the system and reseal all leak location. Re-administer the on-shore leak test until no leaks are present throughout the entire system. Remove all water from the system prior to deployment.
4. Connect all required buoys onto the frame or SWHE in order to suspend it off of the bottom when the coil is submerged. Also connect any other remaining data acquisition thermistors and secure them carefully in their desired locations.
5. Load the SWHE onto the boat and transport it to the testing location on the pond. Gently place the SWHE into the pond so as to avoid flipping of the boat or the coil. Connect the tether line from the frame or coil to the anchor line to prevent the coil from drifting around the test pond.
6. Arrange the valves so the purging loop can be engaged. Start the purging pumps. Allow each section (coil, trailer, and both) to purge for at least 15 minutes. Larger diameter tube will require more purging time. Upon completion of the purging, set valves for the circulation loop.
7. Start the data logger and collect data for the ambient conditions **before** any mechanical devices (pumps or heaters) are turned on. **Typical tests last around 4-6 hours** depending on the size of the tubing used in the SWHE.
8. Start the circulating pumps and heater elements. Observe the transitions between set points. Make sure steady-state conditions are reached before moving to the next set point. Typical transition time is around 30 minutes.
9. Upon the completion of the testing set points, **shut off the heaters first and then the circulating pumps**. Once the pumps and heaters are turned off, so too can the data logger.
10. Close the outside trailer ball valves and disconnect both connecting pipe from the coil at the trailer. Connect one end of the disconnected pipe to the ball valve which is already connected to the air compressor and secure the other end to drain into the pond. When the air compressor is charged to 517 kPa (75 psig) slowly open the valve to about 20% and allow the SWHE to drain of water. **Do not allow valve to fully open! Damage to the SWHE connections may occur.** As the SWHE drains, it should float to the surface of the test pond.

11. Use the boat to retrieve the SWHE from the test pond. Remember to disconnect the tether line from the anchor line. Tow back to shore and remove from the test pond.
12. When the testing is completed, drain all piping and SWHE of water, especially if near or below freezing conditions.
13. Measure the test pond level relative to a set reference point in order to determine the locations of the temperature tree thermistor locations.

7.2 Conclusions: Convection Research

- The spiral-helical SWHE configuration data for 66 tests were analyzed and correlated. Some of the measurements, particularly at low heat transfer rates, had quite high uncertainties.

After some analysis described in Section 5.1.4, 59 of 528 measurements with uncertainties exceeding $\pm 70\%$ were removed from the correlation data set. A number of correlations were investigated, several with similar RMSE, but Equation 5-7 was selected as the recommended correlation:

$$Nu_{f,o,d_o} = 0.16(Ra_{f,o,d_o}^*)^{0.264} \left(\frac{\Delta y}{d_o}\right)^{0.078} \left(\frac{\Delta x}{d_o}\right)^{0.223}$$

See Section 5.1.4 for the range of applicability of the correlation. When used for predicting convection coefficients, the correlation gives an RMSE of 21%. When used to predict heat transfer rates, the RMSE is less than 6%.

- Proximity to the lake bottom was also investigated. A spiral-helical coil was tested while suspended in the testing pond and then lowered onto the pond bottom. No significant reduction in outside heat transfer coefficients was obtained. The reason for this is believed to be the steel frame and coil spacers holding the SWHE out of the mud. Further testing is highly recommended to shed more light on this.
- Factory bundle testing was conducted to provide a lower boundary on the heat transfer rate to show the improvement of spacing out spiral-helical coils. Reductions in heat transfer rates were found between 30% and 60% for a factory bundle compared to a controlled-spacing spiral-helical SWHE. Spaced bundle tests were also conducted and found to show varying

performance levels. The decrease in heat transfer rates for the spaced bundles was found to be between 0-30% when compared to the controlled-spacing spiral-helical SWHE.

- The flat-spiral and slinky configurations were combined and correlated using a modified Rayleigh number to form Equation 5-9.

$$Nu_{f,o,d_o} = 0.047(Ra_{f,o,d_o}^*)^{0.34}$$

The correlation is of a simple form and accurately predicts the outside convection coefficient with an RMSE of 34%. This may be due to the small sample size of tests. Increased testing may further improve this correlation.

- A correlation using a modified Rayleigh number was obtained for the limited testing conducted on the vertical flat-plate heat exchanger.

$$Nu_{f,o,H} = 1.35 \times 10^{-5}(Ra_{f,o,H}^*)^{0.55}$$

Accuracy from the correlation is high with an RMSE of only around 14%. A comparison between the experimental data and the correlation by Churchill and Chu (1975) for vertical flat-plates (Figure 5-23) shows the Churchill and Chu correlation gives reasonable accuracy.

- The dominant thermal resistance in a SWHE made out of HDPE was found to be the tube conductive resistance. Approximately 60% or more of the total thermal resistance was due to the material for SDR-11 tube sizes of 19 mm (¾ in) and larger. This was not the case however for the vertical flat-plate heat exchanger. The outside convective resistance was the dominant thermal resistance in this case at around 88% while the wall conductive resistance was under 2%.

7.3 Conclusions: Applications Research

Sizing design graphs, similar to those presented by Kavanaugh and Rafferty (1997), that give SWHE size per unit heat transfer rate as a function of approach temperature difference were developed. These were shown to be sensitive to a number of parameters not noted to be important by Kavanaugh and Rafferty. These include:

- Lake temperature. At lake temperatures going from 20°C (68°F) to 35°C (95°F) and approach temperature differences greater than 2.8°C (5°F), a 7% decrease in size is demonstrated. The sensitivity increases dramatically as the lake temperature goes below 20°C (68°F). Designers should be aware of these sensitivities, but at low lake temperatures, low approach temperature differences should not be needed.
- Heat pump efficiency. At a lake temperature of 20°C (68°F), approach temperature differences greater than 2.8°C (5°F), and a heat pump efficiency (COP_c) greater than 4, a 13-25% increase in size is shown. Other heat pump efficiencies can and should be used in conjunction with the coil rejection line in order to accurately size the SWHE.
- The spiral-helical SWHE correlation (Equation 5-7) was implemented into a heat exchanger simulation for three different scenarios applicable to the United States and sizing design graphs were generated to aid design engineers. Simply knowing the approach temperature difference, the lake temperature, the efficiency of the heat pump being used, and the tubing used in the SWHE could allow the design engineer to accurately determine the required length of tube per unit of heat pump cooling load. For all scenarios considered together, the largest difference in size was on the order of 2.6-15.6 m/kW (30-180 ft/ton) at approach temperature differences ranging from 1.7-7.2°C (3-13°F).
- Since the conductive resistance is the dominant thermal resistance in an HDPE SWHE, the thickness of the tube walls as well as the use of thermally enhanced HDPE was looked at with respect to allowing a reduction in sizing. SDR-13.5 was shown to give a reduction in size of about 14% while the SDR-15.5 was about 21% for an approach temperature range of 1.7-7.2°C (3-13°F). The thermally enhanced SDR-11 HDPE provided a reduction of around 29% over the same range of approach temperatures.
- Copper as a tubing material was also created into a sizing design graph using the spiral-helical SWHE correlation for outside convection coefficients. The reduction in length when

compared to that of SDR-11 HDPE was found to be 69% for low approach temperature differences and 77% for high ones.

- A vertical flat-plate sizing design graph incorporating a constant COP_c heat pump of four and various lake temperatures was created. The scaling uses surface area, both sides of the plate, instead of the length of tubing.
- A first cost analysis for the material of a SWHE revealed that a copper coil, even though smaller in sizing requirement than the SDR-11 HDPE tubing, is actually more expensive per unit of heat pump cooling load than HDPE tubing smaller than 32 mm (1-1/4 in). Thinner walled HDPE tubing proved to be the most cost effective choice but caution should be used if selected for installment in a high traffic body of water since thinner walls may result in easier damaging.

7.4 Recommendations: Convection Research

- Reduce the uncertainty by increasing the amount of heat input (increase $T_{c,in} - T_{c,out}$) and knowing the tubing geometry and properties. The tolerances on the inside diameter caused the variation in wall thickness (according to the manufacturer) to be quite large. With the thermal conductivity of the HDPE being low, this resulted in high amounts of uncertainty. Knowing the dimensions of the entire tube would allow for more accurate uncertainty.
- Additional coil configurations testing. Aside from the 19 mm (3/4 in) diameter spiral-helical configuration, most of the other SWHEs require further testing in order to adequately capture the results. These additional tests include the remainder of the 25 mm (1 in) and 32 mm (1-1/4 in) spiral-helical plus more spacing combinations, coil diameter variations on the spiral-helical coils, flat-spiral coils at different tube-to-tube spacing and diameters, slinky coils with more loop diameters and pitches, vertical flat-plate heat exchangers with flow and inlet location variations, and finally a copper helical coil with various diameters and pitches. These

suggested tests should help provide an even better comprehension of the geometry influence on the performance of SWHEs.

- Additional testing in lake temperatures below 10°C (50°F) is recommended for both heat rejection and heat extraction. It is important to run supplementary heat rejection tests in cooler water conditions because large deep lakes have vast amounts of untapped cool water. Heat extraction testing is also important for northern climates dominated by heating. Ice formation on coils is also an important area in need of research.

7.5 Recommendations: Applications Research

- Various tests of fouling and lake bottom proximity. Conducting experiments in various water conditions (murky, clear, mud bottom, rock bottom, etc.) would be beneficial to measure the increase/decrease in SWHE performance. This may also help determine to what extent cleaning of the SWHE periodically is beneficial.
- Experiments using the findings of this research. Testing of thin walled tubing should show an improvement in the performance of the SWHE. Durability may be an issue where high human traffic on the water may cause damage to the coils.
- A more detailed economic analysis of the different SWHEs. This would include, but is not limited to, pumping costs, heat pump operation costs, fabrication costs, installation expenses and system maintenance. As an example, even though larger diameter tube may cost more initially, the reduction in pumping costs may offset it. Similar reasons with the other areas of consideration.
- Finally, the best way to validate this research is by having actual performance data from a system in similar conditions that is operating currently. The input conditions may be taken from the actual system and placed into a computer simulation using the findings of this research to predict the SWHE performance. A comparison between results can be made and the research validated.

REFERENCES

- Ali, M. E. 2006. "Natural Convection Heat Transfer from Vertical Helical Coils in Oil." Heat Transfer Engineering 27(3): 79-85.
- Austin III, W. A. 1998. Development of an In Situ System for Measuring Ground Thermal Properties Masters Thesis, Oklahoma State University.
- Chen, X., G. Zhang, J. Peng, X. Lin and T. Liu 2006. "The performance of an open-loop lake water heat pump system in south China." Applied Thermal Engineering 26(17-18): 2255-2261.
- Chiasson, A., S. Rees, J. Spitler and M. Smith 2000. "A Model for Simulating the Performance of a Shallow Pond as a Supplemental Heat Rejecter with Closed-Loop Ground-Source Heat Pump Systems." ASHRAE Transaction 106(2): 1-15.
- Churchill, S. W. and H. H. S. Chu 1975. "Correlating equations for laminar and turbulent free convection from a horizontal cylinder." International journal of heat and mass transfer 18(9): 1049-1053.
- Churchill, S. W. and H. H. S. Chu 1975. "Correlating equations for laminar and turbulent free convection from a vertical plate." International journal of heat and mass transfer 18(11): 1323-1329.
- Hampton, T. V. 2008. "Cool Returns." Retrieved 7/22/2011, 2011, from http://midwest.construction.com/features/archive/0812_feature2.asp.
- Hattermer, B. and S. P. Kavanaugh 2005. "Design Temperature Data for Surface Water Heating and Cooling Systems." ASHRAE Transactions 111(1): 695-701.
- Holman, J. P. and W. J. J. Gajda 1984. Experimental Methods for Engineers, McGraw-Hill Book Company.
- Kavanaugh, S. P. and M. C. Pezent 1989. Water-to-Air Heat Pump Performance with Lakewater. Sixth Symposium on Improving Building Systems in Hot and Humid Climates. Dallas, TX.
- Kavanaugh, S. P. and M. C. Pezent 1990. "Lakewater applications of water-to-air heat pumps." ASHRAE Transaction 90(4): 813-820.
- Kavanaugh, S. P. and K. D. Rafferty 1997. "Ground-Source Heat Pumps - Design of Geothermal Systems for Commercial and Institutional Buildings." ASHRAE.
- Keens, D. 1977. "Case for Seawater Cooling." Institution of Chemical Engineers Symposium Series(52): 3. 1-3. 8.
- Kremposky, M. E. 2007. "Little" Green Schoolhouse Rises in Whitmore Lake. Cam Magazine: 56-66.
- Leraand, T. K. and J. C. Van Ryzin 1995. Air conditioning with deep seawater: a cost-effective alternative for West Beach, Oahu, Hawaii. Proceedings of the 1995 MTS/IEEE Oceans Conference. Part 1 (of 3), October 9, 1995 - October 12, 1995, San Diego, CA, USA, IEEE.
- Looney, C. and S. Oney 2007. "Seawater district cooling and lake source district cooling." Energy Engineering: Journal of the Association of Energy Engineering 104(5): 34-45.
- McCrary, B. H., S. P. Kavanaugh and D. G. Williamson 2006. "Environmental Impacts of Surface Water Heat Pump Systems." ASHRAE Transactions 112(1): 102-110.

- Morgan, V. T. 1975. "The Overall Convective Heat Transfer from Smooth Circular Cylinders." Advances in Heat Transfer 11: 199-264.
- Müller, W. W. 2007. HDPE Geomembranes in Geotechnics. Berlin ;New York, Springer.
- Newman, L. and Y. Herbert 2009. "The use of deep water cooling systems: Two Canadian examples." Renewable Energy 34(3): 727-730.
- Petukhov, B. S. 1970. "Heat transfer and friction in turbulent pipe flow with variable physical properties." Advances in Heat Transfer 6: 503-504.
- Pezent, M. C. and S. P. Kavanaugh 1990. "Development and verification of a thermal model of lakes used with water source heat pumps." ASHRAE Transaction 96(1): 574-582.
- Prabhanjan, D. G., T. J. Rennie and G. S. V. Raghavan 2004. "Natural convection heat transfer from helical coiled tubes." International Journal of Thermal Sciences 43: 359-365.
- Pugh, S. J., G. F. Hewitt and H. Muller-Steinhagen 2005. "Fouling during the use of seawater as coolant - The development of a user guide." Heat Transfer Engineering 26(1): 35-43.
- Rauwendaal, C. 1986. Polymer Extrusion, Hanser Publishers.
- Rogers, G. F. C. and Y. R. Mayhew 1964. "Heat transfer and pressure loss in helically coiled tubes with turbulent flow." International Journal of Heat and Mass Transfer 7(11): 1207-1216.
- Salimpour, M. R. 2009. "Heat transfer coefficients of shell and coiled tube heat exchangers." Experimental Thermal and Fluid Science 33(2): 203-207.
- Seban, R. A. and E. F. McLaughlin 1963. "Heat transfer in tube coils with laminar and turbulent flow." International Journal of Heat and Mass Transfer 6(5): 387-395.
- Sieder, E. N. and G. E. Tate 1936. "Heat Transfer and pressure drop of liquids in tubes." Ind. Engng Chem. 28: 1429.
- Sleicher, C. A. and M. W. Rouse 1975. "A convenient correlation for heat transfer to constant and variable property fluids in turbulent pipe flow." International Journal of Heat and Mass Transfer 18(5): 677-683.
- Spitler, J. D. 2011. Florida Heat Pump Data Sheet Example from 1997. G. Hansen: 1.
- Spitler, J. D. 2011. "Frågetecken för nya borrhållstekniker." Energi & Miljö 82(1): 10.
- Svensson, T. 1985. Experience from a lake heat system at O. Grevie, Sweden. Enerstock Conference. Toronto, Canada: 600-604.
- Viquerat, P.-A., B. Lachal, W. Weber, A. Mermoud and E. Pampaloni. 2007. "Utilization of a Deep Lake Water Direct Cooling Network (DLWDC) for cooling of a large administrative district. Energy and Environmental demonstration and follow-up." Retrieved 1/18/2010, from www.cuepe.ch/html/biblio/pdf/Draft%20paper%20VIQUERAT.pdf
- Zogg, R., K. Roth and J. Brodrick 2008. "Lake-source district cooling systems." ASHRAE Journal 50(2): 55-56.

APPENDIX A

Spiral-Helical Experimental Data & Reference Calculations

152

Test Description	Set Point	Date & Time	H		D _{ci}	D _{co}	V _{ci}	L/s	T _{cin}		T _{cout}		T _p	Q _c	W	R _c		R _t		R _f		R _o		h _o				
			in	cm					ft	m	GPM	°F				°C	°F	°C	Tons	W	hr ⁻² F/Btu	K/W	hr ⁻² F/Btu	K/W	hr ⁻² F/Btu	K/W	hr ⁻² F/Btu	K/W
4.125"V by 4.125"H Helical Coil (3/4")	1	3/17/11 1:52 PM	17.5	44.5	4.0	1.2	8.0	2.4	4.448	0.281	69.7	20.9	63.3	17.4	59.8	15.5	1.2	4169	4.295E-04	8.141E-04	2.574E-04	4.880E-04	1.665E-05	3.157E-05	1.554E-04	2.945E-04	46.8	266
4.125"V by 4.125"H Helical Coil (3/4")	2	3/17/11 2:23 PM	17.5	44.5	4.0	1.2	8.0	2.4	4.445	0.280	75.6	24.2	65.8	18.8	60.8	16.0	1.8	6327	4.174E-04	7.912E-04	2.585E-04	4.899E-04	1.619E-05	3.068E-05	1.427E-04	2.706E-04	51.0	289
4.125"V by 4.125"H Helical Coil (3/4")	3	3/17/11 2:52 PM	17.5	44.5	4.0	1.2	8.0	2.4	4.438	0.280	77.5	25.3	65.9	18.8	60.7	16.0	2.1	7526	3.836E-04	7.272E-04	2.585E-04	4.901E-04	1.610E-05	3.051E-05	1.090E-04	2.065E-04	66.8	379
4.125"V by 4.125"H Helical Coil (3/4")	4	3/17/11 3:24 PM	17.5	44.5	4.0	1.2	8.0	2.4	4.426	0.279	79.2	26.2	67.1	19.5	61.7	16.5	2.2	7823	3.858E-04	7.314E-04	2.590E-04	4.909E-04	1.598E-05	3.028E-05	1.109E-04	2.101E-04	65.6	373
4.125"V by 4.125"H Helical Coil (3/4")	5	3/17/11 3:52 PM	17.5	44.5	4.0	1.2	8.0	2.4	4.416	0.279	79.5	26.4	66.6	19.2	61.3	16.3	2.4	8306	3.697E-04	7.008E-04	2.588E-04	4.907E-04	1.602E-05	3.037E-05	9.485E-05	1.798E-04	76.7	436
4.125"V by 4.125"H Helical Coil (3/4")	6	3/17/11 4:19 PM	17.5	44.5	4.0	1.2	8.0	2.4	4.406	0.278	81.0	27.2	67.8	19.9	61.9	16.6	2.4	8517	3.851E-04	7.300E-04	2.593E-04	4.915E-04	1.591E-05	3.016E-05	1.099E-04	2.084E-04	66.2	376
4.125"V by 4.125"H Helical Coil (3/4")	7	3/17/11 4:49 PM	17.5	44.5	4.0	1.2	8.0	2.4	4.347	0.274	82.0	27.8	68.1	20.0	61.7	16.5	2.5	8818	3.997E-04	7.576E-04	2.594E-04	4.918E-04	1.603E-05	3.038E-05	1.242E-04	2.355E-04	58.6	333
4.125"V by 4.125"H Helical Coil (3/4")	8	3/17/11 5:19 PM	17.5	44.5	4.0	1.2	8.0	2.4	4.322	0.273	82.4	28.0	68.3	20.1	62.1	16.7	2.5	8955	3.885E-04	7.364E-04	2.595E-04	4.919E-04	1.607E-05	3.046E-05	1.129E-04	2.140E-04	64.4	366
4.125"V by 4.125"H Helical Coil (3/4")	1	3/18/11 9:07 AM	17.5	44.5	4.0	1.2	8.0	2.4	4.361	0.275	67.9	19.9	62.7	17.1	59.9	15.5	0.9	3280	4.425E-04	8.387E-04	2.572E-04	4.876E-04	1.708E-05	3.237E-05	1.682E-04	3.188E-04	43.3	246
4.125"V by 4.125"H Helical Coil (3/4")	2	3/18/11 9:32 AM	17.5	44.5	4.0	1.2	8.0	2.4	4.358	0.275	73.4	23.0	64.8	18.2	60.1	15.6	1.6	5456	4.429E-04	8.395E-04	2.581E-04	4.892E-04	1.664E-05	3.155E-05	1.682E-04	3.188E-04	43.3	246
4.125"V by 4.125"H Helical Coil (3/4")	3	3/18/11 9:51 AM	17.5	44.5	4.0	1.2	8.0	2.4	4.355	0.275	75.6	24.2	65.6	18.7	60.1	15.6	1.8	6368	4.430E-04	8.397E-04	2.584E-04	4.899E-04	1.648E-05	3.123E-05	1.681E-04	3.186E-04	43.3	246
4.125"V by 4.125"H Helical Coil (3/4")	4	3/18/11 10:12 AM	17.5	44.5	4.0	1.2	8.0	2.4	4.309	0.272	76.5	24.7	66.0	18.9	60.4	15.8	1.9	6631	4.375E-04	8.293E-04	2.586E-04	4.902E-04	1.656E-05	3.138E-05	1.624E-04	3.078E-04	44.8	254
4.125"V by 4.125"H Helical Coil (3/4")	5	3/18/11 10:37 AM	17.5	44.5	4.0	1.2	8.0	2.4	4.308	0.272	77.6	25.4	66.3	19.1	60.4	15.8	2.0	7146	4.399E-04	8.224E-04	2.587E-04	4.904E-04	1.648E-05	3.124E-05	1.587E-04	3.008E-04	45.9	260
4.125"V by 4.125"H Helical Coil (3/4")	6	3/18/11 10:57 AM	17.5	44.5	4.0	1.2	8.0	2.4	4.303	0.271	78.2	25.7	66.4	19.1	60.3	15.7	2.1	7472	4.278E-04	8.109E-04	2.588E-04	4.905E-04	1.646E-05	3.120E-05	1.526E-04	2.892E-04	47.7	271
4.125"V by 4.125"H Helical Coil (3/4")	7	3/18/11 11:17 AM	17.5	44.5	4.0	1.2	8.0	2.4	4.322	0.273	78.9	26.0	66.5	19.2	60.3	15.7	2.2	7829	4.224E-04	8.008E-04	2.588E-04	4.906E-04	1.635E-05	3.100E-05	1.472E-04	2.791E-04	49.4	281
4.125"V by 4.125"H Helical Coil (3/4")	8	3/18/11 11:38 AM	17.5	44.5	4.0	1.2	8.0	2.4	4.327	0.273	78.8	26.0	66.4	19.1	60.1	15.6	2.2	7846	4.250E-04	8.056E-04	2.588E-04	4.906E-04	1.635E-05	3.098E-05	1.498E-04	2.840E-04	48.6	276
4.125"V by 4.125"H Helical Coil (3/4")	1	3/18/11 1:05 PM	17.5	44.5	4.0	1.2	8.0	2.4	4.342	0.274	68.3	20.2	63.3	17.4	60.3	15.7	0.9	3215	4.641E-04	8.798E-04	2.574E-04	4.879E-04	1.708E-05	3.237E-05	1.896E-04	3.595E-04	38.4	218
4.125"V by 4.125"H Helical Coil (3/4")	2	3/18/11 1:36 PM	17.5	44.5	4.0	1.2	8.0	2.4	4.311	0.272	73.4	23.0	65.0	18.3	60.7	16.0	1.5	5344	4.224E-04	8.007E-04	2.581E-04	4.893E-04	1.678E-05	3.181E-05	1.475E-04	2.796E-04	49.3	280
4.125"V by 4.125"H Helical Coil (3/4")	3	3/18/11 2:02 PM	17.5	44.5	4.0	1.2	8.0	2.4	4.286	0.270	75.7	24.3	65.9	18.9	60.9	16.1	1.7	6091	4.353E-04	8.251E-04	2.585E-04	4.901E-04	1.668E-05	3.162E-05	1.600E-04	3.034E-04	45.5	258
4.125"V by 4.125"H Helical Coil (3/4")	4	3/18/11 2:30 PM	17.5	44.5	4.0	1.2	8.0	2.4	4.299	0.271	76.5	24.7	66.0	18.9	60.7	16.0	1.9	6582	4.280E-04	8.114E-04	2.586E-04	4.902E-04	1.658E-05	3.144E-05	1.529E-04	2.898E-04	47.6	270
4.125"V by 4.125"H Helical Coil (3/4")	5	3/18/11 2:59 PM	17.5	44.5	4.0	1.2	8.0	2.4	4.320	0.273	77.5	25.3	66.5	19.1	60.8	16.0	2.0	6963	4.314E-04	8.178E-04	2.588E-04	4.905E-04	1.644E-05	3.116E-05	1.562E-04	2.961E-04	46.6	264
4.125"V by 4.125"H Helical Coil (3/4")	6	3/18/11 3:30 PM	17.5	44.5	4.0	1.2	8.0	2.4	4.318	0.272	78.4	25.8	66.7	19.3	60.7	15.9	2.1	7326	4.345E-04	8.236E-04	2.589E-04	4.907E-04	1.638E-05	3.105E-05	1.592E-04	3.018E-04	45.7	260
4.125"V by 4.125"H Helical Coil (3/4")	7	3/18/11 4:00 PM	17.5	44.5	4.0	1.2	8.0	2.4	4.309	0.272	79.3	26.3	67.0	19.5	60.8	16.0	2.2	7752	4.273E-04	8.099E-04	2.590E-04	4.910E-04	1.634E-05	3.097E-05	1.519E-04	2.880E-04	47.9	272
4.125"V by 4.125"H Helical Coil (3/4")	8	3/18/11 4:28 PM	17.5	44.5	4.0	1.2	8.0	2.4	4.289	0.271	79.7	26.5	67.2	19.6	60.5	15.9	2.2	7831	4.429E-04	8.396E-04	2.591E-04	4.912E-04	1.638E-05	3.104E-05	1.674E-04	3.174E-04	43.5	247
4.125"V by 4.125"H Helical Coil (3/4")	1	3/18/11 5:36 PM	17.5	44.5	4.0	1.2	8.0	2.4	4.411	0.278	68.1	20.1	63.5	17.5	60.5	15.8	0.8	2971	4.956E-04	9.394E-04	2.575E-04	4.881E-04	1.685E-05	3.194E-05	2.212E-04	4.194E-04	32.9	187
4.125"V by 4.125"H Helical Coil (3/4")	2	3/18/11 6:02 PM	17.5	44.5	4.0	1.2	8.0	2.4	4.399	0.278	73.0	22.8	65.1	18.4	60.6	15.9	1.4	5095	4.460E-04	8.455E-04	2.581E-04	4.893E-04	1.651E-05	3.130E-05	1.714E-04	3.249E-04	42.4	241
4.125"V by 4.125"H Helical Coil (3/4")	3	3/18/11 6:22 PM	17.5	44.5	4.0	1.2	8.0	2.4	4.357	0.275	75.3	24.1	66.0	18.9	60.7	15.9	1.7	5938	4.545E-04	8.615E-04	2.585E-04	4.901E-04	1.647E-05	3.121E-05	1.795E-04	3.403E-04	40.5	230
4.125"V by 4.125"H Helical Coil (3/4")	4	3/18/11 6:42 PM	17.5	44.5	4.0	1.2	8.0	2.4	4.385	0.277	76.3	24.6	66.3	19.1	60.6	15.9	1.8	6437	4.517E-04	8.563E-04	2.587E-04	4.903E-04	1.630E-05	3.091E-05	1.768E-04	3.351E-04	41.2	234
4.125"V by 4.125"H Helical Coil (3/4")	5	3/18/11 7:03 PM	17.5	44.5	4.0	1.2	8.0	2.4	4.374	0.276	77.0	25.0	66.4	19.1	60.5	15.9	1.9	6765	4.447E-04	8.429E-04	2.587E-04	4.904E-04	1.630E-05	3.089E-05	1.697E-04	3.216E-04	42.9	244
4.125"V by 4.125"H Helical Coil (3/4")	6	3/18/11 7:23 PM	17.5	44.5	4.0	1.2	8.0	2.4	4.367	0.276	77.5	25.3	66.5	19.2	60.5	15.8	2.0	7009	4.428E-04	8.393E-04	2.588E-04	4.905E-04	1.628E-05	3.086E-05	1.677E-04	3.179E-04	43.4	246
4.125"V by 4.125"H Helical Coil (3/4")	7	3/18/11 7:43 PM	17.5	44.5	4.0	1.2	8.0	2.4	4.439	0.280	78.2	25.6	66.6	19.2	60.3	15.7	2.1	7500	4.317E-04	8.184E-04	2.588E-04	4.906E-04	1.602E-05	3.037E-05	1.569E-04	2.974E-04	46.4	263
4.125"V by 4.125"H Helical Coil (3/4")	8	3/18/11 8:03 PM	17.5	44.5	4.0	1.2	8.0	2.4	4.429	0.279	79.0	26.1	67.1	19.5	60.4	15.8	2.2	7696	4.458E-04	8.450E-04	2.590E-04	4.910E-04	1.598E-05	3.029E-05	1.708E-04	3.238E-04	424	

Test Description	Set Point	Date & Time	H		D _{c,i}		D _{c,o}		V _{c,i}		T _{c,in}		T _{c,out}		T _p		Q _c		R _c		R _t		R _f		R _o		h _o	
			1-8																									
			in	cm	ft	m	ft	m	GPM	L/s	°F	°C	°F	°C	°F	°C	Tons	W	hr ⁻² /Btu	K/W	hr ⁻² /Btu	K/W	hr ⁻² /Btu	K/W	hr ⁻² /Btu	K/W	Btu/hr-ft ² -°F	W/m ² -K
1.5"V by 2.625"H Helical Coil (3/4")	1	3/28/11 7:37 PM	7.0	17.8	4.0	1.2	6.4	2.0	4.498	0.284	58.7	14.8	55.0	12.8	50.9	10.5	0.7	2420	6.923E-04	1.312E-03	2.546E-04	4.826E-04	1.746E-05	3.309E-05	4.203E-04	7.967E-04	17.3	98
1.5"V by 2.625"H Helical Coil (3/4")	2	3/28/11 8:03 PM	7.0	17.8	4.0	1.2	6.4	2.0	4.485	0.283	60.4	17.8	56.9	13.9	50.9	10.5	1.3	4650	5.736E-04	1.087E-03	2.554E-04	4.841E-04	1.703E-05	3.228E-05	3.012E-04	5.709E-04	24.2	137
1.5"V by 2.625"H Helical Coil (3/4")	3	3/28/11 8:27 PM	7.0	17.8	4.0	1.2	6.4	2.0	4.485	0.283	66.4	19.1	57.8	14.3	50.9	10.5	1.6	5646	5.486E-04	1.040E-03	2.557E-04	4.848E-04	1.683E-05	3.190E-05	2.761E-04	5.233E-04	26.4	150
1.5"V by 2.625"H Helical Coil (3/4")	4	3/28/11 8:48 PM	7.0	17.8	4.0	1.2	6.4	2.0	4.487	0.283	67.3	19.6	58.0	14.5	50.9	10.5	1.7	6074	5.361E-04	1.016E-03	2.558E-04	4.850E-04	1.675E-05	3.175E-05	2.655E-04	4.995E-04	27.6	157
1.5"V by 2.625"H Helical Coil (3/4")	5	3/28/11 9:09 PM	7.0	17.8	4.0	1.2	6.4	2.0	4.491	0.283	68.0	20.0	58.2	14.6	50.8	10.5	1.8	6426	5.276E-04	1.000E-03	2.559E-04	4.852E-04	1.668E-05	3.162E-05	2.550E-04	4.834E-04	28.5	162
1.5"V by 2.625"H Helical Coil (3/4")	6	3/28/11 9:30 PM	7.0	17.8	4.0	1.2	6.4	2.0	4.498	0.284	68.6	20.3	58.4	14.7	50.9	10.5	1.9	6742	5.172E-04	9.804E-04	2.560E-04	4.853E-04	1.661E-05	3.149E-05	2.446E-04	4.636E-04	29.7	169
1.5"V by 2.625"H Helical Coil (3/4")	7	3/28/11 9:50 PM	7.0	17.8	4.0	1.2	6.4	2.0	4.492	0.283	69.6	20.9	58.7	14.8	50.9	10.5	2.0	7154	5.111E-04	9.688E-04	2.561E-04	4.856E-04	1.655E-05	3.138E-05	2.384E-04	4.519E-04	30.5	173
1.5"V by 2.625"H Helical Coil (3/4")	8	3/28/11 10:11 PM	7.0	17.8	4.0	1.2	6.4	2.0	4.502	0.284	70.2	21.2	58.9	15.0	50.9	10.5	2.1	7465	5.054E-04	9.580E-04	2.562E-04	4.857E-04	1.647E-05	3.122E-05	2.327E-04	4.410E-04	31.3	178
1.5"V by 2.625"H Helical Coil (3/4")	1	3/29/11 8:59 AM	7.0	17.8	4.0	1.2	6.4	2.0	4.527	0.286	57.6	14.2	53.9	12.1	50.1	10.0	0.7	2509	6.393E-04	1.212E-03	2.542E-04	4.819E-04	1.751E-05	3.319E-05	3.675E-04	6.967E-04	19.8	112
1.5"V by 2.625"H Helical Coil (3/4")	2	3/29/11 9:25 AM	7.0	17.8	4.0	1.2	6.4	2.0	4.530	0.286	62.9	17.2	55.7	13.1	50.0	10.0	1.4	4793	5.352E-04	1.014E-03	2.550E-04	4.833E-04	1.703E-05	3.229E-05	2.632E-04	4.989E-04	27.6	157
1.5"V by 2.625"H Helical Coil (3/4")	3	3/29/11 9:47 AM	7.0	17.8	4.0	1.2	6.4	2.0	4.538	0.286	65.0	18.4	56.4	13.6	49.9	10.0	1.6	5736	5.212E-04	9.880E-04	2.553E-04	4.839E-04	1.682E-05	3.189E-05	2.491E-04	4.722E-04	29.2	166
1.5"V by 2.625"H Helical Coil (3/4")	4	3/29/11 10:07 AM	7.0	17.8	4.0	1.2	6.4	2.0	4.527	0.286	66.1	19.0	56.8	13.8	49.9	10.0	1.8	6214	5.111E-04	9.689E-04	2.554E-04	4.842E-04	1.677E-05	3.179E-05	2.389E-04	4.529E-04	30.5	173
1.5"V by 2.625"H Helical Coil (3/4")	5	3/29/11 10:27 AM	7.0	17.8	4.0	1.2	6.4	2.0	4.536	0.286	66.9	19.4	57.0	13.9	50.0	10.0	1.9	6549	5.050E-04	9.572E-04	2.555E-04	4.844E-04	1.668E-05	3.161E-05	2.327E-04	4.412E-04	31.3	178
1.5"V by 2.625"H Helical Coil (3/4")	6	3/29/11 10:47 AM	7.0	17.8	4.0	1.2	6.4	2.0	4.529	0.286	68.0	20.0	57.4	14.1	50.0	10.0	2.0	6981	5.020E-04	9.516E-04	2.557E-04	4.847E-04	1.661E-05	3.148E-05	2.297E-04	4.354E-04	31.7	180
1.5"V by 2.625"H Helical Coil (3/4")	7	3/29/11 11:09 AM	7.0	17.8	4.0	1.2	6.4	2.0	4.521	0.285	68.8	20.4	57.8	14.3	50.0	10.0	2.1	7300	5.002E-04	9.482E-04	2.558E-04	4.850E-04	1.657E-05	3.140E-05	2.278E-04	4.318E-04	31.9	181
1.5"V by 2.625"H Helical Coil (3/4")	8	3/29/11 11:30 AM	7.0	17.8	4.0	1.2	6.4	2.0	4.527	0.286	69.4	20.8	57.8	14.3	50.1	10.0	2.2	7671	4.831E-04	9.157E-04	2.559E-04	4.850E-04	1.651E-05	3.130E-05	2.107E-04	3.994E-04	34.5	196
4.125"V by 2.625"H Helical Coil (3/4")	1	3/30/11 6:29 PM	21.7	55.1	4.0	1.2	6.4	2.0	4.470	0.282	56.7	13.7	52.2	11.2	49.6	9.8	0.8	2961	4.400E-04	8.341E-04	2.537E-04	4.809E-04	1.788E-05	3.389E-05	1.684E-04	3.193E-04	43.2	245
4.125"V by 2.625"H Helical Coil (3/4")	2	3/30/11 6:53 PM	21.7	55.1	4.0	1.2	6.4	2.0	4.433	0.280	61.9	16.6	54.0	12.2	49.6	9.8	1.5	5197	4.310E-04	8.171E-04	2.544E-04	4.823E-04	1.752E-05	3.322E-05	1.591E-04	3.016E-04	45.7	260
4.125"V by 2.625"H Helical Coil (3/4")	3	3/30/11 7:13 PM	21.7	55.1	4.0	1.2	6.4	2.0	4.431	0.280	64.2	17.9	54.8	12.6	49.6	9.8	1.7	6122	4.326E-04	8.200E-04	2.548E-04	4.829E-04	1.733E-05	3.285E-05	1.605E-04	3.042E-04	45.3	257
4.125"V by 2.625"H Helical Coil (3/4")	4	3/30/11 7:34 PM	21.7	55.1	4.0	1.2	6.4	2.0	4.440	0.280	65.0	18.3	55.0	12.8	49.6	9.8	1.9	6530	4.279E-04	8.112E-04	2.549E-04	4.831E-04	1.723E-05	3.267E-05	1.558E-04	2.954E-04	46.7	265
4.125"V by 2.625"H Helical Coil (3/4")	5	3/30/11 7:54 PM	21.7	55.1	4.0	1.2	6.4	2.0	4.437	0.280	65.6	18.7	55.1	12.8	49.6	9.8	1.9	6817	4.238E-04	8.033E-04	2.549E-04	4.832E-04	1.720E-05	3.260E-05	1.516E-04	2.875E-04	48.0	272
4.125"V by 2.625"H Helical Coil (3/4")	6	3/30/11 8:16 PM	21.7	55.1	4.0	1.2	6.4	2.0	4.422	0.279	66.3	19.1	55.4	13.0	49.5	9.7	2.0	7113	4.270E-04	8.094E-04	2.550E-04	4.835E-04	1.718E-05	3.257E-05	1.547E-04	2.933E-04	47.0	267
4.125"V by 2.625"H Helical Coil (3/4")	7	3/30/11 8:36 PM	21.7	55.1	4.0	1.2	6.4	2.0	4.404	0.278	67.6	19.8	55.8	13.2	49.5	9.7	2.2	7588	4.308E-04	8.167E-04	2.552E-04	4.838E-04	1.713E-05	3.248E-05	1.585E-04	3.004E-04	45.9	261
4.125"V by 2.625"H Helical Coil (3/4")	8	3/30/11 8:56 PM	21.7	55.1	4.0	1.2	6.4	2.0	4.419	0.279	68.3	20.2	56.1	13.4	49.6	9.8	2.2	7890	4.304E-04	8.158E-04	2.553E-04	4.840E-04	1.703E-05	3.228E-05	1.580E-04	2.995E-04	46.1	261
4.125"V by 2.625"H Helical Coil (3/4")	1	3/31/11 9:13 AM	21.7	55.1	4.0	1.2	6.4	2.0	4.404	0.278	55.2	12.9	50.8	10.5	48.1	8.9	0.8	2841	4.713E-04	8.935E-04	2.533E-04	4.801E-04	1.831E-05	3.471E-05	1.988E-04	3.787E-04	36.4	207
4.125"V by 2.625"H Helical Coil (3/4")	2	3/31/11 9:36 AM	21.7	55.1	4.0	1.2	6.4	2.0	4.394	0.277	60.1	15.6	52.2	11.2	48.1	9.0	1.5	5117	4.215E-04	7.990E-04	2.539E-04	4.812E-04	1.790E-05	3.393E-05	1.497E-04	2.838E-04	48.6	276
4.125"V by 2.625"H Helical Coil (3/4")	3	3/31/11 9:56 AM	21.7	55.1	4.0	1.2	6.4	2.0	4.412	0.278	62.5	17.0	53.1	11.7	48.1	9.0	1.7	6066	4.298E-04	8.147E-04	2.542E-04	4.819E-04	1.761E-05	3.339E-05	1.579E-04	2.994E-04	46.1	262
4.125"V by 2.625"H Helical Coil (3/4")	4	3/31/11 10:17 AM	21.7	55.1	4.0	1.2	6.4	2.0	4.396	0.277	63.4	17.5	53.4	11.9	48.2	9.0	1.8	6441	4.280E-04	8.114E-04	2.544E-04	4.822E-04	1.759E-05	3.334E-05	1.561E-04	2.958E-04	46.6	265
4.125"V by 2.625"H Helical Coil (3/4")	5	3/31/11 10:37 AM	21.7	55.1	4.0	1.2	6.4	2.0	4.396	0.277	64.4	18.0	53.9	12.2	48.2	9.0	1.9	6801	4.346E-04	8.238E-04	2.545E-04	4.825E-04	1.749E-05	3.315E-05	1.626E-04	3.082E-04	44.8	254
4.125"V by 2.625"H Helical Coil (3/4")	6	3/31/11 10:57 AM	21.7	55.1	4.0	1.2	6.4	2.0	4.377	0.276	65.5	18.6	54.2	12.3	48.2	9.0	2.1	7234	4.301E-04	8.153E-04	2.547E-04	4.828E-04	1.747E-05	3.311E-05	1.579E-04	2.994E-04	46.1	262
4.125"V by 2.625"H Helical Coil (3/4")	7	3/31/11 11:18 AM	21.7	55.1	4.0	1.2	6.4	2.0	4.402	0.278	66.8	19.3	54.7	12.6	48.4	9.1	2.2	7794	4.246E-04	8.049E-04	2.549E-04	4.831E-04	1.727E-05	3.273E-05	1.525E-04	2.891E-04	47.7	271
4.125"V by 2.625"H Helical Coil (3/4")	8	3/31/11 11:38 AM	21.7	55.1	4.0	1.2	6.4	2.0	4.370	0.276	67.6	19.8	55.1	12.8	48.6	9.2	2.3	8012	4.249E-04	8.054E-04	2.550E-04	4.834E-04	1.730E-05	3.279E-05	1.526E-04			

Test Description	Set Point	Date & Time	H		D _{ci}		D _{co}		V _{ci}		T _{cin}		T _{cout}		T _p		Q _c		R _c		R _t		R _f		R _o		h _o	
			in	cm	ft	m	ft	m	GPM	L/s	°F	°C	°F	°C	°F	°C	Tons	W	hr ⁻² /Btu	K/W	hr ⁻² /Btu	K/W	hr ⁻² /Btu	K/W	hr ⁻² /Btu	K/W	Btu/hr-ft ² -°F	W/m ² -K
			1-8																									
2.625"V by 2.625"H Helical Coil (3/4")	1	4/13/11 4:23 PM	14.2	36.0	4.0	1.2	6.4	2.0	4.413	0.278	77.1	25.1	71.7	22.1	68.5	20.3	1.0	3499	4.632E-04	8.781E-04	2.603E-04	4.934E-04	1.566E-05	2.968E-05	1.873E-04	3.550E-04	38.9	221
2.625"V by 2.625"H Helical Coil (3/4")	2	4/13/11 4:48 PM	14.2	36.0	4.0	1.2	6.4	2.0	4.406	0.278	82.2	27.9	73.3	22.9	68.6	20.3	1.6	5716	4.314E-04	8.177E-04	2.610E-04	4.947E-04	1.535E-05	2.909E-05	1.551E-04	2.939E-04	46.9	266
2.625"V by 2.625"H Helical Coil (3/4")	3	4/13/11 5:09 PM	14.2	36.0	4.0	1.2	6.4	2.0	4.394	0.277	84.6	29.2	74.3	23.5	68.4	20.2	1.9	6638	4.472E-04	8.477E-04	2.614E-04	4.955E-04	1.521E-05	2.884E-05	1.706E-04	3.234E-04	42.7	242
2.625"V by 2.625"H Helical Coil (3/4")	4	4/13/11 5:26 PM	14.2	36.0	4.0	1.2	6.4	2.0	4.407	0.278	85.5	29.7	74.4	23.6	68.6	20.3	2.0	7103	4.307E-04	8.164E-04	2.615E-04	4.956E-04	1.513E-05	2.868E-05	1.541E-04	2.921E-04	47.2	268
2.625"V by 2.625"H Helical Coil (3/4")	5	4/13/11 5:42 PM	14.2	36.0	4.0	1.2	6.4	2.0	4.407	0.278	86.1	30.0	74.6	23.7	68.8	20.4	2.1	7377	4.203E-04	7.968E-04	2.615E-04	4.958E-04	1.509E-05	2.861E-05	1.437E-04	2.724E-04	50.6	287
2.625"V by 2.625"H Helical Coil (3/4")	6	4/13/11 6:04 PM	14.2	36.0	4.0	1.2	6.4	2.0	4.394	0.277	86.7	30.4	74.8	23.8	68.9	20.5	2.2	7635	4.146E-04	7.860E-04	2.616E-04	4.960E-04	1.509E-05	2.860E-05	1.379E-04	2.615E-04	52.8	300
2.625"V by 2.625"H Helical Coil (3/4")	7	4/13/11 6:19 PM	14.2	36.0	4.0	1.2	6.4	2.0	4.384	0.277	87.6	30.9	75.1	24.0	69.1	20.6	2.3	7952	4.087E-04	7.747E-04	2.618E-04	4.962E-04	1.506E-05	2.855E-05	1.318E-04	2.499E-04	55.2	313
2.625"V by 2.625"H Helical Coil (3/4")	8	4/13/11 6:40 PM	14.2	36.0	4.0	1.2	6.4	2.0	4.386	0.277	87.8	31.0	75.2	24.0	69.0	20.5	2.3	8067	4.125E-04	7.819E-04	2.618E-04	4.963E-04	1.505E-05	2.852E-05	1.356E-04	2.571E-04	53.6	305
2.625"V by 2.625"H Helical Coil (3/4")	1	4/14/11 8:39 AM	14.2	36.0	4.0	1.2	6.4	2.0	4.273	0.270	72.1	22.3	67.9	19.9	65.1	18.4	0.7	2636	5.040E-04	9.553E-04	2.589E-04	4.908E-04	1.658E-05	3.142E-05	2.285E-04	4.331E-04	31.8	181
2.625"V by 2.625"H Helical Coil (3/4")	2	4/14/11 8:59 AM	14.2	36.0	4.0	1.2	6.4	2.0	4.260	0.269	77.3	25.2	69.6	19.9	65.2	18.4	1.4	4807	4.644E-04	8.804E-04	2.597E-04	4.922E-04	1.624E-05	3.079E-05	1.885E-04	3.573E-04	38.6	219
2.625"V by 2.625"H Helical Coil (3/4")	3	4/14/11 9:20 AM	14.2	36.0	4.0	1.2	6.4	2.0	4.219	0.266	79.5	26.4	70.2	21.2	65.2	18.5	1.6	5707	4.532E-04	8.591E-04	2.600E-04	4.928E-04	1.622E-05	3.075E-05	1.770E-04	3.356E-04	41.1	233
2.625"V by 2.625"H Helical Coil (3/4")	4	4/14/11 9:40 AM	14.2	36.0	4.0	1.2	6.4	2.0	4.227	0.267	80.4	26.9	70.5	21.4	65.3	18.5	1.7	6134	4.410E-04	8.359E-04	2.601E-04	4.930E-04	1.614E-05	3.059E-05	1.648E-04	3.123E-04	44.2	251
2.625"V by 2.625"H Helical Coil (3/4")	5	4/14/11 10:00 AM	14.2	36.0	4.0	1.2	6.4	2.0	4.208	0.265	81.2	27.3	70.7	21.5	65.4	18.5	1.8	6451	4.375E-04	8.293E-04	2.602E-04	4.932E-04	1.614E-05	3.060E-05	1.611E-04	3.055E-04	45.2	256
2.625"V by 2.625"H Helical Coil (3/4")	6	4/14/11 10:21 AM	14.2	36.0	4.0	1.2	6.4	2.0	4.201	0.265	82.0	27.8	70.9	21.6	65.4	18.6	1.9	6792	4.313E-04	8.175E-04	2.603E-04	4.934E-04	1.611E-05	3.054E-05	1.549E-04	2.936E-04	47.0	267
2.625"V by 2.625"H Helical Coil (3/4")	7	4/14/11 10:41 AM	14.2	36.0	4.0	1.2	6.4	2.0	4.214	0.266	82.8	28.2	71.2	21.8	65.6	18.7	2.0	7125	4.261E-04	8.078E-04	2.604E-04	4.937E-04	1.602E-05	3.036E-05	1.497E-04	2.838E-04	48.6	276
2.625"V by 2.625"H Helical Coil (3/4")	8	4/14/11 11:02 AM	14.2	36.0	4.0	1.2	6.4	2.0	4.203	0.265	83.3	28.5	71.4	21.9	65.7	18.7	2.1	7287	4.245E-04	8.046E-04	2.605E-04	4.938E-04	1.601E-05	3.036E-05	1.480E-04	2.805E-04	49.2	279
2.625"V by 2.625"H Helical Coil (3/4")	1	4/14/11 1:43 PM	14.2	36.0	4.0	1.2	6.4	2.0	4.253	0.268	75.0	23.9	69.8	21.0	67.1	19.5	0.9	3226	4.439E-04	8.415E-04	2.596E-04	4.921E-04	1.637E-05	3.104E-05	1.679E-04	3.183E-04	43.3	246
2.625"V by 2.625"H Helical Coil (3/4")	2	4/14/11 2:04 PM	14.2	36.0	4.0	1.2	6.4	2.0	4.262	0.269	80.6	27.0	71.8	22.1	67.3	19.6	1.6	5495	4.293E-04	8.139E-04	2.605E-04	4.938E-04	1.594E-05	3.022E-05	1.529E-04	2.899E-04	47.6	270
2.625"V by 2.625"H Helical Coil (3/4")	3	4/14/11 2:24 PM	14.2	36.0	4.0	1.2	6.4	2.0	4.249	0.268	83.1	28.4	72.7	22.6	67.6	19.8	1.8	6419	4.288E-04	8.128E-04	2.609E-04	4.945E-04	1.581E-05	2.997E-05	1.521E-04	2.883E-04	47.8	272
2.625"V by 2.625"H Helical Coil (3/4")	4	4/14/11 2:44 PM	14.2	36.0	4.0	1.2	6.4	2.0	4.205	0.265	83.3	28.5	72.9	22.7	67.7	19.8	1.8	6365	4.369E-04	8.282E-04	2.610E-04	4.947E-04	1.593E-05	3.019E-05	1.600E-04	3.033E-04	45.5	258
2.625"V by 2.625"H Helical Coil (3/4")	5	4/14/11 3:05 PM	14.2	36.0	4.0	1.2	6.4	2.0	4.194	0.265	84.2	29.0	73.2	22.9	67.9	19.9	1.9	6722	4.270E-04	8.094E-04	2.611E-04	4.949E-04	1.591E-05	3.015E-05	1.500E-04	2.844E-04	48.5	275
2.625"V by 2.625"H Helical Coil (3/4")	6	4/14/11 3:25 PM	14.2	36.0	4.0	1.2	6.4	2.0	4.189	0.264	85.2	29.6	73.6	23.1	67.9	19.9	2.0	7128	4.299E-04	8.149E-04	2.612E-04	4.952E-04	1.585E-05	3.005E-05	1.528E-04	2.896E-04	47.6	270
2.625"V by 2.625"H Helical Coil (3/4")	7	4/14/11 3:45 PM	14.2	36.0	4.0	1.2	6.4	2.0	4.180	0.264	86.1	30.0	74.0	23.4	68.0	20.0	2.1	7344	4.386E-04	8.314E-04	2.614E-04	4.956E-04	1.581E-05	2.998E-05	1.613E-04	3.058E-04	45.1	256
2.625"V by 2.625"H Helical Coil (3/4")	8	4/14/11 4:06 PM	14.2	36.0	4.0	1.2	6.4	2.0	4.163	0.263	87.0	30.6	74.3	23.5	68.2	20.1	2.2	7705	4.305E-04	8.161E-04	2.616E-04	4.958E-04	1.581E-05	2.996E-05	1.531E-04	2.903E-04	47.5	270
1.5"V by 1.5"H Helical Coil (3/4")	1	4/19/11 9:01 AM	8.6	21.7	4.0	1.2	5.4	1.7	4.618	0.291	71.4	21.9	67.9	19.9	64.3	17.9	0.7	2359	6.403E-04	1.214E-03	2.589E-04	4.907E-04	1.541E-05	2.921E-05	1.636E-04	6.938E-04	19.9	113
1.5"V by 1.5"H Helical Coil (3/4")	2	4/19/11 9:21 AM	8.6	21.7	4.0	1.2	5.4	1.7	4.589	0.290	75.6	24.2	68.5	20.3	63.5	17.5	1.4	4761	4.921E-04	9.327E-04	2.592E-04	4.914E-04	1.524E-05	2.888E-05	1.276E-04	4.125E-04	33.4	190
1.5"V by 1.5"H Helical Coil (3/4")	3	4/19/11 9:41 AM	8.6	21.7	4.0	1.2	5.4	1.7	4.604	0.290	78.9	26.0	70.4	21.3	63.8	17.7	1.6	5705	5.277E-04	1.000E-03	2.599E-04	4.928E-04	1.493E-05	2.831E-05	1.528E-04	4.792E-04	28.8	163
1.5"V by 1.5"H Helical Coil (3/4")	4	4/19/11 10:02 AM	8.6	21.7	4.0	1.2	5.4	1.7	4.569	0.288	79.9	26.6	70.5	21.4	63.8	17.6	1.8	6250	5.055E-04	9.582E-04	2.600E-04	4.929E-04	1.498E-05	2.839E-05	1.305E-04	4.369E-04	31.6	179
1.5"V by 1.5"H Helical Coil (3/4")	5	4/19/11 10:22 AM	8.6	21.7	4.0	1.2	5.4	1.7	4.510	0.285	80.8	27.1	71.2	21.8	64.5	18.0	1.8	6313	5.011E-04	9.499E-04	2.603E-04	4.934E-04	1.507E-05	2.856E-05	1.257E-04	4.279E-04	32.2	183
1.5"V by 1.5"H Helical Coil (3/4")	6	4/19/11 10:43 AM	8.6	21.7	4.0	1.2	5.4	1.7	4.519	0.285	81.9	27.7	71.8	22.1	64.7	18.1	1.9	6685	5.013E-04	9.504E-04	2.605E-04	4.938E-04	1.496E-05	2.835E-05	1.259E-04	4.282E-04	32.2	183
1.5"V by 1.5"H Helical Coil (3/4")	7	4/19/11 11:03 AM	8.6	21.7	4.0	1.2	5.4	1.7	4.529	0.286	83.4	28.5	72.8	22.6	65.3	18.5	2.0	7022	5.011E-04	9.499E-04	2.609E-04	4.945E-04	1.481E-05	2.808E-05	1.254E-04	4.273E-04	32.3	183
1.5"V by 1.5"H Helical Coil (3/4")	8	4/19/11 11:19 AM	8.6	21.7	4.0	1.2	5.4	1.7	4.546	0.287	83.8	28.8	72.3	22.4	64.3	18.0	2.2	7583	4.985E-04	9.450E-04	2.608E-04	4.943E-04	1.477E-05	2.799E-05	1.230E-04	4.227E-04	32	

Test Description	Set Point	Date & Time	H		D _{c,i}	D _{c,o}	V _{c,i}	L/s	T _{c,in}		T _{c,out}		T _p	Q _c		R _c		R _t		R _f		R _o		h _o				
			in	cm					ft	m	GPM	°F		°C	°F	°C	°F	°C	Tons	W	hr ⁻² /Btu	K/W	hr ⁻² /Btu	K/W	hr ⁻² /Btu	K/W	hr ⁻² /Btu	K/W
			1-8																									
2.625"V by 1.5"H Helical Coil (3/4")	1	4/21/11 5:18 PM	14.2	36.0	4.0	1.2	5.4	1.7	4.409	0.278	69.4	20.8	64.9	18.3	62.0	16.7	0.8	2888	4.793E-04	9.085E-04	2.579E-04	4.889E-04	1.630E-05	3.091E-05	2.051E-04	3.887E-04	35.5	201
2.625"V by 1.5"H Helical Coil (3/4")	2	4/21/11 5:47 PM	14.2	36.0	4.0	1.2	5.4	1.7	4.375	0.276	74.6	23.7	66.6	19.2	62.1	16.7	1.5	5117	4.504E-04	8.538E-04	2.587E-04	4.903E-04	1.602E-05	3.037E-05	1.757E-04	3.331E-04	41.4	235
2.625"V by 1.5"H Helical Coil (3/4")	3	4/21/11 6:07 PM	14.2	36.0	4.0	1.2	5.4	1.7	4.386	0.277	76.6	24.8	67.2	19.6	62.1	16.7	1.7	5998	4.427E-04	8.391E-04	2.589E-04	4.908E-04	1.585E-05	3.004E-05	1.679E-04	3.182E-04	43.3	246
2.625"V by 1.5"H Helical Coil (3/4")	4	4/21/11 6:29 PM	14.2	36.0	4.0	1.2	5.4	1.7	4.364	0.275	77.8	25.5	67.7	19.8	62.0	16.7	1.8	6474	4.456E-04	8.447E-04	2.591E-04	4.912E-04	1.583E-05	3.000E-05	1.707E-04	3.235E-04	42.6	242
2.625"V by 1.5"H Helical Coil (3/4")	5	4/21/11 6:49 PM	14.2	36.0	4.0	1.2	5.4	1.7	4.383	0.277	78.7	25.9	68.0	20.0	62.0	16.7	2.0	6860	4.427E-04	8.391E-04	2.592E-04	4.914E-04	1.571E-05	2.978E-05	1.677E-04	3.179E-04	43.4	246
2.625"V by 1.5"H Helical Coil (3/4")	6	4/21/11 7:09 PM	14.2	36.0	4.0	1.2	5.4	1.7	4.357	0.275	79.3	26.3	68.1	20.1	62.0	16.7	2.0	7131	4.407E-04	8.353E-04	2.593E-04	4.916E-04	1.575E-05	2.985E-05	1.656E-04	3.139E-04	43.9	250
2.625"V by 1.5"H Helical Coil (3/4")	7	4/21/11 7:29 PM	14.2	36.0	4.0	1.2	5.4	1.7	4.383	0.277	80.2	26.8	68.4	20.2	62.0	16.7	2.1	7536	4.380E-04	8.302E-04	2.594E-04	4.918E-04	1.561E-05	2.959E-05	1.629E-04	3.088E-04	44.7	254
2.625"V by 1.5"H Helical Coil (3/4")	8	4/21/11 7:46 PM	14.2	36.0	4.0	1.2	5.4	1.7	4.359	0.275	80.7	27.0	68.6	20.3	62.0	16.7	2.2	7708	4.387E-04	8.315E-04	2.595E-04	4.919E-04	1.565E-05	2.966E-05	1.635E-04	3.099E-04	44.5	253
4.125"V by 1.5"H Helical Coil (3/4")	1	4/22/11 4:26 PM	21.7	55.1	4.0	1.2	5.4	1.7	4.394	0.277	75.5	24.2	68.5	20.3	64.6	18.1	1.3	4507	4.447E-04	8.429E-04	2.592E-04	4.914E-04	1.581E-05	2.998E-05	1.696E-04	3.215E-04	42.9	244
4.125"V by 1.5"H Helical Coil (3/4")	2	4/22/11 4:56 PM	21.7	55.1	4.0	1.2	5.4	1.7	4.461	0.281	80.9	27.1	70.3	21.3	64.7	18.2	2.0	6906	4.203E-04	7.967E-04	2.600E-04	4.929E-04	1.525E-05	2.890E-05	1.450E-04	2.749E-04	50.2	285
4.125"V by 1.5"H Helical Coil (3/4")	3	4/22/11 5:18 PM	21.7	55.1	4.0	1.2	5.4	1.7	4.446	0.280	83.1	28.4	71.1	21.7	64.8	18.2	2.2	7816	4.218E-04	7.995E-04	2.604E-04	4.935E-04	1.514E-05	2.870E-05	1.463E-04	2.773E-04	49.7	282
4.125"V by 1.5"H Helical Coil (3/4")	4	4/22/11 5:39 PM	21.7	55.1	4.0	1.2	5.4	1.7	4.414	0.278	84.0	28.9	71.5	21.9	65.0	18.3	2.3	8085	4.217E-04	7.994E-04	2.605E-04	4.938E-04	1.517E-05	2.876E-05	1.460E-04	2.768E-04	49.8	283
4.125"V by 1.5"H Helical Coil (3/4")	5	4/22/11 5:59 PM	21.7	55.1	4.0	1.2	5.4	1.7	4.407	0.278	84.6	29.2	71.8	22.1	65.2	18.4	2.4	8281	4.206E-04	7.974E-04	2.606E-04	4.941E-04	1.515E-05	2.871E-05	1.449E-04	2.746E-04	50.2	285
4.125"V by 1.5"H Helical Coil (3/4")	6	4/22/11 6:19 PM	21.7	55.1	4.0	1.2	5.4	1.7	4.437	0.280	85.5	29.7	72.1	22.3	65.2	18.4	2.5	8709	4.181E-04	7.926E-04	2.608E-04	4.943E-04	1.500E-05	2.843E-05	1.424E-04	2.699E-04	51.1	290
4.125"V by 1.5"H Helical Coil (3/4")	7	4/22/11 6:38 PM	21.7	55.1	4.0	1.2	5.4	1.7	4.430	0.279	85.8	29.9	71.8	22.1	64.8	18.2	2.6	9090	4.112E-04	7.794E-04	2.607E-04	4.941E-04	1.502E-05	2.848E-05	1.355E-04	2.568E-04	53.7	305
4.125"V by 1.5"H Helical Coil (3/4")	8	4/22/11 6:58 PM	21.7	55.1	4.0	1.2	5.4	1.7	4.427	0.279	86.3	30.2	72.2	22.3	65.2	18.5	2.6	9135	4.079E-04	7.733E-04	2.608E-04	4.944E-04	1.499E-05	2.842E-05	1.321E-04	2.505E-04	55.1	313
4.125"V by 1.5"H Helical Coil (3/4")	1	4/25/11 9:20 AM	21.7	55.1	4.0	1.2	5.4	1.7	4.425	0.279	68.1	20.1	63.6	17.5	60.6	15.9	0.8	2939	4.885E-04	9.261E-04	2.575E-04	4.881E-04	1.640E-05	3.109E-05	2.147E-04	4.069E-04	33.9	192
4.125"V by 1.5"H Helical Coil (3/4")	2	4/25/11 9:43 AM	21.7	55.1	4.0	1.2	5.4	1.7	4.379	0.276	73.6	23.1	65.4	18.5	60.6	15.9	1.5	5245	4.557E-04	8.638E-04	2.583E-04	4.896E-04	1.613E-05	3.058E-05	1.813E-04	3.437E-04	40.1	228
4.125"V by 1.5"H Helical Coil (3/4")	3	4/25/11 10:09 AM	21.7	55.1	4.0	1.2	5.4	1.7	4.360	0.275	75.7	24.3	66.0	18.9	60.6	15.9	1.7	6142	4.500E-04	8.531E-04	2.585E-04	4.901E-04	1.604E-05	3.041E-05	1.754E-04	3.326E-04	41.5	235
4.125"V by 1.5"H Helical Coil (3/4")	4	4/25/11 10:29 AM	21.7	55.1	4.0	1.2	5.4	1.7	4.347	0.274	76.8	24.9	66.4	19.1	60.6	15.9	1.9	6626	4.471E-04	8.475E-04	2.587E-04	4.904E-04	1.600E-05	3.034E-05	1.724E-04	3.268E-04	42.2	240
4.125"V by 1.5"H Helical Coil (3/4")	5	4/25/11 10:49 AM	21.7	55.1	4.0	1.2	5.4	1.7	4.375	0.276	77.8	25.4	66.7	19.3	60.6	15.9	2.0	7044	4.467E-04	8.469E-04	2.589E-04	4.907E-04	1.584E-05	3.003E-05	1.720E-04	3.261E-04	42.3	240
4.125"V by 1.5"H Helical Coil (3/4")	6	4/25/11 11:10 AM	21.7	55.1	4.0	1.2	5.4	1.7	4.398	0.277	78.6	25.9	67.0	19.5	60.6	15.9	2.1	7430	4.429E-04	8.395E-04	2.590E-04	4.909E-04	1.572E-05	2.979E-05	1.682E-04	3.188E-04	43.3	246
4.125"V by 1.5"H Helical Coil (3/4")	7	4/25/11 11:30 AM	21.7	55.1	4.0	1.2	5.4	1.7	4.395	0.277	79.6	26.4	67.4	19.7	60.6	15.9	2.2	7846	4.421E-04	8.381E-04	2.591E-04	4.912E-04	1.565E-05	2.967E-05	1.673E-04	3.172E-04	43.5	247
4.125"V by 1.5"H Helical Coil (3/4")	8	4/25/11 11:50 AM	21.7	55.1	4.0	1.2	5.4	1.7	4.379	0.276	80.1	26.7	67.6	19.8	60.6	15.9	2.3	8036	4.427E-04	8.393E-04	2.592E-04	4.914E-04	1.567E-05	2.970E-05	1.679E-04	3.182E-04	43.3	246
4.125"V by 1.5"H Helical Coil (3/4")	1	4/25/11 3:36 PM	21.7	55.1	4.0	1.2	5.4	1.7	4.394	0.277	69.3	20.7	64.5	18.0	61.4	16.3	0.9	3133	4.788E-04	9.076E-04	2.578E-04	4.887E-04	1.638E-05	3.104E-05	2.046E-04	3.878E-04	35.6	202
4.125"V by 1.5"H Helical Coil (3/4")	2	4/25/11 4:03 PM	21.7	55.1	4.0	1.2	5.4	1.7	4.384	0.277	74.5	23.6	66.0	18.9	60.9	16.1	1.5	5424	4.660E-04	8.833E-04	2.585E-04	4.900E-04	1.603E-05	3.039E-05	1.914E-04	3.629E-04	38.0	216
4.125"V by 1.5"H Helical Coil (3/4")	3	4/25/11 4:28 PM	21.7	55.1	4.0	1.2	5.4	1.7	4.395	0.277	76.8	24.9	66.6	19.2	60.7	16.0	1.9	6560	4.542E-04	8.609E-04	2.588E-04	4.905E-04	1.584E-05	3.003E-05	1.795E-04	3.404E-04	40.5	230
4.125"V by 1.5"H Helical Coil (3/4")	4	4/25/11 4:50 PM	21.7	55.1	4.0	1.2	5.4	1.7	4.391	0.277	77.5	25.3	66.8	19.3	60.7	15.9	2.0	6905	4.478E-04	8.489E-04	2.588E-04	4.907E-04	1.580E-05	2.996E-05	1.731E-04	3.282E-04	42.0	239
4.125"V by 1.5"H Helical Coil (3/4")	5	4/25/11 5:11 PM	21.7	55.1	4.0	1.2	5.4	1.7	4.385	0.277	78.0	25.6	66.9	19.4	61.1	16.2	2.0	7108	4.277E-04	8.107E-04	2.589E-04	4.908E-04	1.579E-05	2.993E-05	1.530E-04	2.899E-04	47.6	270
4.125"V by 1.5"H Helical Coil (3/4")	6	4/25/11 5:31 PM	21.7	55.1	4.0	1.2	5.4	1.7	4.381	0.276	79.1	26.2	67.3	19.6	62.1	16.7	2.2	7568	4.386E-04	7.727E-04	2.590E-04	4.910E-04	1.573E-05	2.982E-05	1.088E-04	2.063E-04	66.8	380
4.125"V by 1.5"H Helical Coil (3/4")	7	4/25/11 5:52 PM	21.7	55.1	4.0	1.2	5.4	1.7	4.393	0.277	80.3	26.8	68.3	20.2	62.5	16.9	2.2	7700	4.407E-04	7.727E-04	2.594E-04	4.917E-04	1.558E-05	2.953E-05	1.326E-04	2.514E-04	54.9	311
4.125"V by 1.5"H Helical Coil (3/4")	8	4/25/11 6:12 PM	21.7	55.1	4.0	1.2	5.4	1.7	4.378	0.276	80.8	27.1	68.3	20.2	62.0	16.7	2.3	7979	4.1.									

157

Test Description	Set Point	Date & Time	H		D _{c,i}	D _{c,o}	V _{c,i}		T _{c,in}	T _{c,out}	T _p	Q _c	R _c		R _t		R _f		R _o		h _o							
			in	cm			ft	m					GPM	L/s	°F	°C	°F	°C	Tons	W	hr ⁻² /Btu	K/W	hr ⁻² /Btu	K/W	hr ⁻² /Btu	K/W	hr ⁻² /Btu	K/W
			1-8																									
1.5"V by 1.5"H Helical Coil (1")	1	10/4/11 8:46 AM	10.0	25.4	4.0	1.2	5.6	1.7	9.460	0.597	71.3	21.8	69.5	20.8	66.8	19.3	0.7	2563	4.034E-04	7.647E-04	2.592E-04	4.913E-04	9.878E-06	1.873E-05	1.343E-04	2.547E-04	43.2	246
1.5"V by 1.5"H Helical Coil (1")	2	10/4/11 9:33 AM	10.0	25.4	4.0	1.2	5.6	1.7	9.448	0.596	75.4	24.1	71.9	22.1	66.7	19.3	1.4	4891	4.028E-04	7.635E-04	2.599E-04	4.927E-04	9.677E-06	1.834E-05	1.332E-04	2.524E-04	43.6	248
1.5"V by 1.5"H Helical Coil (1")	3	10/4/11 10:10 AM	10.0	25.4	4.0	1.2	5.6	1.7	9.464	0.597	77.7	25.1	73.2	22.9	66.8	19.3	1.8	6265	3.973E-04	7.531E-04	2.603E-04	4.934E-04	9.547E-06	1.810E-05	1.275E-04	2.416E-04	45.6	259
1.5"V by 1.5"H Helical Coil (1")	4	10/4/11 10:42 AM	10.0	25.4	4.0	1.2	5.6	1.7	9.441	0.596	79.3	26.3	74.2	23.4	66.7	19.3	2.0	7012	4.090E-04	7.754E-04	2.606E-04	4.940E-04	9.487E-06	1.798E-05	1.389E-04	2.633E-04	41.8	237
1.5"V by 1.5"H Helical Coil (1")	5	10/4/11 11:17 AM	10.0	25.4	4.0	1.2	5.6	1.7	9.439	0.596	80.5	26.9	74.9	23.8	66.8	19.3	2.2	7722	4.049E-04	7.676E-04	2.608E-04	4.944E-04	9.433E-06	1.788E-05	1.347E-04	2.553E-04	43.1	245
1.5"V by 1.5"H Helical Coil (1")	6	10/4/11 11:46 AM	10.0	25.4	4.0	1.2	5.6	1.7	9.464	0.597	81.5	27.5	75.5	24.2	67.0	19.5	2.4	8288	3.966E-04	7.519E-04	2.610E-04	4.947E-04	9.362E-06	1.775E-05	1.263E-04	2.394E-04	46.0	261
1.5"V by 1.5"H Helical Coil (1")	7	10/4/11 12:12 PM	10.0	25.4	4.0	1.2	5.6	1.7	9.406	0.593	82.7	28.2	76.2	24.6	67.2	19.6	2.5	8887	3.936E-04	7.462E-04	2.612E-04	4.952E-04	9.353E-06	1.773E-05	1.231E-04	2.333E-04	47.2	268
1.5"V by 1.5"H Helical Coil (1")	8	10/4/11 12:38 PM	10.0	25.4	4.0	1.2	5.6	1.7	9.424	0.595	83.4	28.5	76.7	24.8	67.1	19.5	2.6	9218	4.022E-04	7.624E-04	2.614E-04	4.954E-04	9.305E-06	1.764E-05	1.315E-04	2.493E-04	44.2	251
1.5"V by 1.5"H Helical Coil (1")	1	10/4/11 1:59 PM	10.0	25.4	4.0	1.2	5.6	1.7	9.458	0.597	78.7	25.9	74.0	23.3	67.7	19.8	1.8	6455	3.834E-04	7.269E-04	2.606E-04	4.939E-04	9.498E-06	1.800E-05	1.134E-04	2.149E-04	51.2	291
1.5"V by 1.5"H Helical Coil (1")	2	10/4/11 2:32 PM	10.0	25.4	4.0	1.2	5.6	1.7	9.456	0.597	81.6	27.6	75.8	24.3	67.4	19.7	2.3	8052	4.006E-04	7.594E-04	2.611E-04	4.949E-04	9.358E-06	1.774E-05	1.302E-04	2.467E-04	44.6	253
1.5"V by 1.5"H Helical Coil (1")	3	10/4/11 2:57 PM	10.0	25.4	4.0	1.2	5.6	1.7	9.429	0.595	82.8	28.2	76.4	24.6	67.3	19.6	2.5	8830	3.970E-04	7.526E-04	2.613E-04	4.953E-04	9.327E-06	1.768E-05	1.264E-04	2.396E-04	46.0	261
1.5"V by 1.5"H Helical Coil (1")	4	10/4/11 3:22 PM	10.0	25.4	4.0	1.2	5.6	1.7	9.418	0.594	83.3	28.5	76.7	24.8	67.3	19.6	2.6	9089	4.009E-04	7.600E-04	2.614E-04	4.955E-04	9.311E-06	1.765E-05	1.302E-04	2.469E-04	44.6	253
1.5"V by 1.5"H Helical Coil (1")	5	10/4/11 3:47 PM	10.0	25.4	4.0	1.2	5.6	1.7	9.402	0.593	83.9	28.8	77.0	25.0	67.5	19.7	2.7	9352	3.951E-04	7.489E-04	2.615E-04	4.957E-04	9.299E-06	1.763E-05	1.243E-04	2.356E-04	46.7	265
1.5"V by 1.5"H Helical Coil (1")	6	10/4/11 4:13 PM	10.0	25.4	4.0	1.2	5.6	1.7	9.409	0.594	83.9	28.8	77.1	25.1	67.5	19.7	2.7	9323	4.012E-04	7.605E-04	2.615E-04	4.957E-04	9.288E-06	1.761E-05	1.304E-04	2.472E-04	44.6	253
1.5"V by 1.5"H Helical Coil (1")	7	10/4/11 4:38 PM	10.0	25.4	4.0	1.2	5.6	1.7	9.399	0.593	83.9	28.7	77.2	25.1	67.5	19.7	2.6	9267	4.052E-04	7.680E-04	2.615E-04	4.958E-04	9.295E-06	1.762E-05	1.343E-04	2.546E-04	43.2	246
1.5"V by 1.5"H Helical Coil (1")	8	10/4/11 5:03 PM	10.0	25.4	4.0	1.2	5.6	1.7	9.380	0.592	83.7	28.7	77.1	25.0	67.6	19.8	2.6	9110	4.004E-04	7.590E-04	2.615E-04	4.957E-04	9.322E-06	1.767E-05	1.296E-04	2.456E-04	44.8	255
1.5"V by 1.5"H Helical Coil (1")	1	10/5/11 8:06 AM	10.0	25.4	4.0	1.2	5.6	1.7	9.441	0.596	70.8	21.5	69.0	20.6	66.8	19.3	0.7	2400	3.737E-04	7.084E-04	2.590E-04	4.911E-04	9.929E-06	1.882E-05	1.047E-04	1.985E-04	55.5	315
1.5"V by 1.5"H Helical Coil (1")	2	10/5/11 8:48 AM	10.0	25.4	4.0	1.2	5.6	1.7	9.414	0.594	74.6	23.7	71.2	21.8	66.7	19.3	1.3	4704	3.804E-04	7.211E-04	2.597E-04	4.923E-04	9.751E-06	1.849E-05	1.109E-04	2.103E-04	52.4	297
1.5"V by 1.5"H Helical Coil (1")	3	10/5/11 9:21 AM	10.0	25.4	4.0	1.2	5.6	1.7	9.374	0.591	76.5	24.7	72.3	22.4	66.6	19.2	1.6	5745	3.886E-04	7.367E-04	2.600E-04	4.929E-04	9.693E-06	1.837E-05	1.189E-04	2.254E-04	48.9	277
1.5"V by 1.5"H Helical Coil (1")	4	10/5/11 9:51 AM	10.0	25.4	4.0	1.2	5.6	1.7	9.383	0.592	76.6	24.8	72.3	22.4	66.6	19.2	1.7	5942	3.797E-04	7.198E-04	2.600E-04	4.929E-04	9.678E-06	1.835E-05	1.100E-04	2.086E-04	52.8	300
1.5"V by 1.5"H Helical Coil (1")	5	10/5/11 10:22 AM	10.0	25.4	4.0	1.2	5.6	1.7	9.389	0.592	79.3	26.3	73.9	23.3	66.6	19.2	2.1	7463	3.815E-04	7.232E-04	2.605E-04	4.938E-04	9.542E-06	1.809E-05	1.115E-04	2.113E-04	52.1	296
1.5"V by 1.5"H Helical Coil (1")	6	10/5/11 10:52 AM	10.0	25.4	4.0	1.2	5.6	1.7	9.403	0.593	80.7	27.0	74.8	23.8	66.8	19.3	2.3	8064	3.887E-04	7.368E-04	2.608E-04	4.943E-04	9.459E-06	1.793E-05	1.184E-04	2.245E-04	49.0	279
1.5"V by 1.5"H Helical Coil (1")	7	10/5/11 11:23 AM	10.0	25.4	4.0	1.2	5.6	1.7	9.397	0.593	80.9	27.2	75.1	23.9	66.8	19.4	2.3	8035	3.976E-04	7.537E-04	2.609E-04	4.945E-04	9.449E-06	1.791E-05	1.273E-04	2.413E-04	45.6	259
1.5"V by 1.5"H Helical Coil (1")	8	10/5/11 11:53 AM	10.0	25.4	4.0	1.2	5.6	1.7	9.395	0.593	81.9	27.7	75.6	24.2	67.0	19.4	2.5	8743	3.851E-04	7.301E-04	2.610E-04	4.948E-04	9.405E-06	1.783E-05	1.147E-04	2.175E-04	50.6	288
2.625"V by 2.625"H Helical Coil (1-1/4")	1	6/15/11 9:45 AM	15.0	38.1	4.0	1.2	6.0	1.8	9.768	0.616	86.7	30.4	83.8	28.8	79.4	26.4	1.2	4217	3.945E-04	7.478E-04	2.655E-04	5.034E-04	1.045E-05	1.980E-05	1.185E-04	2.246E-04	38.8	221
2.625"V by 2.625"H Helical Coil (1-1/4")	2	6/15/11 10:14 AM	15.0	38.1	4.0	1.2	6.0	1.8	9.650	0.609	90.4	32.5	85.9	29.9	79.4	26.3	1.8	6454	3.884E-04	7.363E-04	2.662E-04	5.046E-04	1.037E-05	1.966E-05	1.119E-04	2.121E-04	41.1	234
2.625"V by 2.625"H Helical Coil (1-1/4")	3	6/15/11 10:39 AM	15.0	38.1	4.0	1.2	6.0	1.8	9.707	0.612	92.3	33.5	87.0	30.5	79.5	26.4	2.2	7608	3.825E-04	7.251E-04	2.665E-04	5.052E-04	1.023E-05	1.939E-05	1.058E-04	2.005E-04	43.5	247
2.625"V by 2.625"H Helical Coil (1-1/4")	4	6/15/11 10:51 AM	15.0	38.1	4.0	1.2	6.0	1.8	9.706	0.612	93.0	33.9	87.2	30.7	79.4	26.4	2.3	8083	3.770E-04	7.146E-04	2.666E-04	5.053E-04	1.020E-05	1.934E-05	1.002E-04	1.899E-04	45.9	261
2.625"V by 2.625"H Helical Coil (1-1/4")	5	6/15/11 11:14 AM	15.0	38.1	4.0	1.2	6.0	1.8	9.674	0.610	93.6	34.2	87.7	30.9	79.4	26.3	2.4	8355	3.848E-04	7.294E-04	2.667E-04	5.056E-04	1.020E-05	1.933E-05	1.078E-04	2.044E-04	42.7	242
2.625"V by 2.625"H Helical Coil (1-1/4")	6	6/15/11 11:28 AM	15.0	38.1	4.0	1.2	6.0	1.8	9.664	0.610	94.2	34.5	88.0	31.1	79.5	26.4	2.5	8670	3.816E-04	7.234E-04	2.668E-04	5.058E-04	1.018E-05	1.930E-05	1.046E-04	1.984E-04	44.0	250
2.625"V by 2.625"H Helical Coil (1-1/4")	7	6/15/11 11:42 AM	15.0	38.1	4.0	1.2	6.0	1.8	9.672	0.610	94.9	35.0	88.4	31.3	79.6	26.5	2.6	9157	3.755E-04	7.117E-04	2.669E-04	5.060E-04	1.014E-05	1.922E-05	1.039E-04	1.865E-04	46.8	266
2.625"V by 2.625"H Helical Coil (1-1/4")	8	6/15/11 11:57 AM	15.0	38.1	4.0	1.2	6.0	1.8	9.679	0.611	95.5	35.3	88.8	31.5	79.7	26.5	2.7	9420	3.781E-04	7.167E-04	2.671E-04	5.062E-04	1.011E-05	1.916E-05	1.009E-04	1.913E-04	4	

159

Test Description	Set Point	Date & Time	H		$D_{c,i}$		$D_{c,o}$		$\dot{V}_{c,i}$		$T_{c,in}$		$T_{c,out}$		T_p		Q_c		R_c		R_t		R_f		R_o		h_o	
	1-8		in	cm	ft	m	ft	m	GPM	L/s	°F	°C	°F	°C	°F	°C	Tons	W	hr-°F/Btu	K/W	hr-°F/Btu	K/W	hr-°F/Btu	K/W	hr-°F/Btu	K/W	Btu/hr-ft²-°F	W/m²-K
4.125"V by 4.125"H Helical Coil (1-1/4")	1	9/26/11 12:09 PM	18.0	45.7	4.0	1.2	8.0	2.4	11.143	0.703	77.5	25.3	73.7	23.2	67.9	20.0	1.8	6230	3.540E-04	6.710E-04	2.619E-04	4.964E-04	1.010E-05	1.915E-05	8.204E-05	1.555E-04	56.1	319
4.125"V by 4.125"H Helical Coil (1-1/4")	2	9/26/11 2:01 PM	18.0	45.7	4.0	1.2	8.0	2.4	11.083	0.699	81.3	27.4	76.0	24.5	68.0	20.0	2.4	8495	3.608E-04	6.839E-04	2.625E-04	4.976E-04	9.952E-06	1.887E-05	8.830E-05	1.674E-04	52.1	296
4.125"V by 4.125"H Helical Coil (1-1/4")	3	9/26/11 2:33 PM	18.0	45.7	4.0	1.2	8.0	2.4	11.048	0.697	82.8	28.2	76.9	24.9	68.2	20.1	2.7	9471	3.527E-04	6.686E-04	2.627E-04	4.981E-04	9.905E-06	1.878E-05	8.004E-05	1.517E-04	57.5	326
4.125"V by 4.125"H Helical Coil (1-1/4")	4	9/26/11 3:02 PM	18.0	45.7	4.0	1.2	8.0	2.4	11.062	0.698	83.4	28.6	77.4	25.2	68.3	20.2	2.8	9725	3.564E-04	6.756E-04	2.629E-04	4.984E-04	9.860E-06	1.869E-05	8.362E-05	1.585E-04	55.0	313
4.125"V by 4.125"H Helical Coil (1-1/4")	5	9/26/11 3:34 PM	18.0	45.7	4.0	1.2	8.0	2.4	11.026	0.696	84.0	28.9	77.7	25.4	68.3	20.2	2.9	10100	3.567E-04	6.761E-04	2.630E-04	4.985E-04	9.859E-06	1.869E-05	8.380E-05	1.589E-04	54.9	312
4.125"V by 4.125"H Helical Coil (1-1/4")	6	9/26/11 4:03 PM	18.0	45.7	4.0	1.2	8.0	2.4	11.055	0.697	84.1	28.9	77.9	25.5	68.4	20.2	2.9	10031	3.586E-04	6.798E-04	2.630E-04	4.986E-04	9.830E-06	1.863E-05	8.577E-05	1.626E-04	53.7	305
4.125"V by 4.125"H Helical Coil (1-1/4")	7	9/26/11 4:34 PM	18.0	45.7	4.0	1.2	8.0	2.4	11.079	0.699	83.9	28.8	77.8	25.4	68.3	20.2	2.8	9951	3.614E-04	6.850E-04	2.630E-04	4.986E-04	9.819E-06	1.861E-05	8.853E-05	1.678E-04	52.0	295
4.125"V by 4.125"H Helical Coil (1-1/4")	8	9/26/11 4:59 PM	18.0	45.7	4.0	1.2	8.0	2.4	11.014	0.695	83.7	28.7	77.7	25.4	68.4	20.2	2.7	9623	3.666E-04	6.950E-04	2.630E-04	4.986E-04	9.879E-06	1.873E-05	9.374E-05	1.777E-04	49.1	279
4.125"V by 4.125"H Helical Coil (1-1/4")	1	9/26/11 5:47 PM	18.0	45.7	4.0	1.2	8.0	2.4	11.113	0.701	76.4	24.7	73.3	23.0	68.3	20.2	1.4	5044	3.727E-04	7.064E-04	2.618E-04	4.963E-04	1.017E-05	1.929E-05	1.007E-04	1.909E-04	45.7	260
4.125"V by 4.125"H Helical Coil (1-1/4")	2	9/26/11 6:19 PM	18.0	45.7	4.0	1.2	8.0	2.4	11.112	0.701	78.4	25.8	74.6	23.6	68.6	20.3	1.8	6265	3.621E-04	6.863E-04	2.621E-04	4.969E-04	1.007E-05	1.909E-05	8.985E-05	1.703E-04	51.2	291
4.125"V by 4.125"H Helical Coil (1-1/4")	3	9/26/11 6:46 PM	18.0	45.7	4.0	1.2	8.0	2.4	11.121	0.702	79.1	26.2	74.9	23.8	68.5	20.3	1.9	6773	3.598E-04	6.821E-04	2.622E-04	4.971E-04	1.003E-05	1.901E-05	8.755E-05	1.660E-04	52.6	298
4.125"V by 4.125"H Helical Coil (1-1/4")	4	9/26/11 7:11 PM	18.0	45.7	4.0	1.2	8.0	2.4	11.102	0.700	79.1	26.1	74.9	23.8	68.5	20.3	1.9	6769	3.613E-04	6.849E-04	2.622E-04	4.971E-04	1.005E-05	1.904E-05	8.904E-05	1.688E-04	51.7	293
4.125"V by 4.125"H Helical Coil (1-1/4")	5	9/26/11 7:35 PM	18.0	45.7	4.0	1.2	8.0	2.4	11.063	0.698	79.2	26.2	75.0	23.9	68.4	20.2	1.9	6801	3.658E-04	6.933E-04	2.622E-04	4.971E-04	1.007E-05	1.909E-05	9.344E-05	1.771E-04	49.3	280
4.125"V by 4.125"H Helical Coil (1-1/4")	6	9/26/11 7:58 PM	18.0	45.7	4.0	1.2	8.0	2.4	11.049	0.697	79.3	26.3	75.1	23.9	68.4	20.2	2.0	6918	3.662E-04	6.941E-04	2.623E-04	4.972E-04	1.007E-05	1.909E-05	9.381E-05	1.778E-04	49.1	279
4.125"V by 4.125"H Helical Coil (1-1/4")	7	9/26/11 8:36 PM	18.0	45.7	4.0	1.2	8.0	2.4	11.024	0.695	79.7	26.5	75.3	24.0	68.4	20.2	2.0	7122	3.657E-04	6.933E-04	2.623E-04	4.973E-04	1.007E-05	1.910E-05	9.334E-05	1.769E-04	49.3	280
4.125"V by 4.125"H Helical Coil (1-1/4")	8	9/26/11 9:04 PM	18.0	45.7	4.0	1.2	8.0	2.4	11.023	0.695	79.9	26.6	75.4	24.1	68.4	20.2	2.1	7219	3.650E-04	6.919E-04	2.624E-04	4.974E-04	1.007E-05	1.908E-05	9.256E-05	1.755E-04	49.7	282

APPENDIX B

Bundle Coil Experimental Data & Reference Calculations

Test Description	Set Point	Date & Time	H		C_{minor}		D_{c1}		D_{c0}		V_{c1}		T_{cin}		$T_{c,out}$		T_p		Q_c		R_c		R_t		R_i		R_o		h_o	
	1-8		in	cm	in	cm	ft	m	ft	m	GPM	L/s	°F	°C	°F	°C	°F	°C	Tons	W	hr·°F/Btu	K/W	hr·°F/Btu	K/W	hr·°F/Btu	K/W	hr·°F/Btu	K/W	Btu/hr-ft²·°F	W/m²·K
Loose Bundle Pool Test (3/4")	1	1/15/10 12:00 PM	9.9	25.1	31.0	78.7	4.5	1.4	6.3	1.9	4.471	0.282	54.3	12.4	52.2	11.2	48.9	9.4	0.7	2507	8.970E-04	1.700E-03	2.802E-04	5.311E-04	1.165E-05	2.208E-05	6.051E-04	1.147E-03	12.0	68
Loose Bundle Pool Test (3/4")	2	1/15/10 12:30 PM	9.9	25.1	31.0	78.7	4.5	1.4	6.3	1.9	4.432	0.280	58.6	14.8	54.8	12.7	50.0	10.0	1.2	4365	7.871E-04	1.492E-03	2.822E-04	5.350E-04	1.142E-05	2.165E-05	4.934E-04	9.354E-04	14.7	84
Loose Bundle Pool Test (3/4")	3	1/15/10 1:00 PM	9.9	25.1	31.0	78.7	4.5	1.4	6.3	1.9	4.423	0.279	60.0	15.5	55.6	13.1	50.4	10.2	1.4	5052	7.418E-04	1.406E-03	2.828E-04	5.362E-04	1.135E-05	2.152E-05	4.477E-04	8.486E-04	16.3	92
Loose Bundle Pool Test (3/4")	4	1/15/10 1:30 PM	9.9	25.1	31.0	78.7	4.5	1.4	6.3	1.9	4.436	0.280	61.7	16.5	56.5	13.6	50.9	10.5	1.7	5894	7.077E-04	1.342E-03	2.836E-04	5.376E-04	1.121E-05	2.125E-05	4.129E-04	7.872E-04	17.6	100
Loose Bundle Pool Test (3/4")	5	1/15/10 2:00 PM	9.9	25.1	31.0	78.7	4.5	1.4	6.3	1.9	4.436	0.280	62.9	17.2	57.2	14.0	51.2	10.7	1.9	6533	6.883E-04	1.305E-03	2.842E-04	5.387E-04	1.113E-05	2.111E-05	3.930E-04	7.451E-04	18.5	105
Loose Bundle Pool Test (3/4")	6	1/15/10 2:30 PM	9.9	25.1	31.0	78.7	4.5	1.4	6.3	1.9	4.433	0.280	64.5	18.0	58.1	14.5	51.5	10.8	2.1	7401	6.683E-04	1.267E-03	2.848E-04	5.400E-04	1.104E-05	2.093E-05	3.724E-04	7.060E-04	19.5	111
Loose Bundle Pool Test (3/4")	7	1/15/10 3:00 PM	9.9	25.1	31.0	78.7	4.5	1.4	6.3	1.9	4.428	0.279	65.9	18.8	58.9	14.9	52.0	11.1	2.3	8068	6.543E-04	1.240E-03	2.855E-04	5.412E-04	1.097E-05	2.079E-05	3.578E-04	6.783E-04	20.3	115
Loose Bundle Pool Test (3/4")	8	1/15/10 3:30 PM	9.9	25.1	31.0	78.7	4.5	1.4	6.3	1.9	4.426	0.279	67.0	19.4	59.5	15.3	52.3	11.3	2.4	8581	6.455E-04	1.224E-03	2.860E-04	5.422E-04	1.090E-05	2.067E-05	3.485E-04	6.607E-04	20.9	119
Loose Spaced Bundle Pool Test (3/4")	1	1/19/10 12:00 PM	14.8	37.6	46.6	118.4	4.5	1.4	6.3	1.9	4.492	0.283	53.5	11.9	51.3	10.7	49.2	9.6	0.4	1403	6.391E-04	1.211E-03	2.533E-04	4.802E-04	1.816E-05	3.443E-05	3.676E-04	6.968E-04	19.8	112
Loose Spaced Bundle Pool Test (3/4")	2	1/19/10 12:30 PM	14.8	37.6	46.6	118.4	4.5	1.4	6.3	1.9	4.510	0.285	56.4	13.5	52.6	11.4	49.3	9.6	0.7	2513	5.719E-04	1.084E-03	2.538E-04	4.811E-04	1.781E-05	3.376E-05	3.003E-04	5.692E-04	24.2	138
Loose Spaced Bundle Pool Test (3/4")	3	1/19/10 1:00 PM	14.8	37.6	46.6	118.4	4.5	1.4	6.3	1.9	4.502	0.284	57.5	14.2	53.1	11.7	49.5	9.7	0.8	2910	5.575E-04	1.057E-03	2.540E-04	4.815E-04	1.772E-05	3.359E-05	2.858E-04	5.418E-04	25.5	145
Loose Spaced Bundle Pool Test (3/4")	4	1/19/10 1:30 PM	14.8	37.6	46.6	118.4	4.5	1.4	6.3	1.9	4.512	0.285	58.6	14.8	53.6	12.0	49.6	9.8	0.9	3304	5.485E-04	1.040E-03	2.542E-04	4.819E-04	1.757E-05	3.331E-05	2.768E-04	5.246E-04	26.3	149
Loose Spaced Bundle Pool Test (3/4")	5	1/19/10 2:00 PM	14.8	37.6	46.6	118.4	4.5	1.4	6.3	1.9	4.500	0.284	59.9	15.5	54.2	12.3	49.8	9.9	1.1	3780	5.352E-04	1.015E-03	2.544E-04	4.823E-04	1.748E-05	3.314E-05	2.633E-04	4.992E-04	27.6	157
Loose Spaced Bundle Pool Test (3/4")	6	1/19/10 2:30 PM	14.8	37.6	46.6	118.4	4.5	1.4	6.3	1.9	4.491	0.283	61.3	16.3	54.8	12.7	50.0	10.0	1.2	4249	5.258E-04	9.967E-04	2.547E-04	4.828E-04	1.738E-05	3.295E-05	2.538E-04	4.810E-04	28.7	163
Loose Spaced Bundle Pool Test (3/4")	7	1/19/10 3:00 PM	14.8	37.6	46.6	118.4	4.5	1.4	6.3	1.9	4.493	0.283	62.6	17.0	55.5	13.1	50.2	10.1	1.3	4678	5.229E-04	9.913E-04	2.549E-04	4.833E-04	1.724E-05	3.268E-05	2.508E-04	4.754E-04	29.0	165
Loose Spaced Bundle Pool Test (3/4")	8	1/19/10 3:30 PM	14.8	37.6	46.6	118.4	4.5	1.4	6.3	1.9	4.494	0.284	63.7	17.6	56.1	13.4	50.5	10.3	1.4	4996	5.195E-04	9.847E-04	2.551E-04	4.837E-04	1.713E-05	3.248E-05	2.472E-04	4.686E-04	29.4	167
Factory Banded Spiral-Helical Coil (3/4")	1	4/27/11 6:29 PM	11.0	27.9	34.0	86.4	1.9	0.6	3.5	1.1	4.474	0.282	73.6	23.1	70.1	21.2	60.4	15.8	0.6	2278	1.466E-03	2.779E-03	2.612E-04	4.951E-04	1.474E-05	2.794E-05	1.190E-03	2.256E-03	6.1	35
Factory Banded Spiral-Helical Coil (3/4")	2	4/27/11 7:05 PM	11.0	27.9	34.0	86.4	1.9	0.6	3.5	1.1	4.499	0.284	82.1	27.8	75.9	24.4	60.3	15.7	1.2	4065	1.334E-03	2.529E-03	2.633E-04	4.992E-04	1.400E-05	2.654E-05	1.057E-03	2.003E-03	6.9	39
Factory Banded Spiral-Helical Coil (3/4")	3	4/27/11 7:37 PM	11.0	27.9	34.0	86.4	1.9	0.6	3.5	1.1	4.505	0.284	86.1	30.0	78.8	26.0	60.2	15.7	1.4	4771	1.354E-03	2.567E-03	2.644E-04	5.012E-04	1.368E-05	2.594E-05	1.076E-03	2.040E-03	6.8	38
Factory Banded Spiral-Helical Coil (3/4")	4	4/27/11 8:08 PM	11.0	27.9	34.0	86.4	1.9	0.6	3.5	1.1	4.488	0.283	88.3	31.3	80.4	26.9	60.1	15.6	1.5	5183	1.361E-03	2.580E-03	2.650E-04	5.023E-04	1.357E-05	2.572E-05	1.082E-03	2.052E-03	6.7	38
Factory Banded Spiral-Helical Coil (3/4")	5	4/27/11 8:30 PM	11.0	27.9	34.0	86.4	1.9	0.6	3.5	1.1	4.502	0.284	89.6	32.0	81.3	27.4	60.1	15.6	1.6	5454	1.351E-03	2.561E-03	2.653E-04	5.030E-04	1.344E-05	2.548E-05	1.072E-03	2.033E-03	6.8	39
Factory Banded Spiral-Helical Coil (3/4")	6	4/27/11 8:56 PM	11.0	27.9	34.0	86.4	1.9	0.6	3.5	1.1	4.490	0.283	90.9	32.7	82.2	27.9	60.0	15.6	1.6	5692	1.357E-03	2.572E-03	2.657E-04	5.036E-04	1.338E-05	2.537E-05	1.078E-03	2.043E-03	6.7	38
Factory Banded Spiral-Helical Coil (3/4")	7	4/27/11 9:22 PM	11.0	27.9	34.0	86.4	1.9	0.6	3.5	1.1	4.473	0.282	92.1	33.4	83.0	28.3	59.9	15.5	1.7	5949	1.350E-03	2.559E-03	2.660E-04	5.042E-04	1.335E-05	2.530E-05	1.071E-03	2.030E-03	6.8	39
Factory Banded Spiral-Helical Coil (3/4")	8	4/27/11 9:43 PM	11.0	27.9	34.0	86.4	1.9	0.6	3.5	1.1	4.472	0.282	92.9	33.9	83.6	28.7	59.9	15.5	1.7	6078	1.354E-03	2.567E-03	2.662E-04	5.046E-04	1.329E-05	2.520E-05	1.075E-03	2.037E-03	6.8	38
Factory Banded Spiral-Helical Coil (3/4")	1	4/28/11 9:21 AM	11.0	27.9	34.0	86.4	1.9	0.6	3.5	1.1	4.511	0.285	72.3	22.4	69.0	20.5	58.3	14.6	0.6	2184	1.464E-03	3.120E-03	2.608E-04	4.943E-04	1.475E-05	2.797E-05	1.127E-03	2.597E-03	5.3	30
Factory Banded Spiral-Helical Coil (3/4")	2	4/28/11 10:03 AM	11.0	27.9	34.0	86.4	1.9	0.6	3.5	1.1	4.488	0.283	81.6	27.5	75.7	24.3	58.6	14.8	1.1	3872	1.500E-03	2.840E-03	2.632E-04	4.990E-04	1.406E-05	2.665E-05	1.232E-03	2.318E-03	5.9	34
Factory Banded Spiral-Helical Coil (3/4")	3	4/28/11 10:40 AM	11.0	27.9	34.0	86.4	1.9	0.6	3.5	1.1	4.473	0.282	85.8	29.9	78.6	25.9	58.9	14.9	1.3	4740	1.432E-03	2.714E-03	2.643E-04	5.011E-04	1.379E-05	2.613E-05	1.153E-03	2.187E-03	6.3	36
Factory Banded Spiral-Helical Coil (3/4")	4	4/28/11 11:19 AM	11.0	27.9	34.0	86.4	1.9	0.6	3.5	1.1	4.463	0.282	88.5	31.4	80.4	26.9	58.8	14.9	1.5	5275	1.417E-03	2.687E-03	2.650E-04	5.024E-04	1.362E-05	2.582E-05	1.139E-03	2.159E-03	6.4	36
Factory Banded Spiral-Helical Coil (3/4")	5	4/28/11 11:49 AM	11.0	27.9	34.0	86.4	1.9	0.6	3.5	1.1	4.465	0.282	89.8	32.1	81.3	27.4	59.3	15.2	1.6	5477	1.391E-03	2.637E-03	2.654E-04	5.030E-04	1.353E-05	2.565E-05	1.112E-03	2.109E-03	6.5	37
Factory Banded Spiral-Helical Coil (3/4")	6	4/28/11 12:19 PM	11.0	27.9	34.0	86.4	1.9	0.6	3.5	1.1	4.471	0.282	91.5	33.0	82.4	28.0	59.8	15.4	1.7	5884	1.341E-03	2.541E-03	2.658E-04	5.038E-04	1.340E-05	2.540E-05	1.061E-03	2.012E-03	6.9	39
Factory Banded Spiral-Helical Coil (3/4")	7	4/28/11 12:57 PM	11.0	27.9	34.0	86.4	1.9	0.6	3.5	1.1	4.467	0.282	93.3	34.1	83.9	28.8	59.5	15.3	1.8	6158	1.374E-03	2.604E-03	2.663E-04	5.048E-04	1.328E-05	2.517E-05	1.094E-03	2.074E-03	6.6	38
Factory Banded Spiral-Helical Coil (3/4")	8	4/28/11 1:28 PM	11.0	27.9	34.0	86.4	1.9	0.6	3.5	1.1	4.457	0.281	94.3	34.6	84.4	29.1	60.1	15.6	1.8	6441	1.319E-03	2.500E-03	2.665E-04	5.052E-04	1.325E-05	2.511E-05	1.039E-03	1.969E-03	7.0	40
Factory Banded Spiral-Helical Coil (3/4")	1	4/29/11 11:25 AM	11.0	27.9	34.0	86.4	1.9	0.6	3.5	1.1	4.509	0.284	75.9	24.4	72.3	22.4	62.3	16.8	0.7	2376	1.442E-03	2.733E-03	2.619E-04	4.965E-04	1.442E-05	2.734E-05	1.166E-03	2.209E-03	6.2	35
Factory Banded Spiral-Helical Coil (3/4")	2	4/29/11 12:30 PM	11.0	27.9	34.0	86.4	1.9	0.6	3.5	1.1	4.452	0.281	84.2	29.0	77.9	25.5	62.9	17.2	1.2	4098	1.282E-03	2.430E-03	2.640E-04	5.005E-04	1.394E-05	2.643E-05	1.040E-03	1.903E-03	7.2	41
Factory Banded Spiral-Helical Coil (3/4")	3	4/29/11 1:16 PM	11.0	27.9	34.0	86.4	1.9	0.6	3.5	1.1	4.430	0.279	88.4	31.3	81.0	27.2	63.4	17.4	1.4	4791	1.288E-03	2.442E-03	2.652E-04	5.027E-04	1.369E-05	2.596E-05	1.009E-03	1.914E-03	7.2	41
Factory Banded Spiral-Helical Coil (3/4")	4	4/29/11 1:46																												

Test Description	Set Point	Date & Time	H	C _{minor}	D _{cj}	D _{cD}	V _{cj}	T _{cin}	T _{cout}	T _p	Q _c	W	R _c	R _t	R _i	R _o	h _o											
	1-8		in	cm	ft	m	ft	m	ft	m	GPM	L/s	°F	°C	°F	°C	Tons	W	hr·°F/Btu	K/W	hr·°F/Btu	K/W	hr·°F/Btu	K/W	hr·°F/Btu	K/W	Btu/hr-ft²·°F	W/m²·K
+50% Loose Spiral-Helical Coil (3/4")	1	5/21/11 12:28 PM	16.0	40.6	51.0	129.5	1.9	0.6	3.5	1.1	6.455	0.407	78.3	25.7	75.1	23.9	0.9	3073	5.427E-04	1.029E-03	2.627E-04	4.980E-04	1.045E-05	1.981E-05	2.695E-04	5.109E-04	27.0	153
+50% Loose Spiral-Helical Coil (3/4")	2	5/21/11 1:04 PM	16.0	40.6	51.0	129.5	1.9	0.6	3.5	1.1	6.485	0.409	83.6	28.7	77.8	25.4	1.6	5488	4.751E-04	9.006E-04	2.637E-04	4.998E-04	1.015E-05	1.924E-05	2.013E-04	3.816E-04	36.1	205
+50% Loose Spiral-Helical Coil (3/4")	3	5/21/11 1:30 PM	16.0	40.6	51.0	129.5	1.9	0.6	3.5	1.1	6.469	0.408	85.5	29.7	78.5	25.8	1.9	6646	4.363E-04	8.271E-04	2.639E-04	5.003E-04	1.009E-05	1.913E-05	1.623E-04	3.078E-04	44.8	254
+50% Loose Spiral-Helical Coil (3/4")	4	5/21/11 1:59 PM	16.0	40.6	51.0	129.5	1.9	0.6	3.5	1.1	6.477	0.409	86.9	30.5	79.5	26.4	2.2	6969	4.451E-04	8.438E-04	2.643E-04	5.009E-04	1.001E-05	1.897E-05	1.708E-04	3.239E-04	42.6	242
+50% Loose Spiral-Helical Coil (3/4")	5	5/21/11 2:27 PM	16.0	40.6	51.0	129.5	1.9	0.6	3.5	1.1	6.466	0.408	88.0	31.1	80.1	26.7	2.1	7439	4.479E-04	8.491E-04	2.645E-04	5.014E-04	9.966E-06	1.889E-05	1.735E-04	3.289E-04	41.9	238
+50% Loose Spiral-Helical Coil (3/4")	6	5/21/11 2:54 PM	16.0	40.6	51.0	129.5	1.9	0.6	3.5	1.1	6.464	0.408	89.0	31.7	80.6	27.0	2.2	7896	4.309E-04	8.169E-04	2.647E-04	5.017E-04	9.922E-06	1.881E-05	1.563E-04	2.963E-04	46.5	264
+50% Loose Spiral-Helical Coil (3/4")	7	5/21/11 3:19 PM	16.0	40.6	51.0	129.5	1.9	0.6	3.5	1.1	6.456	0.407	90.2	32.3	81.5	27.5	2.3	8191	4.475E-04	8.483E-04	2.650E-04	5.023E-04	9.872E-06	1.871E-05	1.726E-04	3.273E-04	42.1	239
+50% Loose Spiral-Helical Coil (3/4")	8	5/21/11 3:46 PM	16.0	40.6	51.0	129.5	1.9	0.6	3.5	1.1	6.468	0.408	90.5	32.5	81.5	27.5	2.3	8488	4.331E-04	8.211E-04	2.650E-04	5.023E-04	9.845E-06	1.866E-05	1.583E-04	3.001E-04	46.0	261
+75% Loose Spiral-Helical Coil (3/4")	1	5/26/11 11:26 AM	20.0	50.8	59.5	151.1	1.9	0.6	3.5	1.1	6.218	0.392	78.7	25.9	75.5	24.1	0.8	2935	6.432E-04	1.219E-03	2.629E-04	4.983E-04	1.076E-05	2.040E-05	3.696E-04	7.006E-04	19.7	112
+75% Loose Spiral-Helical Coil (3/4")	2	5/26/11 11:53 AM	20.0	50.8	59.5	151.1	1.9	0.6	3.5	1.1	6.182	0.390	83.6	28.7	78.0	25.6	1.4	5020	5.872E-04	1.113E-03	2.638E-04	5.001E-04	1.056E-05	2.002E-05	3.129E-04	5.931E-04	23.3	132
+75% Loose Spiral-Helical Coil (3/4")	3	5/26/11 12:16 PM	20.0	50.8	59.5	151.1	1.9	0.6	3.5	1.1	6.222	0.393	85.9	29.9	79.2	26.2	1.7	6066	5.616E-04	1.065E-03	2.642E-04	5.008E-04	1.039E-05	1.970E-05	2.870E-04	5.440E-04	25.4	144
+75% Loose Spiral-Helical Coil (3/4")	4	5/26/11 12:36 PM	20.0	50.8	59.5	151.1	1.9	0.6	3.5	1.1	6.219	0.392	86.7	30.4	79.5	26.4	1.9	6571	5.348E-04	1.014E-03	2.643E-04	5.010E-04	1.036E-05	1.964E-05	2.601E-04	4.931E-04	28.0	159
+75% Loose Spiral-Helical Coil (3/4")	5	5/26/11 12:58 PM	20.0	50.8	59.5	151.1	1.9	0.6	3.5	1.1	6.179	0.390	88.0	31.1	80.1	26.7	2.0	7069	5.308E-04	1.006E-03	2.645E-04	5.015E-04	1.036E-05	1.964E-05	2.559E-04	4.851E-04	28.4	161
+75% Loose Spiral-Helical Coil (3/4")	6	5/26/11 1:20 PM	20.0	50.8	59.5	151.1	1.9	0.6	3.5	1.1	6.211	0.392	88.6	31.4	80.3	26.8	2.1	7466	5.250E-04	9.952E-04	2.646E-04	5.016E-04	1.029E-05	1.950E-05	2.501E-04	4.741E-04	29.1	165
+75% Loose Spiral-Helical Coil (3/4")	7	5/26/11 1:40 PM	20.0	50.8	59.5	151.1	1.9	0.6	3.5	1.1	6.210	0.392	89.5	32.0	80.6	27.0	2.3	8069	5.078E-04	9.627E-04	2.647E-04	5.018E-04	1.025E-05	1.943E-05	2.329E-04	4.414E-04	31.2	177
+75% Loose Spiral-Helical Coil (3/4")	8	5/26/11 1:57 PM	20.0	50.8	59.5	151.1	1.9	0.6	3.5	1.1	6.212	0.392	90.0	32.2	81.0	27.2	2.3	8128	5.154E-04	9.771E-04	2.649E-04	5.021E-04	1.022E-05	1.938E-05	2.403E-04	4.556E-04	30.3	172
+75% Loose Spiral-Helical Coil (3/4")	1	5/27/11 10:52 AM	20.0	50.8	59.5	151.1	1.9	0.6	3.5	1.1	6.246	0.394	78.6	25.9	75.9	24.4	0.7	2422	7.431E-04	1.409E-03	2.630E-04	4.986E-04	1.071E-05	2.031E-05	4.694E-04	8.898E-04	15.5	88
+75% Loose Spiral-Helical Coil (3/4")	2	5/27/11 11:25 AM	20.0	50.8	59.5	151.1	1.9	0.6	3.5	1.1	6.233	0.393	83.3	28.5	78.3	25.7	1.3	4533	5.970E-04	1.132E-03	2.639E-04	5.002E-04	1.049E-05	1.989E-05	3.227E-04	6.117E-04	22.5	128
+75% Loose Spiral-Helical Coil (3/4")	3	5/27/11 11:57 AM	20.0	50.8	59.5	151.1	1.9	0.6	3.5	1.1	6.230	0.393	86.0	30.0	79.9	26.6	1.7	5576	5.709E-04	1.082E-03	2.644E-04	5.013E-04	1.036E-05	1.964E-05	2.962E-04	5.614E-04	24.6	139
+75% Loose Spiral-Helical Coil (3/4")	4	5/27/11 12:25 PM	20.0	50.8	59.5	151.1	1.9	0.6	3.5	1.1	6.210	0.392	87.1	30.6	80.5	26.9	1.9	6040	5.495E-04	1.042E-03	2.646E-04	5.017E-04	1.033E-05	1.958E-05	2.745E-04	5.203E-04	26.5	151
+75% Loose Spiral-Helical Coil (3/4")	5	5/27/11 12:53 PM	20.0	50.8	59.5	151.1	1.9	0.6	3.5	1.1	6.250	0.394	88.8	31.6	81.8	27.7	2.2	6420	5.708E-04	1.082E-03	2.651E-04	5.026E-04	1.018E-05	1.930E-05	2.955E-04	5.601E-04	24.6	140
+75% Loose Spiral-Helical Coil (3/4")	6	5/27/11 1:25 PM	20.0	50.8	59.5	151.1	1.9	0.6	3.5	1.1	6.251	0.394	90.1	32.3	82.3	27.9	2.3	7092	5.262E-04	9.976E-04	2.653E-04	5.029E-04	1.013E-05	1.920E-05	2.508E-04	4.755E-04	29.0	165
+75% Loose Spiral-Helical Coil (3/4")	7	5/27/11 1:50 PM	20.0	50.8	59.5	151.1	1.9	0.6	3.5	1.1	6.243	0.394	90.6	32.6	82.5	28.1	2.3	7372	5.246E-04	9.945E-04	2.654E-04	5.031E-04	1.011E-05	1.917E-05	2.492E-04	4.723E-04	29.2	166
+75% Loose Spiral-Helical Coil (3/4")	8	5/27/11 2:13 PM	20.0	50.8	59.5	151.1	1.9	0.6	3.5	1.1	6.258	0.395	91.5	33.0	82.8	28.2	2.7	7900	5.212E-04	9.881E-04	2.655E-04	5.033E-04	1.006E-05	1.906E-05	2.457E-04	4.658E-04	29.6	168
+75% Loose Spiral-Helical Coil (3/4")	1	5/27/11 3:07 PM	20.0	50.8	59.5	151.1	1.9	0.6	3.5	1.1	6.251	0.394	81.6	27.5	78.2	25.6	0.9	3117	6.126E-04	1.161E-03	2.638E-04	5.001E-04	1.052E-05	1.995E-05	3.382E-04	6.412E-04	21.5	122
+75% Loose Spiral-Helical Coil (3/4")	2	5/27/11 3:42 PM	20.0	50.8	59.5	151.1	1.9	0.6	3.5	1.1	6.270	0.396	86.2	30.1	80.4	26.9	1.5	5259	5.710E-04	1.082E-03	2.646E-04	5.016E-04	1.028E-05	1.948E-05	2.961E-04	5.613E-04	24.6	140
+75% Loose Spiral-Helical Coil (3/4")	3	5/27/11 4:10 PM	20.0	50.8	59.5	151.1	1.9	0.6	3.5	1.1	6.246	0.394	88.3	31.3	81.3	27.4	1.8	6386	5.269E-04	9.989E-04	2.649E-04	5.022E-04	1.022E-05	1.937E-05	2.518E-04	4.773E-04	28.9	164
+75% Loose Spiral-Helical Coil (3/4")	4	5/27/11 4:35 PM	20.0	50.8	59.5	151.1	1.9	0.6	3.5	1.1	6.256	0.395	89.0	31.7	81.7	27.6	1.9	6710	5.093E-04	9.655E-04	2.651E-04	5.025E-04	1.017E-05	1.928E-05	2.341E-04	4.438E-04	31.1	176
+75% Loose Spiral-Helical Coil (3/4")	5	5/27/11 4:53 PM	20.0	50.8	59.5	151.1	1.9	0.6	3.5	1.1	6.239	0.394	90.1	32.3	82.2	27.9	2.0	7153	5.233E-04	9.921E-04	2.653E-04	5.029E-04	1.014E-05	1.923E-05	2.479E-04	4.700E-04	29.3	167
+75% Loose Spiral-Helical Coil (3/4")	6	5/27/11 5:11 PM	20.0	50.8	59.5	151.1	1.9	0.6	3.5	1.1	6.277	0.396	90.9	32.7	82.7	28.2	2.1	7529	5.236E-04	1.010E-03	2.654E-04	5.032E-04	1.005E-05	1.906E-05	2.571E-04	4.873E-04	28.3	161
+75% Loose Spiral-Helical Coil (3/4")	7	5/27/11 5:28 PM	20.0	50.8	59.5	151.1	1.9	0.6	3.5	1.1	6.266	0.395	91.5	33.0	82.8	28.2	2.3	7952	5.097E-04	9.663E-04	2.655E-04	5.032E-04	1.005E-05	1.905E-05	2.342E-04	4.440E-04	31.1	176
+75% Loose Spiral-Helical Coil (3/4")	8	5/27/11 5:43 PM	20.0	50.8	59.5	151.1	1.9	0.6	3.5	1.1	6.252	0.394	91.9	33.3	83.0	28.3	2.3	8139	5.038E-04	9.550E-04	2.656E-04	5.034E-04	1.005E-05	1.905E-05	2.282E-04	4.326E-04	31.9	181
Factory Banded Spiral-Helical Coil (1")	1	5/2/11 7:25 PM	9.0	22.9	36.0	91.4	2.6	0.8	4.1	1.2	5.431	0.343	73.4	23.0	69.6	20.9	0.9	3050	1.003E-03	1.901E-03	2.619E-04	4.964E-04	1.513E-05	2.869E-05	7.256E-04	1.376E-03	8.0	45
Factory Banded Spiral-Helical Coil (1")	2	5/2/11 8:21 PM	9.0	22.9	36.0	91.4	2.6	0.8	4.1	1.2	5.411	0.341	81.3	27.4	75.1	24.0	1.4	4910	1.028E-03	1.949E-03	2.639E-04	5.002E-04	1.452E-05	2.753E-05	7.496E-04	1.421E-03	7.7	44
Factory Banded Spiral-Helical Coil (1")	3	5/2/11 9:10 PM	9.0	22.9	36.0	91.4	2.6	0.8	4.1	1.2	5.438	0.343	84.4	29.1	77.2	25.1	1.6	5709	1.017E-03	1.928E-03	2.646E-04	5.016E-04	1.423E-05	2.697E-05	7.380E-04	1.399E-03	7.9	45
Factory Banded Spiral-Helical Coil (1")	4	5/2/11 9:45 PM	9.0	22.9	36.0	91.4	2.6	0.8	4.1	1.2	5.411	0.341	85.9	30.0	78.1	25.6	1.8	6155	1.007E-03	1.910E-03	2.650E-04	5.023E-04	1.418E-05	2.688E-05	7.282E-04	1.380E-03	8.0	45
Factory Banded Spiral-Helical Coil (1")	5	5/2/11 10:19 PM	9.0	22.9	36.0	91.4	2.6	0.8	4.1	1.2	5.427	0.342	86.9	30.5	78.8	26.0	1.8	6393	1.012E-03	1.919E-03	2.652E-04	5.028E-04	1.407E-05	2.668E-05	7.331E-04	1.390E-03	7.9	45
Factory Banded Spiral-Helical Coil (1")	6	5/2/11 10:47 PM	9.0	22.9	36.0	91.4	2.6	0.8	4.1	1.2	5.408	0.341	87.9	31.0	79.5	26.4	1.9	6615	1.017E-									

Test Description	Set Point	Date & Time	H	C _{minor}	D _{ci}	D _{co}	V _{ci}	T _{cin}	T _{cout}	T _p	Q _c	W	R _c	R _t	R _i	R _o	h _o													
	1-8		in	cm	ft	m	ft	m	ft	m	GPM	L/s	°F	°C	°F	°C	°F	°C	Tons	hr·°F/Btu	K/W	hr·°F/Btu	K/W	hr·°F/Btu	K/W	hr·°F/Btu	K/W	Btu/hr-ft²·°F	W/m²·K	
50% Loose Spiral-Helical Coil (1")	1	5/31/11 9:20 AM	17.0	43.2	52.0	132.1	2.6	0.8	4.1	1.2	8.466	0.534	83.0	28.3	81.5	27.5	75.9	24.4	0.5	1777	1.036E-03	1.963E-03	6.659E-04	5.040E-04	9.681E-06	1.835E-05	7.601E-04	1.441E-03	7.6	43
50% Loose Spiral-Helical Coil (1")	2	5/31/11 9:50 AM	17.0	43.2	52.0	132.1	2.6	0.8	4.1	1.2	8.429	0.532	87.5	30.8	84.1	28.9	76.0	24.4	1.2	4157	6.822E-04	1.293E-03	2.667E-04	5.055E-04	9.511E-06	1.803E-05	4.060E-04	7.697E-04	14.3	81
50% Loose Spiral-Helical Coil (1")	3	5/31/11 10:13 AM	17.0	43.2	52.0	132.1	2.6	0.8	4.1	1.2	8.416	0.531	89.6	32.0	85.3	29.6	76.1	24.5	1.5	5346	6.166E-04	1.169E-03	2.787E-04	5.063E-04	9.429E-06	1.787E-05	3.401E-04	6.447E-04	17.1	97
50% Loose Spiral-Helical Coil (1")	4	5/31/11 10:35 AM	17.0	43.2	52.0	132.1	2.6	0.8	4.1	1.2	8.416	0.531	90.5	32.5	85.7	29.9	76.1	24.5	1.7	5843	5.947E-04	1.127E-03	2.672E-04	5.066E-04	9.391E-06	1.780E-05	3.181E-04	6.030E-04	18.3	104
50% Loose Spiral-Helical Coil (1")	5	5/31/11 10:56 AM	17.0	43.2	52.0	132.1	2.6	0.8	4.1	1.2	8.430	0.532	91.4	33.0	86.3	30.2	76.2	24.5	1.8	6223	5.888E-04	1.116E-03	2.674E-04	5.069E-04	9.337E-06	1.770E-05	3.120E-04	5.915E-04	18.6	106
50% Loose Spiral-Helical Coil (1")	6	5/31/11 11:17 AM	17.0	43.2	52.0	132.1	2.6	0.8	4.1	1.2	8.425	0.532	92.3	33.5	86.8	30.4	76.3	24.6	1.9	6751	5.664E-04	1.074E-03	2.676E-04	5.072E-04	9.306E-06	1.764E-05	2.896E-04	5.490E-04	20.1	114
50% Loose Spiral-Helical Coil (1")	7	5/31/11 11:35 AM	17.0	43.2	52.0	132.1	2.6	0.8	4.1	1.2	8.410	0.531	93.0	33.9	87.3	30.7	76.4	24.7	2.0	7053	5.642E-04	1.070E-03	2.677E-04	5.075E-04	9.284E-06	1.760E-05	2.872E-04	5.445E-04	20.2	115
50% Loose Spiral-Helical Coil (1")	8	5/31/11 12:06 PM	17.0	43.2	52.0	132.1	2.6	0.8	4.1	1.2	8.409	0.531	93.5	34.2	87.4	30.8	76.4	24.7	2.1	7460	5.424E-04	1.028E-03	2.678E-04	5.076E-04	9.271E-06	1.758E-05	2.654E-04	5.030E-04	21.9	124
50% Loose Spiral-Helical Coil (1")	1	5/31/11 3:27 PM	17.0	43.2	52.0	132.1	2.6	0.8	4.1	1.2	8.429	0.532	85.5	29.7	82.9	28.3	76.7	24.8	0.9	3236	6.696E-04	1.269E-03	2.663E-04	5.048E-04	9.603E-06	1.820E-05	3.937E-04	7.463E-04	14.8	84
50% Loose Spiral-Helical Coil (1")	2	5/31/11 3:58 PM	17.0	43.2	52.0	132.1	2.6	0.8	4.1	1.2	8.435	0.532	90.1	32.3	85.4	29.6	77.0	25.0	1.6	5778	5.339E-04	1.012E-03	2.671E-04	5.063E-04	9.395E-06	1.781E-05	2.574E-04	4.879E-04	22.6	128
50% Loose Spiral-Helical Coil (1")	3	5/31/11 4:20 PM	17.0	43.2	52.0	132.1	2.6	0.8	4.1	1.2	8.425	0.532	92.2	33.4	86.5	30.3	77.0	25.0	2.0	6980	5.076E-04	9.622E-04	2.674E-04	5.070E-04	9.316E-06	1.766E-05	2.308E-04	4.375E-04	25.2	143
50% Loose Spiral-Helical Coil (1")	4	5/31/11 4:38 PM	17.0	43.2	52.0	132.1	2.6	0.8	4.1	1.2	8.448	0.533	92.7	33.7	86.7	30.4	76.9	24.9	2.1	7370	5.000E-04	9.478E-04	2.675E-04	5.071E-04	9.274E-06	1.758E-05	2.232E-04	4.231E-04	26.0	148
50% Loose Spiral-Helical Coil (1")	5	5/31/11 4:59 PM	17.0	43.2	52.0	132.1	2.6	0.8	4.1	1.2	8.420	0.531	93.1	34.0	87.0	30.6	76.8	24.9	2.1	7458	5.112E-04	9.690E-04	2.676E-04	5.073E-04	9.280E-06	1.759E-05	2.343E-04	4.441E-04	24.8	141
50% Loose Spiral-Helical Coil (1")	6	5/31/11 5:19 PM	17.0	43.2	52.0	132.1	2.6	0.8	4.1	1.2	8.406	0.530	93.8	34.3	87.4	30.8	76.9	25.0	2.2	7787	5.050E-04	9.572E-04	2.678E-04	5.076E-04	9.264E-06	1.756E-05	2.280E-04	4.321E-04	25.5	145
50% Loose Spiral-Helical Coil (1")	7	5/31/11 5:46 PM	17.0	43.2	52.0	132.1	2.6	0.8	4.1	1.2	8.410	0.531	94.2	34.5	87.6	30.9	76.9	25.0	2.3	8029	5.009E-04	9.496E-04	2.678E-04	5.077E-04	9.246E-06	1.753E-05	2.239E-04	4.244E-04	26.0	147
50% Loose Spiral-Helical Coil (1")	8	5/31/11 6:10 PM	17.0	43.2	52.0	132.1	2.6	0.8	4.1	1.2	8.399	0.530	94.7	34.9	87.9	31.1	77.1	25.0	2.4	8340	4.918E-04	9.323E-04	2.679E-04	5.079E-04	9.232E-06	1.750E-05	2.147E-04	4.069E-04	27.1	154
75% Loose Spiral-Helical Coil (1")	1	6/3/11 9:58 AM	23.0	58.4	60.0	152.4	2.6	0.8	4.1	1.2	8.478	0.535	84.6	29.2	83.8	28.8	78.2	25.7	0.3	960	1.832E-03	3.473E-03	2.667E-04	5.056E-04	9.553E-06	1.811E-05	1.556E-03	2.950E-03	3.7	21
75% Loose Spiral-Helical Coil (1")	2	6/3/11 10:28 AM	23.0	58.4	60.0	152.4	2.6	0.8	4.1	1.2	8.420	0.531	89.0	31.7	86.3	30.2	78.4	25.8	0.9	3316	8.086E-04	1.533E-03	2.675E-04	5.071E-04	9.413E-06	1.784E-05	5.316E-04	1.008E-03	10.9	62
75% Loose Spiral-Helical Coil (1")	3	6/3/11 10:53 AM	23.0	58.4	60.0	152.4	2.6	0.8	4.1	1.2	8.435	0.532	91.5	33.1	87.6	30.9	78.7	25.9	1.4	4807	6.559E-04	1.243E-03	2.679E-04	5.079E-04	9.294E-06	1.762E-05	3.878E-04	7.179E-04	15.3	87
75% Loose Spiral-Helical Coil (1")	4	6/3/11 11:12 AM	23.0	58.4	60.0	152.4	2.6	0.8	4.1	1.2	8.406	0.530	92.4	33.5	88.1	31.2	78.9	26.1	1.5	5186	6.342E-04	1.202E-03	2.681E-04	5.082E-04	9.283E-06	1.760E-05	3.568E-04	6.763E-04	16.3	92
75% Loose Spiral-Helical Coil (1")	5	6/3/11 11:30 AM	23.0	58.4	60.0	152.4	2.6	0.8	4.1	1.2	8.393	0.530	92.9	33.8	88.3	31.3	79.1	26.2	1.6	5670	5.846E-04	1.108E-03	2.681E-04	5.083E-04	9.278E-06	1.759E-05	3.072E-04	5.824E-04	18.9	107
75% Loose Spiral-Helical Coil (1")	6	6/3/11 11:50 AM	23.0	58.4	60.0	152.4	2.6	0.8	4.1	1.2	8.365	0.528	93.7	34.3	89.0	31.6	79.2	26.2	1.6	5776	6.057E-04	1.148E-03	2.684E-04	5.088E-04	9.265E-06	1.756E-05	3.281E-04	6.219E-04	17.7	101
75% Loose Spiral-Helical Coil (1")	7	6/3/11 12:07 PM	23.0	58.4	60.0	152.4	2.6	0.8	4.1	1.2	8.393	0.530	94.4	34.7	89.1	31.7	79.4	26.3	1.8	6463	5.524E-04	1.047E-03	2.684E-04	5.088E-04	9.214E-06	1.747E-05	2.474E-04	5.208E-04	21.1	120
75% Loose Spiral-Helical Coil (1")	8	6/3/11 12:27 PM	23.0	58.4	60.0	152.4	2.6	0.8	4.1	1.2	8.362	0.528	95.2	35.1	89.6	32.0	79.8	26.5	1.9	6803	5.343E-04	1.013E-03	2.686E-04	5.091E-04	9.211E-06	1.746E-05	2.565E-04	4.862E-04	22.6	129
75% Loose Spiral-Helical Coil (1")	1	6/3/11 1:04 PM	23.0	58.4	60.0	152.4	2.6	0.8	4.1	1.2	8.391	0.529	86.7	30.4	85.0	29.4	80.1	26.7	0.6	2073	8.105E-04	1.536E-03	2.671E-04	5.063E-04	9.543E-06	1.809E-05	5.339E-04	1.012E-03	10.9	62
75% Loose Spiral-Helical Coil (1")	2	6/3/11 1:30 PM	23.0	58.4	60.0	152.4	2.6	0.8	4.1	1.2	8.361	0.527	91.2	32.9	87.5	30.8	80.4	26.9	1.3	4527	6.681E-04	1.077E-03	2.679E-04	5.078E-04	9.377E-06	1.778E-05	2.908E-04	5.513E-04	20.0	113
75% Loose Spiral-Helical Coil (1")	3	6/3/11 1:53 PM	23.0	58.4	60.0	152.4	2.6	0.8	4.1	1.2	8.368	0.528	93.4	34.1	88.8	31.5	80.6	27.0	1.6	5707	5.304E-04	1.005E-03	2.683E-04	5.086E-04	9.274E-06	1.758E-05	2.528E-04	4.793E-04	23.0	130
75% Loose Spiral-Helical Coil (1")	4	6/3/11 2:09 PM	23.0	58.4	60.0	152.4	2.6	0.8	4.1	1.2	8.352	0.527	94.1	34.5	89.1	31.7	80.5	26.9	1.7	6112	5.243E-04	9.938E-04	2.684E-04	5.088E-04	9.263E-06	1.756E-05	2.664E-04	4.674E-04	23.6	134
75% Loose Spiral-Helical Coil (1")	5	6/3/11 2:35 PM	23.0	58.4	60.0	152.4	2.6	0.8	4.1	1.2	8.358	0.527	95.6	35.3	90.3	32.4	81.0	27.2	1.8	6461	5.358E-04	1.016E-03	2.688E-04	5.096E-04	9.184E-06	1.741E-05	2.578E-04	4.887E-04	22.5	128
75% Loose Spiral-Helical Coil (1")	6	6/3/11 2:53 PM	23.0	58.4	60.0	152.4	2.6	0.8	4.1	1.2	8.343	0.526	96.7	35.9	91.0	32.8	81.3	27.4	2.0	6889	5.274E-04	9.997E-04	2.691E-04	5.101E-04	9.152E-06	1.735E-05	2.491E-04	4.722E-04	23.3	132
75% Loose Spiral-Helical Coil (1")	7	6/3/11 3:08 PM	23.0	58.4	60.0	152.4	2.6	0.8	4.1	1.2	8.339	0.526	97.1	36.2	91.2	32.9	81.3	27.4	2.0	7200	5.133E-04	9.730E-04	2.691E-04	5.102E-04	9.141E-06	1.733E-05	2.350E-04	4.455E-04	24.7	140
75% Loose Spiral-Helical Coil (1")	8	6/3/11 3:27 PM	23.0	58.4	60.0	152.4	2.6	0.8	4.1	1.2	8.318	0.525	97.7	36.5	91.6	33.1	81.3	27.4	2.1	7426	5.160E-04	9.782E-04	2.693E-04	5.105E-04	9.134E-06	1.731E-05	2.376E-04	4.504E-04	24.5	139
75% Loose Spiral-Helical Coil (1")	1	6/6/11 8:26 AM	23.0	58.4	60.0	152.4	2.6	0.8	4.1	1.2	8.379	0.529	87.3	30.7	85.4	29.7	80.6	27.0	0.7	2291	7.338E-04	1.391E-03	2.672E-04	5.066E-04	9.524E-06	1.805E-05	4.570E-04	8.664E-04	12.7	72
75% Loose Spiral-Helical Coil (1")	2	6/6/11 8:57 AM	23.0	58.4	60.0	152.4	2.6	0.8	4.1	1.2	8.361	0.528	91.6	33.1	87.6	30.9	80.7	27.1	1.4	4851	5.264E-04	9.979E-04	2.679E-04	5.079E-04	9.362E-06	1.775E-05	2.491E-04	4.722E-04	23.3	132
75% Loose Spiral-Helical Coil (1")	3	6/6/11 9:22 AM	23.0	58.4	60.0	152.4	2.6	0.8	4.1	1.2	8.347	0.527	93.6	34.2	88.6	31.4	80.8	27.1	1.7	6079	4.851E-04	9.197E-04	2.682E-04	5.085E-04	9.294E-06	1.762E-05	2.076E-04	3.936E-04	28.0	159
75% Loose Spiral-Helical Coil (1")	4	6/6/11 9:47 AM	23.0	58.4	60.0	152.4	2.6	0.8	4.1	1.2	8.343	0.526	94.6	34.8	89.2	31.8	81.0	27.2	1.9	6543	4.763E-04	9.029E-04	2.684E-04	5.089						

Test Description	Set Point	Date & Time	<i>H</i>		<i>C_{minor}</i>		<i>D_{cj}</i>		<i>D_{cD}</i>		<i>V_{cj}</i>		<i>T_{cjin}</i>		<i>T_{cjout}</i>		<i>T_p</i>		<i>Q_c</i>		<i>R_c</i>		<i>R_t</i>		<i>R_i</i>		<i>R_o</i>		<i>h_o</i>	
	1-8		in	cm	ft	m	ft	m	ft	m	GPM	L/s	°F	°C	°F	°C	°F	°C	Tons	W	hr-°F/Btu	K/W	hr-°F/Btu	K/W	hr-°F/Btu	K/W	hr-°F/Btu	K/W	Btu/hr-ft²-°F	W/m²-K
50% Loose Spiral-Helical Coil (1.25")	1	6/7/11 10:10 AM	13.0	33.0	55.0	139.7	4.0	1.2	6.0	1.8	9.788	0.618	87.2	30.7	83.4	28.6	78.6	25.9	1.5	5397	3.552E-04	6.173E-04	2.653E-04	5.030E-04	1.042E-05	1.976E-05	7.939E-05	1.505E-04	58.0	329
50% Loose Spiral-Helical Coil (1.25")	2	6/7/11 10:36 AM	13.0	33.0	55.0	139.7	4.0	1.2	6.0	1.8	9.793	0.618	91.0	32.8	85.7	29.8	79.2	26.2	2.2	7608	3.427E-04	6.497E-04	2.660E-04	5.043E-04	1.023E-05	1.940E-05	6.646E-05	1.260E-04	69.3	393
50% Loose Spiral-Helical Coil (1.25")	3	6/7/11 11:14 AM	13.0	33.0	55.0	139.7	4.0	1.2	6.0	1.8	9.774	0.617	93.5	34.1	87.4	30.8	78.3	25.7	2.5	8653	3.028E-04	7.635E-04	2.666E-04	5.054E-04	1.012E-05	1.919E-05	1.261E-04	2.390E-04	36.5	207
50% Loose Spiral-Helical Coil (1.25")	4	6/7/11 11:30 AM	13.0	33.0	55.0	139.7	4.0	1.2	6.0	1.8	9.768	0.616	94.2	34.5	87.9	31.1	77.4	25.2	2.5	8901	3.396E-04	8.334E-04	2.668E-04	5.057E-04	1.009E-05	1.913E-05	1.628E-04	3.085E-04	28.3	161
50% Loose Spiral-Helical Coil (1.25")	5	6/7/11 11:49 AM	13.0	33.0	55.0	139.7	4.0	1.2	6.0	1.8	9.767	0.616	94.9	34.9	88.3	31.3	78.2	25.7	2.6	9284	4.149E-04	7.865E-04	2.669E-04	5.059E-04	1.006E-05	1.907E-05	1.379E-04	2.615E-04	33.4	189
50% Loose Spiral-Helical Coil (1.25")	6	6/7/11 12:10 PM	13.0	33.0	55.0	139.7	4.0	1.2	6.0	1.8	9.743	0.615	95.6	35.3	88.9	31.6	77.1	25.0	2.7	9568	4.580E-04	8.682E-04	2.671E-04	5.063E-04	1.004E-05	1.904E-05	1.809E-04	3.429E-04	25.4	144
50% Loose Spiral-Helical Coil (1.25")	7	6/7/11 12:26 PM	13.0	33.0	55.0	139.7	4.0	1.2	6.0	1.8	9.716	0.613	96.4	35.8	89.4	31.9	77.6	25.3	2.8	9850	4.476E-04	8.485E-04	2.672E-04	5.066E-04	1.003E-05	1.902E-05	1.703E-04	3.229E-04	27.0	153
50% Loose Spiral-Helical Coil (1.25")	8	6/7/11 12:46 PM	13.0	33.0	55.0	139.7	4.0	1.2	6.0	1.8	9.712	0.613	96.9	36.1	89.8	32.1	78.1	25.6	2.8	9993	4.394E-04	8.330E-04	2.674E-04	5.069E-04	1.001E-05	1.897E-05	1.620E-04	3.071E-04	28.4	161
50% Loose Spiral-Helical Coil (1.25")	1	6/7/11 1:31 PM	13.0	33.0	55.0	139.7	4.0	1.2	6.0	1.8	9.830	0.620	89.2	31.8	85.6	29.8	78.6	25.9	1.5	5152	4.962E-04	9.406E-04	2.662E-04	5.045E-04	1.025E-05	1.944E-05	2.198E-04	4.167E-04	20.9	119
50% Loose Spiral-Helical Coil (1.25")	2	6/7/11 2:01 PM	13.0	33.0	55.0	139.7	4.0	1.2	6.0	1.8	9.805	0.619	92.9	33.9	87.8	31.0	78.4	25.8	2.1	7382	4.683E-04	8.877E-04	2.668E-04	5.058E-04	1.010E-05	1.915E-05	1.914E-04	3.628E-04	24.0	137
50% Loose Spiral-Helical Coil (1.25")	3	6/7/11 2:23 PM	13.0	33.0	55.0	139.7	4.0	1.2	6.0	1.8	9.769	0.616	94.7	34.8	88.8	31.6	78.8	26.0	2.4	8369	4.478E-04	8.489E-04	2.671E-04	5.064E-04	1.005E-05	1.905E-05	1.706E-04	3.235E-04	27.0	153
50% Loose Spiral-Helical Coil (1.25")	4	6/7/11 2:40 PM	13.0	33.0	55.0	139.7	4.0	1.2	6.0	1.8	9.745	0.615	95.4	35.2	89.2	31.8	78.4	25.8	2.5	8814	4.532E-04	8.590E-04	2.672E-04	5.066E-04	1.004E-05	1.904E-05	1.759E-04	3.334E-04	26.2	149
50% Loose Spiral-Helical Coil (1.25")	5	6/7/11 3:03 PM	13.0	33.0	55.0	139.7	4.0	1.2	6.0	1.8	9.745	0.615	96.1	35.6	89.6	32.0	78.6	25.9	2.6	9203	4.434E-04	8.405E-04	2.673E-04	5.068E-04	1.001E-05	1.898E-05	1.660E-04	3.147E-04	27.7	157
50% Loose Spiral-Helical Coil (1.25")	6	6/7/11 3:26 PM	13.0	33.0	55.0	139.7	4.0	1.2	6.0	1.8	9.732	0.614	96.7	35.9	89.8	32.1	78.2	25.6	2.8	9705	4.483E-04	8.499E-04	2.674E-04	5.069E-04	1.001E-05	1.895E-05	1.709E-04	3.240E-04	26.9	153
50% Loose Spiral-Helical Coil (1.25")	7	6/7/11 3:48 PM	13.0	33.0	55.0	139.7	4.0	1.2	6.0	1.8	9.714	0.613	97.6	36.4	90.3	32.4	78.1	25.6	2.9	10268	4.459E-04	8.452E-04	2.676E-04	5.072E-04	9.974E-06	1.891E-05	1.683E-04	3.191E-04	27.3	155
50% Loose Spiral-Helical Coil (1.25")	8	6/7/11 4:36 PM	13.0	33.0	55.0	139.7	4.0	1.2	6.0	1.8	9.741	0.615	97.8	36.5	90.2	32.3	78.0	25.6	3.0	10698	4.294E-04	8.140E-04	2.675E-04	5.071E-04	9.948E-06	1.886E-05	1.520E-04	2.881E-04	30.3	172
50% Loose Spiral-Helical Coil (1.25")	1	6/8/11 9:31 AM	13.0	33.0	55.0	139.7	4.0	1.2	6.0	1.8	9.889	0.624	85.7	29.8	82.5	28.1	79.7	26.5	1.3	4574	2.675E-04	5.070E-04	2.651E-04	5.025E-04	1.041E-05	1.973E-05	-7.999E-06	-1.516E-05	-575.3	-3267
50% Loose Spiral-Helical Coil (1.25")	2	6/8/11 9:59 AM	13.0	33.0	55.0	139.7	4.0	1.2	6.0	1.8	9.869	0.623	89.8	32.1	84.9	29.4	79.8	26.6	2.0	6998	3.026E-04	5.736E-04	2.658E-04	5.038E-04	1.022E-05	1.938E-05	2.660E-05	5.042E-05	173.0	982
50% Loose Spiral-Helical Coil (1.25")	3	6/8/11 10:21 AM	13.0	33.0	55.0	139.7	4.0	1.2	6.0	1.8	9.854	0.622	91.6	33.1	86.0	30.0	80.0	26.7	2.3	8026	3.100E-04	5.876E-04	2.661E-04	5.045E-04	1.015E-05	1.924E-05	3.372E-05	6.393E-05	136.5	775
50% Loose Spiral-Helical Coil (1.25")	4	6/8/11 10:40 AM	13.0	33.0	55.0	139.7	4.0	1.2	6.0	1.8	9.833	0.620	92.5	33.6	86.6	30.3	80.2	26.8	2.4	8451	3.135E-04	5.943E-04	2.663E-04	5.048E-04	1.012E-05	1.919E-05	3.708E-05	7.028E-05	124.1	705
50% Loose Spiral-Helical Coil (1.25")	5	6/8/11 10:55 AM	13.0	33.0	55.0	139.7	4.0	1.2	6.0	1.8	9.818	0.619	93.3	34.0	87.2	30.6	80.3	26.9	2.5	8708	3.215E-04	6.095E-04	2.665E-04	5.052E-04	1.010E-05	1.914E-05	4.495E-05	8.521E-05	102.4	581
50% Loose Spiral-Helical Coil (1.25")	6	6/8/11 11:12 AM	13.0	33.0	55.0	139.7	4.0	1.2	6.0	1.8	9.824	0.620	94.1	34.5	87.8	31.0	80.4	26.9	2.5	8894	3.367E-04	6.382E-04	2.667E-04	5.056E-04	1.005E-05	1.905E-05	5.988E-05	1.135E-04	76.9	436
50% Loose Spiral-Helical Coil (1.25")	7	6/8/11 11:28 AM	13.0	33.0	55.0	139.7	4.0	1.2	6.0	1.8	9.822	0.620	94.9	34.9	88.4	31.3	80.3	26.9	2.6	9291	3.464E-04	6.567E-04	2.669E-04	5.059E-04	1.001E-05	1.898E-05	6.953E-05	1.318E-04	66.2	376
50% Loose Spiral-Helical Coil (1.25")	8	6/8/11 11:42 AM	13.0	33.0	55.0	139.7	4.0	1.2	6.0	1.8	9.793	0.618	95.4	35.2	88.7	31.5	80.0	26.7	2.7	9447	3.649E-04	6.917E-04	2.670E-04	5.062E-04	1.001E-05	1.898E-05	8.788E-05	1.666E-04	52.4	297
75% Loose Spiral-Helical Coil (1.25")	1	6/8/11 3:42 PM	21.0	53.3	64.0	162.6	4.0	1.2	6.0	1.8	9.693	0.612	94.0	34.5	88.2	31.2	84.1	28.9	2.3	8228	2.342E-04	4.439E-04	2.669E-04	5.059E-04	1.016E-05	1.925E-05	-4.284E-05	-8.121E-05	-107.4	-610
75% Loose Spiral-Helical Coil (1.25")	2	6/8/11 4:08 PM	21.0	53.3	64.0	162.6	4.0	1.2	6.0	1.8	9.645	0.609	97.7	36.5	90.2	32.3	84.1	29.0	3.0	10479	2.597E-04	4.924E-04	2.675E-04	5.070E-04	1.004E-05	1.902E-05	-1.778E-05	-3.370E-05	-258.9	-1470
75% Loose Spiral-Helical Coil (1.25")	3	6/8/11 4:29 PM	21.0	53.3	64.0	162.6	4.0	1.2	6.0	1.8	9.613	0.607	99.2	37.4	91.1	32.9	83.7	28.7	3.2	11332	2.846E-04	5.395E-04	2.678E-04	5.076E-04	9.993E-06	1.894E-05	6.808E-06	1.291E-05	675.9	3838
75% Loose Spiral-Helical Coil (1.25")	4	6/8/11 4:45 PM	21.0	53.3	64.0	162.6	4.0	1.2	6.0	1.8	9.597	0.605	99.8	37.6	91.4	33.0	83.6	28.7	3.3	11669	2.879E-04	5.457E-04	2.679E-04	5.078E-04	9.985E-06	1.893E-05	1.001E-05	1.898E-05	459.7	2610
75% Loose Spiral-Helical Coil (1.25")	5	6/8/11 5:01 PM	21.0	53.3	64.0	162.6	4.0	1.2	6.0	1.8	9.593	0.605	100.2	37.9	91.7	33.1	83.8	28.8	3.4	11902	2.849E-04	5.400E-04	2.679E-04	5.079E-04	9.970E-06	1.890E-05	6.970E-06	1.321E-05	660.3	3749
75% Loose Spiral-Helical Coil (1.25")	6	6/8/11 5:18 PM	21.0	53.3	64.0	162.6	4.0	1.2	6.0	1.8	9.625	0.607	100.8	38.2	92.1	33.4	83.5	28.6	3.5	12225	2.966E-04	5.623E-04	2.681E-04	5.081E-04	9.914E-06	1.879E-05	1.866E-05	3.537E-05	246.7	1401
75% Loose Spiral-Helical Coil (1.25")	7	6/8/11 5:33 PM	21.0	53.3	64.0	162.6	4.0	1.2	6.0	1.8	9.628	0.607	101.5	38.6	92.5	33.6	84.4	29.1	3.6	12641	2.777E-04	5.264E-04	2.682E-04	5.084E-04	9.881E-06	1.873E-05	-3.468E-07	-6.574E-07	-13269.9	-75350
75% Loose Spiral-Helical Coil (1.25")	8	6/8/11 5:48 PM	21.0	53.3	64.0	162.6	4.0	1.2	6.0	1.8	9.601	0.606	101.7	38.7	92.5	33.6	82.7	28.2	3.6	12807	3.174E-04	6.017E-04	2.682E-04	5.084E-04	9.897E-06	1.876E-05	3.931E-05	7.452E-05	117.1	665
75% Loose Spiral-Helical Coil (1.25")	1	6/9/11 1:30 PM	21.0	53.3	64.0	162.6	4.0	1.2	6.0	1.8	9.801	0.618	90.7	32.6	86.4	30.2	82.4	28.0	1.7	6142	2.788E-04	5.285E-04	2.663E-04	5.049E-04	1.021E-05	1.936E-05	2.236E-06	4.238E-06	2058.6	11689
75% Loose Spiral-Helical Coil (1.25")	2	6/9/11 1:57 PM	21.0	53.3	64.0	162.6	4.0	1.2	6.0	1.8	9.755	0.615	94.3	34.6	88.4	31.3	82.4	28.0	2.4	8399	2.992E-04	5.671E-04	2.669E-04	5.060E-04	1.009E-05	1.912E-05	2.216E-05	4.200E-05	207.7	1179
75% Loose Spiral-Helical Coil (1.25")	3	6/9/11 2:19 PM	21.0	53.3	64.0	162.6	4.0	1.2	6.0	1.8	9.720	0.613																		

APPENDIX C

Flat-Spiral Experimental Data & Reference Calculations

Test Description	Set Point	Date & Time	Δx		$D_{c,i}$		$D_{c,o}$		$V_{c,i}$		$T_{c,in}$		$T_{c,out}$		T_p		Q_c		R_c		R_t		R_i		R_o		h_o	
	1-8		in	cm	ft	m	ft	m	GPM	L/s	°F	°C	°F	°C	°F	°C	Tons	W	hr-°F/Btu	K/W	hr-°F/Btu	K/W	hr-°F/Btu	K/W	hr-°F/Btu	K/W	Btu/hr-ft ² -°F	W/m ² -K
Flat-Spiral Coil (3/4") (Test 1)	1	9/3/10 12:00 PM	2.0	5.1	3.0	0.9	11.5	3.5	3.517	0.222	85.2	29.6	81.5	27.5	79.3	26.3	0.5	1892	5.843E-04	1.108E-03	3.168E-04	6.006E-04	2.035E-05	3.858E-05	2.471E-04	4.684E-04	35.4	201
Flat-Spiral Coil (3/4") (Test 1)	2	9/3/10 12:30 PM	2.0	5.1	3.0	0.9	11.5	3.5	3.510	0.221	88.0	31.1	82.4	28.0	79.5	26.4	0.8	2853	5.331E-04	1.011E-03	3.173E-04	6.015E-04	2.016E-05	3.823E-05	1.957E-04	3.709E-04	44.7	254
Flat-Spiral Coil (3/4") (Test 1)	3	9/3/10 1:00 PM	2.0	5.1	3.0	0.9	11.5	3.5	3.422	0.216	88.9	31.6	82.4	28.0	79.1	26.2	0.9	3274	5.288E-04	1.002E-03	3.174E-04	6.016E-04	2.054E-05	3.895E-05	1.909E-04	3.619E-04	45.8	260
Flat-Spiral Coil (3/4") (Test 1)	4	9/3/10 1:30 PM	2.0	5.1	3.0	0.9	11.5	3.5	3.549	0.224	90.0	32.2	83.0	28.3	79.6	26.4	1.0	3633	5.079E-04	9.628E-04	3.176E-04	6.021E-04	1.982E-05	3.757E-05	1.705E-04	3.231E-04	51.3	291
Flat-Spiral Coil (3/4") (Test 1)	5	9/3/10 2:00 PM	2.0	5.1	3.0	0.9	11.5	3.5	3.415	0.215	91.4	33.0	83.5	28.6	79.7	26.5	1.1	3912	5.303E-04	1.005E-03	3.180E-04	6.027E-04	2.036E-05	3.859E-05	1.920E-04	3.640E-04	45.5	259
Flat-Spiral Coil (3/4") (Test 1)	6	9/3/10 2:30 PM	2.0	5.1	3.0	0.9	11.5	3.5	3.504	0.221	92.1	33.4	83.6	28.7	79.5	26.4	1.2	4332	5.159E-04	9.779E-04	3.180E-04	6.028E-04	1.987E-05	3.767E-05	1.780E-04	3.374E-04	49.1	279
Flat-Spiral Coil (3/4") (Test 1)	7	9/3/10 3:00 PM	2.0	5.1	3.0	0.9	11.5	3.5	3.536	0.223	93.3	34.0	84.0	28.9	79.6	26.5	1.4	4782	4.973E-04	9.427E-04	3.182E-04	6.032E-04	1.963E-05	3.721E-05	1.595E-04	3.023E-04	54.8	311
Flat-Spiral Coil (3/4") (Test 1)	8	9/3/10 3:30 PM	2.0	5.1	3.0	0.9	11.5	3.5	3.532	0.223	93.9	34.4	84.2	29.0	79.7	26.5	1.4	5003	4.961E-04	9.404E-04	3.183E-04	6.034E-04	1.960E-05	3.716E-05	1.582E-04	2.999E-04	55.3	314
Flat-Spiral Coil (3/4") (Test 2)	1	9/14/10 8:00 AM	2.0	5.1	3.0	0.9	11.5	3.5	3.226	0.204	81.2	27.4	78.8	26.0	77.3	25.2	0.3	1135	6.571E-04	1.246E-03	3.156E-04	5.983E-04	2.236E-05	4.239E-05	3.191E-04	6.048E-04	27.4	156
Flat-Spiral Coil (3/4") (Test 2)	2	9/14/10 8:30 AM	2.0	5.1	3.0	0.9	11.5	3.5	3.129	0.197	83.7	28.7	79.6	26.4	77.2	25.1	0.5	1896	6.338E-04	1.202E-03	3.161E-04	5.992E-04	2.272E-05	4.307E-05	2.950E-04	5.593E-04	29.6	168
Flat-Spiral Coil (3/4") (Test 2)	3	9/14/10 9:00 AM	2.0	5.1	3.0	0.9	11.5	3.5	3.032	0.191	83.9	28.9	79.8	26.5	77.2	25.1	0.5	1857	6.883E-04	1.305E-03	3.162E-04	5.994E-04	2.331E-05	4.418E-05	3.488E-04	6.613E-04	25.1	142
Flat-Spiral Coil (3/4") (Test 2)	4	9/14/10 9:30 AM	2.0	5.1	3.0	0.9	11.5	3.5	3.451	0.218	84.3	29.1	79.5	26.4	77.1	25.1	0.7	2412	5.307E-04	1.006E-03	3.160E-04	5.991E-04	2.087E-05	3.956E-05	1.938E-04	3.673E-04	45.1	256
Flat-Spiral Coil (3/4") (Test 2)	5	9/14/10 10:00 AM	2.0	5.1	3.0	0.9	11.5	3.5	3.332	0.210	86.2	30.1	80.1	26.7	77.2	25.1	0.9	3004	5.198E-04	9.853E-04	3.164E-04	5.997E-04	2.134E-05	4.045E-05	1.821E-04	3.451E-04	48.0	273
Flat-Spiral Coil (3/4") (Test 2)	6	9/14/10 10:30 AM	2.0	5.1	3.0	0.9	11.5	3.5	3.178	0.200	87.6	30.9	80.6	27.0	77.3	25.2	0.9	3225	5.601E-04	1.062E-03	3.167E-04	6.004E-04	2.208E-05	4.186E-05	2.213E-04	4.195E-04	39.5	224
Flat-Spiral Coil (3/4") (Test 2)	7	9/14/10 11:00 AM	2.0	5.1	3.0	0.9	11.5	3.5	3.086	0.195	88.4	31.3	80.9	27.1	77.3	25.1	1.0	3404	5.768E-04	1.093E-03	3.169E-04	6.007E-04	2.257E-05	4.278E-05	2.374E-04	4.499E-04	36.8	209
Flat-Spiral Coil (3/4") (Test 2)	8	9/14/10 11:30 AM	2.0	5.1	3.0	0.9	11.5	3.5	3.067	0.193	89.9	32.1	81.4	27.5	77.5	25.3	1.1	3774	5.717E-04	1.084E-03	3.172E-04	6.013E-04	2.255E-05	4.275E-05	2.320E-04	4.398E-04	37.7	214
Flat-Spiral Coil (3/4") (Test 3)	1	9/16/10 6:00 PM	2.0	5.1	3.0	0.9	11.5	3.5	3.263	0.206	84.1	28.9	81.6	27.5	79.4	26.3	0.3	1180	8.117E-04	1.539E-03	3.168E-04	6.005E-04	2.177E-05	4.127E-05	4.731E-04	8.969E-04	18.5	105
Flat-Spiral Coil (3/4") (Test 3)	2	9/16/10 6:30 PM	2.0	5.1	3.0	0.9	11.5	3.5	3.218	0.203	86.2	30.1	82.5	28.0	79.4	26.4	0.5	1781	7.651E-04	1.450E-03	3.173E-04	6.014E-04	2.182E-05	4.136E-05	4.260E-04	8.075E-04	20.5	117
Flat-Spiral Coil (3/4") (Test 3)	3	9/16/10 7:00 PM	2.0	5.1	3.0	0.9	11.5	3.5	3.207	0.202	87.0	30.6	82.6	28.1	79.4	26.4	0.6	2055	7.257E-04	1.376E-03	3.174E-04	6.017E-04	2.182E-05	4.136E-05	3.865E-04	7.327E-04	22.6	128
Flat-Spiral Coil (3/4") (Test 3)	4	9/16/10 7:30 PM	2.0	5.1	3.0	0.9	11.5	3.5	3.209	0.202	87.9	31.1	82.8	28.2	79.3	26.3	0.7	2377	6.982E-04	1.323E-03	3.175E-04	6.019E-04	2.174E-05	4.121E-05	3.589E-04	6.803E-04	24.4	138
Flat-Spiral Coil (3/4") (Test 3)	5	9/16/10 8:00 PM	2.0	5.1	3.0	0.9	11.5	3.5	3.157	0.199	89.1	31.7	83.3	28.5	79.3	26.3	0.8	2679	7.157E-04	1.357E-03	3.178E-04	6.024E-04	2.193E-05	4.157E-05	3.760E-04	7.127E-04	23.3	132
Flat-Spiral Coil (3/4") (Test 3)	6	9/16/10 8:30 PM	2.0	5.1	3.0	0.9	11.5	3.5	3.176	0.200	90.2	32.3	83.7	28.7	79.3	26.3	0.9	3004	6.989E-04	1.325E-03	3.180E-04	6.028E-04	2.172E-05	4.118E-05	3.591E-04	6.808E-04	24.3	138
Flat-Spiral Coil (3/4") (Test 3)	7	9/16/10 9:00 PM	2.0	5.1	3.0	0.9	11.5	3.5	3.165	0.200	91.0	32.8	84.0	28.9	79.3	26.3	0.9	3223	6.994E-04	1.326E-03	3.182E-04	6.031E-04	2.172E-05	4.116E-05	3.595E-04	6.815E-04	24.3	138
Flat-Spiral Coil (3/4") (Test 3)	8	9/16/10 9:30 PM	2.0	5.1	3.0	0.9	11.5	3.5	3.184	0.201	91.6	33.1	84.1	28.9	79.2	26.2	1.0	3500	6.802E-04	1.289E-03	3.182E-04	6.033E-04	2.156E-05	4.087E-05	3.404E-04	6.453E-04	25.7	146

*Testing times are approximate

APPENDIX D

Vertical and Horizontal Slinky Experimental Data & Reference Calculations

Test Description	Set Point	Date & Time	Pitch		D _{loop}	V _{cl}		T _{cin}		T _{cout}		T _p	Q _c	R _c		R _t		R _i		R _o		h _o				
			ft			GPM		°F		°F				hr-°F/Btu		K/W		hr-°F/Btu		K/W		hr-°F/Btu		K/W		Btu/hr-ft ² -°F
			cm	m	L/s																					
10" Pitch Vertical Slinky	1	9/30/10 6:00 PM	0.8	25.4	3.0	0.9	3.641	0.230	75.7	24.3	73.1	22.8	71.8	22.1	0.4	1393	4.956E-04	9.395E-04	2.607E-04	4.941E-04	1.243E-05	2.356E-05	2.225E-04	4.218E-04	32.7	186
10" Pitch Vertical Slinky	2	9/30/10 6:30 PM	0.8	25.4	3.0	0.9	3.557	0.224	78.2	25.7	73.8	23.2	71.8	22.1	0.7	2295	4.818E-04	9.134E-04	2.610E-04	4.948E-04	1.255E-05	2.378E-05	2.083E-04	3.948E-04	34.9	198
10" Pitch Vertical Slinky	3	9/30/10 7:00 PM	0.8	25.4	3.0	0.9	3.499	0.221	79.2	26.2	74.1	23.4	71.8	22.1	0.7	2616	4.855E-04	9.204E-04	2.612E-04	4.951E-04	1.267E-05	2.402E-05	2.117E-04	4.013E-04	34.4	195
10" Pitch Vertical Slinky	4	9/30/10 7:30 PM	0.8	25.4	3.0	0.9	3.509	0.221	80.6	27.0	74.5	23.6	71.9	22.2	0.9	3085	4.824E-04	9.145E-04	2.614E-04	4.955E-04	1.256E-05	2.382E-05	2.085E-04	3.952E-04	34.9	198
10" Pitch Vertical Slinky	5	9/30/10 8:00 PM	0.8	25.4	3.0	0.9	3.527	0.223	81.6	27.5	74.7	23.7	72.0	22.2	1.0	3540	4.511E-04	8.551E-04	2.615E-04	4.957E-04	1.247E-05	2.363E-05	1.771E-04	3.358E-04	41.1	233
10" Pitch Vertical Slinky	6	9/30/10 8:30 PM	0.8	25.4	3.0	0.9	3.505	0.221	82.5	28.0	74.8	23.8	72.0	22.2	1.1	3896	4.365E-04	8.275E-04	2.616E-04	4.959E-04	1.249E-05	2.368E-05	1.624E-04	3.079E-04	44.8	254
10" Pitch Vertical Slinky	7	9/30/10 9:00 PM	0.8	25.4	3.0	0.9	3.539	0.223	83.7	28.7	75.3	24.0	72.1	22.3	1.2	4331	4.368E-04	8.280E-04	2.618E-04	4.963E-04	1.232E-05	2.336E-05	1.627E-04	3.084E-04	44.7	254
10" Pitch Vertical Slinky	8	9/30/10 9:30 PM	0.8	25.4	3.0	0.9	3.534	0.223	84.6	29.2	75.6	24.2	72.3	22.4	1.3	4620	4.353E-04	8.251E-04	2.620E-04	4.966E-04	1.229E-05	2.330E-05	1.610E-04	3.053E-04	45.2	257
10" Pitch Vertical Slinky	1	10/5/10 12:00 PM	0.8	25.4	3.0	0.9	4.461	0.281	69.4	20.8	67.4	19.6	66.0	18.9	0.4	1360	4.889E-04	9.268E-04	2.586E-04	4.903E-04	1.089E-05	2.064E-05	2.194E-04	4.158E-04	33.2	188
10" Pitch Vertical Slinky	2	10/5/10 12:30 PM	0.8	25.4	3.0	0.9	4.403	0.278	71.8	22.1	68.3	20.2	66.1	19.0	0.6	2231	4.771E-04	9.044E-04	2.590E-04	4.910E-04	1.089E-05	2.064E-05	2.072E-04	3.927E-04	35.1	199
10" Pitch Vertical Slinky	3	10/5/10 1:00 PM	0.8	25.4	3.0	0.9	4.515	0.285	72.8	22.7	68.8	20.5	66.3	19.1	0.8	2656	4.638E-04	8.792E-04	2.592E-04	4.914E-04	1.060E-05	2.010E-05	1.940E-04	3.677E-04	37.5	213
10" Pitch Vertical Slinky	4	10/5/10 1:30 PM	0.8	25.4	3.0	0.9	4.562	0.288	73.8	23.2	69.3	20.7	66.5	19.2	0.9	3034	4.562E-04	8.647E-04	2.594E-04	4.917E-04	1.046E-05	1.982E-05	1.863E-04	3.532E-04	39.1	222
10" Pitch Vertical Slinky	5	10/5/10 2:00 PM	0.8	25.4	3.0	0.9	4.598	0.290	75.2	24.0	69.9	21.1	66.7	19.3	1.0	3549	4.495E-04	8.520E-04	2.597E-04	4.922E-04	1.032E-05	1.956E-05	1.795E-04	3.403E-04	40.5	230
10" Pitch Vertical Slinky	6	10/5/10 2:30 PM	0.8	25.4	3.0	0.9	4.534	0.286	76.3	24.6	70.5	21.4	66.9	19.4	1.1	3893	4.514E-04	8.556E-04	2.599E-04	4.926E-04	1.038E-05	1.968E-05	1.811E-04	3.433E-04	40.2	228
10" Pitch Vertical Slinky	7	10/5/10 3:00 PM	0.8	25.4	3.0	0.9	4.548	0.287	77.4	25.2	71.0	21.6	67.0	19.4	1.2	4251	4.623E-04	8.763E-04	2.601E-04	4.930E-04	1.031E-05	1.953E-05	1.919E-04	3.637E-04	37.9	215
10" Pitch Vertical Slinky	8	10/5/10 3:30 PM	0.8	25.4	3.0	0.9	4.543	0.287	78.0	25.6	71.2	21.8	67.1	19.5	1.3	4544	4.465E-04	8.464E-04	2.602E-04	4.932E-04	1.028E-05	1.949E-05	1.761E-04	3.338E-04	41.3	235
10" Pitch Horizontal Slinky	1	10/11/10 12:00 PM	0.8	25.4	3.0	0.9	4.473	0.282	71.8	22.1	69.7	21.0	68.2	20.1	0.4	1353	5.208E-04	9.873E-04	2.594E-04	4.918E-04	1.069E-05	2.027E-05	2.507E-04	4.752E-04	29.0	165
10" Pitch Horizontal Slinky	2	10/11/10 12:30 PM	0.8	25.4	3.0	0.9	4.456	0.281	74.2	23.5	70.8	21.6	68.2	20.1	0.6	2205	5.425E-04	1.028E-03	2.599E-04	4.927E-04	1.060E-05	2.009E-05	2.720E-04	5.155E-04	26.8	152
10" Pitch Horizontal Slinky	3	10/11/10 1:00 PM	0.8	25.4	3.0	0.9	4.459	0.281	75.3	24.1	71.4	21.9	68.4	20.2	0.7	2567	5.366E-04	1.017E-03	2.601E-04	4.931E-04	1.053E-05	1.997E-05	2.660E-04	5.042E-04	27.4	155
10" Pitch Horizontal Slinky	4	10/11/10 1:30 PM	0.8	25.4	3.0	0.9	4.455	0.281	76.5	24.7	71.9	22.2	68.5	20.3	0.8	2967	5.339E-04	1.012E-03	2.603E-04	4.935E-04	1.048E-05	1.987E-05	2.631E-04	4.987E-04	27.7	157
10" Pitch Horizontal Slinky	5	10/11/10 2:00 PM	0.8	25.4	3.0	0.9	4.453	0.281	77.5	25.3	72.3	22.4	68.4	20.2	1.0	3370	5.384E-04	1.021E-03	2.605E-04	4.938E-04	1.044E-05	1.979E-05	2.675E-04	5.070E-04	27.2	154
10" Pitch Horizontal Slinky	6	10/11/10 2:30 PM	0.8	25.4	3.0	0.9	4.485	0.283	78.5	25.8	72.8	22.7	68.5	20.3	1.1	3706	5.354E-04	1.015E-03	2.607E-04	4.942E-04	1.032E-05	1.957E-05	2.644E-04	5.012E-04	27.5	156
10" Pitch Horizontal Slinky	7	10/11/10 3:00 PM	0.8	25.4	3.0	0.9	4.504	0.284	79.5	26.4	73.4	23.0	68.6	20.3	1.2	4071	5.340E-04	1.012E-03	2.609E-04	4.946E-04	1.024E-05	1.940E-05	2.629E-04	4.984E-04	27.7	157
10" Pitch Horizontal Slinky	8	10/11/10 3:30 PM	0.8	25.4	3.0	0.9	4.503	0.284	80.1	26.7	73.6	23.1	68.9	20.5	1.2	4281	5.145E-04	9.754E-04	2.610E-04	4.948E-04	1.021E-05	1.935E-05	2.433E-04	4.613E-04	29.9	170
10" Pitch Horizontal Slinky	1	10/11/10 6:00 PM	0.8	25.4	3.0	0.9	4.536	0.286	72.9	22.7	71.1	21.7	69.4	20.8	0.3	1207	5.953E-04	1.128E-03	2.599E-04	4.927E-04	1.048E-05	1.986E-05	3.249E-04	6.159E-04	22.4	127
10" Pitch Horizontal Slinky	2	10/11/10 6:30 PM	0.8	25.4	3.0	0.9	4.532	0.286	75.1	23.9	72.0	22.2	69.6	20.9	0.6	2017	5.470E-04	1.037E-03	2.603E-04	4.934E-04	1.038E-05	1.968E-05	2.763E-04	5.238E-04	26.3	150
10" Pitch Horizontal Slinky	3	10/11/10 7:00 PM	0.8	25.4	3.0	0.9	4.532	0.286	75.8	24.3	72.3	22.4	69.3	20.7	0.7	2338	5.668E-04	1.075E-03	2.604E-04	4.936E-04	1.034E-05	1.961E-05	2.961E-04	5.613E-04	24.6	140
10" Pitch Horizontal Slinky	4	10/11/10 7:30 PM	0.8	25.4	3.0	0.9	4.552	0.287	76.8	24.9	72.7	22.6	69.3	20.7	0.8	2684	5.629E-04	1.067E-03	2.606E-04	4.939E-04	1.026E-05	1.944E-05	2.920E-04	5.536E-04	24.9	141
10" Pitch Horizontal Slinky	5	10/11/10 8:00 PM	0.8	25.4	3.0	0.9	4.565	0.288	77.8	25.4	73.1	22.8	69.5	20.8	0.9	3097	5.364E-04	1.017E-03	2.607E-04	4.942E-04	1.019E-05	1.931E-05	2.654E-04	5.032E-04	27.4	156
10" Pitch Horizontal Slinky	6	10/11/10 8:30 PM	0.8	25.4	3.0	0.9	4.548	0.287	78.5	25.8	73.3	22.9	69.2	20.7	1.0	3429	5.393E-04	1.022E-03	2.608E-04	4.944E-04	1.019E-05	1.931E-05	2.683E-04	5.086E-04	27.1	154
10" Pitch Horizontal Slinky	7	10/11/10 9:00 PM	0.8	25.4	3.0	0.9	4.546	0.287	79.1	26.1	73.5	23.1	69.3	20.7	1.0	3680	5.296E-04	1.004E-03	2.609E-04	4.946E-04	1.017E-05	1.927E-05	2.586E-04	4.901E-04	28.1	160
10" Pitch Horizontal Slinky	8	10/11/10 9:30 PM	0.8	25.4	3.0	0.9	4.552	0.287	79.6	26.5	73.7	23.2	69.1	20.6	1.1	3933	5.361E-04	1.016E-03	2.610E-04	4.947E-04	1.013E-05	1.920E-05	2.650E-04	5.023E-04	27.5	156
5" Pitch Vertical Slinky	1	10/26/10 12:00 PM	0.8	25.4	3.0	0.9	3.413	0.215	66.4	19.1	64.2	17.9	62.8	17.1	0.3	1095	6.427E-04	1.218E-03	2.576E-04	4.884E-04	1.397E-05	2.649E-05	3.711E-04	7.034E-04	19.6	111
5" Pitch Vertical Slinky	2	10/26/10 12:30 PM	0.8	25.4	3.0	0.9	3.364	0.212	69.0	20.5	64.9	18.3	63.0	17.2	0.6	1973	5.372E-04	1.018E-03	2.580E-04	4.891E-04	1.398E-05	2.651E-05	2.652E-04	5.027E-04	27.4	156
5" Pitch Vertical Slinky	3	10/26/10 1:00 PM	0.8	25.4	3.0	0.9	3.313	0.209	70.0	21.1	65.4	18.6	62.9	17.2	0.6	2208	5.833E-04	1.106E-03	2.582E-04	4.895E-04	1.409E-05	2.672E-05	3.110E-04	5.894E-04	23.4	133
5" Pitch Vertical Slinky	4	10/26/10 1:30 PM	0.8	25.4	3.0	0.9	3.262	0.206	71.1	21.7	65.5	18.6	63.1	17.3	0.8	2652	5.180E-04	9.819E-04	2.583E-04	4.89						

Test Description	Set Point	Date & Time	Pitch		D _{loop}	V _{cl}		T _{cin}		T _{cout}		T _p		Q _c		R _c		R _t		R _i		R _o		h _o		
			ft	cm		ft	m	GPM	L/s	°F	°C	°F	°C	°F	°C	Tons	W	hr-°F/Btu	K/W	hr-°F/Btu	K/W	hr-°F/Btu	K/W	hr-°F/Btu	K/W	Btu/hr-ft ² -°F
15" Pitch Vertical Slinky	1-8																									
15" Pitch Vertical Slinky	1	1/4/11 8:00 AM	0.8	25.4	3.0	0.9	4.116	0.260	48.0	8.9	46.3	8.0	39.8	4.3	0.3	989	2.159E-03	4.092E-03	2.517E-04	4.772E-04	1.371E-05	2.600E-05	1.893E-03	3.589E-03	3.8	22
15" Pitch Vertical Slinky	2	1/4/11 8:30 AM	0.8	25.4	3.0	0.9	4.085	0.258	53.4	11.9	47.7	8.7	39.6	4.2	1.0	3412	9.127E-04	1.730E-03	2.524E-04	4.785E-04	1.343E-05	2.545E-05	6.469E-04	1.226E-03	11.2	64
15" Pitch Vertical Slinky	3	1/4/11 9:00 AM	0.8	25.4	3.0	0.9	4.079	0.257	55.9	13.3	48.3	9.1	39.5	4.2	1.3	4524	7.917E-04	1.501E-03	2.527E-04	4.791E-04	1.327E-05	2.515E-05	5.258E-04	9.966E-04	13.8	79
15" Pitch Vertical Slinky	4	1/4/11 9:30 AM	0.8	25.4	3.0	0.9	4.070	0.257	57.2	14.0	48.7	9.3	39.4	4.1	1.4	5095	7.522E-04	1.426E-03	2.529E-04	4.794E-04	1.321E-05	2.503E-05	4.861E-04	9.215E-04	15.0	85
15" Pitch Vertical Slinky	5	1/4/11 10:00 AM	0.8	25.4	3.0	0.9	4.062	0.256	57.8	14.3	48.7	9.3	39.5	4.2	1.5	5426	7.105E-04	1.347E-03	2.529E-04	4.794E-04	1.320E-05	2.502E-05	4.444E-04	8.424E-04	16.4	93
15" Pitch Vertical Slinky	6	1/4/11 10:30 AM	0.8	25.4	3.0	0.9	4.075	0.257	59.2	15.1	49.3	9.6	39.7	4.3	1.7	5956	6.849E-04	1.298E-03	2.532E-04	4.799E-04	1.306E-05	2.475E-05	4.187E-04	7.937E-04	17.4	99
15" Pitch Vertical Slinky	7	1/4/11 11:00 AM	0.8	25.4	3.0	0.9	4.099	0.259	60.4	15.8	49.8	9.9	39.9	4.4	1.8	6417	6.633E-04	1.257E-03	2.534E-04	4.803E-04	1.291E-05	2.447E-05	3.971E-04	7.527E-04	18.3	104
15" Pitch Vertical Slinky	8	1/4/11 11:30 AM	0.8	25.4	3.0	0.9	4.086	0.258	61.2	16.2	50.2	10.1	40.0	4.4	1.9	6602	6.685E-04	1.267E-03	2.535E-04	4.806E-04	1.288E-05	2.441E-05	4.021E-04	7.622E-04	18.1	103
15" Pitch Vertical Slinky	1	1/5/11 12:00 PM	0.8	25.4	3.0	0.9	3.934	0.248	51.1	10.6	48.4	9.1	41.1	5.1	0.4	1569	1.592E-03	3.018E-03	2.525E-04	4.786E-04	1.395E-05	2.645E-05	1.325E-03	2.513E-03	5.5	31
15" Pitch Vertical Slinky	2	1/5/11 12:30 PM	0.8	25.4	3.0	0.9	3.888	0.245	56.7	13.7	50.3	10.2	41.6	5.3	1.0	3669	9.246E-04	1.753E-03	2.533E-04	4.802E-04	1.367E-05	2.591E-05	6.576E-04	1.247E-03	11.1	63
15" Pitch Vertical Slinky	3	1/5/11 1:00 PM	0.8	25.4	3.0	0.9	3.920	0.247	59.3	15.2	51.0	10.6	41.8	5.5	1.4	4765	7.946E-04	1.506E-03	2.537E-04	4.809E-04	1.340E-05	2.540E-05	5.276E-04	1.000E-03	13.8	78
15" Pitch Vertical Slinky	4	1/5/11 1:30 PM	0.8	25.4	3.0	0.9	3.990	0.252	60.5	15.8	51.6	10.9	42.1	5.6	1.5	5204	7.592E-04	1.439E-03	2.539E-04	4.813E-04	1.310E-05	2.484E-05	4.922E-04	9.331E-04	14.8	84
15" Pitch Vertical Slinky	5	1/5/11 2:00 PM	0.8	25.4	3.0	0.9	3.998	0.252	61.4	16.3	51.9	11.0	42.3	5.7	1.6	5575	7.274E-04	1.379E-03	2.540E-04	4.815E-04	1.303E-05	2.469E-05	4.604E-04	8.727E-04	15.8	90
15" Pitch Vertical Slinky	6	1/5/11 2:30 PM	0.8	25.4	3.0	0.9	4.000	0.252	62.2	16.8	52.1	11.2	42.3	5.7	1.7	5896	7.097E-04	1.345E-03	2.541E-04	4.817E-04	1.297E-05	2.459E-05	4.426E-04	8.390E-04	16.4	93
15" Pitch Vertical Slinky	7	1/5/11 3:00 PM	0.8	25.4	3.0	0.9	3.982	0.251	62.7	17.0	52.1	11.1	42.3	5.7	1.8	6196	6.835E-04	1.296E-03	2.541E-04	4.817E-04	1.300E-05	2.464E-05	4.163E-04	7.892E-04	17.5	99
15" Pitch Vertical Slinky	8	1/5/11 3:30 PM	0.8	25.4	3.0	0.9	3.970	0.250	63.3	17.4	52.3	11.3	42.2	5.7	1.8	6404	6.830E-04	1.295E-03	2.542E-04	4.820E-04	1.299E-05	2.461E-05	4.158E-04	7.882E-04	17.5	99
15" Pitch Horizontal Slinky	1	1/7/11 8:00 AM	0.8	25.4	3.0	0.9	4.173	0.263	49.7	9.8	47.3	8.5	40.9	4.9	0.4	1469	1.512E-03	2.866E-03	2.521E-04	4.779E-04	1.340E-05	2.541E-05	1.246E-03	2.363E-03	5.8	33
15" Pitch Horizontal Slinky	2	1/7/11 8:30 AM	0.8	25.4	3.0	0.9	4.161	0.263	55.0	12.8	48.7	9.3	41.0	5.0	1.1	3847	8.061E-04	1.528E-03	2.528E-04	4.791E-04	1.307E-05	2.478E-05	5.402E-04	1.024E-03	13.5	76
15" Pitch Horizontal Slinky	3	1/7/11 9:00 AM	0.8	25.4	3.0	0.9	4.150	0.262	57.5	14.2	49.6	9.8	41.3	5.2	1.4	4851	7.137E-04	1.353E-03	2.531E-04	4.798E-04	1.293E-05	2.451E-05	4.476E-04	8.485E-04	16.3	92
15" Pitch Horizontal Slinky	4	1/7/11 9:30 AM	0.8	25.4	3.0	0.9	4.147	0.262	58.7	14.8	49.9	10.0	41.4	5.2	1.5	5331	6.782E-04	1.286E-03	2.533E-04	4.801E-04	1.286E-05	2.438E-05	4.120E-04	7.811E-04	17.7	100
15" Pitch Horizontal Slinky	5	1/7/11 10:00 AM	0.8	25.4	3.0	0.9	4.150	0.262	59.9	15.5	50.4	10.2	41.6	5.3	1.7	5808	6.542E-04	1.240E-03	2.535E-04	4.805E-04	1.276E-05	2.420E-05	3.880E-04	7.355E-04	18.8	106
15" Pitch Horizontal Slinky	6	1/7/11 10:30 AM	0.8	25.4	3.0	0.9	4.146	0.262	61.0	16.1	50.8	10.5	41.9	5.5	1.8	6198	6.313E-04	1.197E-03	2.537E-04	4.808E-04	1.270E-05	2.408E-05	3.649E-04	6.917E-04	19.9	113
15" Pitch Horizontal Slinky	7	1/7/11 11:00 AM	0.8	25.4	3.0	0.9	4.146	0.262	62.2	16.8	51.3	10.7	42.2	5.7	1.9	6623	6.143E-04	1.165E-03	2.539E-04	4.812E-04	1.262E-05	2.391E-05	3.479E-04	6.594E-04	20.9	119
15" Pitch Horizontal Slinky	8	1/7/11 11:30 AM	0.8	25.4	3.0	0.9	4.128	0.260	63.1	17.3	51.8	11.0	42.5	5.8	1.9	6812	6.114E-04	1.159E-03	2.540E-04	4.816E-04	1.260E-05	2.388E-05	3.448E-04	6.536E-04	21.1	120
15" Pitch Horizontal Slinky	1	1/7/11 12:00 PM	0.8	25.4	3.0	0.9	4.159	0.262	52.9	11.6	49.7	9.8	43.3	6.3	0.5	1928	1.197E-03	2.269E-03	2.529E-04	4.794E-04	1.314E-05	2.491E-05	9.310E-04	1.765E-03	7.8	44
15" Pitch Horizontal Slinky	2	1/7/11 12:30 PM	0.8	25.4	3.0	0.9	4.155	0.262	58.1	14.5	51.2	10.7	43.4	6.3	1.2	4178	7.679E-04	1.456E-03	2.536E-04	4.808E-04	1.280E-05	2.427E-05	5.015E-04	9.506E-04	14.5	82
15" Pitch Horizontal Slinky	3	1/7/11 1:00 PM	0.8	25.4	3.0	0.9	4.141	0.261	60.4	15.8	51.9	11.0	43.4	6.3	1.5	5189	6.905E-04	1.309E-03	2.539E-04	4.813E-04	1.269E-05	2.406E-05	4.239E-04	8.036E-04	17.2	97
15" Pitch Horizontal Slinky	4	1/7/11 1:30 PM	0.8	25.4	3.0	0.9	4.144	0.261	61.1	16.2	52.2	11.2	43.8	6.6	1.5	5378	6.720E-04	1.274E-03	2.540E-04	4.816E-04	1.263E-05	2.395E-05	4.054E-04	7.684E-04	17.9	102
15" Pitch Horizontal Slinky	5	1/7/11 2:00 PM	0.8	25.4	3.0	0.9	4.144	0.261	61.8	16.6	52.3	11.3	43.7	6.5	1.6	5781	6.494E-04	1.231E-03	2.541E-04	4.817E-04	1.259E-05	2.387E-05	3.827E-04	7.255E-04	19.0	108
15" Pitch Horizontal Slinky	6	1/7/11 2:30 PM	0.8	25.4	3.0	0.9	4.133	0.261	62.5	17.0	52.5	11.4	43.7	6.5	1.7	6091	6.364E-04	1.206E-03	2.542E-04	4.819E-04	1.258E-05	2.384E-05	3.696E-04	7.007E-04	19.7	112
15" Pitch Horizontal Slinky	7	1/7/11 3:00 PM	0.8	25.4	3.0	0.9	4.126	0.260	63.0	17.2	52.6	11.4	43.5	6.4	1.8	6312	6.345E-04	1.203E-03	2.542E-04	4.820E-04	1.257E-05	2.383E-05	3.677E-04	6.970E-04	19.8	112
15" Pitch Horizontal Slinky	8	1/7/11 3:30 PM	0.8	25.4	3.0	0.9	4.124	0.260	63.5	17.5	52.8	11.6	43.5	6.4	1.8	6440	6.349E-04	1.204E-03	2.543E-04	4.821E-04	1.254E-05	2.377E-05	3.680E-04	6.976E-04	19.8	112

APPENDIX E

Vertical Flat-Plate Experimental Data & Reference Calculations

Test Description	Set Point	Date & Time	Δx		Δy		H		L		\dot{V}_{ej}	$T_{c,in}$	$T_{c,out}$	T_p	Q_c		R_c		R_w		R_j		R_o		h_o					
			in	cm	in	cm	ft	m	ft	m					Tons	W	hr ⁻² F/Btu	K/W	hr ⁻² F/Btu	K/W	hr ⁻² F/Btu	K/W	hr ⁻² F/Btu	K/W	Btu/hr-ft ² -°F	W/m ² -K				
Flat-Vertical Plate HX Test 1	1	4/1/11 6:00 PM	0.3	0.6	11.0	27.9	22.8	6.9	3.7	1.1	6.007	0.379	65.9	18.8	63.0	17.2	53.4	11.9	0.7	2511	1.286E-03	2.439E-03	1.408E-05	2.670E-05	1.104E-04	2.093E-04	1.162E-03	2.203E-03	21.5	122
Flat-Vertical Plate HX Test 1	2	4/1/11 6:30 PM	1.3	3.2	12.0	30.5	23.8	7.2	4.7	1.4	5.986	0.378	71.3	21.8	65.9	18.8	53.2	11.8	1.3	4668	9.563E-04	1.813E-03	1.408E-05	2.670E-05	1.121E-04	2.124E-04	8.302E-04	1.574E-03	30.1	171
Flat-Vertical Plate HX Test 1	3	4/1/11 7:00 PM	2.3	5.7	13.0	33.0	24.8	7.5	5.7	1.7	5.982	0.377	73.6	23.1	67.2	19.5	53.2	11.8	1.6	5589	8.891E-04	1.685E-03	1.408E-05	2.670E-05	1.127E-04	2.136E-04	7.623E-04	1.445E-03	32.8	186
Flat-Vertical Plate HX Test 1	4	4/1/11 7:30 PM	3.3	8.3	14.0	35.6	25.8	7.8	6.7	2.0	5.975	0.377	74.5	23.6	67.7	19.9	53.5	11.9	1.7	5909	8.652E-04	1.640E-03	1.408E-05	2.670E-05	1.130E-04	2.143E-04	7.381E-04	1.399E-03	33.9	192
Flat-Vertical Plate HX Test 1	5	4/1/11 8:00 PM	4.3	10.8	15.0	38.1	26.8	8.2	7.7	2.3	5.960	0.376	75.3	24.1	68.0	20.0	53.3	11.8	1.8	6349	8.387E-04	1.590E-03	1.408E-05	2.670E-05	1.134E-04	2.151E-04	7.112E-04	1.348E-03	35.2	200
Flat-Vertical Plate HX Test 1	6	4/1/11 8:30 PM	5.3	13.3	16.0	40.6	27.8	8.5	8.7	2.6	6.010	0.379	75.7	24.3	68.2	20.1	53.4	11.9	1.9	6571	8.175E-04	1.550E-03	1.408E-05	2.670E-05	1.128E-04	2.138E-04	6.907E-04	1.309E-03	36.2	206
Flat-Vertical Plate HX Test 1	7	4/1/11 9:00 PM	6.3	15.9	17.0	43.2	28.8	8.8	9.7	2.9	5.531	0.349	76.6	24.8	68.6	20.3	53.2	11.8	1.8	6480	8.678E-04	1.645E-03	1.408E-05	2.670E-05	1.208E-04	2.289E-04	7.330E-04	1.389E-03	34.1	194
Flat-Vertical Plate HX Test 1	8	4/1/11 9:30 PM	7.3	18.4	18.0	45.7	29.8	9.1	10.7	3.3	5.474	0.345	77.3	25.2	69.0	20.6	53.4	11.9	1.9	6599	8.626E-04	1.635E-03	1.408E-05	2.670E-05	1.219E-04	2.312E-04	7.266E-04	1.377E-03	34.4	195
Flat-Vertical Plate HX Test 2	1	4/4/11 8:00 AM	8.3	21.0	19.0	48.3	30.8	9.4	11.7	3.6	5.322	0.336	68.3	20.2	67.5	19.7	61.0	16.1	0.2	616	3.271E-03	6.200E-03	1.408E-05	2.670E-05	1.229E-04	2.329E-04	3.134E-03	5.940E-03	8.0	45
Flat-Vertical Plate HX Test 2	2	4/4/11 8:30 AM	9.3	23.5	20.0	50.8	31.8	9.7	12.7	3.9	5.345	0.337	70.2	21.2	68.1	20.1	61.0	16.1	0.5	1631	1.455E-03	2.759E-03	1.408E-05	2.670E-05	1.229E-04	2.330E-04	1.318E-03	2.499E-03	19.0	108
Flat-Vertical Plate HX Test 2	3	4/4/11 9:00 AM	10.3	26.0	21.0	53.3	32.8	10.0	13.7	4.2	5.443	0.343	75.1	24.0	70.8	21.6	60.8	16.0	1.0	3410	1.033E-03	1.959E-03	1.408E-05	2.670E-05	1.224E-04	2.321E-04	8.968E-04	1.700E-03	27.9	158
Flat-Vertical Plate HX Test 2	4	4/4/11 9:30 AM	11.3	28.6	22.0	55.9	33.8	10.3	14.7	4.5	5.422	0.342	75.8	24.3	70.9	21.6	60.8	16.0	1.1	3830	9.500E-04	1.801E-03	1.408E-05	2.670E-05	1.229E-04	2.330E-04	8.129E-04	1.541E-03	30.8	175
Flat-Vertical Plate HX Test 2	5	4/4/11 10:00 AM	12.3	31.1	23.0	58.4	34.8	10.6	15.7	4.8	5.411	0.341	76.1	24.5	70.6	21.5	60.6	15.9	1.2	4304	8.539E-04	1.619E-03	1.408E-05	2.670E-05	1.232E-04	2.335E-04	7.166E-04	1.358E-03	34.9	198
Flat-Vertical Plate HX Test 2	6	4/4/11 10:30 AM	13.3	33.7	24.0	61.0	35.8	10.9	16.7	5.1	5.404	0.341	77.5	25.3	71.6	22.0	60.7	15.9	1.3	4679	8.588E-04	1.628E-03	1.408E-05	2.670E-05	1.237E-04	2.345E-04	7.210E-04	1.367E-03	34.7	197
Flat-Vertical Plate HX Test 2	7	4/4/11 11:00 AM	14.3	36.2	25.0	63.5	36.8	11.2	17.7	5.4	5.415	0.342	78.4	25.8	72.3	22.4	60.7	16.0	1.4	4850	8.707E-04	1.651E-03	1.408E-05	2.670E-05	1.237E-04	2.346E-04	7.329E-04	1.389E-03	34.1	194
Flat-Vertical Plate HX Test 2	8	4/4/11 11:30 AM	15.3	38.7	26.0	66.0	37.8	11.5	18.7	5.7	5.430	0.343	78.5	25.8	72.2	22.3	60.7	15.9	1.4	5034	8.382E-04	1.589E-03	1.408E-05	2.670E-05	1.235E-04	2.340E-04	7.007E-04	1.328E-03	35.7	203
Flat-Vertical Plate HX Test 3	1	4/4/11 12:00 PM	16.3	41.3	27.0	68.6	38.8	11.8	19.7	6.0	5.776	0.364	70.1	21.2	68.8	20.4	61.5	16.4	0.3	1079	2.153E-03	4.081E-03	1.408E-05	2.670E-05	1.156E-04	2.191E-04	2.023E-03	3.835E-03	12.4	70
Flat-Vertical Plate HX Test 3	2	4/4/11 12:30 PM	17.3	43.8	28.0	71.1	39.8	12.1	20.7	6.3	5.738	0.362	75.3	24.0	71.5	21.9	61.6	16.5	0.9	3186	1.071E-03	2.031E-03	1.408E-05	2.670E-05	1.175E-04	2.227E-04	9.398E-04	1.782E-03	26.6	151
Flat-Vertical Plate HX Test 3	3	4/4/11 1:00 PM	18.3	46.4	29.0	73.7	40.8	12.4	21.7	6.6	5.716	0.361	77.1	25.1	72.2	22.4	61.7	16.5	1.2	4073	9.218E-04	1.747E-03	1.408E-05	2.670E-05	1.183E-04	2.242E-04	7.894E-04	1.496E-03	31.7	180
Flat-Vertical Plate HX Test 3	4	4/4/11 1:30 PM	19.3	48.9	30.0	76.2	41.8	12.7	22.7	6.9	5.702	0.360	78.1	25.6	72.7	22.6	61.7	16.5	1.3	4510	8.746E-04	1.658E-03	1.408E-05	2.670E-05	1.187E-04	2.251E-04	7.418E-04	1.406E-03	33.7	191
Flat-Vertical Plate HX Test 3	5	4/4/11 2:00 PM	20.3	51.4	31.0	78.7	42.8	13.0	23.7	7.2	5.720	0.361	79.5	26.4	73.7	23.2	61.7	16.5	1.4	4824	8.919E-04	1.691E-03	1.408E-05	2.670E-05	1.188E-04	2.253E-04	7.589E-04	1.439E-03	32.9	187
Flat-Vertical Plate HX Test 3	6	4/4/11 2:30 PM	21.3	54.0	32.0	81.3	43.8	13.3	24.7	7.5	5.713	0.360	79.6	26.4	73.2	22.9	61.7	16.5	1.5	5375	7.860E-04	1.490E-03	1.408E-05	2.670E-05	1.189E-04	2.254E-04	6.530E-04	1.238E-03	38.3	217
Flat-Vertical Plate HX Test 3	7	4/4/11 3:00 PM	22.3	56.5	33.0	83.8	44.8	13.6	25.7	7.8	5.698	0.359	79.7	26.5	73.1	22.8	61.7	16.5	1.6	5509	7.709E-04	1.461E-03	1.408E-05	2.670E-05	1.191E-04	2.259E-04	6.376E-04	1.209E-03	39.2	223
Flat-Vertical Plate HX Test 3	8	4/4/11 3:30 PM	23.3	59.1	34.0	86.4	45.8	13.9	26.7	8.1	5.727	0.361	80.9	27.2	74.3	23.5	61.6	16.4	1.6	5554	8.333E-04	1.580E-03	1.408E-05	2.670E-05	1.191E-04	2.257E-04	7.001E-04	1.327E-03	35.7	203
Flat-Vertical Plate HX Test 4	1	4/4/11 6:00 PM	24.3	61.6	35.0	88.9	46.8	14.2	27.7	8.4	5.887	0.371	68.8	20.4	67.8	19.9	61.1	16.2	0.2	870	2.400E-03	4.550E-03	1.408E-05	2.670E-05	1.135E-04	2.151E-04	2.272E-03	4.308E-03	11.0	62
Flat-Vertical Plate HX Test 4	2	4/4/11 6:30 PM	25.3	64.1	36.0	91.4	47.8	14.6	28.7	8.7	5.855	0.369	73.6	23.1	70.1	21.2	60.9	16.1	0.9	3043	1.043E-03	1.978E-03	1.408E-05	2.670E-05	1.151E-04	2.182E-04	9.142E-04	1.733E-03	27.3	155
Flat-Vertical Plate HX Test 4	3	4/4/11 7:00 PM	26.3	66.7	37.0	94.0	48.8	14.9	29.7	9.0	5.860	0.370	75.6	24.2	71.0	21.7	60.7	16.0	1.1	3940	9.239E-04	1.751E-03	1.408E-05	2.670E-05	1.155E-04	2.190E-04	7.943E-04	1.506E-03	31.5	179
Flat-Vertical Plate HX Test 4	4	4/4/11 7:30 PM	27.3	69.2	38.0	96.5	49.8	15.2	30.7	9.3	5.843	0.369	77.3	25.2	72.3	22.4	60.6	15.9	1.2	4242	9.707E-04	1.840E-03	1.408E-05	2.670E-05	1.163E-04	2.204E-04	8.403E-04	1.593E-03	29.8	169
Flat-Vertical Plate HX Test 4	5	4/4/11 8:00 PM	28.3	71.8	39.0	99.1	50.8	15.5	31.7	9.7	5.825	0.367	78.8	26.0	73.4	23.0	60.6	15.9	1.3	4595	9.793E-04	1.856E-03	1.408E-05	2.670E-05	1.170E-04	2.217E-04	8.482E-04	1.608E-03	29.5	167
Flat-Vertical Plate HX Test 4	6	4/4/11 8:30 PM	29.3	74.3	40.0	101.6	51.8	15.8	32.7	10.0	5.839	0.368	79.7	26.5	73.9	23.3	60.5	15.8	1.4	4976	9.490E-04	1.799E-03	1.408E-05	2.670E-05	1.170E-04	2.217E-04	8.179E-04	1.551E-03	30.6	174
Flat-Vertical Plate HX Test 4	7	4/4/11 9:00 PM	30.3	76.8	41.0	104.1	52.8	16.1	33.7	10.3	5.852	0.369	80.8	27.1	74.5	23.6	60.5	15.8	1.5	5394	9.217E-04	1.747E-03	1.408E-05	2.670E-05	1.170E-04	2.218E-04	7.907E-04	1.499E-03	31.6	180
Flat-Vertical Plate HX Test 4	8	4/4/11 9:30 PM	31.3	79.4	42.0	106.7	53.8	16.4	34.7	10.6	5.862	0.370	81.1	27.3	74.5	23.6	60.4	15.8	1.6	5652	8.868E-04	1.681E-03	1.408E-05	2.670E-05	1.169E-04	2.216E-04	7.559E-04	1.433E-03	33.1	188
Flat-Vertical Plate HX Test 5	1	4/5/11 8:00 AM	32.3	81.9	43.0	109.2	54.8	16.7	35.7	10.9	5.861	0.370	67.1	19.5	66.3	19.1	58.0	14.5	0.2	622	4.084E-03	7.742E-03	1.408E-05	2.670E-05	1.133E-04	2.149E-04	3.957E-03	7.501E-03	6.3	36
Flat-Vertical Plate HX Test 5	2	4/5/11 8:30 AM	33.3	84.5	44.0	111.8	55.8	17.0	36.7	11.2	5.851	0.369	72.3	22.4	68.9	20.5	58.1	14.5	0.8	2839	1.281E-03	2.427E-03	1.408E-05	2.670E-05	1.148E-04	2.176E-04	1.152E-03	2.183E-03	21.7	123
Flat-Vertical Plate HX Test 5	3	4/5/11 9:00 AM	34.3	87.0	45.0	114.3	56.8	17.3	37.7	11.5	5.844	0.369	74.7	23.7	70.2	21.2	58.2	14.5	1.1	3844	1.079E-03	2.046E-03	1.408E-05	2.670E-05	1.155E-04	2.189E-04	9.499E-04	1.801E-03	26.3	149
Flat-Vertical Plate HX Test 5	4	4/5/11 9:30 AM	35.3	89.5</																										

VITA

Garrett Michael Hansen

Candidate for the Degree of

Master of Science

Thesis: EXPERIMENTAL TESTING AND ANALYSIS OF SURFACE WATER
HEAT EXCHANGERS

Major Field: Mechanical Engineering

Biographical:

Education: Graduated from Washington High School in Sioux Falls, South Dakota in May 2004; received Bachelor of Science in Mechanical Engineering at South Dakota State University, Brookings, South Dakota in May, 2009; completed the requirements for the Master of Science in mechanical engineering at Oklahoma State University, Stillwater, Oklahoma in December, 2011.

Experience: Worked two summers as a mechanical engineer intern at Adams Thermal Systems in Canton, South Dakota from 2006-2007. Was a mechanical engineering intern at Showplace Wood Products in Harrisburg, South Dakota in the summer of 2008 and into the spring of 2009. Worked as an engineering intern at Smithfield Foods Inc. in Sioux Falls, South Dakota for the summer of 2009. Was employed by Oklahoma State University as a research assistant and a teaching assistant from the end of the 2009 summer and going through October 2011.

Certifications:

Engineer in Training (EIT)

Professional Memberships:

American Society of Heating, Refrigerating, and Air Conditioning Engineers, Inc. (ASHRAE student member). Pi Tau Sigma Mechanical Engineering Honor Society.

Name: Garrett Michael Hansen

Date of Degree: December, 2011

Institution: Oklahoma State University

Location: Stillwater, Oklahoma

Title of Study: EXPERIMENTAL TESTING AND ANALYSIS OF SURFACE WATER
HEAT EXCHANGERS

Pages in Study: 172

Candidate for the Degree of Master of Science

Major Field: Mechanical Engineering

Scope and Method of Study: When looking at the heat exchanger of a surface water heat pump (SWHP) system the material of choice these days is high density polyethylene (HDPE). HDPE coils provide high corrosion resistance and minimal impact on the surrounding environment, but at a cost of high thermal resistance. Although the internal convective resistance and conductive resistance are well known, the exterior resistance due to natural convection is poorly understood. In this thesis, 119 experiments were conducted on heat exchangers in the following forms: controlled spacing spiral-helical coils, bundled coils, flat-spirals, vertical slinky, horizontal slinky, and vertical flat-plate heat exchangers. Exterior convective resistances were estimated using an ϵ -NTU heat exchanger analysis. For each geometry, natural convection correlations were developed. Applications of the results to design procedures and heat exchanger design are also investigated.

Findings and Conclusions: A correlation for spiral-helical surface water heat exchangers (SWHE) that gives Nusselt number as a function of modified Rayleigh number, with corrections for horizontal spacing and vertical spacing is developed. This correlation yields an RMSE error of 21% for the outside convection coefficient which results in an RMSE error in the heat transfer of less than 6%. Using this correlation, design graphs for SWHE were created giving the size as a function of approach temperature difference. The second-order effects of lake temperature and heat pump efficiency on SWHE sizing are also determined. Three scenarios for the continental United States (northern, central, and southern) using the design graphs are provided. Using findings in the research regarding the distribution of thermal resistances, several design improvements such as the use of thinner walled HDPE, thermally enhanced HDPE, and metal heat exchangers are also provided. Reduction in sizing for the suggested design improvements ranged from 14% – 77% when compared to SDR-11 HDPE tubing with sizes of 19 mm – 32 mm ($\frac{3}{4}$ " – $1\frac{1}{4}$ ").

ADVISER'S APPROVAL: Dr. Jeffrey Spitler